

Cellular Responses to Jasmonate in *Arabidopsis* Roots

Hsuan-Fu Chen

**Thesis submitted for the degree of
Doctor of Philosophy**

**University of East Anglia
Norwich, U.K.
School of Biological Sciences**

September 2011

© This copy of the thesis has been supplied on condition that anyone who consults it is understood to recognise that its copyright rests with the author and that no quotation from the thesis, nor any information derived therefrom, may be published without the author's prior, written consent.

Abstract

Higher plants respond to biotic and abiotic stress through activation of the JA pathway, which suppresses growth and activates defence. This project describes the expression and subcellular localisation of two of the JA signalling proteins, and the mechanism of MeJA-mediated root growth inhibition. By using immunolocalisation and reporter gene expression, localisation of COI1 was shown at the subcellular and tissue level. Although COI1 was constitutively expressed in the root and shoot, increased expression of COI1 in MeJA-treated roots suggested that the *COI1* gene and the COI1 protein were also regulated by the JA pathway. Co-localisation of COI1 and JAZ3 protein in the nucleus confirmed that the previously-reported interaction between COI1 and JAZ3 took place in the nucleus.

To investigate the morphological basis of root growth inhibition by MeJA, time-lapse and still imaging by confocal microscopy was used to compare root growth parameters in untreated and MeJA-treated roots. MeJA inhibited root growth by reducing the number of dividing cells and rapidly-elongating cells, and causing earlier maturation of the elongating cells, so that they ceased elongating before reaching normal mature cell length. However, the rate of individual cell elongation was unaltered. The physiological basis of MeJA-mediated growth inhibition was investigated by examining the orientation of microtubules, acid efflux from the root elongation zone, and the effect of low water potential on root elongation. MeJA-treated roots had reduced acid efflux and water uptake in the elongating cells, while microtubule orientation was not required for the inhibitory effect.

The crosstalk between JA, auxin, GA and ABA was studied by measuring the change of morphological growth parameters in mutants under different hormone treatment. The impaired MeJA-mediated growth inhibition in *aux1* indicated that MeJA reduced root growth by altering auxin transportation. However, MeJA-mediated growth inhibition was DELLA- and ABA- independent. In summary, MeJA reduced cell division by decreasing rate of mitosis, and inhibited cell elongation by reducing acid efflux, which reduced water uptake, possibly by regulating the auxin transportation, in the *Arabidopsis* root.

List of Contents

Statement of Originality	x
Acknowledgements	xi
Glossary	xii
Chapter 1. General Introduction	1
1.1 JA Signal Pathway	1
1.1.1 JA Biosynthesis	1
1.1.2 JA Signal Perception Pathway	3
1.1.3 JA-Mediated Regulation of Gene Expression	6
1.2 JA Responses	7
1.2.1 Defence	7
1.2.2 Development	8
1.2.3 Growth	9
1.3 Crosstalk between JA and the Other Hormones	11
1.3.1 Auxin	11
1.3.2 ABA	13
1.3.3 GA	14
1.4 Plant Root Growth	16
1.4.1 Cytoskeleton	18
1.4.2 Cell Wall and the Acid Growth Hypothesis	19
1.5 Aim and Objective	20
Chapter 2. General Methodology	21
2.1 Preparation of Material	21
2.1.1 LB Medium	21
2.1.2 SOB Medium	22
2.1.3 Half MS Medium	22
2.1.4 Johnson's Medium	22
2.1.5 Medium for Testing pH of the Maize Seedlings	23

2.1.6 Low-Water-Potential Medium.....	23
2.2 Plant and Plant Growth Handling.....	24
2.2.1 Preparation of Chemicals	24
2.2.2 Surface Sterilisation of <i>Arabidopsis</i> Seeds.....	26
2.2.3 Growth Condition for <i>Arabidopsis</i>	26
2.2.4 Cross of <i>Arabidopsis</i> Transgenic Lines.....	26
2.2.5 List of <i>Arabidopsis</i> Lines and Mutants Used	27
2.2.6 Surface Sterilisation of Maize Seeds.....	28
2.2.7 Growth Condition for Maize	28
2.3 Molecular Biology Methods.....	29
2.3.1 Extraction of DNA from <i>E. coli</i>	29
2.3.2 Plasmid Construction	29
2.3.2.1 Digestion of DNA with Restriction Enzymes	29
2.3.2.2 Extraction of DNA from Agarose Gel.....	30
2.3.2.3 Ligation Reaction.....	31
2.3.2.4 Transformation of <i>E. coli</i> with Plasmid DNA.....	31
2.3.3 Polymerase Chain Reaction (PCR)	32
2.3.3.1 General PCR Protocols	32
2.3.3.2 Primer Design	32
2.3.3.3 DNA Sequencing	32
2.3.4 Gateway System.....	33
2.3.5 Electrophoresis of DNA	33
2.3.5.1 Electrophoresis.....	33
2.3.5.2 DNA Quantification.....	34
2.3.6 Histochemical Assay of GUS (β -Glucuronidase).....	34
2.3.7 Small Scale Extraction of Plant DNA	35
2.3.8 Western Blotting.....	36
2.3.8.1 Preparation of Plant Protein Extract.....	36
2.3.8.2 Preparation of SDS Polyacrylamide Gel.....	36
2.3.8.3 Running the SDS Polyacrylamide Gel.....	37
2.3.8.4 Western Blotting	37
2.3.9 pH Measurement of the Suspended <i>Arabidopsis</i> Roots	38
2.4 Immunolocalisation of HA-Tagged COII Protein.....	38
2.4.1 Whole-Mount Immunolocalisation	38
2.4.2 Antibody Used in Whole-Mount Immunolocalisation	39

2.5 Microscopy	40
2.5.1 Bright Field Microscopy	40
2.5.2 Fluorescence Microscopy	40
2.5.3 Confocal Microscopy	40
2.6 Use of Online Database	41
2.6.1 Genevestigator	41
2.6.2 Tair	41
2.6.3 Motif Scan	42
2.6.4 NEBcutter V2.0	42
2.6.5 Clustal W2	42
Chapter 3. Localisation of Components of the Jasmonate Signal Pathway	43
3.1 Introduction	43
3.2 Method	44
3.2.1 Selection of A Line Homozygous for <i>35S::COII::HA</i> and the <i>coil-16</i> Mutation	44
3.3 Results	46
3.3.1 Localisation of <i>pCOII:: uidA β-glucuronidase</i>	46
3.3.2 <i>35S::COII::HA/coil-16</i> is as Sensitive as <i>Col-gl</i> to MeJA Treatment	49
3.3.2.1 Effect of MeJA Treatment on Root Length of <i>35S::COII::HA/coil-16</i> and <i>Col-gl</i>	49
3.3.2.2 Effect of MeJA Treatment on LEH of <i>35S::COII::HA/coil-16</i> and <i>Col-gl</i>	51
3.3.3 Expression of <i>35S::COII::HA/coil-16</i> and <i>pCOI::COII::HA/coil-16</i>	53
3.3.4 Localisation of Constitutively Expressed <i>COI1::HA</i>	56
3.3.4.1 Identifying Homozygous <i>35S::COII::HA/coil-16</i>	56
3.3.4.2 Identification of the NLS Motif in <i>COI1</i> Protein Sequence	59
3.3.4.3 Control of Autofluorescence in Whole-Mount Immunolocalisation	60
3.3.4.4 Choice of Antibody	61
3.3.4.5 Whole-Mount Immunolocalisation of Constitutively Expressed <i>COI1::HA</i>	61
3.3.5 Localisation of <i>COI1::HA</i> in <i>pCOII::COII::HA /coil-16</i> Plants	63
3.3.6 Co-localisation of <i>COI1</i> and <i>JAI3</i>	65
3.3.6.1 Localisation of <i>JAI3::GFP</i>	65
3.3.6.2 Production of Homozygous Lines for the <i>35S::JAI3::GFP</i> Transgenic Line and <i>35S::COII::HA/coil-16</i>	66
3.3.6.3 Co-localisation of <i>JAI3::GFP</i> and <i>COI1::HA</i>	68

3.3.6.4 JAZ Degradation is COI1-Dependent.....	73
3.4 Discussion.....	75
Chapter 4. Construction of pCOI1::COI1::RFP	78
4.1 Introduction	78
4.2 Methods	79
4.2.1 PCR-based Confirmation of the Presence of p8.6 in pBlueScript.....	80
4.2.2 High Fidelity PCR for Gateway Construction	81
4.2.3 PCR-based Confirmation of the Presence of p8.6 in the p8.6/ pDONR TM 221... ..	82
4.2.4 PCR-based Confirmation of the Presence of COI1 in the p8.6/ pDONR TM 221. ..	83
4.2.5 PCR-based Confirmation of COI1 Native Promoter and COI1 Gene in the p8.6/pDONR TM 221.....	84
4.2.6 Primers with attB Recombination Used to Amplify p8.6 Site for Gateway [®] Cloning System	85
4.2.7 Primers Used in Full-Length Sequencing of the COI1 Native Promoter	85
4.3 Results	86
4.3.1 Making of p8.6/pBS	86
4.3.2 p8.6-RFP Construction Using the Gateway [®] Cloning System.....	88
4.3.3 Analysis of the p8.6 Construct	98
4.4 Discussion.....	105
Chapter 5. Arabidopsis Root Growth in Response to MeJA: the Cell Pattern in QC-LEH.....	108
5.1 Introduction	108
5.2 Results	109
5.2.1 Johnson's Medium and Half MS Medium	109
5.2.2 Root Growth Response to MeJA.....	112
5.2.2.1 Effect of MeJA Treatment on Root Cells in Meristem and Elongation Zone	112
5.2.2.2 Effect of MeJA Treatment on Cell Division	118
5.2.2.3 Effect of MeJA Treatment on Root Cells in JA and Auxin Mutants	119
5.3 Discussion.....	126
Chapter 6. Arabidopsis Root Growth in Response to MeJA: Setting Up the Parameters	129

6.1 Introduction	129
6.2 Results	131
6.3 Discussion.....	139
 Chapter 7. <i>Arabidopsis</i> Root Growth in Response to MeJA, GA and ABA: Crosstalk Between Plant Hormone Signal Pathways	142
7.1 Introduction	142
7.2 Results	144
7.2.1 The Effect of MeJA, GA and ABA Treatments on Root Growth of <i>coil-16</i> , <i>abi</i> , <i>aux1</i> , and <i>della4</i> Mutants Insensitive to JA, ABA, auxin and GA, Respectively	144
7.2.1.1 The Role of <i>COI1</i> on JA, GA and ABA Signaling.....	146
7.2.1.2 The Role of <i>AUX1</i> on JA, GA and ABA Signaling	152
7.2.1.3 The Role of <i>ABI</i> on JA, GA and ABA Signaling.....	156
7.2.1.4 The Role of <i>DELLAs</i> on JA, GA and ABA Signaling	159
7.2.1.5 The Effect of MeJA, GA and ABA Treatment on Cyclin B1 Expression .	163
7.2.2 The Effect of the MeJA and PAC Treatments on <i>della 4</i> , <i>gal-3</i> , <i>gai</i> and <i>coil-16</i>	166
7.2.3 The Effect of the ABA Treatment on <i>aos</i> , <i>coil-16</i> , <i>jai3</i> , <i>jin1-1</i> and <i>jut</i>	169
7.3 Discussion.....	171
 Chapter 8. <i>Arabidopsis</i> Root Growth in Response to MeJA: Role of Microtubules, Acid Efflux and Water Potential	176
8.1 Introduction	176
8.2 Results	178
8.2.1 Effect of MeJA Treatment on Microtubule Orientation.....	178
8.2.2 Effect of MeJA treatment on Acid Efflux	188
8.2.3 Effect of MeJA treatment on Cellular Water Potential	190
8.3 Discussion.....	192
 Chapter 9. General Discussion	195

List of Figures

1-1. Model of the 9-LOX and 13-LOX pathways and the JA biosynthesis	2
1-2. Crystal structure of the COI1-ASK1 complex with JA-Ile and the JAZ1 peptide	3
1-3. Model of switching the JA signaling on and off	5
1-4. SCF complexes in auxin and JA signaling	13
1-5. Model of the GA signaling	15
1-6. Root structure and the localisation of key factors in <i>Arabidopsis</i>	17
1-7. Five day old wild type <i>Arabidopsis</i> root	17
1-8. Model of a cellulose synthase complex in the plasma membrane	19
3-1. GUS staining of <i>pCOI1::GUS</i>	47
3-2. Histochemical GUS detection of <i>pCOI1::GUS</i>	48
3-3. Root length of Col- <i>gl</i> and <i>35S::COI1::HA/coi1-16</i> treated with MeJA	50
3-4. LEH of Col- <i>gl</i> and <i>35S::COI1::HA/coi1-16</i> treated with MeJA	52
3-5. Detection of COI1::HA in <i>35S::COI1::HA-116/coi1-16</i> and <i>35S::COI1::HA-99/coi1-16</i>	54
3-6. Detection of COI1::HA in <i>35S::COI1::HA-116/coi1-16</i> and <i>P8.6/coi1-16</i>	55
3-7. PCR-based detection of the <i>coi1-16</i> mutation	57
3-8. The result of the scanning of COI1 protein sequence in Motif Scan Webpage	59
3-9. Amino acid sequence of the COI1 protein and NLS	60
3-10. Immunolocalisation of Col- <i>gl</i> and <i>35S::COI1::HA-116/coi1-16</i>	62
3-11. Immunolocalisation of Col- <i>gl</i> and <i>p8.6/coi1-16</i>	64
3-12. Localisation of JAI3::GFP	66
3-13. Selection of <i>35S::JAI3::GFP</i> ; <i>35S::COI1::HA/coi1-16</i> seedlings	67
3-14. Immunolocalisation of COI1::HA in <i>35S::JAI3::GFP</i> ; <i>35S::COI1::HA/coi1-16</i>	69
3-15. Immunolocalisation of JAI3::GFP and COI1::HA in <i>35S::JAI3::GFP</i> ; <i>35S::COI1::HA/coi1-16</i>	70
3-16. Immunolocalisation of JAI3::GFP and COI1::HA in MeJA-treated <i>35S::JAI3::GFP</i> ; <i>35S::COI1::HA/coi1-16</i>	72
3-17. Histochemical GUS detection of <i>35S::JAZ1::GUS/coi1-1</i>	74

3-18.	Subcellular localisation of JAZ1/TIFY10A	77
4-1.	Flow chart of p8.6/pDONR TM 221 construction	80
4-2.	The map of primers in p8.6	86
4-3.	Sall/KpnI digestion of pBluescript and p8.6/pBIN19	87
4-4.	Identification of the p8.6/pBS candidates	88
4-5.	Identification of the p8.6/ pDONR TM 221 candidates	89
4-6.	PCR reactions for p8.6/pDONR TM 221 candidates using three sets of primer pairs ..	90
4-7.	DNA alignment of Tair genome sequence, p8.6/pBS and p8.6/pDONR TM 221 #8... 96	
4-8.	Diagram of sequencing and aligning processes.....	97
4-9.	The result of p8.6/pBIN19 sequenced with the ADs29 primer	99
4-10.	Online searching result of the 225 bps known fragment in p8.6.....	99
4-11.	Restriction sites in p8.6	103
4-12.	Restriction sites in the multiple restriction site region of p8.6/pBIN19.....	104
4-13.	Restriction enzyme digestion for p8.6/pBIN19.....	105
5-1.	Col- <i>gl</i> seedlings grown in half MS medium and Johnson's medium.....	110
5-2.	Root length and LEH of MeJA-treated Col- <i>gl</i>	111
5-3.	Time-lapse observation of <i>GFP-TUA6</i> seedlings.....	113
5-4.	Accumulated individual cell length of <i>GFP-TUA6</i>	114
5-5.	Accumulated cell length of <i>GFP-TUA6</i> untreated or treated with MeJA	117
5-6.	GUS detection of <i>CYCBI::GUS</i> treated with 20 μ M MeJA	119
5-7.	Accumulated cell length of <i>aos/GFP-TUA6</i> untreated or treated with MeJA	122
5-8.	Accumulated cell length of <i>coi1-16</i> untreated or treated with MeJA.....	123
5-9.	Accumulated cell length of <i>jin1-1/GFP-TUA6</i> untreated or treated with MeJA....	124
5-10.	Accumulated cell length of <i>aux1-7/GFP-TUA6</i> untreated or treated with MeJA	125
5-11.	The cell cycle in root meristem.....	127
6-1.	Confocal image of <i>Arabidopsis</i> root apex.....	130
6-2.	Confocal image of <i>Arabidopsis</i> root apex untreated or treated with MeJA	131
6-3.	Meristem size of <i>CYCBI::GUS</i> treated with 0, 1, 5 or 20 μ M MeJA	132
6-4.	Cell number in meristem of <i>CYCBI::GUS</i> treated with 0, 1, 5 or 20 μ M MeJA... 133	
6-5.	Mature cell length of <i>CYCBI::GUS</i> treated with 0, 1, 5 or 20 μ M MeJA	134
6-6.	Cell production rate of <i>CYCBI::GUS</i> treated with 0, 1, 5 or 20 μ M MeJA	135
6-7.	Mitotic cell number of <i>CYCBI::GUS</i> treated with 0, 1, 5 or 20 μ M MeJA.....	137
6-8.	Increased root length of <i>CYCBI::GUS</i> treated with 0, 1, 5 or 20 μ M MeJA.....	138
7-1.	Root growth parameters of Col- <i>gl</i> treated with MeJA or GA	147
7-2.	Root growth parameters of <i>coi1-16</i> treated with MeJA or GA	148

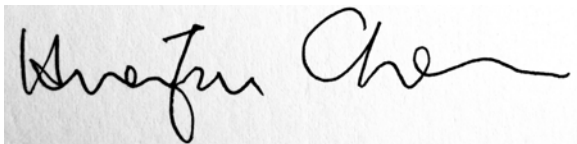
7-3. Root growth parameters of <i>CYCBI::GUS/Col-0</i> treated with MeJA or GA.....	149
7-4. Root growth parameters of <i>Col-gl</i> treated with ABA	150
7-5. Root growth parameters of <i>coil-16</i> treated with ABA	153
7-6. Root growth parameters of <i>CYCBI::GUS/Col-0</i> treated with ABA	154
7-7. Cyclin B1 expression of <i>CYCBI::GUS/Col-0</i> treated with MeJA, GA or ABA ...	157
7-8. Root growth parameters of <i>Col-0</i> treated with MeJA, GA or ABA.....	160
7-9. Root growth parameters of <i>aux1-7</i> treated with MeJA, GA or ABA.....	161
7-10. Root growth parameters of <i>abi</i> treated with MeJA, GA or ABA.....	164
7-11. Root growth parameters of <i>Ler</i> treated with MeJA, GA or ABA	165
7-12. Root growth parameters of <i>della 4</i> treated with MeJA, GA or ABA.....	166
7-13. Rate of root growth of <i>Ler</i> , <i>della 4</i> and <i>gal-3</i> treated with MeJA or PAC	167
7-14. Rate of root growth of <i>gai</i> treated with MeJA	168
7-15. Rate of root growth of <i>Col-gl</i> and <i>coil-16</i> treated with PAC	168
7-16. Rate of root growth of <i>Col-gl</i> , <i>aos</i> and <i>coil-16</i> treated with ABA	170
7-17. Rate of root growth of <i>Col-0</i> , <i>jai3</i> , <i>jin1-1</i> and <i>jut</i> treated with ABA	171
8-1. Confocal image of <i>GFP-TUB6</i> roots.....	179
8-2. Confocal image of <i>aos/GFP-TUB6</i> roots.....	180
8-3. Confocal image of <i>jin1-1/GFP-TUB6</i> roots.....	181
8-4. Confocal image of <i>aux1-7/GFP-TUB6</i> roots	182
8-5. Confocal image of oryzalin-treated <i>GFP-TUB6</i> roots	183
8-6. Oryzalin-treated <i>GFP-TUB6</i> roots	184
8-7. Oryzalin and MeJA-treated <i>GFP-TUB6</i> roots.....	186
8-8. Oryzalin and MeJA-treated <i>GFP-TUB6</i> roots with individual cell diameter measurement.....	187
8-9. How to test if microtubules are required for MeJA-mediated growth inhibition...	187
8-10. <i>Zea mays</i> seedlings untreated or treated with MeJA	189
8-11. pH measuring of medium with suspended <i>Col-gl</i> or <i>coil-16</i> roots.....	190
8-12. Increased root length and growth inhibition rate of PEG8000 and MeJA-treated <i>Col-gl</i> and <i>coil-16</i>	192
9-1. Listed effects of MeJA on root growth inhibition	198

List of Tables

2-1. List of <i>Arabidopsis</i> lines and mutants used.....	27
3-1. The sequences of primers.....	45
3-2. The rationale of the PCR-based detection of the <i>COII</i> and <i>coil</i> -16 alleles.....	45
3-3. Examples of identifying the homozygous <i>coil</i> -16.....	58
4-1. The sequences of primers.....	86
4-2. List of base substitutions occurred in p8.6/pDONR TM 221 candidates.....	91
4-3. Description of 18 Blast hits from the NCBI blast searching result.....	100
5-1. Summary of parameters from Figure 5-7 to 5-10.....	120
6-1. Meristem size from Fig 6-3 and significant analysis.....	132
6-2. Cell number in meristem from Fig 6-4 and significant analysis.....	133
6-3. Mature cell length from Fig 6-5 and significant analysis.....	134
6-4. Rate of cell production from Fig 6-6 and significant analysis.....	136
6-5. Mitotic cell number from Fig 6-7 and significant analysis.....	137
6-6. Increased root length from Fig 6-8 and significant analysis.....	138
7-1. The significance of the parameters differences between Col- <i>gl</i> and <i>coil</i> -16.....	151
7-2. The significance of the parameters differences between Col-0 and <i>aux1</i> -7.....	155
7-3. The significance of the parameters differences between Col-0 and <i>abi</i>	158
7-4. The significance of the parameters differences between Ler and <i>della</i> 4.....	162

Statement of Originality

Unless otherwise noted or referenced in the text, the work described in this thesis is, to the best of my knowledge and belief, original and my own work. It has not been submitted, either in whole or in part, for any degree at this or any other academic or professional institution.

A handwritten signature in black ink on a light-colored background. The signature is written in a cursive style, with the first part appearing to be 'Hsuan-Fu' and the second part being 'Chen' followed by a long, sweeping horizontal stroke.

Hsuan-Fu Chen

22 September, 2011

Acknowledgements

I would not be able to complete this thesis without the help and support from several people. To name just a few:

I owe thousand thanks to Prof John Turner, Dr. Henrik Buschmann and Dr Mette Mogensen (my supervisor and two advisors, respectively) for their guidance and encouragement during this project. I am particularly grateful for John for giving advices, sharing his marvelous scientific knowledge with me and sparing no effort on correcting and commenting on this thesis.

I would like to thank Dr. Paul Thomas for helping with the microscope matter, and Dr. Swarup Ranjan from University of Nottingham and Dr. Jiri Friml from VIB/University Gent for providing the immunolocalisation protocol and the troubleshooting. I would also like to thank Narisa Kunpratun, who cooperated with me in some of the Chapters.

I am also thankful to many friends and colleagues with who I have worked at UEA, particularly Elaine Patrick, Fran Robson, Zhang Yi, Thuong Nguyen, Kawee Sujipali and Liyuan Chen from the Turner's lab. I can never be grateful enough for the help and friendships they offered throughout this project.

Finally, I would like to dedicate this thesis to my family back in Taiwan, Japan and the States, and my friends, wherever they are. Without their support, this PhD mission would be impossible.

Glossary

ABA	abscisic acid
anti-HA	anti-hemagglutinin
AOS	allene oxide synthase
AOC	allene oxide cyclase
bp	base pair
CDK	cyclin-dependent kinase
DAG	day after germination
DNA	deoxyribonucleic acid
EDZ	elongation-differentiation zone
GA	Gibberellin
GFP	green fluorescent protein
GUS	β -glucuronidase
IAA	indole-3-acetic acid
JA	jasmonate
JA-Ile	jasmonoyl-isoleucine
kb	kilo base
LD	long-day
LEH	Length of the first Epidermal cell with a visible root Hair bulge
LOX	lipoxygenase
LRRs	leucine-rich repeats
MeJA	methyl jasmonate
MS	Murashige and Skoog
MTSB	microtubule-stabilising buffer
NLS	nuclear localisation signal
PAC	paclobutrazol
PBS	phosphate buffered saline
PCR	polymerase chain reaction
PEG8000	Polyethylene Glycol 8000
PFA	paraformaldehyde
PM	proximal meristem
QC	quiescent centre
RNA	ribonucleic acid
RNAi	RNA interference
SA	Salicylic acid
SAM	shoot apical meristem
SD	short-day
SDS	sodium dodecyl sulfate
SOB	super optimal broth
TF	transcription factor
TZ	transition zone
UDPG	uracil-diphosphate glucose
WT	wild type
X-Gluc	5-bromo-4-chloro-3-indolyl- β -D-glucuronic acid

Chapter 1

General Introduction

Hormones are a group of small molecules which, when released from a cell, carry chemical messages to protein receptors in cells or tissues in other parts of the organism, and modulate their metabolic processes. Plant hormones regulate physiological processes such as general growth, development, and responses to environmental stresses. Auxins, gibberellins (GAs), cytokinins, ethylene and abscisic acid (ABA) were identified early as major types of hormones, while additional compounds, including brassinosteroids, jasmonates (JAs), salicylic acid (SA), nitric oxide and strigolactones, were more recently identified (Santner and Estelle, 2009). These hormones are not structurally related, but some of their signal pathways share similar features. In addition, the crosstalk between hormone signaling is evidently extensive (Kasan and Manners, 2008). The hormone, JA, is introduced here from its synthesis, to perception and downstream gene responses.

1.1 JA Signal Pathway

1.1.1 JA Biosynthesis

Oxylipin is a family of oxygenated products derived from fatty acids, and JA is an oxylipin signaling molecule (Vick and Zimmerman, 1984). Linolenic acid is released from plastid lipids by lipases and forms the substrate for synthesis of JA (Koo and Howe, 2009). Hydroperoxides, including (13S)-hydroperoxy-octadecatrienoic acid (13-HPOT) and (9S)- hydroperoxyoctadecatrienoic acid (9-HPOT), are generated from linolenic acid by lipoxygenases (LOXs). The first step of JA biosynthesis starts from conversion of 13-HPOT by allene oxide synthase

(AOS) and allene oxide cyclase (AOC), to form *cis*(+)-12-oxophytodienoic acid (OPDA), the final product produced in the plastid. OPDA is then transported to peroxisomes, where its cyclopentanone ring is reduced by OPR3, a peroxisomal OPDA reductase, and its acidic side-chain is shortened by the β -oxidation enzymes, to form the final JA product (**Figure 1-1**) (Wasternack, 2007).

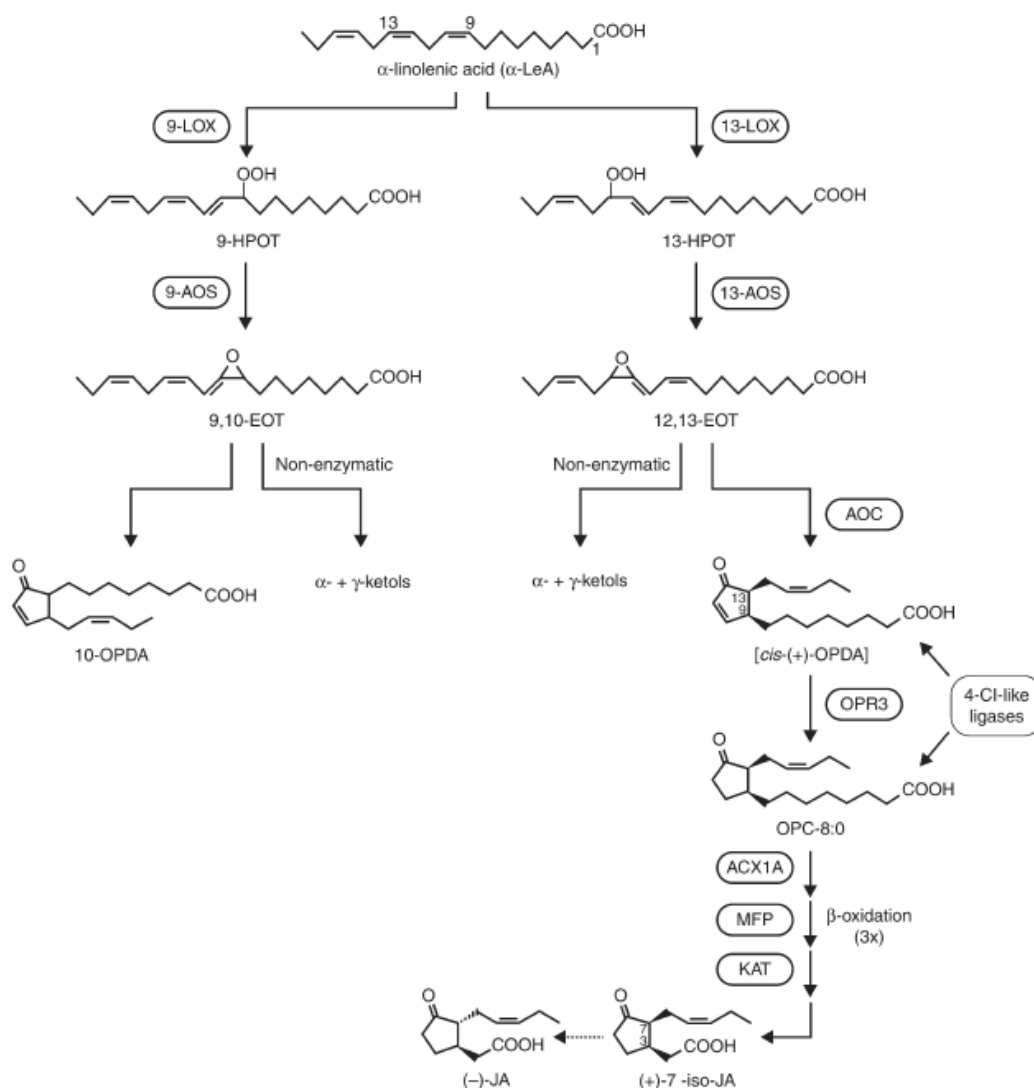


Figure 1-1 Diagram of the 9-LOX and 13-LOX pathways and the JA biosynthesis (Wasternack, 2007)

1.1.2 JA Signal Perception Pathway

JA is not the active form for signal perception. There are several metabolic routes for the modification of JA, such as methylation by a methyl transferase to form methyl jasmonate (MeJA) (Seo *et al.*, 2001), or conjugation with amino acids (Sembdner and Parthier, 1993, Staswick and Tiryaki, 2004). The amide conjugates jasmonoyl-isoleucine (JA-Ile), which is synthesised by a JA conjugate synthase (JAR1) (Staswick and Tiryaki, 2004), is the active ligand that binds to and stimulates the formation of COI1-JAZ co-receptor (**Figure 1-2**) (Thines *et al.*, 2007, Sheard *et al.*, 2010).

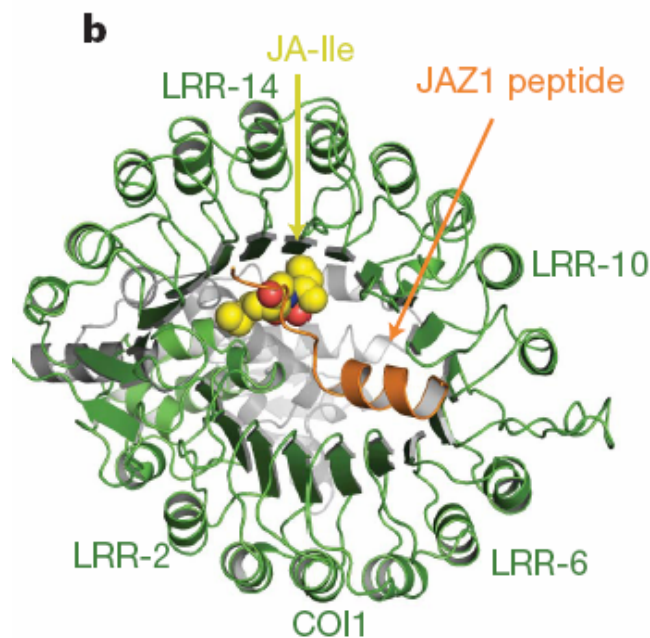


Figure 1-2 Crystal structure of the COI1-*Arabidopsis SKP1-like 1* (ASK1) (green and grey ribbons, respectively) complex with JA-Ile and the JAZ1 peptide (Sheard *et al.*, 2010). In COI1, there are 16 imperfect leucine-rich repeats (LRRs). The three long intra-repeat loops (loop-2, -12 and -14) are involved in hormone and polypeptide substrate binding.

Isolation and identification of some important mutants had helped to clarify the JA signal perception pathway. *jar1* was isolated as an ethyl methanesulfonate mutant with decreased sensitivity to MeJA-induced root growth inhibition (Staswick *et al.*, 1992). Using a molecular mapping approach, *JAR1* was found to encode a protein

structurally related to adenylate-forming enzymes of the firefly luciferase superfamily (Staswick *et al.*, 2002). Further examination of the biochemical activity of JAR1 and the ability of JA conjugates to complement the *jar1-1* mutation revealed that JAR1 is a JA-amino synthetase which converts JA to the active JA-Ile (Staswick and Tiriyaki, 2004). The mutant, *coronatine-insensitive 1 (coi1)*, was selected in a screen for plants insensitive to the phytotoxin coronatine (Feys *et al.*, 1994). By a map-based cloning, COI1 was identified as an F-box protein, which associates with SKP1 (S-phase kinase-associated protein), CULLIN (CUL) and RING-box proteins (Rbx) to form the SCF^{COI1} ubiquitin ligase complex (**Figure 1-2**) (Xie *et al.*, 1998; Zheng *et al.*, 2002; Devoto *et al.*, 2002; Sheard *et al.*, 2010).

The discovery of the JASMONATE ZIM-domain (*JAZ*) genes was more tortuous. From a transcriptional profiling experiment in flower buds of the *opr3* mutant, which is defective in OPDA reductase3 and is male sterile, 31 genes were specifically induced by JA application. Eight proteins from these genes with unknown function all contain a ~28-amino acid motif (ZIM), but none of the T-DNA insertion mutants of these genes showed an obvious JA-related phenotype, suggesting that some JAZ proteins are functionally redundant. However, *JAZ1Δ3A*, a mutant lacking the conserved domain 3, exhibited dominant-negative phenotype, such as male sterility and resistance to JA-mediated growth inhibition, indicating that the altered JAZ1 protein blocked the JA responsiveness. It was subsequently revealed that the COI1-dependent degradation of the JAZ1 protein is essential for activating JA-dependant gene expression, and that JAZ1 might be a repressor for the JA signaling pathway (Thines *et al.*, 2007).

The functional domains of JAZ proteins include Jas, N-terminus (NT) and ZIM domains. Located near the C-terminus, Jas domain is unique for its participation in the protein-protein interaction with both MYC2 and COI1, and for determining the nuclear localisation of the JAZ proteins (Thines *et al.*, 2007; Melotto *et al.*, 2008; Grunewald *et al.*, 2009). NT is a weakly conserved region at the N-terminus (Thines *et al.*, 2007). ZIM domain is necessary and sufficient for the JAZ-JAZ interactions to form homodimers or heterodimers, and is a defining feature of the TIFY family, named after the conserved amino acid pattern “TIF[F/Y]XG” (Vanholmes *et al.*, 2007; Chung and Howe, 2009; Chini *et al.*, 2009). Removing the ZIM domain from *JAZ1* abolished JAZ1's nuclear localisation as discrete speckles in the tobacco BY-2 cells, indicating that the protein-protein interaction mediated by ZIM domain is

possibly crucial for the proper localisation of JAZ1 in the nucleoplasm (Grunewald *et al.*, 2009).

In unstressed cells, JAZ proteins repress transcription factors (TFs) which promote the expression of JA-responsive genes. In stressed cells, JA is synthesised, JA-Ile induces the recruitment of JAZ proteins to the (Skp1/Cullin/F-box) SCF^{COI1} complex, and JAZ proteins are subsequently destroyed via the 26S proteasome pathway, thus releasing the MYC2 TF from repression (Thines *et al.*, 2007, Chini *et al.*, 2007). As a feedback control, the induction of early JA-responsive genes by MYC2 includes the *JAZ* genes, and the newly-produced JAZ proteins resume the repression (**Figure 1-3**) (Chung *et al.*, 2009).

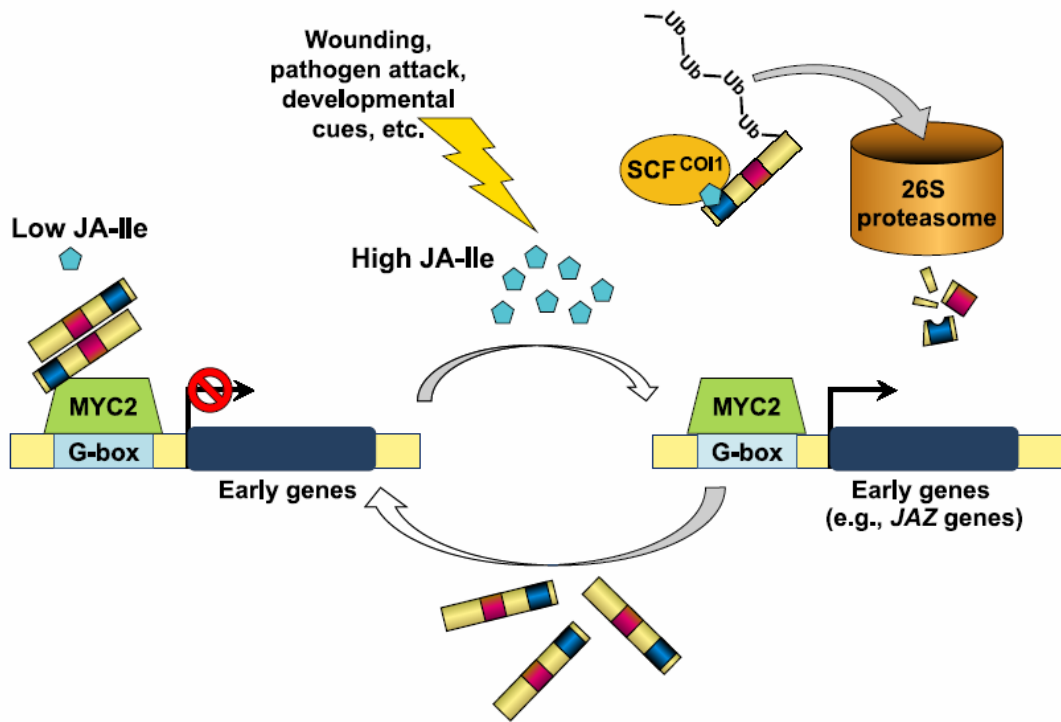


Figure 1-3 Model for JA signaling pathway. When the signaling is inactive, JAZ binds to MYC2, hence suppresses the expression of JA responsive genes (Left). When the signaling is activated, synthesis of JA-Ile stimulates the binding of JAZ to SCF^{COI1}, which promotes ubiquitination and degradation of JAZ via the 26S proteasome. MYC2 is then capable of inducing the transcription of early JA responsive genes, including the *JAZ*s. The newly synthesised JAZ proteins bind to MYC2 and turn off the JA signaling. (Chung *et al.*, 2009)

1.1.3 JA-Mediated Regulation of Gene Expression

The most-studied TF for JA-responsive gene expression is MYC2, a nuclear-localized basic helix-loop-helix-leucine zipper TF encoded by *JASMONATE-INSENSITIVE1 (JAI1/JIN1)* (Lorenzo *et al.*, 2004). Compared to wild type plants, the *jin1/myc2* mutant is more susceptible to some insect pests, but also more resistant to fungal and bacterial pathogens, indicating that JIN1/MYC2 can either positively or negatively regulate JA-dependant expression (Dombrecht *et al.*, 2007). However, *jin1/myc2* exhibits weaker JA-dependent phenotypes than *coi1*, suggesting that MYC2 is only required for some of the JA responses (Lorenzo *et al.*, 2004, Berger *et al.*, 1996). Other TFs shown to be involved in modulating JA-responsive genes include ERF1 (ETHYLENE RESPONSE FACTOR1), WRKYs, MYBs and zinc fingers (Fonseca *et al.*, 2009). However, no interaction between these TFs and the JAZ proteins has been reported so far.

JIN1/MYC2 was the first TF found to be targeted by JAZ proteins (Chini *et al.*, 2007). Although it was hypothesised that JAZ proteins can target specific TFs, which leads to different JA-dependent functions, it was only recently found that the other TFs also interact with JAZ proteins (Ferna'ndez-Calvo *et al.*, 2011). MYC3 and MYC4 are bHLH TFs closely related to MYC2. The double *myc2 myc3* mutant and the triple *myc2 myc3myc4* mutant are less sensitive to JA than *myc2*, and each of the mutants showed differential phenotypes in different JA-mediated responses, indicating that MYC3 and MYC4 have functions additional to MYC2 in regulating JA-responsive gene expression, and they are not completely redundant (Ferna'ndez-Calvo *et al.*, 2011). MYC2, MYC3 and MYC4 might not be the only three TFs which interact with JAZ proteins. More investigation is required to understand how JA responses are specifically regulated.

1.2 JA Responses

The range of JA-dependent control of development and metabolism is much wider than JA's initial characterisation as a defence hormone (Koo and Howe, 2009). A recent study on the MeJA-induced genes in a fast-dividing *Arabidopsis* cell culture revealed that JA signaling alters the metabolism and cell cycle progression via a programmed transcriptional cascade. Early MeJA responsive genes encode the protein components of JA biosynthesis pathway and the transcriptional regulators such as MYC TF and JAZ proteins, whereas later MeJA responses arrest the cell cycle in the G2-M transition, and activate transcription of genes for biosynthesis of phenylpropanoid and monolignol, which might activate subsequent defence responses (Pauwels *et al.*, 2008). To date, JA has been shown to be involved in carbon partitioning (Stepansky and Galili, 2003), mechanotransduction (Stelmach *et al.*, 1998), senescence (Buchanan-Wollaston *et al.*, 2005), resistance to insects and pathogens (Creelman and Mullet, 1997), response to salt stress and ultraviolet radiation (Moons *et al.*, 1997, Conconi *et al.*, 1996), reproductive and vegetative development (Feys *et al.*, 1994, Li *et al.*, 2004), and control of growth through regulation of mitosis in the shoot apical meristem (SAM) (Zhang and Turner, 2008). The following sub-sections give further detail on JA's role in defence and development.

1.2.1 Defence

JA was initially regarded as a plant secondary compound, which induced the production of proteinase inhibitor in tomato when applied exogenously (Farmer and Ryan, 1990). It became evident that JA is a defence hormone, when the JA biosynthesis mutants exhibit altered phenotype for disease and herbivores resistance. An octadecanoid pathway mutant (JL5) of tomato is deficient in DEFENCELESS1 (DEF1), which affects the JA biosynthesis between the lipoxygenase conversion and the conversion of PDA to JA. JL5 has reduced resistance to hornworm, and is unable to accumulate defence proteins when treated with elicitors of the wound response (Howe *et al.*, 1996). Likewise, a triple fatty acid desaturation (FAD) mutant *fad3-2 fad7-2 fad8*, which is deficient in the jasmonate precursor linolenic acid, is

devastatingly susceptible to the fungal gnat larva attack, but this can be rescued by applying jasmonate (McConn *et al.*, 1997). *fad3-2 fad7-2 fad8* is also susceptible to the fungal root pathogen *Pythium mastophorum*, and applied jasmonate again retrieves the mutant's resistibility back to wild type level (Vijayan *et al.*, 1998). The LOX3-, AOS-, and hydroperoxide lyase (HPL)-deficient *N. attenuata* plants made with antisense (as) RNA silencing technique showed different response to the herbivores attack. The as-*lox* plants attract more *Manduca sexta*, leaf beetle *Diabrotica undecimpunctata tenella* Le Conte, and *Empoasca* sp., an unusual herbivore on *N. attenuata* plants, than wild type, as-*hpl*, or as-*aos* plants. This indicates that LOX3-dependent octadecanoids may affect the host-plant selection of herbivores by allowing them to distinguish between plants with and without intact JA signaling (Kessler *et al.*, 2004). These studies clearly demonstrate the essential role of JA signaling in defence resistance, and the diverse role of the intermediates in the JA biosynthesis pathway.

1.2.2 Development

The JA insensitive mutant *coil* has shorter stamen filaments than those in the wild types, its anthers do not dehisce, and the pollen inside have obvious vacuoles and are smaller than those in the wild type anthers. However, *coil* has a normal stigma and style, and produce siliques when pollinated by wild type *Arabidopsis*, indicating that COI1-dependent JA signaling is crucial for male fertility (Feys *et al.*, 1994). Two-dimensional electrophoresis of proteins from the flowers of wild type and *coil* shows the mutant lacks a protein of approximately 31 kD, which was unidentified but apparently required for normal anther development (Feys *et al.*, 1994). The referred protein was later confirmed as a coronatine-induced vegetative storage protein (VSP), which has abundant expression in flowers and siliques, and the expression is entirely *COI1*-dependent (Benedetti *et al.*, 1995). Subsequent studies revealed that the *fad3-2 fad7-2 fad8* triple mutant is also male sterile, with anthers which do not dehisce and pollen with very low viability (McConn and Browse, 1996). It was suggested that the JA signaling is at least responsible for two distinctive functions during flower development. One is to assure the successful dehiscence of the anthers by controlling the dehydration of endothecium cells and the degeneration of the stomium and septum cells, and the other is to promote pollen

maturation (McConn and Browse, 1996). The *Arabidopsis* mutant, *defective in anther dehiscence1* (*dad1*), is defective in JA biosynthesis, and also has failed anther dehiscence and immature pollen. DAD1 is a phospholipase localised in the chloroplast. Its expression is induced by wounding, and the expression is restricted to stamen filaments (Ishiguro *et al.*, 2001). These findings link the male sterility of *dad1* to impaired water transportation during flower development. It was postulated that JA regulates water transportation into the filaments and petals, which promotes water uptake and cell elongation. Impaired water transportation in *dad1* causes failure of filament elongation, anther dehiscence and pollen maturation (Ishiguro *et al.*, 2001).

Interestingly, in tomato, the recessive *jasmonic acid-insensitive1-1* (*jail-1*) and *jail-2* mutants, which are mutated in the tomato homolog of the *Arabidopsis* *COI1* gene, exhibit maternal sterility instead of male sterility. Such difference between *jail-1* (tomato) and *coil* (*Arabidopsis*) may be because *Arabidopsis* produces dehiscent dry siliques, whereas tomato is a nondehiscent fleshy fruit (Li *et al.*, 2004). *jail-1* also shows developmental abnormality in glandular trichomes, which are absent in *jail-1* fruit and decrease hugely in *jail-1* leaves and sepals. Increased trichome density had been observed as one of the induced responses to herbivore attack (Karban and Baldwin, 1997). Therefore, change of glandular trichome density by COI1/JA signaling can be regarded as one of the JA-mediated defence responses. Indeed, the bHLH TF GLABRA3 (GL3), whose expression is induced by JA treatment, was later shown to interact with the product of *TRANSPARENT TESTA GLABRA1* (*TTG1*). Mutation of *TTG1* gene in *Arabidopsis* effectively disrupts JA-induced trichome formation, without abolishing normal JA responses. These findings indicate that GL3 is the key TF for JA-induced trichome formation, and change of the morphological appearance can be part of the anti-stress strategy regardless of the developmental stages. (Yoshida *et al.*, 2009)

1.2.3 Growth

It was demonstrated that 10 μ M MeJA treatment significantly inhibit primary root growth in some plant species (Corbineau *et al.*, 1988). This response to MeJA was later recognised to be specific to the hormone instead of a toxic effect, and was used

to screen JA insensitive mutants in *Arabidopsis* (Staswick *et al.*, 1992, Feys *et al.*, 1994). Subsequent studies revealed that JA-mediated growth-inhibition is perhaps a consequence of several physiological activities combined together. In tobacco BY-2 cells, 50 μ M MeJA treatment disrupts microtubules in the S phase, indicating that microtubules are only sensitive to MeJA when the cells are in the process of DNA synthesis (Abe *et al.*, 1990). Świątek *et al.* further confirmed that MeJA specifically blocks G1/S and G2/M transitions in the cell cycle of BY-2 cells, and suggested that MeJA prevents mitosis by decreasing the cyclin-dependent kinase (CDK) activity (Świątek *et al.*, 2002). On the other hand, JA effectively inhibits the IAA-induced elongation of oat coleoptile segments, possibly due to the prevention of glucose incorporation into the cell wall polysaccharides, which suggests JA inhibits cell elongation by interfering the sugar metabolism (Ueda *et al.*, 1995). Although both reduction of cell mitosis and cell elongation were proved to be associated with JA-induced growth inhibition, the molecular mechanism behind it is largely unknown. However, it has been shown that MeJA suppresses *DR5::GUS*, an auxin reporter, in the root elongation zone in *Arabidopsis*, which in turn blocks the polar auxin transportation (T. Nguyen, 2007, unpublished data).

A large-scale attempt to screen for genes involved in the MeJA-induced growth inhibition in *Arabidopsis* identified *JASMONATE-ASSOCIATED1* (*JAS1*), later recognised as *JAZ10*. Overexpression of *JAS1* partially recovers the wounding (endogenous JA) and exogenous MeJA-induced growth inhibition, and RNA interference (RNAi) transgenic plants of *JAS1* is more sensitive to MeJA than the wild type plant. These results indicate that *JAS1* is a key mediator for wounding-induced growth response in JA signaling (Yan *et al.*, 2007). However, it is not certain yet if *JAS1/JAZ10* is the only repressor that mediates growth inhibition in the JA signal pathway, and what are the genes regulated by *JAS1/JAZ10* in order to suppress growth. The JA-responsive and COI1-dependent growth inhibition by wounding in *Arabidopsis* leaves was further investigated recently by Zhang and Turner, who found that the growth inhibition is due to reduction of the growth rate and mitotic cell number, and not reduction of cell size. It is also evident that OPDA, though capable of activating defence response itself, is unable to promote wound-induced growth inhibition before it is converted to JA or JA's amide conjugates (Zhang and Turner, 2008).

1.3 Crosstalk between JA and the Other Hormones

Crosstalk between plant hormones has been a popular research category. Hormones can interact antagonistically or synergistically in fine-tuning physiological activities in response to environmental stresses, and this is often revealed by finding mutants of certain signal pathway that also exhibit altered responses to another hormone (Santner and Estelle, 2009). Although rough pictures have been drawn for interactions between plant hormones, a lot still waits to be discovered to understand this complex network. Many observations have confirmed the extensive crosstalk between JA and other hormones, such as auxin, ethylene, ABA, GA and SA (Kazan and Manners, 2008). Here, auxin, ABA and GA are reviewed exclusively for their relationships with JA.

1.3.1 Auxin

Auxin is the first identified plant hormone. It is a dominant figure in regulating growth and development throughout the plant's life cycle. The crosstalk between JA and auxin is mostly regarded as positive (Kazan and Manners, 2009). Microarray analysis first suggested that wounding and MeJA possibly affect auxin level in *Arabidopsis* (Devoto *et al.*, 2005), and it was confirmed later that MeJA indeed activates transcription of auxin biosynthesis genes, which might contribute to MeJA-induced growth regulation (Dombrecht *et al.*, 2007). Interestingly, expression of the JA biosynthesis genes *LOX2* and *AOS* (1.1.1) were induced by IAA, and induction of these genes decreased in the auxin response mutant *axr1*, indicating that auxin also activates the JA biosynthesis genes (Tiryaki and Staswick, 2002). Many mutants were already found to have altered phenotypes in both JA and auxin pathways. Mutations in *AUXIN RESISTANT1* (*AXR1*) and *CULLINI/AXR6* attenuate sensitivity to both JA and auxin in *Arabidopsis* (Tiryaki and Staswick, 2002, Quint *et al.*, 2005). *GH3.9* belongs to the auxin-responsive family *GH3*. The *gh3.9* mutant and the *GH3.9* RNAi lines are less sensitive to MeJA and more sensitive to IAA than the wild type plant, indicating that *GH3.9* has a role in both IAA- and MeJA-mediated root growth inhibition (Khan and Stone, 2007). Two auxin response factors (ARF) genes, *ARF6* and *ARF8*, are responsible for both male and female

fertility. The double mutant *arf6/arf8* shows reduction of *LOX2* and *OPR3* expression, suggesting *ARF6* and *ARF8* regulate flower development by inducing JA production (Naqpal *et al.*, 2005). Finally, the *Arabidopsis eta3/sgt1b* mutant, which is compromised in SCF^{TIR1}-mediated auxin response, also shows reduced sensitivity to MeJA (Gray *et al.*, 2003).

The similarities between JA and auxin signaling are apparent. They both use signaling perception mechanism associated with F-box proteins and the ubiquitin-proteasome pathway (Santner and Estelle, 2009). In JA signaling, COI1 is the key F-box protein in the SCF^{COI1} complex, which receives JA-Ile as the hormone messenger, and JAZ proteins are the repressors degraded via ubiquitination after being recruited by the JA-Ile-activated SCF^{COI1} complex. In auxin signaling, TRANSPORT INHIBITOR RESPONSE1 (TIR1) is the key F-box protein in the SCF^{TIR1} complex, which receives biologically active auxins as the hormone messenger, and Aux/IAA protein is the repressor degraded via ubiquitination after being recruited by the auxin-activated SCF^{TIR1} complex. TOPLESS (TPL) is a transcriptional co-repressor associated with Aux/IAA protein in repressing the ARF transcription factors (**Figure 1-4**) (Santner and Estelle, 2009). There is so far no evidence for a co-repressor which works with MYC2 in mediating expression of the JA-responsive genes. However, Novel Interactor of JAZ (NINJA), an adaptor protein which acts as a transcriptional repressor to negatively regulate JA responses, is shown to interact with both JAZ and TPL. This suggests that TPL works in multiple signaling pathways, and provides a further link between JA and auxin signaling (Pauwels *et al.*, 2010).

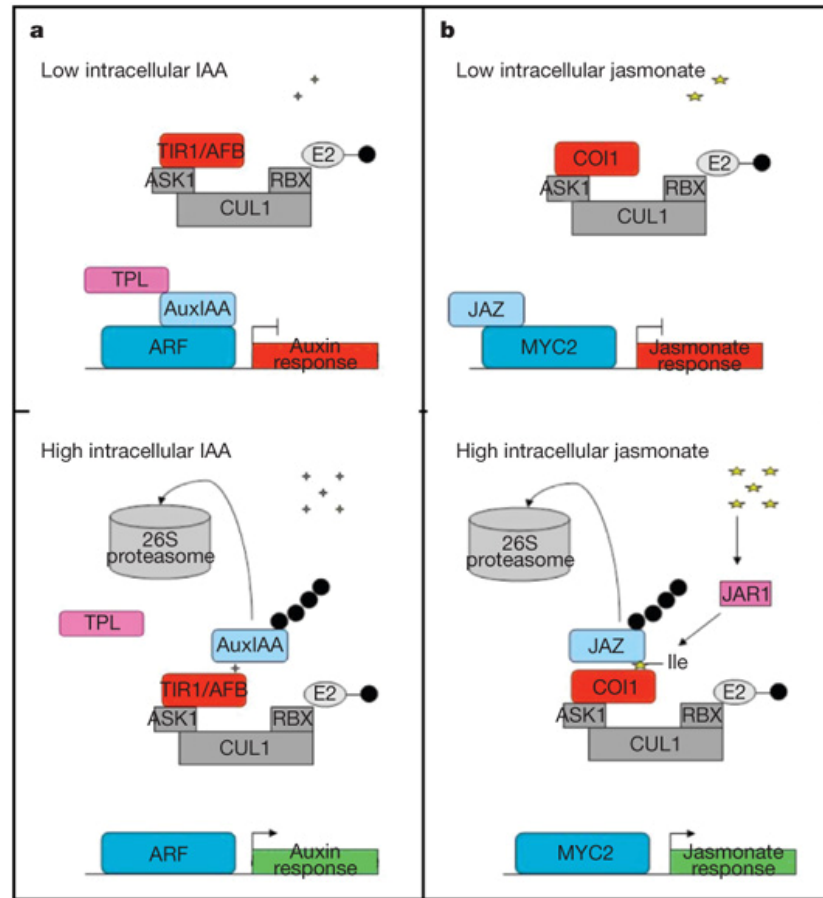


Figure 1-4 SCF complexes are required for both auxin and JA signaling. (a) TIR1/AFB is the auxin receptor. The SCF^{TIR1}, which consists of ASK, CUL and RBX, recruits Aux/IAA and promotes its degradation via the 26S proteasome when the auxin signaling is activated. Degradation of Aux/IAA releases TPL and induces ARF-dependent transcription. (b) See the text in 1.1.2 for detail of JA signaling. (Santner and Estelle, 2009)

1.3.2 Abscissic Acid

ABA is reported to be involved in regulating many developmental stages, including seed germination, embryo maturation and leaf senescence (Wasilewska *et al.*, 2008), and also takes part in plant defence responses (Mauch-Mani and Mauch, 2005; Adie *et al.*, 2007). ABA exhibits both antagonistic and synergistic interactions with JA (Kazan and Manners, 2008). Although both ABA and MeJA significantly reduce the elongation of *Zea mays* coleoptile segments, the fact that MeJA-mediated growth

inhibition is not attenuated by adding norflurazon, a carotenoid synthesis inhibitor that reduces ABA levels, clearly showed that the inhibitory processes apparently work independently in this circumstance (Irving *et al.*, 1999).

In *Arabidopsis*, both endogenous and exogenous ABA decreases the expression of JA-ethylene responsive defence genes extensively. In addition, both *jin1-9/myc2* and *aba2-1* mutants show higher transcript levels of JA-ethylene responsive defence genes, and are less susceptible to the necrotrophic fungal pathogen *F. oxysporum* than the wild type plant, suggesting antagonism between the ABA and JA-ethylene signaling pathways in pathogen defence (Anderson *et al.*, 2004). On the other hand, type III effectors (T3Es), chemical virulence factors produced by *Pseudomonas syringae* pv *tomato* DC3000, increases both ABA and JA levels in treated leaves. Microarray analysis of the transcripts differentially induced by T3E, JA or ABA application indicated significant overlap of the up-regulated transcripts between these three treatment, suggesting that JA and ABA work synergistically in resistance to the hemi-biotroph DC3000 (de Torres-Zabala *et al.*, 2007). In the case of *Arabidopsis* and the necrotrophic pathogen *Pythium irregulare*, JA signaling is the main weapon used to defend against the oomycete. The investigation in the *aba2-12* biosynthetic mutant revealed that ABA is required for JA biosynthesis and the expression of JA-responsive defence genes induced by *P. irregulare* infection, indicating another synergistic interaction between the two hormones (Adie *et al.*, 2007).

1.3.3 Gibberellins

Like auxin and ABA, GA is also closely related to various developmental processes, such as seed germination, leaf expansion, stem elongation, and floral initiation (Richards *et al.*, 2001). The perception of a GA signal also has similar features to JA and auxin signaling. SLEEPY1 (SLY1) and GIBBERELLIN-INSENSITIVE DWARF2 (GID2) are the key F-box proteins in the SCF^{GID2/SLY} complex. GID1, the receptor for GA, interacts with DELLA proteins in a GA-dependent manner (Ueguchi-Tanaka *et al.*, 2005). Named after their conserved domain, DELLA proteins are the repressors for phytochrome-interacting factor 3 (PIF3, a bHLH-type transcription factor) and PIF4. The interaction between DELLA proteins, GID1 and

GID2/SLY promotes the degradation of the DELLA proteins via ubiquitination, hence activates expression of genes regulated by PIF3 and PIF4, and other GA-responsive genes (**Figure 1-5**) (Hedden, 2008; Santner and Estelle, 2009).

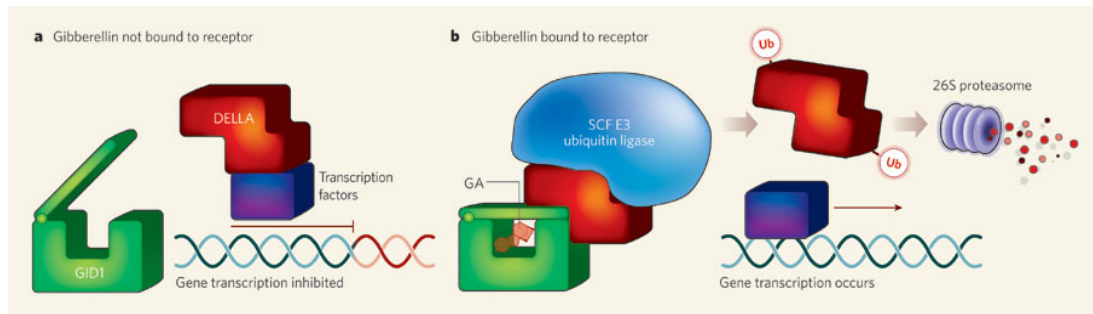


Figure 1-5 Model of the GA signaling. (a) When GA signaling is inactive, the GID1 receptor is unbound and DELLA suppresses the expression of GA-responsive genes. (b) When GA binds to GID1, GID1 promotes the association of DELLA and the SCF E3 ubiquitin ligase, which leads to degradation of DELLA via the 26S proteasome, hence releasing the TFs to promote GA-responsive gene expression. (Hedden, 2008)

Not surprisingly, the connection between the JA and GA signaling pathways largely depends on the DELLA proteins. A quadruple-DELLA mutant, which is deficient in GAI, RGA, RGL1, and RGL2, is partially insensitive to MeJA, while the dominant DELLA mutant *gai* has higher JA-responsive gene expression than the wild type plant. In addition, the quadruple-DELLA mutant displays altered resistance to both necrotrophic and biotrophic infection and changed JA-dependent gene expression during the infection, suggesting that DELLA proteins play a role in JA perception and signaling (Navarro *et al.*, 2008). A subset of genes named *GAMYBs* encode TFs involved in GA-mediated stamen development. It was shown that the expression of *MYB21*, *MYB24*, and *MYB57* are reduced in the quadruple DELLA mutant *gal-3 gai-t6 rga-t2 rgl1-1*, whereas exogenous JA treatment restores the expression of *MYB21*, *MYB24*, and *MYB57* back to wild-type level. By examining gene expression in the wild type plant and various GA/DELLA mutants, it was also clear that GA destabilised DELLA proteins to upregulate the JA biosynthesis genes *LOX1* and *DAD1*, and the induction of *DAD1* expression is

before the induction of *MYB21*, *MYB24*, and *MYB57*. These results demonstrate that GA promotes JA biosynthesis by modulating expression of *LOX1* and *DAD1*, which in turn induces the expression of *MYB21*, *MYB24*, and *MYB57* for GA-mediated stamen development (Cheng *et al.*, 2009). A recent break-through report further revealed that DELLA proteins, including RGA, GAI, RGL1, and RGL2, interact with JAZ1 in the NT and Jas domain, while ZIM domain is not required for the interaction. DELLA proteins bind to JAZ1 by competing with MYC2, and enhancing the binding between MYC2 and the G-box motifs (Hou *et al.*, 2010). This provides yet another link between JA and GA signaling, and also suggests a more complex network between the two hormones.

1.4 Plant Root Growth

JA's effect on growth of a plant has been wildly demonstrated (see 1.2.3). In this thesis, the root was chosen to be the subject for observing the morphological changes caused by MeJA. It is hence important to understand the process of root growth in advance. In *Arabidopsis*, the primary root is composed of four cell layers: stele, endodermis, cortex and epidermis. A file of cells initiated from the apical meristem forms each layer. The quiescent centre (QC) is surrounded by the initial cells of each layer, and QC promotes continuous cell division of the initial cells (**Figure 1-6**) (Ueda *et al.*, 2005).

There are three developmental stages in root growth: cell division, cell elongation and cell differentiation. Cell division occurs in the meristem, bringing new cells which expand for a short time period. The length of cells in the meristem is mostly identical until these cells progress to the transition zone (TZ), where cell expansion is restricted to the lateral sides of the cells. The cells gradually lose the ability to divide, and begin to elongate rapidly. Cell elongation occurs along the TZ and the elongation-differentiation zone (EDZ). While elongation continues in EDZ, cells begin to differentiate and form the root hairs, until they reach their mature length (**Figure 1-7**) (Dolan and Davies, 2004; Dello Ioio *et al.*, 2008).

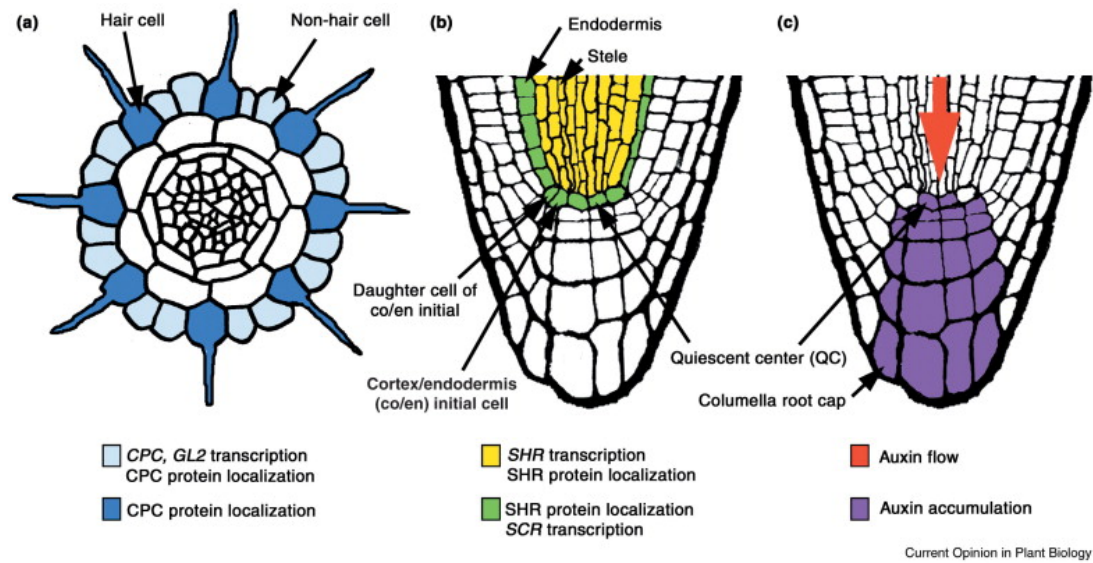


Figure 1-6 Root structure and the localisation of key factors in *Arabidopsis*. (a) The transverse and (b,c) longitudinal views of a root. (a,b) The key genes expressed in the specialised cell types are named and coloured. (c) The flow and accumulating of auxin. CPC: CAPRICE; GL2: GLABRA2; SHR: SHORT-ROOT; and SCR: SCARECROW. (Ueda *et al.*, 2005)

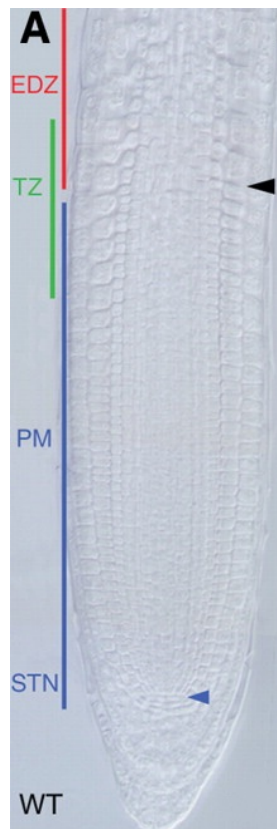


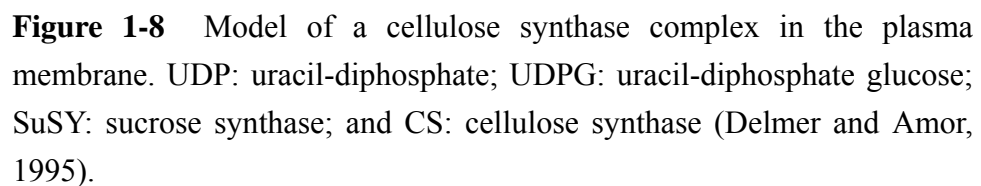
Figure 1-7 Five day old wild type (WT) *Arabidopsis* root. STN: stem cell niche; PM: proximal meristem; EDZ: elongation-differentiation zone; and TZ: transition zone. Blue arrow: the beginning of PM; and black arrow: the boundary between PM and EDZ (Dello Ioio *et al.*, 2008).

The process of cell elongation involves several elements. For instance, the change of arrangements of the cytoskeleton which controls the plasticity of the cell wall; the breaking of the hydrogen bonds between the cell wall components, loosening the wall; the water/fluid uptake which increases the vacuolar volume inside the cells, and the formation of new cell wall components which is required for the concomitant increase of the cell surface area during elongation (Dolan and Davies, 2004). In the following sub-sections, more details are given to illustrate the cytoskeleton function in the elongating cells.

1.4.1 Cytoskeleton

Cytoskeleton is the cellular skeleton inside the cytoplasm. In plants, microtubules are a component of the cytoskeleton and are composed of α - and β -tubulin heterodimers. These are in a constant and dynamic cycle of polymerisation, pausing, and depolymerisation (Sedbrook and Kaloriti, 2008). By visualising cellulose synthase and microtubules in living plant cells, it was confirmed that the cellulose synthase complexes are organised in the plasma membrane by a functional association with the cortical microtubules (Paredes *et al.*, 2006). During cell elongation, cellulose synthase complex, which is in the cell membrane and associated with microtubules in cytoplasm, moves along the microtubules and synthesises cellulose by converting sucrose into uracil-diphosphate glucose (UDPG), and the polymerisation of UDPG to form the cellulose microfibrils (**Figure 1-8**) (Delmer and Amor, 1995; Somerville, 2006).

The directed and controlled cell elongation is modulated by the placement of newly formed cellulose microfibrils, whose orientation is closely related to that of microtubules (Sedbrook and Kaloriti, 2008). Immunofluorescence showed that the orientation of both microfibrils and microtubules change according to the progress of development. In the root cap cells, the microtubules orientation is mainly transverse. In the end of the cell division zone and in rapid elongation zone, the microtubules orientation remain transverse, but with slight deviation from the transverse axis. In cells in the end of the elongation zone, the number of the microtubules declines, and their orientation becomes oblique. However, the orientation of microfibrils displays slight difference from that of microtubules in the



The cell wall is composed of polysaccharides that are made up of monosaccharides. Cellulose, which consists of several thousands of individual glucose molecules, is a polysaccharide and a structural component of the primary cell wall. The

intra-molecular hydrogen bonds form within the cellulose chain, while the inter-molecular hydrogen bonds form between the cellulose chains. In the actively elongating cells, the primary cell wall is mainly comprised of cellulose, hemicellulose and pectin. The hemicellulose polysaccharides are hydrogen bonded to the cellulose microfibrils, and the hydrogen bonds between components are temporarily broken to loosen the cell wall for further expansion (Delmer and Amor, 1995).

It was hypothesised that in the expanding cells, auxin activates the membrane-bound proton pumps, which release protons from the cytoplasm into the cell wall, and decrease pH of the wall solution. Subsequently, the enzymes responsible for wall loosening are activated due to lower pH, hence cells enlarge (Evans, 1974; Rayle and Cleland, 1977). Indeed, the IAA-induced proton secretion is observed in corn coleoptile segments and also intact corn roots, and the area of proton secretion coincides with the elongation zone (Evans and Vesper, 1980, Mulkey and Evans, 1981). In addition, IAA treatment decreases cytosolic pH in maize coleoptiles and parsley hypocotyls (Brummer *et al.*, 1985, Gehring *et al.*, 1990). Auxin accelerates cell elongation and acid secretion, possibly by activating the H⁺-ATPase pump in the cell membrane, and by stimulating synthesis of the H⁺-ATPase pump (Rober-Kleber *et al.*, 2003). Using antibody detection, Hager *et al.* showed that auxin increases the synthesis of a pool of H⁺-ATPase in the plasma membrane of maize coleoptile segments, supporting the acid growth hypothesis and the involvement of auxin (Hager *et al.*, 1991)

1.5 Aim and Objectives

Growth inhibition is a plant's most apparent morphological response induced by endogenous and exogenous JA. This phenomenon is seemingly part of the defence mechanism, however, little is known about the cellular basis of root growth inhibition by JAs and the possible crosstalk from other plant hormones. This study therefore investigates the cellular and intracellular responses to MeJA-mediated root growth inhibition, and examines the possible involvement of other plant hormones in this circumstance.

Chapter 2

General Methodology

2.1 Preparation of Material

2.1.1 LB Medium

Luria-Bertani (LB) media was prepared as below unless stated otherwise.

Composition:

Tryptone (Formedium™, Norwich, UK)	10 g
Yeast extract (Duchefa, Haarlem, Netherlands)	5 g
NaCl (Fisher Scientific, UK)	10 g

The above was dissolved in one litre of distilled water and pH was adjusted to 7.0 by adding diluted potassium hydroxide (KOH) solution. This solution was added to Erlenmeyer flasks containing agar (Formedium™, Norwich, UK) sufficient to give a final concentration of 1.4% (w/v). The medium was sterilised (121°C for 15 min), cooled to 50°C, supplemented with chemicals as appropriate, and poured into petri dishes.

2.1.2 SOB Medium

Super Optimal Broth (SOB) media was prepared as below.

Composition:

Tryptone (Formedium™, Norwich, UK)	20 g
Yeast extract (Duchefa, Haarlem, Netherlands)	5 g
NaCl (Fisher Scientific, UK)	0.5 g
1 M KCl	2.5 mL

The above was dissolved in one litre of distilled water and pH was adjusted to 7.0 by adding diluted KOH solution. The medium was sterilised (121°C for 15 min), and 10 mL of 1 M MgCl₂ was added before use.

2.1.3 Half MS Medium

Half Murashige & Skoog (MS) (1962) media was prepared as below.

Composition:

MS salt (Duchefa, Haarlem, Netherlands)	2.215 g
MES hydrate, minimum (SIGMA)	0.5 g
Sucrose	5 g

The above was dissolved in one litre of distilled water and pH was adjusted to 5.9 (or as stated otherwise) by adding diluted KOH solution. This solution was added to Erlenmeyer flasks containing plant agar (Duchefa) sufficient to give a final concentration of 0.7% (w/v). The medium was sterilised (121°C for 15 min), cooled to 50°C, supplemented with chemicals as appropriate, and poured into petri/square dishes.

2.1.4 Johnson's Medium

The medium was prepared as described by Johnson *et al.* (1956).

2.1.5 Medium for Testing pH of the Maize Seedlings

The medium was modified from Mulkey and Evans (1981).

Composition:

Ca(NO ₃) ₂	1.5 mM
MgSO ₄ , KH ₂ PO ₄ and KNO ₃	1 mM each
H ₃ BO ₃	20 µM
ZnCl ₂	3.8 µM
MoO ₃	0.18 µM
CuCl ₂	0.14 µM

500 mL medium was made with the above composition. The medium was then sterilised (121°C for 15 min), cooled and stored in 4 °C.

Before each experiment, 0.6 % rapid agarose (Life Technologies, INC. USA) and 0.71 mM bromocresol purple (MW: 540.2, Sigma) were added into 50 mL sterilised media. The colour of medium was adjusted to dark red/purple by adding diluted KOH solution.

The medium was then heated until the agarose dissolved, supplemented with chemicals as appropriate, and poured into petri dishes. The primary roots of 3 to 5-day-old maize seedlings were gently pressed into the media before it completely solidified. The embedded seedlings were left in a long-day (LD) growth chamber for regular observation (over 72 hrs).

2.1.6 Low-Water-Potential Medium

Low-water-potential medium was prepared as below.

Step 1:

Prepare half MS agar plates as described in 2.1.3. The solution was added into Erlenmeyer flasks containing plant agar (Duchefa) sufficient to give a final concentration of 1.5% (w/v).

The medium was sterilised (121°C for 15 min), cooled to 50°C, and volume of 20 mL medium was pipetted into each plate (100 mm x 20 mm depth).

Step 2:

Prepare half MS liquid medium as described in 2.1.3. To make low-water-potential overlay solution, appropriate amount of Polyethylene Glycol 8000 (PEG 8000, Sigma-Aldrich) was added and dissolved while the medium remained hot after sterilisation. The concentrations of PEG 8000 were 0%, 15%, 25%, 40% and 55% (w/v), respectively.

Thirty mL medium from step 2 was pipetted into a plate from step 1. The plates were allowed to equilibrate for one night. Before using the media, the liquid layer was poured off carefully as the agar layer may be floating on top of the solution. The low water potential media were always freshly made before each experiment.

2.2 Plant and Plant Growth Handling

2.2.1 Preparation of Chemicals

Methyl jasmonate (MeJA, MW: 224.3, Bedoukian Research, Danbury, USA)

MeJA was kept at room temperature and 200 µL (4590 mM) was diluted in ethanol to give 10 mL of a 100 mM solution. This stock solution was filter-sterilised and stored at -20°C. Plants were exposed to MeJA by two methods.

- 1). MeJA was added to the molten medium to give a concentration of 20 µM, unless otherwise stated, before the medium was poured directly into plates and allowed to set.
- 2). MeJA was also used to restore fertility to mature *aos* plants. Flower buds were sprayed with fine mist of 500 µM MeJA using a chromatomiser.

Indoleacetic acid (IAA, MW: 175.2, Sigma-Aldrich)

IAA powder was kept at -20°C. An amount (43.8 mg) was dissolved in a minimum volume of ethanol and then diluted in sterilised distilled water to give 50 ml of a 5 mM solution. This stock solution was filter-sterilised and stored at -20°C. Plants were

exposed to 0.1 μM IAA by adding the IAA stock into molten half MS medium before it was poured into petri/square dishes.

Gibberellic acid (GA, MW: 346.4, Sigma-Aldrich)

GA powder was kept in a desiccator at room temperature. An amount (17.32 mg) was dissolved in a minimum volume of ethanol and then diluted in sterilised distilled water to give 5 ml of a 10 mM solution. This stock solution was filter-sterilised and stored at -20°C . Plants were exposed to 2 μM GA by adding the GA stock into molten half MS medium before it was poured into petri/square dishes.

Absciscic acid (ABA, MW: 264.3, Duchefa)

ABA powder was kept at -20°C . An amount (66.1 mg) was dissolved in 5 mL ethanol to give a 50 mM solution. This stock solution was filter-sterilised and stored at -20°C . Plants were exposed to 0.5 μM ABA by adding the ABA stock into molten half MS medium before it was poured into petri/square dishes.

Paclobutrazol (PAC, MW: 293.79, Sigma-Aldrich)

PAC powder was kept at -20°C . An amount (250 mg in a glass bottle packed and seal by the supplier) was dissolved in 42.55 mL ethanol to give a 50 mM solution. This stock solution was filter-sterilised and stored at -20°C . Plants were exposed to 1 μM PAC by adding the PAC stock into molten half MS medium before it was poured into petri/square dishes.

Oryzalin (MW: 346.36, Supelco, USA)

Oryzalin was kept at room temperature. An amount (1 mg) was diluted in 5.774 mL DMSO to give 0.5 mM solution. This stock solution was filter-sterilised and stored at room temperature in dark. Plants were exposed to either 0.2 or 0.5 μM oryzalin by adding the oryzalin stock into molten half MS medium before it was poured into petri/square dishes.

2.2.2 Surface Sterilisation of *Arabidopsis* Seeds

Seed sterilisation was carried out in a laminar flow hood in 1.5 mL Eppendorf tubes. A volume (500 μ L) of each solution (100% ethanol, 20% (v/v) bleach and sterile water) was used in each step of the sterilisation process: the seeds were washed once in 100% ethanol for 2 min, sterilised in 20% bleach for 15 min, and rinsed for 5 min, three times, with sterilised distilled water. The sterilised seeds were then kept at 4°C for vernalisation for at least 1 day before they were sown individually on media plates.

2.2.3 Growth Condition for *Arabidopsis*

Media plates were placed in a SANYO (Illinois, USA) growth chamber of specific photoperiods at 22°C with light intensity of 70-90 μ mol/m²/sec in LD (16/8 hours light/dark) unless stated otherwise. For most of the experiments, plates were placed vertically to prevent the hypocotyls from reaching to the lids of the plates and the roots from penetrating deeply into the medium.

Soil-grown plants were raised in a LD growth room at 22-23°C. Trays that contained the pots were covered with plastic lids to ensure high humidity required for seed germination. Two small openings on the top of plastic lids were opened 1 to 2 days post germination to allow ventilation. *Arabidopsis* seedlings grew on for approximately 1-2 weeks before being individually transplanted into fresh soil.

2.2.4 Cross of *Arabidopsis* Transgenic Lines

Pollen recipients were immature flowers, from which the stigma had not emerged through the petals and the sepals. Adjacent flowers and leaves were removed to prevent confusion over which developing siliques were the products of hand-pollination.

Immature flowers of the pollen recipient were emasculated by hand with fine forceps. The petals of the pollen donors were open slightly but not yet perpendicular to the floral axis, with yellow pollen presented on the anthers. Pollen was carefully applied from the pollen donor to the recipient stigma. The crossed flowers were loosely covered

with cling film. The style began to elongate 2 to 3 days after the hand-pollination. The siliques developed and elongated in the same manner as in self-pollinated siliques.

2.2.5 List of *Arabidopsis* Lines and Mutants Used

Table 2-1 List of *Arabidopsis* lines and mutants used

Name	Background ecotype and description	Source
<i>aos</i>	Columbia-0 (Col-0). JA synthesis deficient mutant.	Lab stock
pL7/ <i>pCOII::uidA</i> <i>β-glucuronidase</i> (<i>GUS</i>)	Col-0. Inserting 5' upstream untranslated region of <i>COII</i> coding sequence in front of the reporter gene <i>uidA</i> coding region.	Lab stock (Harmston and Turner, unpublished data, 2003)
35S:: <i>JAI3</i> ::GFP	Col-0.	Chini <i>et al.</i> , 2007
<i>jai3</i>	Col-0. Mutated Jas domain of JAZ3	Lorenzo <i>et al.</i> , 2004; Chini <i>et al.</i> , 2007
<i>jin1-1</i>	Col-0. AtMYC2 defective mutant	Lorenzo <i>et al.</i> , 2004
<i>jut</i>	Col-0.	Lab stock
<i>CYCB1::GUS</i>	Col-0. The transgenic line with visible mitotic cells after GUS staining.	Ferreira <i>et al.</i> , 1994
<i>aux1-7</i>	Col-0. Mutation in a permease that helped to facilitate IAA transportation.	Pickett <i>et al.</i> , 1990
<i>abi</i>	Col-0. ABA insensitive mutant.	Lab stock
<i>coil-16</i>	Columbia glabrous (Col- <i>gl</i>). <i>Coil</i> mutant. Insensitive to MeJA.	Lab stock (Ellis and Turner, 2002)
35S:: <i>COII</i> ::HA-11 6/ <i>coil-16</i>	Col- <i>gl</i> . 35S:: <i>COII</i> ::HA transgenic line in the <i>coil-16</i> mutant background.	Lab stock (Devoto <i>et al.</i> , 2002)
35S:: <i>COII</i> ::HA-99 / <i>coil-16</i>	Col- <i>gl</i> . 35S:: <i>COII</i> ::HA transgenic line in the <i>coil-16</i> mutant background.	Lab stock (Devoto <i>et al.</i> , 2002)
P8.6 (<i>pCOII::COII</i> ::H A)	Col- <i>gl</i> . <i>pCOII::COII</i> ::HA transgenic line in the <i>coil-16</i> mutant background.	Lab stock (Devoto and Turner, 2002 unpublished)
GFP- <i>TUA6</i>	Col- <i>gl</i> . The transgenic line with visible α tubulin-GFP.	NASC (Loughborough, UK)

Name	Background ecotype and description	Source
GFP- <i>TUB6</i>	Col- <i>gl</i> . The transgenic line with visible β tubulin-GFP.	NASC (Loughborough, UK)
<i>della 4</i>	Landsberg (Ler). A quadruple-DELLA protein mutant lacking GAI, RGA, RGL1 and RGL2.	Achard <i>et al.</i> , 2006
<i>gal-3</i>	Ler. GA synthesis deficient mutant.	Sun and Kamiya, 1994
<i>gai</i>	Ler. A mutant with un-degradable GAI protein.	Ubeda-Tomás <i>et al.</i> , 2008
Ecotype (wild type)	Col-0, Col- <i>gl</i> , Ler and 2M.	Lab stock

2.2.6 Surface Sterilisation of Maize Seeds

Seed sterilisation was carried out in a laminar flow hood in 30 mL plastic container (Sterilin, UK). A volume (15 mL) of each solution (100% ethanol, 5% (v/v) bleach and sterile water) was used in each step of the sterilisation process: approximately 10 seeds were washed once in 100% ethanol for 2 min, sterilised in 5% bleach for 5 min, and rinsed for 5 min, three times, with sterilised distilled water. The sterilised seeds were then sown immediately on the sterilised water-soaked tissue in plastic container.

2.2.7 Growth Condition for Maize

Seeds were placed on moist tissue in plastic containers, which were sealed and were placed in a SANYO (Illinois, USA) growth chamber of specific photoperiods at 22°C with light intensity of 70-90 $\mu\text{mol}/\text{m}^2/\text{sec}$ in LD (16/8 hours light/dark) unless stated otherwise.

2.3 Molecular Biology Methods

2.3.1 Extraction of DNA from *E. coli*

All procedures were processed at room temperature unless otherwise stated. Plasmid DNA was obtained with QIAprep[®] spin miniprep and QIAGEN[®] midi kits for mini- and large-scale preparations, respectively.

An alternative method for mini-preparation of plasmid DNA was by using alkaline lysis procedure developed by Birnboim and Doly (1979). For 4 mL cell culture volumes, the cells were spun down at 13,000 rpm for 30 s. The supernatant was removed and the cell pellets were re-suspended with 0.3 ml of resuspension buffer (10 mM EDTA and 50 mM Tris HCl, pH 8.0). Two μ L of 100 μ g/mL RNase was added and the tubes were left at room temperature for 5 min after a thorough vortex. The cells were then treated with 0.3 mL of freshly made lysis solution (0.2 N NaOH, 1% (w/v) SDS), inverted gently 2-3 times, and left at room temperature for 3 min.

Potassium acetate (KAc) solution (0.3 mL, 3M KAc, pH5.5, which was adjusted by glacial acetic acid) was then added. The tubes were gently inverted 4-5 times and left on ice for 10 min. The lysates were centrifuged at 13,000 rpm for 10 min. The cleared supernatant was transferred into new tubes and 400 μ L of phenol/chloroform was added. The suspension was mixed and centrifuged at 13,000 rpm for 5 min. The upper aqueous phase was transferred into a new tube and mixed with 650 μ L isopropanol, and centrifuged at 13,000 rpm for 20 min to form the DNA pellets. The pellets were washed with 500 μ L of 75% (v/v) ethanol, and air-dried. The air-dried pellets were re-suspended in 40 μ L of sterile water.

2.3.2 Plasmid Construction

2.3.2.1 Digestion of DNA with Restriction Enzymes

The restriction enzyme digestions were carried out by following the instruction from the suppliers. Here is an example of *Kpn*I and *Sa*I double-digestions.

Restriction digest was set up in 1.5 mL microcentrifuge tubes on ice as below:

Plasmid DNA	1.0 µL (250 ng)
10× SuRE/ Cut Buffer L (Roche)	1.5 µL
<i>Kpn</i> I (Roche)	1.0 µL
10× BSA	1.5 µL
Sterilised distilled water	To make up to 15.0 µL

Restriction digest (15.0 µL) was added to each of three 1.5 mL microcentrifuge tubes. DNA was digested overnight at 37°C. The extent of the reaction was checked by electrophoresis of 5 µL of aliquots on 1% agarose gel.

Next, 40 µL digested linear DNA were eluted from the restriction digest using QIAquick[®] gel extraction kits supplied by QIAGEN[®] according to the manufacture's instruction. This process gave 30 µL purified linear DNA product for the next step.

The second restriction digest was set up in 1.5 mL microcentrifuge tubes on ice as below:

Purified linear DNA	10.0 µL
10× SuRE/ Cut Buffer H (Roche)	1.5 µL
<i>Sa</i> II (Roche)	1.0 µL
10× BSA	1.5 µL
Sterilised distilled water	To make up to 15.0 µL

Restriction digest (15.0 µL) was added to each of three 1.5 mL microcentrifuge tubes. DNA was digested overnight at 37°C. The total reaction mixture was then combined and run by electrophoresis in three lanes on 1% agarose gel before eluting the target DNA bands from the gel.

2.3.2.2 Extraction of DNA from Agarose Gel

After electrophoresis, the agarose gel was checked under UV light and the target DNA bands were cut with a sharp, clean razor. The extra gel which did not contain DNA was removed from the cut bands.

DNA product was eluted from the cut agarose gel using QIAquick[®] gel elution kits supplied by QIAGEN[®] according to the manufacture's instruction.

2.3.2.3 Ligation Reaction

Ligation reaction was set up in 1.5 mL microcentrifuge tubes on ice as below:

pBlueScript vector digested with <i>KpnI/SalI</i>	0.5 µL
Insert digested with <i>KpnI/SalI</i>	12.0 µL
10× ligation buffer (Roche)	1.5 µL
T4 DNA ligase (Roche)	1.0 µL
Sterilised distilled water	To make up to 15.0 µL

Ligation reaction (15.0 µL) was placed in 1.5 mL microcentrifuge tube and incubated at 15°C for one night. The ligation product was then purified using MICROCON[®] Centrifugal Filter Devices (Microcon YM-100) from Amicon[®] Bioseparations before next step of cloning.

2.3.2.4 Transformation of *E. coli* with Plasmid DNA

Competent *E. coli* strain DH10B was prepared using a protocol from GIBCO BRL, with refinements. SOB medium (100 mL) in a 250 mL flask was inoculated with 0.1 mL of an overnight culture of bacteria and incubated for about 4 hrs at 37°C with vigorous shaking (250 rpm). When the culture reached OD₅₅₀ 0.8, it was chilled on ice for 30 min. the cells were harvested at 2600×g for 10 min, at 4°C, and then washed twice with 100 mL of ice-cold 10% (v/v) glycerol. The cells were resuspended in a final volume of 0.5 mL with ice-cold 10% (v/v) glycerol and snap-frozen in aliquots of 45 µL at -80°C for further use as a stock of competent cells.

Transformation was carried out by electroporation using a GIBCO BRL electroporator (Cell-porator and Voltage Booster) in a pre-chilled 0.15 cm cuvette under conditions suggested by the manufacturer (Capacitance: 330 µF, Resistance: 4 kΩ, Voltage: 410 V, Impedance: low Ω, Charge rate: fast). For 20 µL competent cells, 1 µL of purified ligation mix from 2.3.2.3 was added. The electroporated cells were

immediately incubated in 0.8 mL of LB medium at 37°C for one hour on a shaker, and then plated out onto solid LB containing IPTG (5 µL from 200 mg/mL stock) and X-gal (50 µL from 20 mg/mL stock) for blue/white colony selection. LB plates were kept at 37°C for one night. Positive (white) colonies were then checked by PCR (2.3.3.1) or restriction enzyme digestion (2.3.2.1).

2.3.3 Polymerase Chain Reaction (PCR)

2.3.3.1 General PCR Protocols

DNA amplification was carried out in a Peltier Thermal Cycler (DNA Engine, DYAD™, MJ Research, USA). PCR products were run in 1% (w/v) TAE agarose gel containing 0.001% of 10mg/mL ethidium bromide. DNA was visualised under UV light using a UVP-Trans illuminator after electrophoresis.

2.3.3.2 Primer Design

Primers were generally designed to be 21-24 nucleotides long with at least 50% GC content. Recombination site-adapted primers for Gateway cloning were up to 50 nucleotides long. The primers were from Sigma-Aldrich Company Ltd. (Dorset, UK) and were dissolved in distilled water to produce 100 µM stocks. These stock solutions were stored at -20°C and were diluted to a working concentration of 5 µM.

2.3.3.3 DNA Sequencing

Sequencing solution was prepared as below on ice:

50~100 ng DNA (plasmid)	1.0-6.0 µL
Sequencing buffer (Genetix, Hampshire, UK)	1.0 µL
5 µM primer (Sigma-Aldrich, Dorset, UK)	1.0 µL
BigDye 3.1 (Genetix)	1.0 µL
halfBD 3.1 (Genetix)	1.0 µL
Sterilised distilled water	Make up to 10 µL

A Peltier Thermal Cycler (DNA Engine, DYADTM, MJ Research, USA) was used for PCR reactions. The amplification condition was 96°C for 30 sec, 46°C for 15 sec and 60°C for 4 min. The cycle was repeated 28 times and preceded by 1 min at 96°C.

The PCR products were sent off to the John Innes Sequencing Centre: Genome Laboratory (Norwich, UK) to be processed. The sequencing data were then returned and analysed using the Lasergene 6 programme (DNASTAR, Madison, USA) and online tool (NCBI BLAST: <http://www.ncbi.nlm.nih.gov/BLAST/>) to confirm that the amplified DNA matched the published DNA sequence.

2.3.4 Gateway System

The protocol of “Gateway[®] Technology with ClonaseTM II” was carried out according to the manufacturer’s instruction (Version A, 24 June 2004, InvitrogenTM). The Gateway[®] Technology is to efficiently transfer DNA fragments between plasmids using the “Gateway att” recombination sites, and two enzyme mixes, LR Clonase and BP Clonase. For cloning detail and primer design, refer to 2.3.2 and 2.3.3.

2.3.5 Electrophoresis of DNA

2.3.5.1 Electrophoresis

TAE buffer (Sambrook, 1989)

One liter of 50× TAE stock solution contained 252 g Tris-acetate, 57.1 mL glacial acetic acid and 18.6 g EDTA. The pH of the stock solution was adjusted to pH8.0. This stock solution was diluted with water to make 1× TAE buffer, which was used for running and making agarose gels.

Loading buffer (Sambrook, 1989)

An aqueous solution of glycerol 30% (v/v) was sterilised (121°C for 15 min) and cooled to room temperature. Bromophenol blue and xylene cyanol were added to give a concentration of 0.25% (v/v) each. The loading buffer was then filter-sterilised and stored at room temperature.

1 Kb plus DNA ladder (GibcoBRL[®])

The DNA ladder (1µg/µL) was kept in -20°C before use and applied according to manufacturer's instructions.

Agarose (1%) was suspended in 1× TAE buffer and heated in a microwave until it melted. This solution was cooled to 50°C and supplemented with 0.001% (v/v) ethidium bromide (Sigma, Dorset, UK). The solution was then poured into the gel mould, and the appropriate comb was placed. The solidified gel was placed in a gel tank containing 1× TAE buffer. The DNA samples were supplemented with 2 µL loading buffer prepared as below, loaded on the gel with a ladder marker, and electrophoresed at 50-80 V. The gel images were taken under UV light (BIO-RED, Hercules, USA).

2.3.5.2 DNA Quantification

DNA samples and Lambda DNA (50 ng and 500 ng, run in two lanes) were run on the same 1% agarose gel. DNA was quantified by comparing the intensity of ethidium bromide-stained bands of samples and Lambda DNA.

2.3.6 Histochemical Assay of GUS (β-Glucuronidase)

β-glucuronidase (GUS) a widely used reporter gene encoded by *gusA*. X-Gluc (5-bromo-4-chloro-3-indolyl-beta-D- glucuronic acid, cyclohexylammonium salt) is a substrate for GUS. GUS cleaves X-Gluc to produce colourless glucuronic acid and an intense blue precipitate of chloro-bromoindigo (Jefferson *et al.*, 1987).

Plant tissues were submerged in GUS solution and incubated in the dark at room temperature. The incubation time was from 1 hr to overnight and depended on the intensity of the blue colour that showed up after starting the staining. Cells containing the β-glucuronidase enzyme turned blue (Jefferson *et al.*, 1987). In older plants, the X-Gluc solution was vacuum infiltrated into the tissue (5 min, repeated three times) and the samples were then incubated overnight at 37°C. To remove the chlorophyll from tissue, the stained plant tissues were cleared with 3:1 methanol/ acetic acid solution for a minimum of 2 hr at room temperature. The samples were then to be fixed in 70% (v/v) ethanol and kept in 4°C before microscope observation.

The histochemical detection of GUS activity in plant tissues was based on Jefferson (1987). The staining solution was prepared as follows:

	Stock	Working concentration
NaPO ₄ Buffer	1 M	0.1 M
EDTA (pH 8.0)	0.5 M	10 mM
Potassium ferricyanide	100 mM	0.5 mM
Potassium ferrocyanide	100 mM	0.5 mM
Triton X-100	10%	0.5%
Methanol	100%	20%
X-Gluc	100 mg/mL	0.5 mg/mL

For X-Gluc stock solution, 1 g X-Gluc powder (Melford laboratories) was dissolved in 10 mL N, N Dimethylformamide and stored at -80°C. The phosphate buffer and EDTA were autoclaved before use. Potassium ferricyanide, Potassium ferrocyanide, Triton X-100 and X-Gluc were all filter-sterilised before use.

2.3.7 Small Scale Extraction of Plant DNA

The small scale extraction method is modified from the protocol by Dellaporta *et al.* (1983) and was primarily used for PCR amplification. About 2-3 leaves, depending on size, were ground with liquid nitrogen in 1.5 mL Eppendorf tube using a mini pestle. The leaf tissues were then homogenised in 700 µL extraction buffer (100 mM Tris-HCl pH 8.0, 50 mM EDTA pH 8.0, 500 mM NaCl, 10 mM β-mercaptoethanol and 2% SDS) and placed on ice before incubating at 65°C for 12 min with occasional inversions. Afterwards, 200 µL, 5M KAc were added to each tube, which was then put on ice for 10 min.

Plant debris was spun down at 13,000 rpm for 8 min. DNA in the aqueous phase was then mixed with an equal volumes of phenol/ chloroform (1:1) and spun at 13,000 rpm for 8 min. DNA in the aqueous phase was precipitated with 60 µL of 3 M sodium acetate (pH 5.2) and 500 µL of isopropanol. After incubating the samples for 30 min on -20°C, the DNA was pelleted by centrifugation at 13,000 rpm for 15 min, washed with 500 µL, 75% ethanol, allowed to dry and dissolved in 50 µL TE buffer (10 mM Tris and 1 mM EDTA, pH 8.0).

2.3.8 Western Blotting

2.3.8.1 Preparation of Plant Protein Extract

Arabidopsis total protein was extracted as described below. About 2-3 leaves, weighing approximately 100-200 mg, were ground in liquid nitrogen in 1.5 mL Eppendorf tube using a mini pestle. The leaf tissue was then homogenised in 300 μ L extraction buffer (25 mM Tris (pH7.5), 100 mM NaCl, 1 mM EDTA, 10% glycerol and 0.15% NP40. 5 mM DTT, 1 mM NaF, 10 mM β -glycol phosphate, 1 mM orthovanadate, 1 mM PEFA and 1 tablet of Sigma Cocktail was added before use) and placed on ice with occasional inversions. Plant debris was then spun down at 13,000 rpm for 15 min, at 4°C. Proteins in the aqueous phase were then collected into a new 1.5 ml Eppendorf tube.

Total protein was then quantified with the Coomassie Blue reagent from Bio-Rad according to manufacturer's instruction. After quantification, 1 volume of the total proteins was mixed with 0.25 volume of sample buffer (60 mM Tris-HCl (pH6.8), 2% SDS, 10 % glycerol, 0.025% bromophenol blue and 5% β -mercaptoethanol) and boiled for 5 min before loading to SDS polyacrylamide gel.

2.3.8.2 Preparation of SDS Polyacrylamide Gel

Sodium dodecyl sulfate (SDS) polyacrylamide gel was prepared as stated below:

15% resolving gel:

Sterilised distilled water	1.1 mL
30% Acrylamide/Bis solution (Bio-Red Laboratories)	2.5 mL
1.5 M Tris (pH 8.8)	1.3 mL
10% SDS	50 μ L
TEMED (Bio-Red Laboratories)	2 μ L
10% APS	50 μ L

5% stacking gel:

Sterilised distilled water	1.4 mL
30% Acrylamide/Bis solution (Bio-Red Laboratories)	0.33 mL
1 M Tris (pH 6.8)	0.25 mL
10% SDS	20 µL
TEMED (Bio-Red Laboratories)	2 µL
10% APS	20 µL

2.3.8.3 Running the SDS Polyacrylamide Gel

Plant protein samples and Kaleidoscope Prestained Standards (Bio-Red Laboratories) were loaded and run into the polyacrylamide gel with constant voltage (80-110 V) for approximately 2 hrs. The polyacrylamide gel could then either be stained with gel staining buffer or processed to Western Blotting.

Gel staining buffer was prepared as followed:

Coomassie blue	0.75 g
Methanol	150 mL
Acetic acid	30 mL
Distilled water	120 mL

After coomassie blue staining, SDS PAGE was destained with destaining buffer (10% methanol and 10% acetic acid) until the blue separated protein bands were clear enough for analysis.

2.3.8.4 Western Blotting

The separated plant proteins on the polyacrylamide gel were blotted to a nitrocellulose membrane (Protran, Schleicher & Schuell) in a Bio-Rad's Transblot with constant current (400 mA) according to manufacturers' instruction. After blotting, the membrane was washed with PBST (10 mM sodium phosphate, 150 mM NaCl, pH 7.3, 0.05% Tween-20) before incubating with a peroxidase-coupled monoclonal anti-HA antibody

(Boehringer Mannheim) at 4°C for one night. The epitope-tagged proteins were then detected using an enhanced chemiluminescence system (ECL, Amersham) as described (Ausubel *et al.*, 1999)

2.3.9 pH Measurement of the Suspended Arabidopsis Roots

All procedures were processed at room temperature unless otherwise stated. Eight to 10-day-old *Arabidopsis* seedlings were decapitated (removal of the shoot apex) and transferred to 48-multi-well plate immediately. More than 50 decapitated seedlings were placed in one well containing 200 µL half MS medium. This medium was specially prepared following section 2.1.3 without adding MES hydrate. The medium pH was adjusted to pH6.0.

The medium and seedling mixture was aerated by using an aquarium pump. A Hanna Instruments semi-micro electrode (model HI-1330B) connected to a Hanna Instruments pH meter (model pH210) was used to measure the pH of the medium. The decapitated seedlings were incubated for no more than 60 min to avoid the fluid evaporation from affecting the pH value.

2.4 Immunolocalisation of HA-Tagged COI1 Protein

2.4.1 Whole-Mount Immunolocalisation

This technique was undertaken as described by Friml *et al.* (2003), or according to manufacturers' instructions. This protocol was then improved by Dr. Ranjan Swarup as stated below.

Whole-mount immunolocalisation by Dr. Ranjan Swarup

Three-day-old plant seedlings were collected and placed in wells of a multiwell plate containing 500 µL fixation solution (5% paraformaldehyde (PFA) in microtubule-stabilising buffer (MTSB: 50 mM Pipes, 5 mM EGTA, 5 mM MgSO₄; adjusted to pH 6.9 - 7.0 with KOH)). The multiwell plate was then placed under vacuum for 1 hr at room temperature. Seedlings were then washed for 4× 10 min in phosphate buffered saline (PBS: dissolving 8 g NaCl, 0.2 g KCl, 1.44 g Na₂HPO₄ and 0.24 g

KH₂PO₄ in 1 litre distilled water), and 2× 10 min in distilled water. A Driselase (Driselase[®] from *Basidiomycetes sp.*, Sigma) solution was prepared as 0.5% -1.0% (w/v) in MTSB. The seedlings were immersed in driselase solution for 1 hr at room temperature and washed for 6× 10 min in PBS.

Next, the seedlings were permeabilised with permeabilisation solution (20% DMSO and 2% NP-40 in PBS) for 1 hr at room temperature and washed for 6× 10 min in PBS. The permeabilised seedlings were transferred to blocking solution (2% Bovine serum albumin in PBS) for 1 hr at 37°C and then incubated with primary antibody for 4-5 hr at 37°C. The seedlings were then washed again for 6× 10 min in PBS and then incubated with the secondary antibody for 4-5 hr at 37°C.

2.4.2 Antibody Used in Whole-Mount Immunolocalisation

Two methods were used to detect the hemagglutinin (HA)-tagged proteins.

A. Indirect immunolocalisation:

Primary antibody

A peroxidase-coupled monoclonal anti-hemagglutinin (anti-HA) antibody (Boehringer Mannheim) was used. The concentration of antibody was determined according to manufacturers' instructions.

Secondary antibody

An Oregon Green[®] 488 goat anti-rat IgG (H+L) antibody (Invitrogen) was used for observation of the target proteins in green fluorescence. Alternatively, an Alexa Fluor[®] 568 goat anti-mouse IgG (H+L) antibody (Invitrogen) was used for observation of the target proteins in red fluorescence. The concentration of antibody was determined according to manufacturers' instructions.

B. Single-step immunolocalisation:

A Slowfade-antifade antibody (anti-HA, mouse IgG monoclonal Alexa Fluor[®] 488 conjugate, Invitrogen) was used with *Slowfade*[®] Antifade Kit and then no more secondary antibody was needed. This method produced fluorescent images with less background compared to the indirect immunolocalisation.

2.5 Microscopy

2.5.1 Bright Field Microscopy

Two Zeiss microscopes were used for bright field microscopy. The CCD Upright (Axioplan 2 Imaging, HBO 100) was equipped with AxioCam HRm camera and took images of *Arabidopsis* roots for cell length measurement and detection of GUS activity. The CCD Inverted I (Axiovert 200M, HAL 100) was equipped with AxioCam HRm camera and took images for *Arabidopsis* root growth as extended observations under physiologically-controlled conditions. *AxioVision* Viewer (<http://www.zeiss.de/viewer>) was used as the software to take images and to view and analyse the photomicrographs taken and saved in zvi format.

One low power Nikon SMZ-U microscope was also used for observation of GUS staining in bright field. This microscope was fitted with a Nikon Coolpix 4500 digital camera, which was used to take pictures of *Arabidopsis* sample in JPEG format.

2.5.2 Fluorescence Microscopy

A Zeiss microscope in Biomedical Research Centre (BMRC) was used for fluorescence microscopy. The Zeiss microscope (Axioplan 2 Imaging, HAL 100) was equipped with AxioCam MRm camera and took images of green fluorescent protein (GFP) transgenic lines and the HA-tagged COI1 protein in whole mount immunolocalisation experiments. *AxioVision* Viewer (<http://www.zeiss.de/viewer>) was used as the software to take images and to view and analyse the photomicrographs taken and saved in zvi format.

2.5.3 Confocal Microscopy

A Leica TCS SP2 UV system and a Zeiss LSM510 META were used as laser-scanning confocal microscopes. Both microscopes were equipped with Argon and HeNe lasers, giving lines at 458, 476, 488, 514, 543 and 633 nm, which allow excitation of visible-light fluorophores (typically cyan, green, yellow, orange and red).

For the Leica TCS SP2 UV system, LCS Lite (<http://www.leica->

microsystems.com/website/lms.nsf) was used as the software to take and view the images saved in TIFF format. Additionally, Viocity LE version 5.1 (<http://www.improvision.com/downloads/>) was used as the software to view and analyse the TIFF images taken and saved with LCS Lite software.

For Zeiss LSM510 META confocal microscope, LSM 510 (<http://www.zeiss.com>) was used as the software to take and view the images saved in lsm format. Additionally, Andor iQ 1.9.1 (http://www.andor.com/pdfs/downloads/iq_release.pdf) was used as the software to analyse the lsm images taken and saved with LSM 510 software.

2.6 Use of Online Database

2.6.1 Genevestigator (<https://www.genevestigator.ethz.ch>)

To investigate the expression and regulation of genes, Genevestigator offers access to interrogate the microarray database of thousands of gene expression studies in *Arabidopsis*, which make it possible to identify genes with expression similarity to that of the interested jasmonate-regulated genes, and thereby identify new targets.

By selecting the “start analysis tool” in the main page and login to Genevestigator version 3, the expression of a gene of interest can be visualised in different tissues, at multiple developmental stages, or in response to large sets of stimuli, diseases, drug treatments, or genetic modifications.

2.6.2 The Arabidopsis Information Resource (<http://www.arabidopsis.org/>)

The Arabidopsis Information Resource (TAIR) is a database of genetic and molecular biology data for the model plant *Arabidopsis thaliana*. Complete genome sequence of *Arabidopsis* can be accessed by searching genes of interest in the main page. The information of target gene: *CORONATINE INSENSITIVE 1 (COI1)* at locus At2g39940 can be found in <http://www.arabidopsis.org/servlets/TairObject?id=34748&type=locus>, under “Sequence Viewer” in the “Map Links” section. In the page “Sequence Viewer”, the target gene, At2g39940, is highlighted in yellow. By clicking Sequence ruler to open the 10 kb sequence window, the nucleotide view will provide the exact sequence

in detail, including promoter, exon, intron, and 5' untranslated region (5' UTR).

Many analysis tools can also be found by clicking “Tools” in the main page, including BLAST (<http://www.arabidopsis.org/Blast/>) and WU-BLAST2 (<http://www.arabidopsis.org/wublast/index2.jsp>).

2.6.3 Motif Scan (<http://hits.isb-sib.ch/cgi-bin/PFSCAN>)

To analyse the nucleotide sequence of the native promoter of *COII*, Motif Scan was used to scan for the known motifs in that sequence. To analyse the amino acid sequence of a protein, Motif Scan was used to produce a list of motif matches, match details and the references.

2.6.4 NEBcutter V2.0 (<http://tools.neb.com/NEBcutter2/index.php>)

To analyse the existing restriction enzyme sites in one construct, NEBcutter, provided by New England BioLabs, was used. A DNA sequence was entered in the main page and submitted. The results page gave the linear DNA map with a list of restriction enzyme sites, and the cleavage type of these enzymes.

2.6.5 Clustal W2 (<http://www.ebi.ac.uk/Tools/msa/clustalw2/>)

This tool was especially useful for finding point mutations in DNA sequences. To align DNA sequence to each other and to a database, Clustal W2, a multiple sequencing alignment program for DNA or proteins, was used.

Chapter 3

Localisation of Components of the JA Signal Pathway

3.1 Introduction

COI1 was originally identified in a screen for coronatine-resistant mutants of *Arabidopsis* (Feys *et al.*, 1994). In subsequent studies, *COI1* was found to be an F-box protein and also a protein component in SCF^{COI1} complex, which plays an important role in the process of perception and response to JA (Xie *et al.*, 1998, Zheng *et al.*, 2002). The targets of the SCF^{COI1} complex are JAZ proteins. As the repressors of the MYC2 TF, JAZ proteins are destroyed in response to a JA signal in a process that requires COI1. This process is believed to require COI1-dependent ubiquitination of the JAZ proteins, and their degradation in the 26S proteasome (Thines *et al.*, 2007, Chini *et al.*, 2007). Studies using GFP fusions to JAZ1, JAZ6 and JAI3/JAZ3 revealed that they are localised in the nucleus, and that these fusion proteins disappear in a COI1-dependent response to JA.

The expression pattern of the *COI1* gene, and the subcellular localisation of the COI1 protein are, however, not known. Considering the fact that COI1 physically interacts with the ZIM domain of JAI3/JAZ3 (Chini *et al.*, 2007), co-localisation of COI1 and JAZ will give further evidence of where the JA perception happens.

In this chapter, I have used *pCOI1::uidA β-glucuronidase* to report the expression of the COI1 transcript. I have also used *35S::COI1::HA/coil-16* and *pCOI1::COI1::HA/coil-16* to investigate regulation of expression of COI1 and

localisation of the COI1 protein. I then constructed a transgenic line that expresses both JAI3::GFP and COI1::HA, and used this to investigate the co-localisation of these proteins.

3.2 Method

3.2.1 Selection of A Line Homozygous for 35S::COI1::HA and the *coil*-16 Mutation

F2 seeds from a cross of a 35S::COI1::HA transgenic line to the *coil*-16 mutant were provided (Harmston and Turner, unpublished data, 2003). Seeds were surface sterilised (2.2.2), and sown in half MS medium (2.1.3) containing 25 µg/mL Kanamycin for 35S::COI1::HA selection. After incubating in standard condition (2.2.3) for 10 days, Kanamycin-resistant seedlings were transferred to soil and grew for another 20 days. Leaf samples were collected, plant DNA was extracted (2.3.7), and PCR-based detection of the *coil*-16 mutation was performed.

The *coil*-16 mutant locus contains a point mutation, which causes Leu245 to become phenylalanine in the sixth leucine-rich repeat (Ellis and Turner, 2002). This results from a C to T transition. To identify the homozygous *coil*-16 plants from the F2 generation of 35S::COI1::HA crossed to *coil*-16, 3 primers, 2-COI1, 3-COI1 and 4-COI1 (Table 3-1), were designed to distinguish WT from the *coil*-16 sequence (F. Robson, unpublished data, 2006). Table 3-2 represents the rationale of the design. DNA sample from each F2 plant was amplified separately with two combinations of the primer pairs, 2-COI1 + 3-COI1 and 2-COI1 + 4-COI1. The 2-COI1 + 3-COI1 pair yielded a product of about 350 bps in plants with *coil*-16 mutant allele, while the 2-COI1 + 4-COI1 pair yielded a product of about 350 bps in plants with COI1 allele.

As predicted, one band (PCR product) was obtained with each of primer pairs 2-COI1 + 3-COI1 and 2-COI1 + 4-COI1 from heterozygous lines. One band was obtained with the 2-COI1 + 3-COI1 pair but not 2-COI1 + 4-COI1 pair from homozygous *coil*-16 lines. Finally, one band was obtained with the 2-COI1 + 4-COI1 pair but not 2-COI1 + 3-COI1 pair from WT plants.

Table 3-1 The sequences of primers.

Name	Sequence
2-COI1	5'-GAA CAC AAT TTA GTA CTA AGG ACG CAT TCC CAA -3'
3-COI1	5'-AAC TAG TTG GGT TCT TTA AGG CTG CAG CTA ACT -3'
4-COI1	5'- AAC TAG TTG GGT TCT TTA AGG CTG CAG CTA TTC -3'

Table 3-2 The rationale of the PCR-based detection of the *COI1* and *coil-16* alleles.

	3-COI1 (for the <i>coil-16</i> allele)	4-COI1 (for the <i>COI1</i> allele)
<i>COI1</i> sequence	GAT TAG xx CTA ACT	GAT TAG x CTA TTC
<i>coil-16</i> sequence	GAT TAA x CTA ACT	GAT TAA x x CTA TTC

Briefly, the PCR solution was prepared as below on ice:

10× NH ₄ reaction buffer (Bioline, London, UK)	2.0 µL
2 mM dNTP (Bioline, London, UK)	2.0 µL
50 mM MgCl ₂ (Bioline, London, UK)	0.6 µL
5 µM forward primer (Sigma-Genosys)	2.0 µL
5 µM reverse primer (Sigma-Genosys)	2.0 µL
BioTaq TM DNA polymerase (Bioline, London, UK)	0.3 µL
Genomic DNA	1.0 µL
Sterilised distilled water	To make up to 20 µL

General PCR protocols were given in 2.3.3.1. The specific PCR conditions were as follows: initial denaturation at 94°C for 2 min; amplification for 30 cycles of 94°C for 30 sec, 62°C for 1 min and 72°C for 1 min, and final extension at 72°C for 5 min.

3.3 Results

3.3.1 Localisation of *pCOII:: uidA β -glucuronidase*

An *uidA GUS* reporter gene was fused to a 2 kb fragment named *pCOII*, which was isolated from the 5' upstream untranslated region of the *COII* gene. The resulting construct, *pCOII::GUS*, was used to transform *Arabidopsis thaliana* ecotype Col-0 (Harmston and Turner, unpublished data, 2003).

Seeds homozygous for *pCOII::GUS* were surface sterilized (2.2.2) and germinated on half MS or on half MS containing 20 μ M MeJA (2.1.3 and 2.2.1). Six to 8 days old seedlings were collected and assayed for GUS activity (2.3.6).

In untreated seedlings, GUS protein accumulated extensively in the root tip (Figure 3-1, A). However, when seeds were grown in the half MS containing 20 μ M MeJA, the blue precipitate was observed in both the root tip and the stele (Figure 3-1, B. Stele is marked with arrow). This suggested that MeJA enhanced the transcription of the GUS product in the vascular tissue in the root. Nevertheless, it was also possible that the GUS staining was more intensive at the stunted roots. This echoes to the finding of root growth inhibition caused by MeJA treatment (Staswick *et al.*, 1992). The root hair zone was closer to the root tip of the MeJA-treated root (Figure 3-1, B) than the control (Figure 3-1, A), which was consistent with stunted growth following the MeJA treatment.

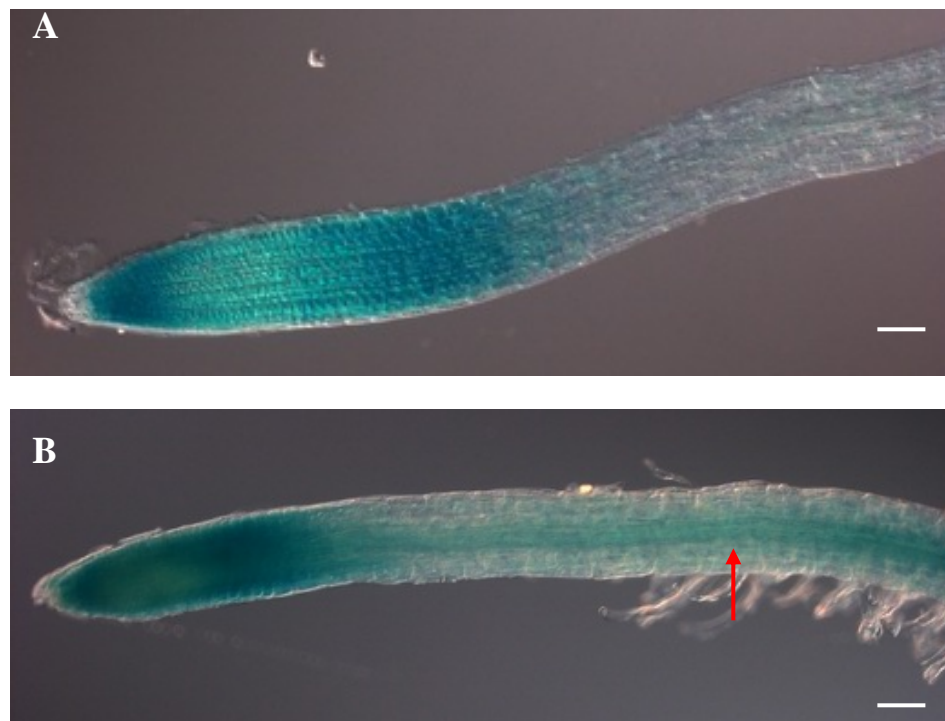


Figure 3-1 GUS staining of *pCOII::GUS*. (A) The root tip of 6 day old *pCOII::GUS* seedling grown in half MS medium. (B) The root tip of 6 day old *pCOII::GUS* seedling grown in half MS medium containing 20 μ M MeJA. Arrow indicates the stele. Scale bar 50 μ m.

Seedlings were also allowed to grow in half MS for more than 3 weeks until they developed rosette leaves and reproductive tissues. This time, the whole plants were assayed for GUS activity (Figure 3-2). In mature tissues, GUS product accumulated in both vegetative and reproductive organs, including the rosette leaves, cauline leaves and flowers (Figure 3-2, A). Observation of the floral tissue revealed that the GUS product only appeared in sepals and stamen filaments (arrows), but not carpel, pollen, petals and the pedicel (Figure 3-2, B).

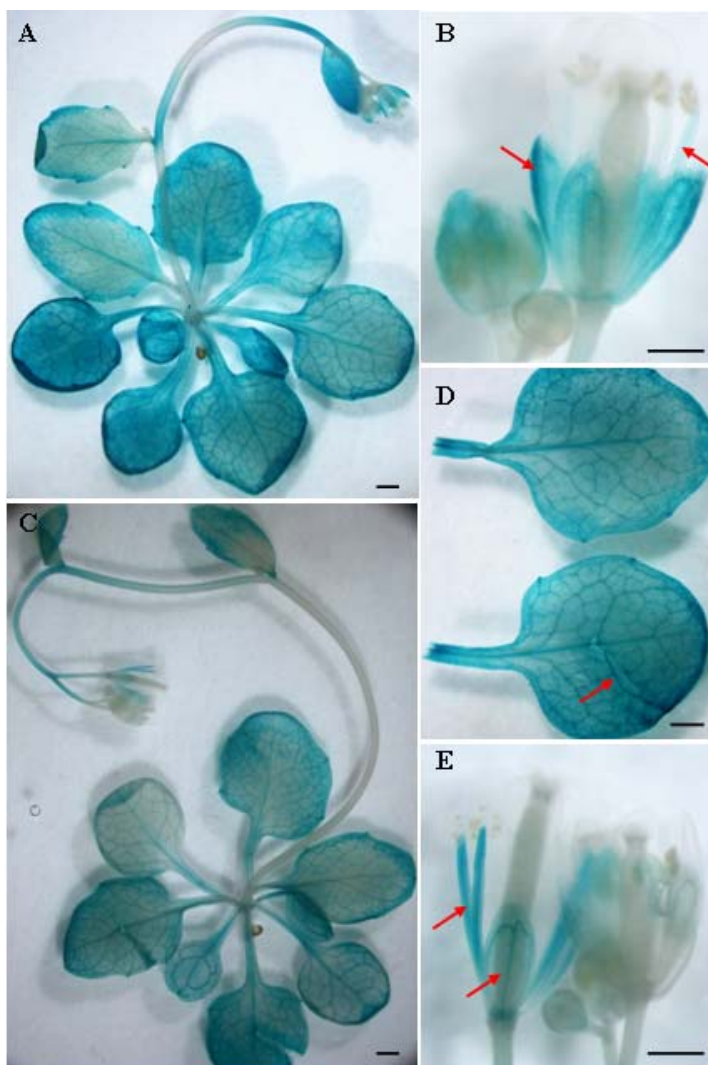


Figure 3-2 Histochemical GUS detection of *pCOII::GUS*. (A) Four week old *pCOII::GUS* plant. (B) Magnification shot of the flower buds from (A). Arrows indicate sepal (left) and stamen filament (right). (C) Four week old *pCOII::GUS* plant. Two rosette leaves were wounded 24 hrs before collection. (D) Unwounded and wounded leaves from (C). Arrow indicates the wound area. (E) Magnification shot of the flower buds from (C). Arrows indicate stamen filament (left) and sepal (right). Scale bar 1 mm.

The effect of wounding on *COI1* transcription pattern was examined. Wounding was expected to induce biosynthesis of the endogenous JA and activate JA signaling (Zhang and Turner, 2008). Rosette leaves were wounded with forceps, and the whole plants were harvested 24 hrs later for GUS activity assay. The intensity and localisation of GUS product in the entire plant was not noticeably altered by wounding (Figure 3-2 A and C), and the wounded leaves had no difference of GUS production in the tissue around the wounded area (Figure 3-2 D, arrow). However, closer examination of floral tissue indicated that the GUS product in the wounded plant accumulated to higher level in stamen filaments but less in sepals (Figure 3-2 E, arrows).

3.3.2 *35S::COI1::HA/coi1-16* is as Sensitive as *Col-gl* to MeJA Treatment

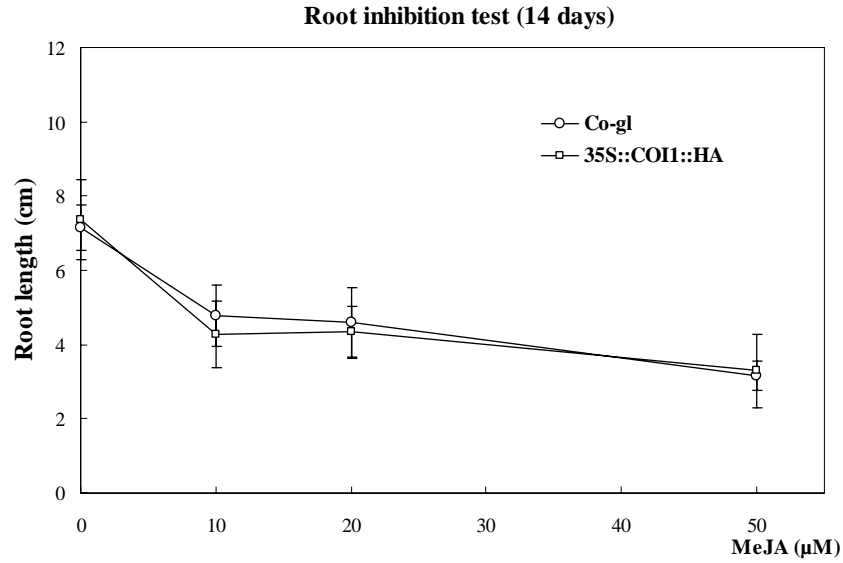
The sensitivity of *35S::COI1::HA-99/coi1-16* roots to MeJA treatment was examined, because it was suggested that *35S::COI1::HA/coi1-16* transgenic seedlings were slightly more sensitive to MeJA than *Col-gl* seedlings (Devoto and Turner, unpublished data, 2005). Considering this line would be used for protein expression examination and immunolocalisation of *COI1::HA* under MeJA treatment, it was important to confirm this claim.

3.3.2.1 Effect of MeJA Treatment on Root Length of *35S::COI1::HA/coi1-16* and *Col-gl*

Ten μ M, 20 μ M and 50 μ M MeJA treatment was tested to evaluate the effect of MeJA on primary root growth. The *Col-gl* and *35S::COI1::HA/coi1-16* seeds were surface sterilized, put in dark for overnight, and then grown in half MS medium for 6 days before they were transferred to MeJA containing half MS medium. These roots were measured on day 14 (Figure 3-3, B). To test the effect of MeJA on germination, another group of *Col-gl* and *35S::COI1::HA/coi1-16* seeds were surface sterilized, put in dark for overnight, and then grown on half MS medium and half MS medium containing 10 μ M MeJA, 20 μ M MeJA or 50 μ M MeJA for 14 days. Roots were measured on day 14 (Figure 3-3, A). Results from both examinations suggested that *Col-gl* and *35S::COI1::HA/coi1-16* were similarly sensitive to MeJA. Moreover, the root length of

Col-gl and *35S::COI1::HA/coi1-16* were also similarly inhibited by MeJA treatment.

A



B

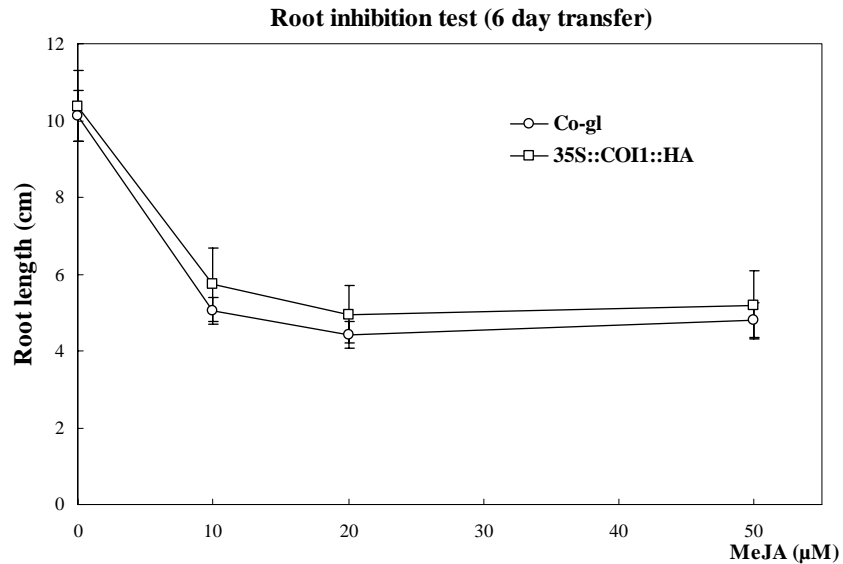


Figure 3-3 Root length of *Col-gl* and *35S::COI1::HA/coi1-16* grown in half MS medium containing 0 μM, 10 μM, 20 μM or 50 μM MeJA. (A) Seeds were germinated on half MS medium containing MeJA. Roots were measured on day 14. (B) Seeds were germinated on half MS medium for 6 days before transferring to half MS medium containing MeJA. Roots were measured on day 14.

The effect of MeJA on root length inhibition in 50 μ M was not different from those in 10 μ M and 20 μ M MeJA (Figure 3-3, B). However, for the seedlings directly germinated in MeJA containing medium, those treated with 50 μ M MeJA were slightly shorter than those treated with 10 μ M and 20 μ M MeJA (Figure 3-3, A). Judging from the nearly 100% germination rate in control and every treated group (data not shown), it was also clear that the MeJA treatment inhibited primary root growth but not germination. In short, these experiments justified using *35S::COII::HA/coi1-16* as the plant material for studies in 3.3.4.

3.3.2.2 Effect of MeJA Treatment on LEH of *35S::COII::HA/coi1-16* and *Col-gl*

Length of the first Epidermal cell with a visible root Hair bulge (LEH) was introduced as a new parameter of root development by Le (Le *et al.*, 2001). With this developmental marker that separates the rapid expansion and slow expansion of root cells, how various concentrations of MeJA could affect LEH and how quickly MeJA inhibited root growth were studied. Six day old *Col-gl* and *35S::COII::HA/coi1-16* seedlings were transferred to half MS medium (as control) and half MS medium containing 10 μ M MeJA, 20 μ M MeJA and 50 μ M MeJA, and incubated for 3hrs, 6 hrs and 24 hrs. Results in Figure 3-4 showed that the LEH became longer, from 130 μ m to 200 μ m, in untreated controls. In seedlings treated with 10 μ M MeJA, the LEH was slightly shorter after 3 hrs and remained similar in size until 24 hrs (Figure 3-4, A) In seedlings treated with 20 μ M MeJA, the LEH was shorter and, remarkably, decreased after 24 hrs (Figure 3-4, B). In seedlings treated with 50 μ M MeJA, the LEH showed the greatest decrease after 6 hrs of treatment (Figure 3-4, C).

These experiments indicated that the effect of MeJA on LEH happened within 3 hrs after the treatment started. They also suggested that MeJA treated seedlings had shorter root comparing to untreated ones was because of shorter LEH. Finally, with the best demonstration of growth inhibition, 20 μ M MeJA was chosen to be the treatment concentration in Chapter 5, 6, 7 and 8.

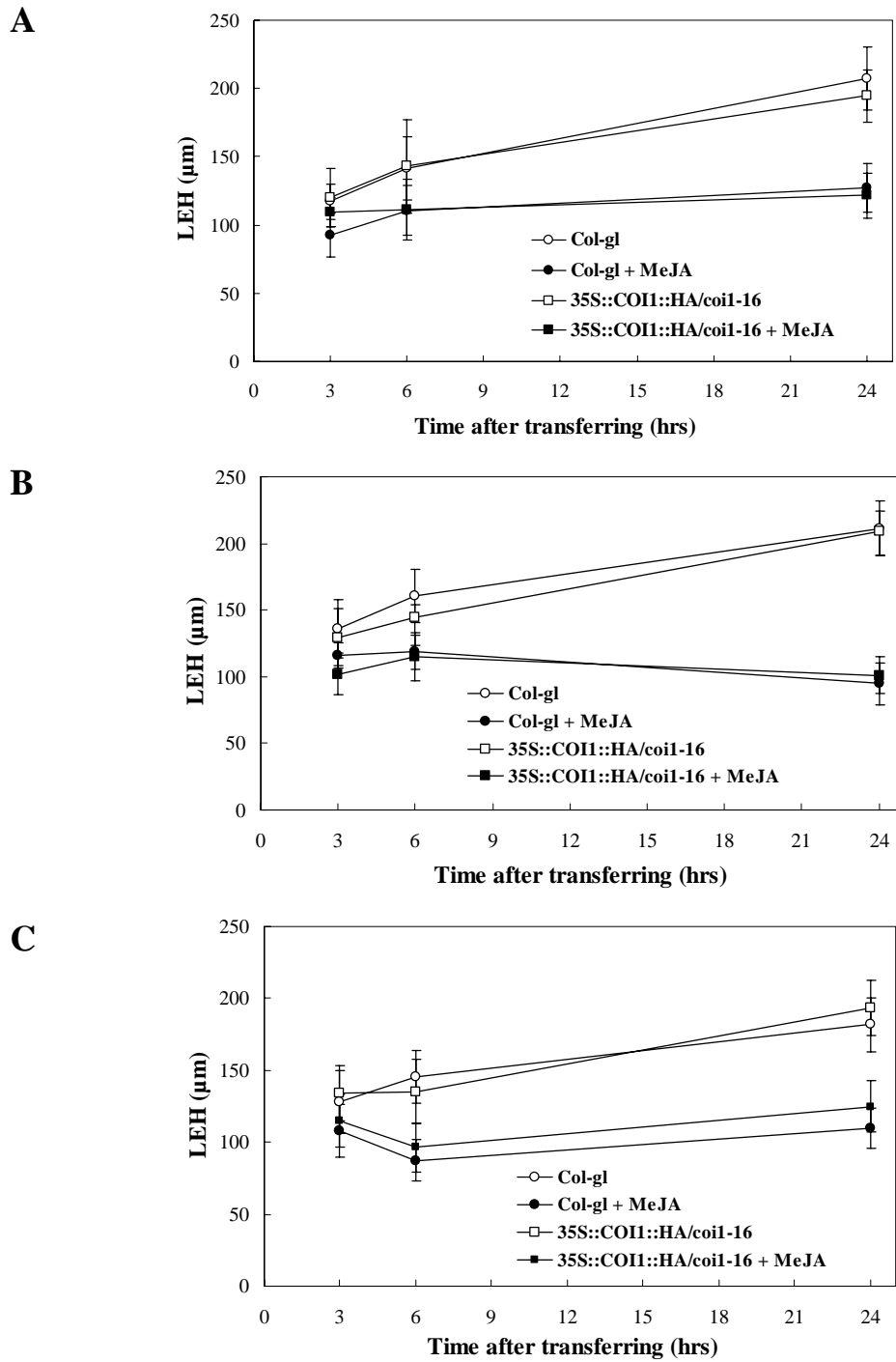


Figure 3-4 Six day old Col-gl and 35S::COI1::HA/coi1-16 seedlings were transferred to half MS medium containing various concentrations of MeJA. LEH was measured at 3 hr, 6 hr and 24 hr after transferring. (A) 10 μM MeJA (B) 20 μM MeJA. (C) 50 μM MeJA.

3.3.3 Expression of *35S::COI1::HA/coi1-16* and *pCOI1::COI1::HA/coi1-16*

Western Blotting was used to confirm expression of COI1 in the transgenic lines, *35S::COI1::HA-116/coi1-16*, *35S::COI1::HA-99/coi1-16* (Devoto *et al.*, 2002), and p8.6 (*pCOI1::COI1::HA*)/*coil-16* (Devoto and Turner, unpublished data, 2002). The MeJA treatment was applied to investigate if the expression of COI1 protein was altered by the presence of MeJA.

For this, seedlings were grown on half MS under standard conditions for 20 days (2.2.3), harvested, and divided into the root and shoot. Protein was extracted (2.3.8.1), samples were run on a SDS polyacrylamide gel (2.3.8.2) and blotted to membranes (2.3.8.3). The COI1:HA protein was detected by hybridization to peroxidase-coupled anti-HA antibody (2.3.8.4). The result of Western Blotting (Figure 3-5) showed that the COI1:HA protein migrated approximately mid-way between the 38kD and 82kD markers, consistent with its molecular weight of 67 kD. Both *35S::COI1::HA-116/coi1-16* and *35S::COI1::HA-99/coi1-16* transgenic lines had detectable levels of COI1 protein in both the root and shoot. Protein from the root and shoot tissue of Col-*gl*, as the negative control, gave no bands, as expected. The positive control was from a confirmed *35S::COI1::HA* transgenic line (Devoto *et al.*, 2002).

To determine the level of the COI1 protein in the p8.6/*coil-16* transgenic line, the seedlings were grown in half MS medium with or without 20 μ M MeJA for 20 days (2.2.3), harvested and divided into the root and shoot. Protein was extracted (2.3.8.1), samples were run on a SDS polyacrylamide gel (2.3.8.2) and blotted to membranes (2.3.8.3). The COI1:HA protein was detected by hybridization to peroxidase-coupled anti-HA antibody (2.3.8.4). Samples from *35S::COI1::HA-99 /coil-16* transgenic lines was included as a control.

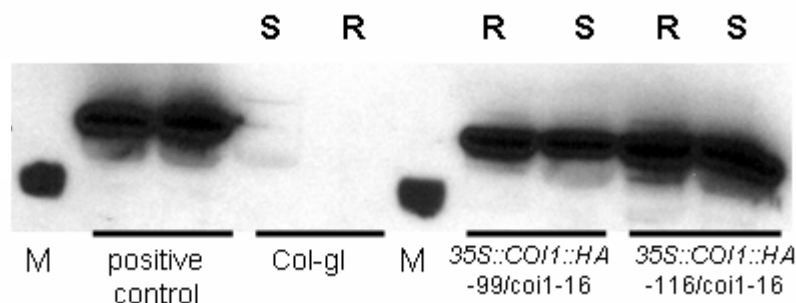


Figure 3-5 Detection of COI1::HA in *35S::COI1::HA-116/coi1-16* and *35S::COI1::HA-99/coi1-16* transgenic lines by Western Blotting. Ten µg total protein extract of either root (R) or shoot (S) tissue from 20 days old seedlings was loaded onto wells in a SDS polyacrylamide gel. Positive control came from a confirmed *35S::COI1::HA Arabidopsis* transgenic line (Devoto *et al.*, 2002). *Arabidopsis thaliana* ecotype Col-*gl* was used as the negative control. The gel was run, blotted to membranes, and hybridised to peroxidase-coupled monoclonal anti-HA antibody 3F10 (1:1000, Roche). Marker (M) was Kaleidoscope Prestained Standards (Bio-Rad), in which only the 38 kD band was detected by the antibody. The detected bands from the transgenic lines ran between the 38 and 82 kD markers.

The Western Blot (Figure 3-6) confirmed that in *35S::COI1::HA-99/coi1-16*, the level of COI1::HA expression was the same in both the root and shoot, in untreated and MeJA treated plants. However, expression of the COI1::HA protein in *p8.6/coi1-16* was significantly increased in the root tissue treated with MeJA, compared to untreated roots, while the level of COI1::HA in shoot was similar in both untreated and MeJA-treated plants. This suggested that the expression of COI1:HA protein under the control of native promoter was induced by MeJA treatment. This is consistent with the observation that COI1 transcription in the *pCOI1::GUS* root was induced by MeJA (Figure 3-1, B). To summarise, the Western Blotting analysis confirmed the expression of COI1 protein in the tested transgenic lines, which were subsequently used for immunolocalisation of COI::HA.

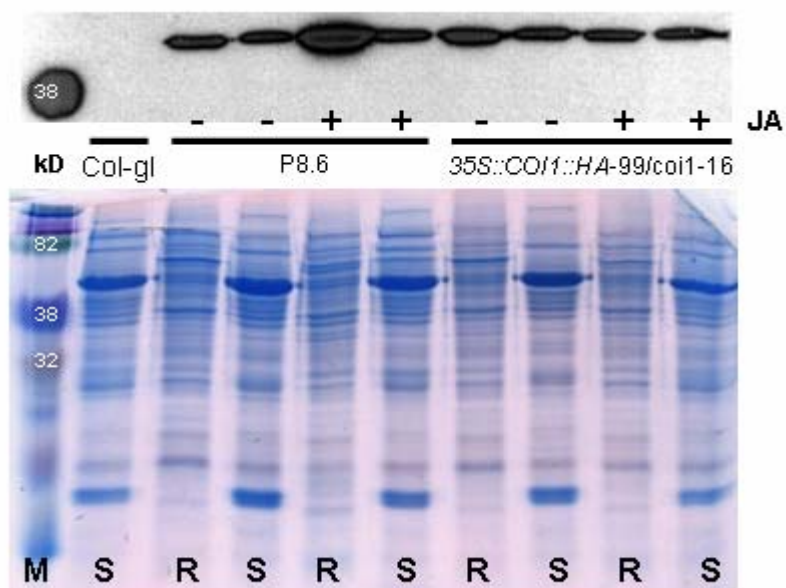


Figure 3-6 Detection of COI1::HA in *35S::COI1::HA-116/coi1-16* and *P8.6/coi1-16* transgenic lines by Western Blotting. Seedlings were grown for 20 days on half MS or MS containing 20 μ M MeJA (JA -, and JA +), harvested, divided into root (R) and shoot (S), and protein was extracted. Ten μ g total protein extract was loaded onto wells in a SDS polyacrylamide gel. *Arabidopsis thaliana* ecotype *Col-gl* was used as the negative control. The gel was run, blotted to membranes, and hybridised to peroxidase-coupled monoclonal anti-HA antibody 3F10 (1:1000, Roche). Marker (M) was Kaleidoscope Prestained Standards (Bio-Rad), in which only the 38 kD band was detected by the antibody. The detected bands from the transgenic lines ran between the 38 and 82 kD markers.

3.3.4 Localisation of Constitutively Expressed COI1::HA

Overview

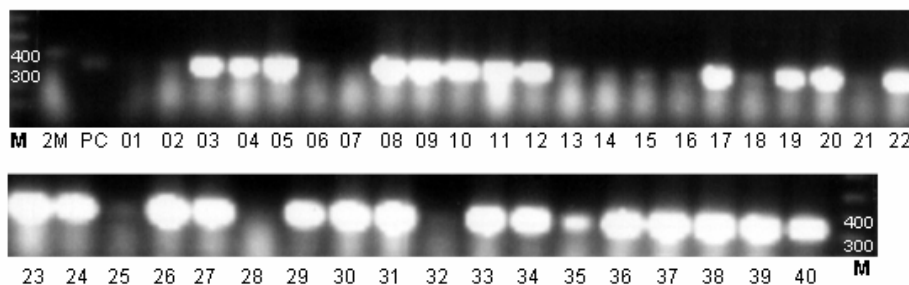
35S::*COI1*::*HA*-116/*coil*-16 and 35S::*COI1*::*HA*-99/*coil*-16 transgenic lines were used in the primary search of COI1's subcellular localisation. Both lines were first checked for the homozygous *coil*-16 background before entering the immunolocalisation step. The condition of whole mount immunolocalisation was then optimised to give best observation quality under confocal microscope.

3.3.4.1 Identifying Homozygous 35S::*COI1*::*HA*/*coil*-16

Before starting to localise COI1::HA in the 35S::*COI1*::*HA*-116/*coil*-16 and 35S::*COI1*::*HA*-99/*coil*-16 transgenic lines, it was confirmed that the transgenic lines were indeed *coil*-16 homozygous. From an original cross of 35S::*COI1*::*HA* to *coil*-16, 40 F2 plants resistant to Kanamycin were tested for the presence of *COI1* and *coil*-16 alleles. The PCR-based detection of the *coil*-16 mutation is described in 3.2.1.

The PCR results in Figure 3-7 are summarised in Table 3-3. This identified the following lines as homozygous for *coil*-16: 1, 2, 6, 13, 14, 15, 16, 18, 21, 25 and 32. F3 seeds were collected from these lines, and seedlings were grown in Kanamycin-contained half MS medium to identify F4 lines homozygous for the 35S::*COI1*::*HA* transgene and *coil*-16 mutation. The identified transgenic lines were used in the following sections.

Primer: 2-COI1 and 4-COI1



Primer: 2-COI1 and 3-COI1

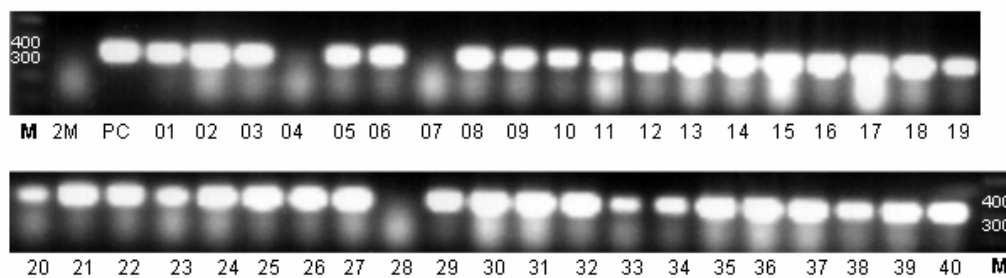


Figure 3-7 PCR-based detection of the *coil-16* mutation. The PCR products from two combinations (primer pairs 2-COI1 + 3-COI1 and 2-COI1 + 4-COI1) in separate PCR reactions were loaded and run in the same agarose gel. The DNA band sized in approximately 350 bp represented the target PCR product for both primer sets. Ten µl of the PCR product was loaded onto each lane. Marker (M) was 1 Kb plus DNA ladder. *Arabidopsis* ecotype 2M was used as negative control. Genomic DNA extracted from confirmed homozygous *coil-16* transgenic plant was used as positive control (PC).

Table 3-3 Examples of identifying the homozygous *coil-16* by using two combinations (primer pairs 2-COI1 + 3-COI1 and 2-COI1 + 4-COI1) in separate PCR reactions.

Plant No	2-COI1 + 4-COI1	2-COI1 + 3-COI1	Genotype
01	-	+	Homozygous <i>coil-16</i>
02	-	+	Homozygous <i>coil-16</i>
03	+	+	Heterozygous
04	+	-	Homozygous WT
05	+	+	Heterozygous
06	-	+	Homozygous <i>coil-16</i>
07	-	-	N/A
08	+	+	Heterozygous
09	+	+	Heterozygous
10	+	+	Heterozygous
11	+	+	Heterozygous
12	+	+	Heterozygous
13	-	+	Homozygous <i>coil-16</i>
14	-	+	Homozygous <i>coil-16</i>
15	-	+	Homozygous <i>coil-16</i>
16	-	+	Homozygous <i>coil-16</i>
17	+	+	Heterozygous
18	-	+	Homozygous <i>coil-16</i>
19	+	+	Heterozygous
20	+	+	Heterozygous
21	-	+	Homozygous <i>coil-16</i>
22	+	+	Heterozygous
23	+	+	Heterozygous
24	+	+	Heterozygous
25	-	+	Homozygous <i>coil-16</i>
26	+	+	Heterozygous
27	+	+	Heterozygous
28	-	-	N/A
29	+	+	Heterozygous
30	+	+	Heterozygous
31	+	+	Heterozygous
32	-	+	Homozygous <i>coil-16</i>
33	+	+	Heterozygous

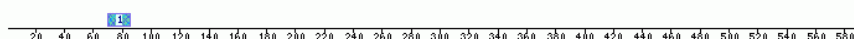
Plant No	2-COI1 + 4-COI1	2-COI1 + 3-COI1	Genotype
34	+	+	Heterozygous
35	+	+	Heterozygous
36	+	+	Heterozygous
37	+	+	Heterozygous
38	+	+	Heterozygous
39	+	+	Heterozygous
40	+	+	Heterozygous

3.3.4.2 Identification of the NLS Motif in COI1 Protein Sequence

COI1 protein was predicted as a 592-amino acid protein, in which a degenerate F-box motif and 16 imperfect leucine-rich repeats (LRRs) were found (Xie *et al.*, 1998). Online searching by using Motif Scan (<http://hits.isb-sib.ch/cgi-bin/PFSCAN>) discovered a bipartite nuclear localisation signal (NLS), consisted of “RRFPNLRSLK-LKGKPR”, and situated at the 70th to 85th amino acids in the COI1 protein (Figure 3-8). The NLS was localised between the F-box and the leucine-rich repeats (Figure 3-9). This suggested that the COI1 protein was likely to be transferred to the nucleus after translation.

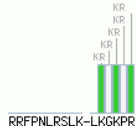
Subject

ID RAW_TEXT TEMPORARY; PRT; 592 AA.



Match 1

>prf:NLS_BP 3.000 3 pos. 70 - 85 [1, -1] PS50079|prf:NLS_BP Bipartite nuclear localization signal profile.



Legends: 1, Match 1 (scan).

Figure 3-8 The result of scanning of COI1 protein sequence in Motif Scan Webpage (<http://hits.isb-sib.ch/cgi-bin/>). The NLS was detected in the region on upper line shown in blue. The NLS sequence is given in Match 1.

this, I increased the concentration of the antibody. For the single-step immunolocalisation, the antibody was increased from 1:10,000 to 1:1,000, and for the two-step immunolocalisation, the secondary antibody was increased from 1:10,000 to 1:1,000. These changes improved the signal so that it became more distinguishable from the background.

3.3.4.4 Choice of Antibody

The Slowfade-antifade antibody (anti-HA, mouse IgG monoclonal Alexa Fluor[®] 488 conjugate) was initially used in whole-mount immunolocalisation due to its merit of providing a convenient single-step immunolocalisation methodology. This procedure produced fluorescent images which had less background fluorescence compared to the indirect staining method. The indirect immunolocalisation method required a primary anti-HA antibody and a secondary anti-mouse IgG antibody. The benefits of the indirect methodology are that it gave more flexibility to choose the antibodies conjugated with different fluorophore molecules. In addition, hybridisation of the secondary antibody allowed more amplification of the signal (2.4.2).

3.3.4.5 Whole-Mount Immunolocalisation of Constitutively Expressed COI1::HA

After solving the problem of autofluorescence and determining the appropriate antibodies, the technique of whole mount immunolocalisation was finally implemented properly. Three to four day old *35S::COI1::HA-116/coil-16 Arabidopsis* seedlings were fixed, treated with drieslase, permeabilised (2.4.1), and hybridised with anti-HA Alexa Fluor[®] 488 conjugate antibody (2.4.2). The seedlings were then covered with a glass coverslip and observed under the Leica confocal microscope (2.5.3). The signals of COI1::HA protein were exclusively distributed in the nucleus of the root cells (Figure 3-10, B). When the *35S::COI1::HA-116/coil-16* seedlings were treated 50 μ M MeJA for 3 hrs before they were harvested, the distribution of the COI1::HA protein and the intensity of the fluorescence signal were unaffected (data not shown). In agreement with

the Western blot results (3.3.3), this indicates that the stability of COI1::HA protein is unaltered by MeJA.

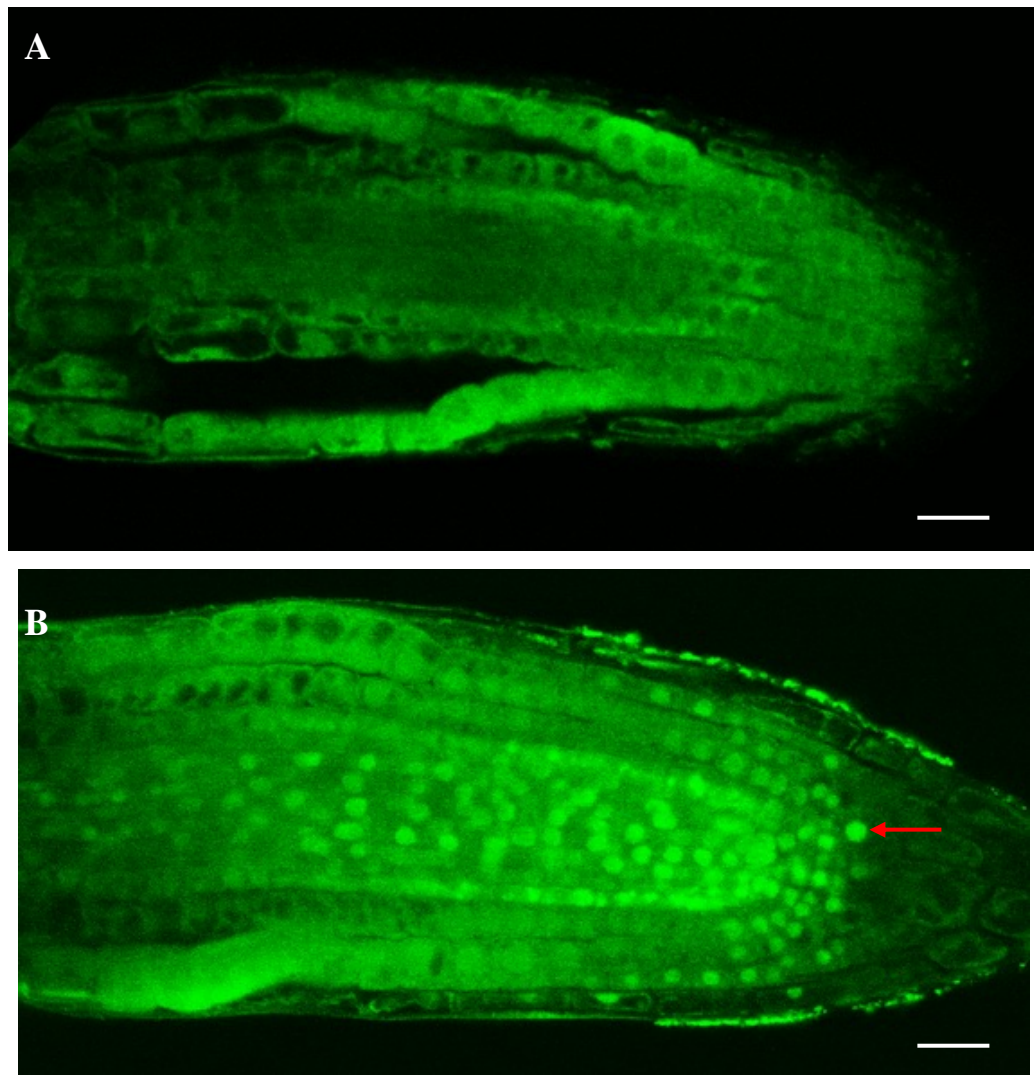


Figure 3-10 Immunolocalisation of Col-*gl* and 35S::COI1::HA-116/*coil*-16 *Arabidopsis* transgenic lines. COI1::HA was detected by anti-HA, mouse IgG1, monoclonal 16B12, Alexa Fluor® 488 conjugate antibody (1:200, Invitrogen A21287). (A) Root tip of 3 day old Col-*gl* seedling grown in half MS medium. (B) Root tip of 3 day old 35S::COI1::HA-116/*coil*-16 seedling grown in half MS medium. The COI1::HA protein was detected in the nucleus (arrow). Scale bar 30 µm.

3.3.5 Localisation of COI1::HA in *pCOI1::COI1::HA/coil-16* Plants

The p8.6 (*pCOI1::COI1::HA*)/*coil-16* transgenic line was used for whole-mount immunolocalisation. The p8.6 construct contains the *COI1* native promoter, and was predicted to reveal any tissue- or intensity-specific differences from the *35S::COI1::HA* construct. Three to 4 day old p8.6/*coil-16* *Arabidopsis* seedlings were fixed, were treated with drieslase, permeabilised (2.4.1), and hybridised with anti-HA Alexa Fluor[®] 488 conjugate antibody (2.4.2). The seedlings were then covered with a glass coverslip and observed under the Leica confocal microscope (2.5.3).

The fluorescence signal shown in Col-*gl* roots (Fig 3-11, A) was similar to that seen in fixed Col-*gl* roots untreated with anti-HA Alexa Fluor[®] 488 conjugate antibody (data not shown), indicating that this is autofluorescence, while p8.6/*coil-16* roots showed strong signal inside the nucleus (Figure 3-11, B). Interestingly, in p8.6/*coil-16* plants, the signal was strongest in the centre of the nucleus and close to the nuclear membrane (Figure 3-11, B, arrow). In p8.6/*coil-16* plants treated with 50 µM MeJA for 3 hrs before harvest, the distribution of signal was also restricted to the nucleus, but was more equally distributed in this organelle than in untreated p8.6/*coil-16* (Figure 3-11, C). These findings are consistent with the increased level of the COI1:HA protein in roots of p8.6/*coil-16* plants treated with MeJA. (3.3.3).

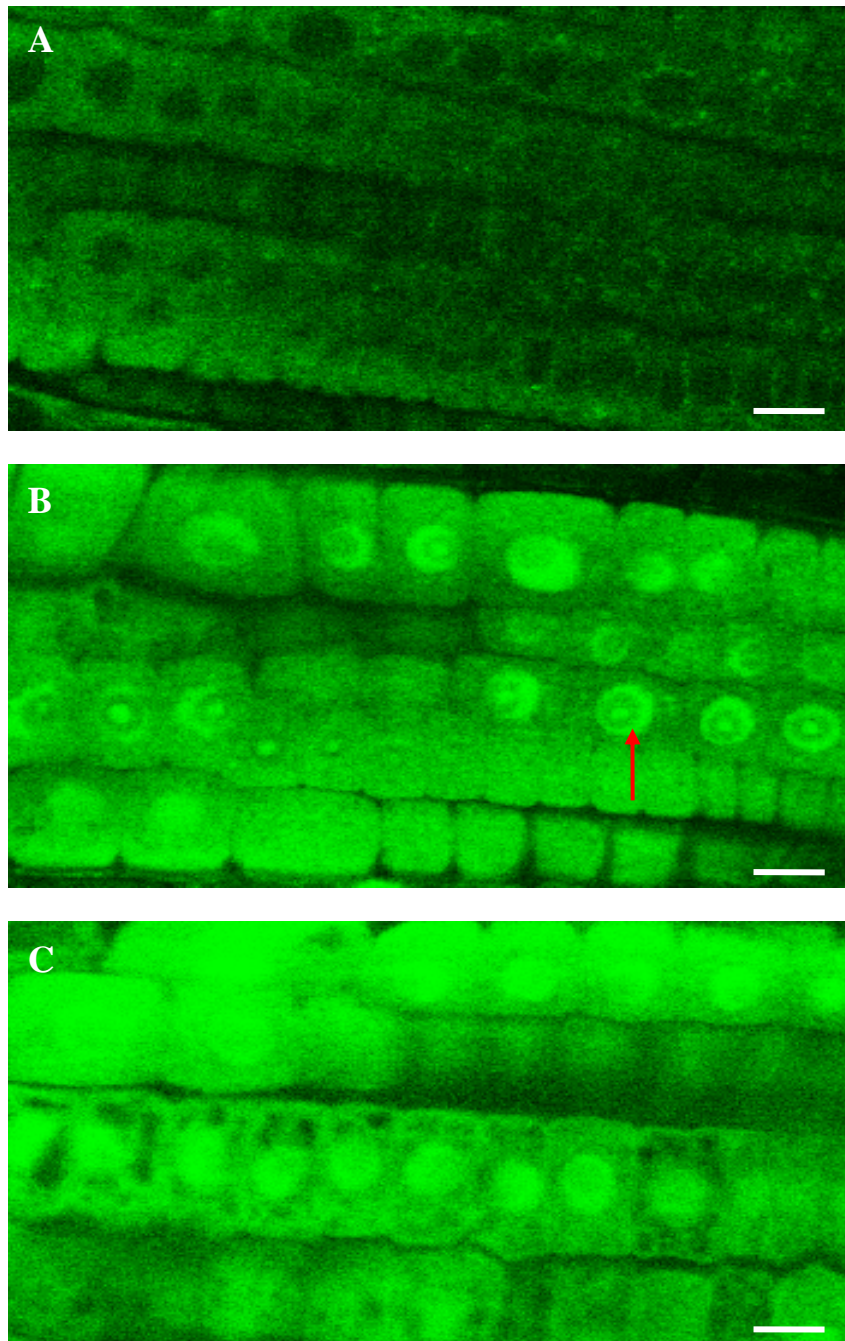


Figure 3-11 Immunolocalisation of Col-*gl* and p8.6/*coil*-16. COI1::HA was detected by anti-HA, Alexa Fluor[®] 488 antibody (1:200, Invitrogen). (A) Root cells in 3 day old Col-*gl* seedling. (B) Root cells in 3 day old p8.6/*coil*-16 seedling. (C) Root cells in 3 day old p8.6/*coil*-16 seedling treated with 50 µM MeJA for 3 hrs before it was harvested. Scale bar: 10 µm.

3.3.6 Co-localisation of COI1 and JAI3

The binding of the COI1 protein with members from the JAZ family had been reported by Chini *et al.* (2007) *in vitro*. In order to investigate the physical interaction between COI1 and the JAZ proteins *in situ*, a cross of *35S::COI1::HA/coi1-16* and the *35S::JAI3::GFP* transgenic line (Chini *et al.*, 2007) was made.

3.3.6.1 Localisation of JAI3::GFP

The localisation of JAI3::GFP was checked in the *35S::JAI3::GFP* transgenic line provided by Chini *et al.* Seeds were surface sterilised and grown in half MS medium under standard conditions (2.2.3). Because JAI3 protein is degraded soon after binding with the SCF^{COI1} complex, which is assembled when the JA signal pathway is activated, the JAI3::GFP signal was unstable in plants under stress or the MeJA treatment. Therefore, 5 day old *35S::JAI3::GFP* transgenic seedling was rapidly transferred to a glass slide with a drop of water added, and then observed immediately using a fluorescence microscope (2.5.2).

In Figure 3-12, GFP signals localised noticeably in the nucleus of root cells. However, the green fluorescence light faded quickly and disappeared completely within 10 minutes after being transferred to the glass slide. This occurred whether or not the tissues were being continuously observed under the fluorescence microscope, indicating that the fading fluorescence was not due to bleaching by the UV light. Treating the *35S::JAI3::GFP* transgenic seedlings with 20 μ M MeJA for 1 hr before observation also caused disappearance of the JAI3::GFP signal (data not shown). These findings confirmed the localisation of the JAI3::GFP protein to the nucleus, and its instability promoted by MeJA. The *35S::JAI3::GFP* transgenic line was next crossed with *35S::COI1::HA/coi1-16* in 3.3.6.2.

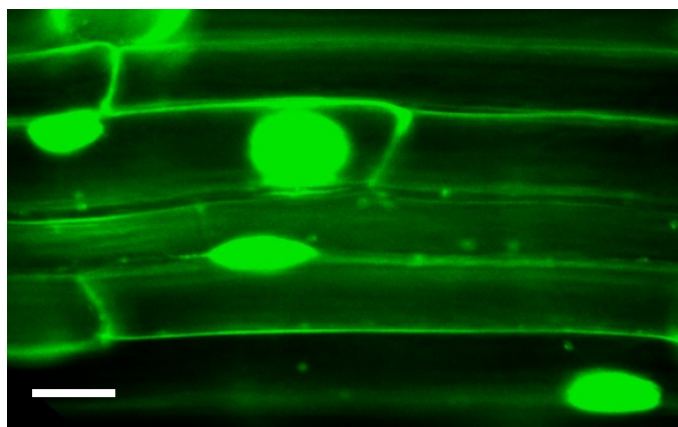


Figure 3-12 Observation of mature root cells in the *35S::JAI3::GFP* *Arabidopsis* transgenic lines. Five day old *35S::JAI3::GFP* transgenic seedlings were observed with a Zeiss fluorescence microscope. Scale bar 10 μ m.

3.3.6.2 Production of Homozygous Lines for the *35S::JAI3::GFP* Transgenic Line and *35S::COI1::HA/coi1-16*

Crossing of *35S::JAI3::GFP* transgenic line and *35S::COI1::HA/coi1-16* was carried out by applying pollen from *35S::JAI3::GFP* transgenic line anthers to the stigma of *35S::COI1::HA/coi1-16* flowers. The *Arabidopsis* background of *35S::JAI3::GFP* transgenic line is *Columbia* (Col-0), which has trichomes as a dominant phenotype, whereas the *Arabidopsis* ecotype of *35S::COI1::HA/coi1-16* is Col-*gl*, which is derived from Col-0, has no trichomes. The merit of crossing phenotypically distinguishable parents is that it helps to confirm F1 seedlings from cross pollination instead of self-pollination. With a Col-0 ecotype pollen donor and a Col-*gl* ecotype recipient, F1 seedlings, which had trichomes, were grown in soil and seeds from the F2 generation were collected.

To select plants homozygous for the *35S::JAI3::GFP* and *35S::COI1::HA* transgenes, F2 seeds were grown in half MS medium containing kanamycin (25 μ g/ml) and hygromycin (20 μ g/ml) under standard conditions (2.2.3). The *35S::JAI3::GFP* construct contains *HPT* for hygromycin resistance and the *35S::COI1::HA* construct

contains *Kan^R* conferring kanamycin resistance. The hygromycin resistant seedlings were selected by putting the plates in light for 4-12 hrs to promote germination, then transferring plates to the dark for 5 days, before observing the phenotype of the seedlings. As expected, the hygromycin sensitive seedlings laid on medium with very short hypocotyls and open cotyledons, while hygromycin resistant seedlings were upright like normal dark-grown seedlings, with long hypocotyls and closed cotyledons (Figure 3-13). More than half of the seeds gave seedlings that were resistant to both kanamycin and hygromycin, consistent with the ratio of 9:16 expected if there was independent segregation of the two transgenes. The kanamycin and hygromycin resistant F2 seedlings were then selected and 40 were transferred to soil.

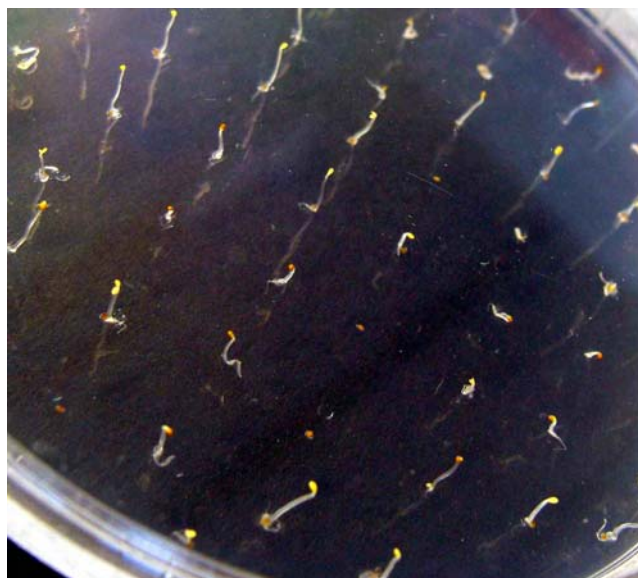


Figure 3-13 After crossing of the *35S::JAI3::GFP* transgenic line and *35S::COI1::HA/coi1-16*, the F2 segregated seeds were grown in half MS containing kanamycin (25 µg/ml) and hygromycin (20 µg/ml). Seeds which did not germinate were kanamycin sensitive. Seedlings which laid on medium with very short hypocotyls were kanamycin resistant but hygromycin sensitive. Seedlings appeared standing up tall like normal dark-grown seedlings were both kanamycin and hygromycin resistant.

The F3 seeds were collected from F2 plants individually. F3 seeds were grown in half MS medium containing kanamycin (25 µg/ml) and hygromycin (20 µg/ml) under standard conditions (2.2.3). For each individual F2 plant, 100 F3 seeds were sown. Plants that gave 100% kanamycin and hygromycin resistant F3 seedlings were considered homozygous for *35S::JAI3::GFP* and *35S::COI1::HA* transgenes, and were used to examine the co-localisation of COI1::HA and JAI3::GFP.

3.3.6.3 Co-localisation of JAI3::GFP and COI1::HA

Three day old homozygous *35S::JAI3::GFP*; *35S::COI1::HA/coil-16* seedlings were fixed, treated with drieslase, permeabilised (2.4.1), and hybridised with Oregon Green[®] 488 goat anti-rat IgG (H+L) antibody and Alexa Fluor[®] 568 goat anti-mouse IgG antibody (2.4.2), separately. The seedlings were then covered with a glass coverslip and root tips were observed under the Leica confocal microscope (2.5.3). Because JAI3::GFP gives green fluorescence, the red fluorescent Alexa Fluor[®] 568 anti-HA antibody was used as secondary antibody for simultaneously co-localising the COI1::HA signals.

The first step was to confirm that in the transgenic line *35S::JAI3::GFP*; *35S::COI1::HA/coil-16*, COI1::HA was localised in the nucleus as it was in the *35S::COI1::HA/coil-16* (Figure 3-10). For this, in *35S::JAI3::GFP*; *35S::COI1::HA/coil-16*, COI1::HA was localised with Oregon Green[®] 488 anti-HA antibody. As shown in Figure 3-14, B (arrow), COI1::HA was localised in the nucleus of *35S::JAI3::GFP*; *35S::COI1::HA/coil-16*.

To test whether COI1 co-localised with JAI3 in *35S::JAI3::GFP*; *35S::COI1::HA/coil-16*, the localisation of COI1::HA (detected with Alexa Fluor[®] 568 anti-HA antibody, gives red fluorescence) and JAI3::GFP (detected by green fluorescence) was determined simultaneously (Figure 3-15). Figure 3-15, A and figure 3-15, B show co-localisation of COI1::HA and JAI3::GFP in a single nucleus (arrows). This is confirmed in the overlay (Figure 3-15, C).

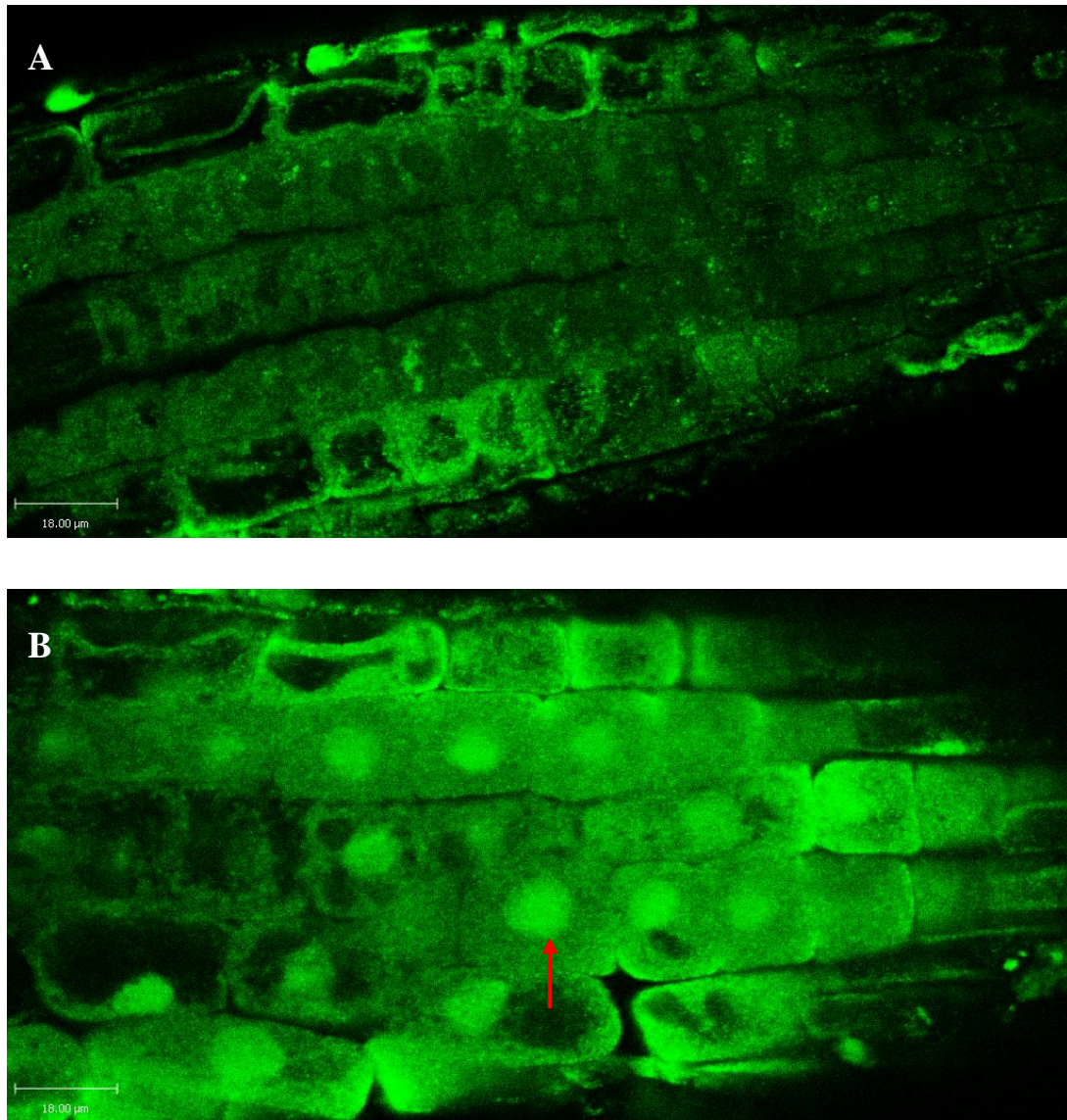


Figure 3-14 Immunolocalisation of COI1::HA in homozygous *35S::JAI3::GFP*; *35S::COI1::HA/coil-16* root. COI1::HA was detected by Oregon Green[®] 488 goat anti-rat IgG (H+L) antibody (Invitrogen). (A) Root cells in 3 day old Col-*gl* seedling as control. (B) Root cells in 3 day old *35S::JAI3::GFP*; *35S::COI1::HA/coil-16*. The COI1::HA signal is marked (arrow). Scale bar 18 µm.

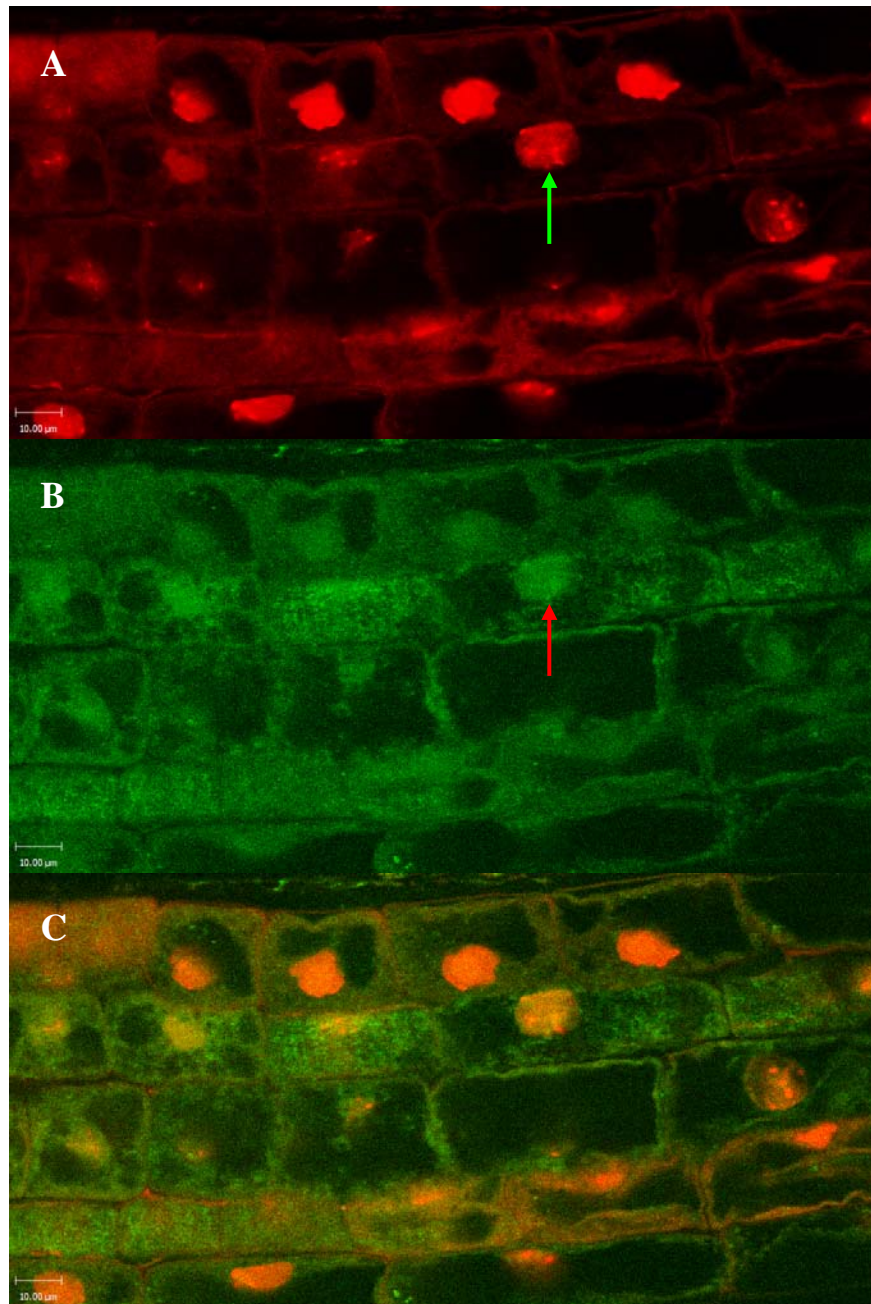


Figure 3-15 Immunolocalisation of JAI3::GFP and COI1::HA in homozygous *35S::JAI3::GFP*; *35S::COI1::HA/coi1-16* root. COI1::HA was detected by Alexa Fluor® 568 goat anti-mouse IgG antibody (Invitrogen). (A) Red fluorescence of COI1::HA (arrow). (B) Green fluorescence of JAI3::GFP (arrow). (C) Overlay of (A) and (B). Where both red and green fluorescence came from the same location, the image appeared yellow. Scale bar 10 µm.

It is interesting to see that the distribution of COI1::HA was not uniform inside the nucleus when detected with Alexa Fluor[®] 568 anti-HA antibody. In some of the root cells, COI1::HA signals were distributed as several bright red dots (speckles) in the nucleus (Figure 3-15, A, arrow). Evidently, Alexa Fluor[®] 568 anti-HA antibody localises COI1::HA to speckles within the nucleus (Figure 3-15, A), whereas Oregon Green[®] 488 anti-HA antibody localises COI1::HA evenly within the nucleus (Figure 3-14, B).

Although the autofluorescence presented in both green and red fluorescence (Figure 3-14, B and Figure 3-15, A), considering the autofluorescence under the green fluorescence is higher than those under the red fluorescence, it is possible that the greater noise/signal ratio in Figure 3-14 caused artificial distribution of the COI1::HA signal, while in Figure 3-15, less autofluorescence under the red fluorescence allows more accurate detection of the COI1::HA signal.

To investigate the effect of MeJA treatment on the localisation of JAI3 and COI1, 3 day old homozygous *35S::JAI3::GFP*, *35S::COI1::HA/coi1-16* seedlings were treated with 20 μ M MeJA for 24 hrs before harvesting for whole-mount immuno-observation. Seedlings were fixed, treated with drieslase, permeabilised (2.4.1), and hybridised with Alexa Fluor[®] 568 goat anti-mouse IgG antibody (2.4.2). The seedlings were then covered with a glass coverslip and observed under the Leica confocal microscope (2.5.3).

After the MeJA treatment, the result showed that the COI1::HA signal was detected in nucleus as red speckles (Figure 3-16, A, arrow). However, in the MeJA treated root, the JAI3::GFP signals had disappeared from the nucleus (Figure 3-16, B). This was confirmed in the merged image, which showed only the COI1::HA signal in the nucleus (Figure 3-16, C). This finding indicated that the COI1::HA signal was not altered by MeJA treatment, but the JAI3 signal was undetectable in the MeJA-treated plants.

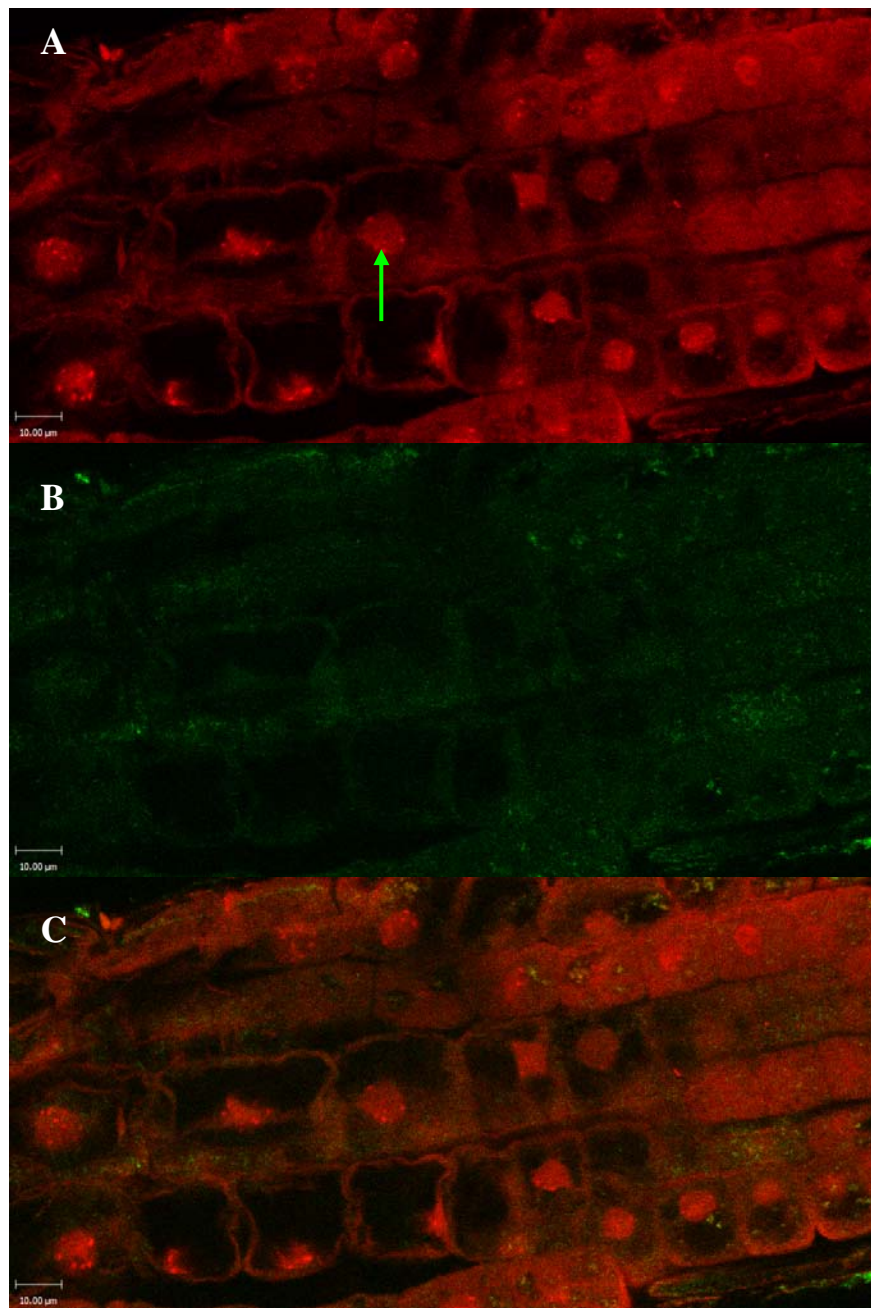


Figure 3-16 Immunolocalisation of JAI3::GFP and COI1::HA in homozygous *35S::JAI3::GFP*; *35S::COI1::HA/coi1-16* root treated with 20 μM MeJA 24 hrs before it was harvested. COI1::HA was detected by Alexa Fluor[®] 568 goat anti-mouse IgG antibody (Invitrogen). (A) Red fluorescence of COI1::HA (arrow). (B) Green fluorescence of JAI3::GFP. (C) Overlay of (A) and (B). Where both red and green fluorescence came from the same location, the image appeared yellow. Scale bar 10 μm.

3.3.6.4 JAZ Degradation is COI1-Dependent

The COI1-dependence of JAZ degradation was examined. For this, the *35S::JAZ1::GUS/coi1-1* transgenic line (Thines *et al.*, 2007) was used.

35S::JAZ1::GUS/coi1-1 was maintained in a population segregating for the *COI1* and *coi1-1* alleles. To obtain results from homozygous *35S::JAZ1::GUS/coi1-1*, 90 seeds from the segregating F2 generation were surface sterilised, and grown in half MS medium under standard conditions (2.2.3). Four day old seedlings were transferred to medium containing 20 μ M MeJA for 1hr, harvested, and assayed for GUS activity (2.3.6). The GUS product was detected in the cotyledons, root tips, and hypocotyls of 24 of the 90 seedlings tested (Figure 3-17, A, B and E), while 66 seedlings showed no detectable GUS product (Figure 3-17, C and D). The ratio of 24 to 66 was close to 1 to 3, which agreed with the F2 ratio of homozygous *coi1-1* (1) to heterozygous *coi1-1/COI1* (2) plus wild type *COI1/COI1* (1). This indicated that the degradation of JAZ1 protein after MeJA treatment may be COI1-dependent.

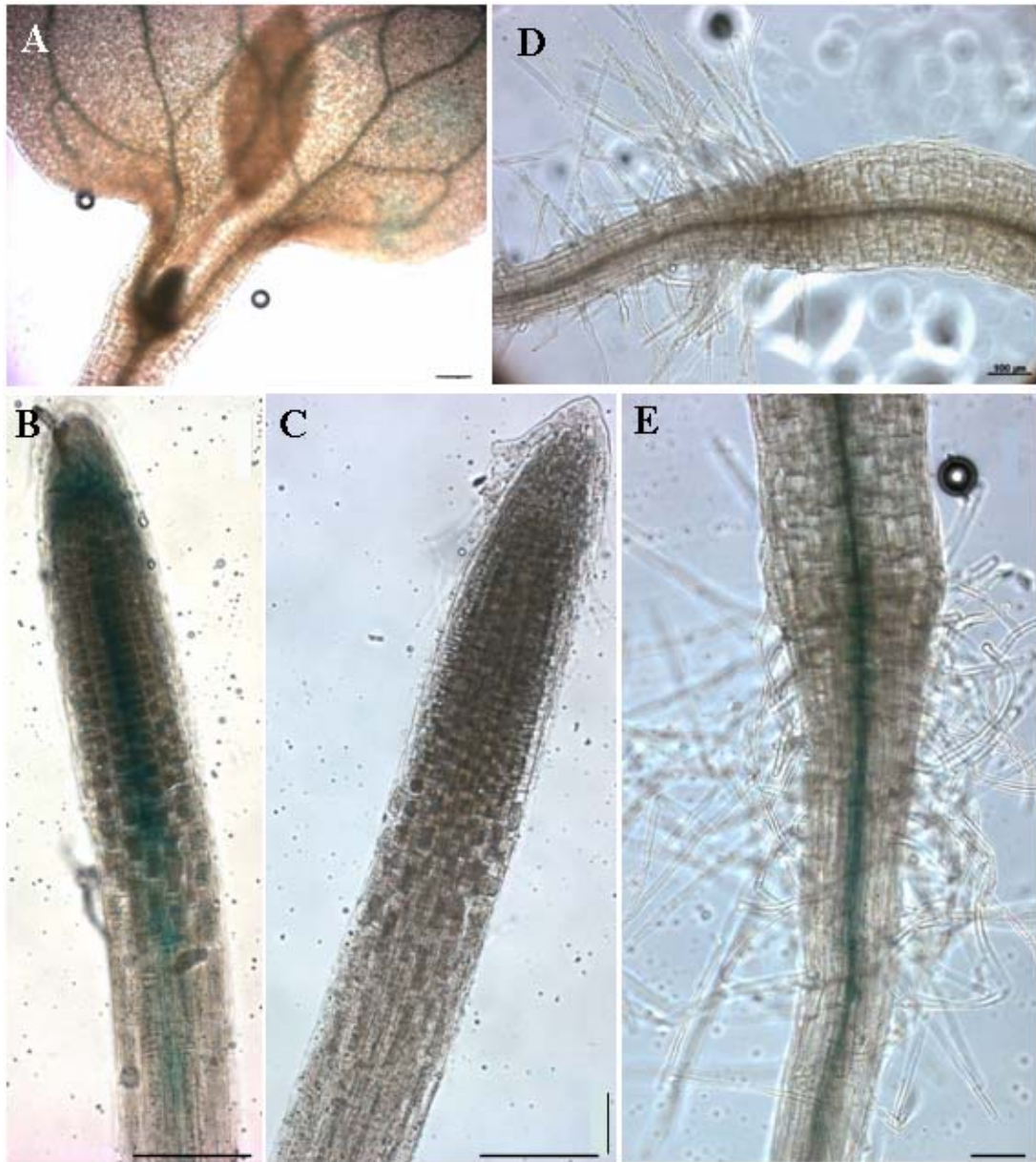


Figure 3-17 Histochemical GUS detection of *35S::JAZ1::GUS* transgenic lines. Four day old *35S::JAZ1::GUS/coi1-1* seedlings treated with 20 μ M MeJA for 1hr. (A) Cotyledon, (B) root tip, and (E) hypocotyl and part of the mature root. Four day old *35S::JAZ1::GUS* in heterozygous *coi1-1* or wild type background seedlings treated with 20 μ M MeJA for 1hr. (C) Root tip and (D) hypocotyl and part of the mature root. Scale bar 100 μ m.

3.4 Discussion

The localisation and expression of the COI1 protein has been studied in this chapter. In the *pCOI1::GUS* transgenic plant, the GUS product was present in plant tissues, especially the vascular bundles (**Figure 3-2**). When the plants were treated with 20 μ M MeJA, there was increased expression of the reporter in the root vascular bundle (**Figure 3-1**). When the plants were wounded in order to activate the JA signaling, there was increased expression of the reporter in the stamen filaments but not in other tissues or the wounded leaves (**Figure 3-2**, B and E). A feature of the *coil* mutant and some other mutants in the JA biosynthesis pathway is that they are male sterile, have short stamens, and pollen grains do not develop properly (Feys *et al.*, 1994). This is consistent with a role for JA in development of male fertility. Therefore, the expression of the COI1 reporter in sepal and stamen filaments and the altered expression when plant was wounded may relate to its function on floral development.

Interestingly, when the p8.6/*coil*-16 transgenic lines were treated with 20 μ M MeJA, there was increased expression of the COI1 protein in the root, but not in the shoot tissue (**Figure 3-6**). This finding corresponds to the increased expression of the reporter in root vascular bundle in **Figure 3-1**, B. However, Northern (RNA) blot analysis showed similar expression level of the *COI1* transcript in untreated, wounded and JA-treated *Arabidopsis* (Xie *et al.*, 1998), and there was no distinguishable difference between the expression in the untreated and wounded leaves of *pCOI1::GUS* transgenic plant (**Figure 3-2**). Taken together, it is possible that the COI1 expression is slightly induced in the root tissue when the JA signal pathway is activated, but this increase in transcription and translation is not sufficient enough to be revealed by Northern blotting.

Previous work has indicated that other components of the JA signal pathway, including MYC2, JAZ1, JAZ6, JAI3/JAZ3 and JAS1, a downstream growth mediator later to be identified as JAZ10 from the JAZ family, are also localised to the nucleus (Lorenzo *et al.*, 2004, Thines *et al.*, 2007, Chini *et al.*, 2007, Yan *et al.*, 2007). The experiments described in this chapter are the first in which the COI1 protein has been localised. When transcription was driven by either the 35S promoter or the *COI1* native promoter, COI1::HA protein was shown to specifically accumulate in the nucleus (**Figure 3-10** and **3-11**). Moreover, immunolocalisation of COI1::HA in the

homozygous *35S::JAI3::GFP*; *35S::COI1::HA/coi1-16* root revealed the co-localisation of JAI3::GFP and COI1::HA in the nucleus (**Figure 3-15**). These results suggest that the SCF^{COI1} complex is very likely formed inside the nucleus, and also confirmed that the SCF^{COI1}-JAZ3 interaction takes place in the nucleus.

Although the COI1 protein was only detectable in the nucleus, its distribution in the organelle varied in different transgenic lines. In *35S::COI1::HA/coi1-16*, COI1::HA was distributed uniformly throughout the nucleus, whereas in *p8.6/coi1-16*, COI1::HA was distributed in the centre of the nucleus and close to the nucleus membrane in the root cells (**Figure 3-10**, B and **Figure 3-11**, B). More interestingly, COI1::HA in *p8.6/coi1-16* treated with MeJA was distributed evenly inside the nucleus (**Figure 3-11**, C), suggesting that the expression of COI1::HA increased in the MeJA-treated *p8.6/coi1-16* root. This finding is consistent with the increased expression of the COI1 protein in the *p8.6/coi1-16* root (**Figure 3-6**). Taken together, the results from both Western Blot and confocal imaging indicated a possible post-transcription and/or translation regulation mediated by the native promoter and the 5' untranslated region on the expression of COI1.

The speckle-like distribution of COI1::HA in the homozygous *35S::JAI3::GFP*; *35S::COI1::HA/coi1-16* root nucleus was an unexpected observation. This uneven distribution was only detected by the Alexa Fluor[®] 568 goat anti-mouse IgG antibody in red fluorescence without or with MeJA (**Figure 3-15** and **3-16**), but not by the Oregon Green[®] 488 goat anti-rat IgG antibody (**Figure 3-14**). Evidently, the distribution of COI1::HA is not the same when detected by different antibodies. Although it was suggested that the speckle-like distribution of COI1::HA shown in the red fluorescence might be covered by the autofluorescence when detected in the green fluorescence (3.3.6.3), the reason why COI1::HA distributes evenly (**Figure 3-10**, B and **Figure 3-14**, B), or as speckle (**Figure 3-15**) under the regulation of the 35S promoter, and distributes unevenly (**Figure 3-11**, B) under the regulation of the native promoter, remains unknown. It is interesting though, that an uneven distribution is also observed with the JAZ1/TIFY10A-GFP in tobacco BY-2 cells, in which JAZ1/TIFY10A-GFP is distributed as nuclear bodies (**Figure 3-18**; Grunewald *et al.*, 2009). It is suggested that the tify domain might contain a nucleoplasm retention signal, and the protein-protein interaction between JAZ proteins, which is mediated by the tify motif, may be necessary for the distribution of JAZ to the nucleoplasm (Grunewald *et al.*, 2009). It is therefore

possible that the protein-protein interaction between COI1 and JAZ also regulates the localisation of COI1 in the nucleus. In addition, the speckle-like distribution of COI1::HA (**Figure 3-15**) does not resemble the nuclear bodies in **Figure 3-18**, suggesting that the sub-nuclear structures observed in **Figure 3-15** and **Figure 3-18** might not be the same. It is therefore important to make a further detailed examination of the sub-nuclear localisation of the COI1 protein at high resolution. Considering the interference from autofluorescence, future work should focus on making a *COI1::GFP* or a *COI1::RFP* construct.

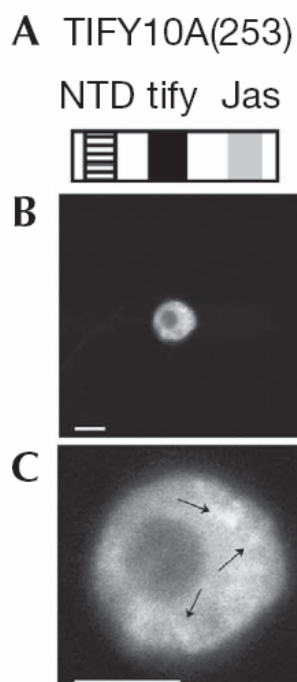


Figure 3-18 Subcellular localization of JAZ1/TIFY10A-GFP in a tobacco BY-2 cell. (A) Schematic representation of JAZ1/TIFY10A protein. (B) GFP signal in a BY-2 cell. (C) Close-up of nuclear GFP localisations. Arrows indicate nuclear bodies. Scale bars, 10 μm. Jas, jasmonate-associated; NTD, amino-terminal domain. (Grunewald *et al.*, 2009, Figure 2)

Chapter 4

Construction of pCOII::COII::RFP

4.1 Introduction

The *COII* gene (Feys *et al.*, 1994, Xie *et al.*, 1998) has been manipulated, cloned into many vectors and introduced back into *Arabidopsis* (Devoto *et al.*, 2002, Devoto and Turner, unpublished data, 2002-2005). In Chapter 3, one of the unpublished transgenic lines, p8.6/*coil*-16, was used to investigate the expression and subcellular localisation of COI1 (3.3.3 and 3.3.5), and a different subcellular expression pattern was observed from the constitutively expressed COI1 in transgenic line 35S::*COII*::*HA*/*coil*-16 (3.3.4). However, a difficulty encountered was that the fixation step required for the immunolocalisation process gave rise to green autofluorescence which interfered with the detection of a GFP signal and with the Alexa Fluor[®] 488 anti-HA antibody signal (3.3.4.3). In this chapter, p8.6 was used to make a construct with the red fluorescent protein (*RFP*) gene fused to the native *COII* promoter and the *COII* gene. Detection of this construct would not require the fixation step, and would also allow more flexibility in detecting the COI1 protein at the subcellular level, and co-localising COI1 with other protein components in JA signal pathway.

Furthermore, in order to determine the restriction enzymes used for cloning and to ensure the construct was made in frame, the full-length of p8.6 was sequenced.

4.2 Methods

SUMMARY

P8.6 (pCOII::COII::HA) construct was cloned into pBIN19, a binary vector, by A. Devoto (Devoto and Turner, unpublished data, 2002). To achieve easier manipulation of the construct, p8.6 from p8.6/pBIN19 was cloned into pBluescript (2.3.2.1). For this, p8.6/pBIN19 was digested with *SalI* and *KpnI*. The digest was fractionated by electrophoresis (2.3.5.1), and the p8.6 fragment was extracted from the DNA gel (2.3.2.2). pBluescript was also cut with *SalI* and *KpnI* (2.3.2.1). The digest was fractionated by electrophoresis (2.3.5.1), and the pBluescript fragment was extracted from the DNA gel (2.3.2.2). The linear pBlueScript was added to the p8.6 fragment and ligated (2.3.2.3). The resulting plasmid, p8.6/pBS, was introduced into *E. coli* by electroporation, and transformants were identified by blue/white selection (2.3.2.4). Next, p8.6 was PCR amplified from p8.6/pBS to add the *attB* recombination site in both ends of p8.6. This PCR product was then introduced into a donor vector, pDONRTM221, by recombination reaction (Figure 4-1). The involved PCR reactions and the full-length sequencing are described below.

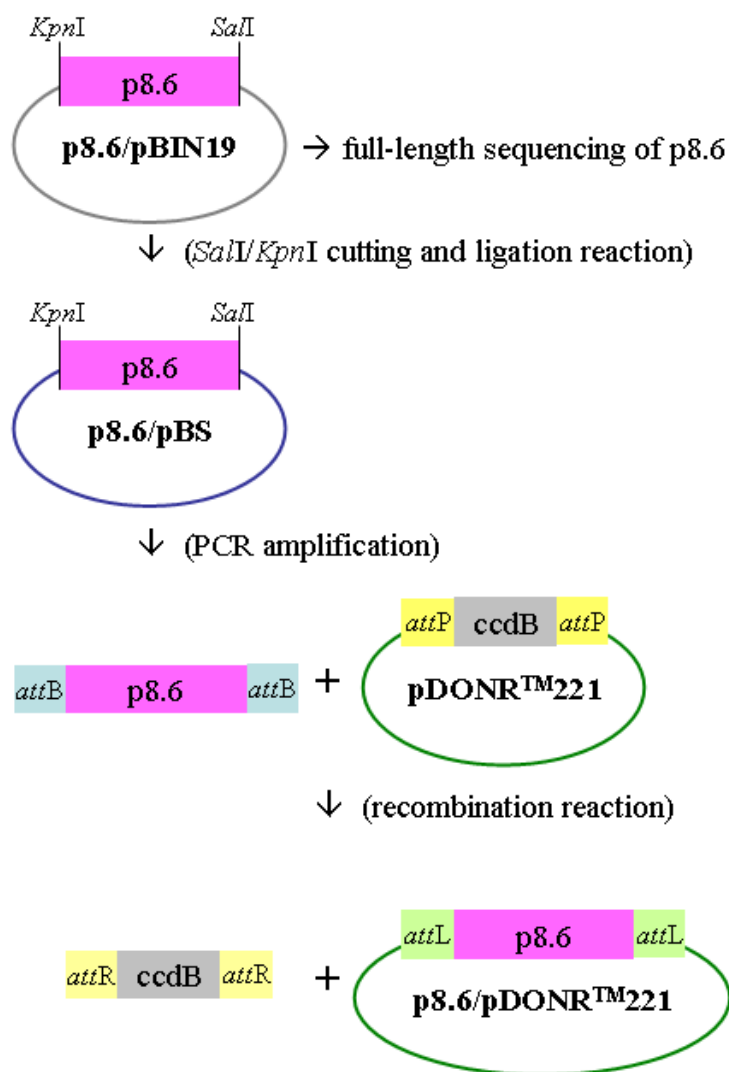


Figure 4-1 Flow chart of the construction of p8.6/pBIN19 to p8.6/pDONR™221. See text (4.2 Summary) for the chart detail.

4.2.1 PCR-based Confirmation of the Presence of p8.6 in pBlueScript

To identify the presence of p8.6 fragment in p8.6/pBS, two primers, T7 forward primer and M13 reverse primer (Table 4-1, 4.2.7), which were present in the pBlueScript vector, were used to amplify a product of about 4,000 bps as determined by gel electrophoresis, representing the DNA fragment between the templates of these two primers in

p8.6/pBS.

Briefly, the PCR solution was prepared as below on ice:

10× NH ₄ reaction buffer (Bioline, London, UK)	2.0 µL
2 mM dNTP (Bioline, London, UK)	2.0 µL
50 mM MgCl ₂ (Bioline, London, UK)	0.6 µL
5 µM T7 forward primer (Sigma-Aldrich, Dorset, UK)	2.0 µL
5 µM M13 reverse primer (Sigma-Aldrich, Dorset, UK)	2.0 µL
BioTaq TM DNA polymerase (Bioline, London, UK)	0.3 µL
Plasmid DNA	0.25 µL
Sterilised distilled water	To make up to 20 µL

General PCR protocols are given in 2.3.3.1. The specific PCR condition was as follows: initial denaturation at 94°C for 2 min; amplification for 30 cycles of 94°C for 1 min, 58°C for 30 sec and 72°C for 4 min 30 sec, and final extension at 72°C for 5 min.

4.2.2 High Fidelity PCR for Gateway Construction

To fuse p8.6 with RFP, the Gateway[®] cloning System was used. A 4,000 bps fragment was amplified with 5pCOI1HA_{att}B and 3pCOI1HA_{att}B primer pairs (Table 4-1, 4.2.7) from p8.6/pBS and the Expand High Fidelity PCR System (Roche, UK) was applied. The Expand High Fidelity PCR System is optimized to efficiently amplify DNA fragments up to 5 kb and it gives better results (higher yield, higher specificity and greater fidelity) than Taq DNA polymerase in PCR reactions. The unique enzyme mix contains thermostable Taq DNA polymerase and Tgo DNA polymerase, a thermostable DNA polymerase with proofreading activity. Therefore, this system is used for amplification of long DNA fragments for cloning.

PCR solution was prepared as below on ice:

Mix 1 (for one reaction)

Reagent	Volume	Final concentration
Sterilised distilled water	Add up to 25 μ L	
Deoxynucleotide mix, 10 mM of each dNTP	1.0 μ L	200 μ M of each dNTP
Forward primer (Sigma-Aldrich, Dorset, UK)	Variable	300 nM
Reverse primer (Sigma-Aldrich, Dorset, UK)	Variable	300 nM
Template DNA	Variable	0.1-250 ng
Final volume	25μL	

Mix 2 (for one reaction)

Reagent	Volume	Final concentration
Sterilised distilled water	19.25 μ L	
Expand High Fidelity buffer, 10 \times conc. With 15 mM MgCl ₂	5 μ L	1 \times (1.5 mM MgCl ₂)
Expand High Fidelity enzyme mix	0.75 μ L	2.6 U/reaction
Final volume	25μL	

General PCR protocols are given in 2.3.3.1. The specific PCR condition was as follows: initial denaturation at 94°C for 2 min; amplification for 30 cycles of 94°C for 15 sec, 65°C for 30 sec and 71°C for 3 min, and final extension at 72°C for 7 min.

4.2.3 PCR-based Confirmation of the Presence of p8.6 in the p8.6/pDONRTM221

To confirm the presence of p8.6 fragment in the p8.6/pDONRTM221, two primers, M13 forward primer and M13 reverse primer (Table 4-1, 4.2.7), were used to amplify a product of about 4,000 bps, representing the DNA between the templates of these two primers in the p8.6/pDONRTM221.

Briefly, the PCR solution was prepared as below on ice:

10× NH ₄ reaction buffer (Bioline, London, UK)	2.0 µL
2 mM dNTP (Bioline, London, UK)	2.0 µL
50 mM MgCl ₂ (Bioline, London, UK)	0.6 µL
5 µM M13 forward primer (Sigma-Aldrich, Dorset, UK)	2.0 µL
5 µM M13 reverse primer (Sigma-Aldrich, Dorset, UK)	2.0 µL
BioTaq TM DNA polymerase (Bioline, London, UK)	0.3 µL
Plasmid DNA	0.5 µL
Sterilised distilled water	To make up to 20 µL

General PCR protocols are given in 2.3.3.1. The specific PCR condition was as follows: initial denaturation at 94°C for 2 min; amplification for 30 cycles of 94°C for 1 min, 58°C for 30 sec and 72°C for 4 min, and final extension at 72°C for 5 min.

4.2.4 PCR-based Confirmation of the Presence of *COII* in the p8.6/pDONRTM221

To identify the presence of *COII* gene in the p8.6/pDONRTM221, two primers, ADs23 forward primer and ADa32 reverse primer (Table 4-1 and Figure 4-1, 4.2.7, Devoto and Turner, unpublished data, 2002), were used to amplify a product of about 1,700 bps that confirmed the presence of the *COII*-specific fragment in the p8.6/pDONRTM221.

Briefly, the PCR solution was prepared as below on ice:

10× NH ₄ reaction buffer (Bioline, London, UK)	2.0 µL
2 mM dNTP (Bioline, London, UK)	2.0 µL
50 mM MgCl ₂ (Bioline, London, UK)	0.6 µL
0.1 µg/µL ADs23 primer (Sigma-Aldrich, Dorset, UK)	1.0 µL
0.1 µg/µL ADa32 primer (Sigma-Aldrich, Dorset, UK)	1.0 µL
BioTaq TM DNA polymerase (Bioline, London, UK)	0.3 µL
Plasmid DNA	0.5 µL
Sterilised distilled water	To make up to 20 µL

General PCR protocols are given in 2.3.3.1. The specific PCR condition was as follows: initial denaturation at 94°C for 2 min; amplification for 30 cycles of 94°C for 1 min, 55°C for 30 sec and 72°C for 2 min, and final extension at 72°C for 5 min.

4.2.5 PCR-based Confirmation of the Presence of *COI1* Native Promoter and *COI1* Gene in the p8.6/pDONRTM221

To identify the presence of *pCOI1::COI1* in the p8.6/pDONRTM221 and to check the specificity of two primers designed for sequencing the *COI1* native promoter, two forward primers, pCOI1f01 and pCOI1f02 (Table 4-1, 4.2.7), were paired with ADa32 reverse primer, separately, for the PCR amplification. The pCOI1f01 forward primer + ADa32 reverse primer pairs amplified a 2,900 bps PCR product. The pCOI1f02 forward primer + ADa32 reverse primer pairs amplified a 2,400 bps PCR product. Both fragment confirmed the presence of *pCOI1::COI1* in p8.6/pDONRTM221.

The PCR solution was prepared as below on ice:

pCOI1f01 forward primer + ADa32 reverse primer

10× NH ₄ reaction buffer (Bioline, London, UK)	2.0 µL
2 mM dNTP (Bioline, London, UK)	2.0 µL
50 mM MgCl ₂ (Bioline, London, UK)	0.6 µL
5 µM pCOI1f01 primer (Sigma-Aldrich, Dorset, UK)	2.0 µL
0.1 µg/µL ADa32 primer (Sigma-Aldrich, Dorset, UK)	1.0 µL
BioTaq TM DNA polymerase (Bioline, London, UK)	0.3 µL
Plasmid DNA	0.5 µL
Sterilised distilled water	To make up to 20 µL

General PCR protocols are given in 2.3.3.1. The specific PCR condition was as follows: initial denaturation at 94°C for 2 min; amplification for 30 cycles of 94°C for 1 min, 55°C for 30 sec and 72°C for 3 min 30 sec, and final extension at 72°C for 5 min.

pCOI1f02 forward primer + ADa32 reverse primer

10× NH ₄ reaction buffer (Bioline, London, UK)	2.0 µL
2 mM dNTP (Bioline, London, UK)	2.0 µL
50 mM MgCl ₂ (Bioline, London, UK)	0.6 µL
5 µM pCOI1f02 primer (Sigma-Aldrich, Dorset, UK)	2.0 µL
0.1 µg/µL ADa32 primer (Sigma-Aldrich, Dorset, UK)	1.0 µL
BioTaq TM DNA polymerase (Bioline, London, UK)	0.3 µL
Plasmid DNA	0.5 µL
Sterilised distilled water	To make up to 20 µL

General PCR protocols are given in 2.3.3.1. The specific PCR condition was as follows: initial denaturation at 94°C for 2 min; amplification for 30 cycles of 94°C for 1 min, 44°C for 30 sec and 72°C for 3 min, and final extension at 72°C for 5 min.

4.2.6 Primers with *attB* Recombination Used to Amplify p8.6 Site for Gateway[®] Cloning System

Primers were designed to amplify the p8.6 fragment, which is 4,027 kb, from p8.6/pBS. The designed gene-specific primers were left genomic primer (5pCOI1HA*attB*) and right genomic primer (3pCOI1HA*attB*). The primer pairs were designed to incorporate the *attB* recombination site into the PCR products. Guidelines for primer design were provided in the Gateway[®] Technology with ClonaseTM II user manual, page 12-15.

All primer sequences are shown in Table 4-1 (4.2.7).

4.2.7 Primers Used in Full-Length Sequencing of the *COI1* Native Promoter

To perform full-length sequencing of p8.6, two forward primers, pCOI1f01 and pCOI1f02 (Table 4-1), were designed specifically for the *COI1* native promoter region, because the p*COI* fragment was too long to be completely sequenced with just one forward and one reverse primer. The existing primers, ADs23, ADs25, and ADa32

(Table 4-1, Devoto and Turner, unpublished data, 2002), were also used for full-length sequencing of p8.6. The positions of the primers in p8.6 are shown in Figure 4-2.

Table 4-1 The sequences of primers.

Name	Sequence
T7 forward primer	5' - TAA TAC GAC TCA CTA TAG GG -3'
M13 reverse primer	5' - CAG GAA ACA GCT ATG ACC -3'
M13 forward primer	5' - TGT AAA ACG ACG GCC AGT -3'
ADs23	5' -AGT CTT CTC CGA TTC ACC-3'
ADs25	5' -TGC TCA GCA CAA CAC ATC TC-3'
ADs29	5' -ATG GAA TTC TCA AGA GGC TG-3'
ADa32	5' -ACA AGT ATC TCA GTG AAG GC-3'
5pCOI1HA <i>att</i> B	5'-GGG GAC AAG TTT GTA CAA AAA AGC AGG CTT TTG GAA TCA GAC AAA TTA TTG CT-3'
3pCOI1HA <i>att</i> B	5'-GGG GAC CAC TTT GTA CAA GAA AGC TGG GTA CTC AGC ATA ATC TGG AAC CTG CAC-3'
pCOI1f01	5' -CGC TGG TCG AGA AAG G-3'
pCOI1f02	5' -CAC TGA AAG AAA TTT C-3'

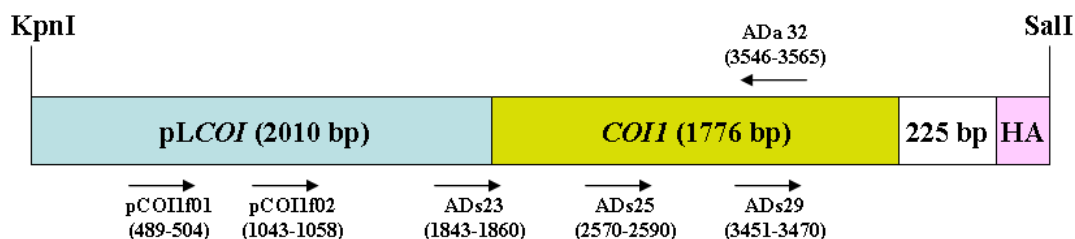


Figure 4-2 The map of primers in p8.6 (*pCOI1::COI1::HA*).

4.3 Results

4.3.1 Making of p8.6/pBS

First, the p8.6/pBIN19 plasmid was digested with *SalI* and *KpnI*. Reaction products of the double digestion were then run on an agarose gel (2.3.5). In Figure 4-3, lanes 4, 5

and 6, two linear fragments were separated, one was bigger than 12,000 bps and represented the pBIN19 vector, and the other was about 4,000 bps and represented p8.6. Likewise, the pBluescript vector was digested with *SalI* and *KpnI* and the reaction products of the double digestion were run on an agarose gel (2.3.5). In Figure 4-3, lane 1, 2 and 3, one linear fragment of about 3,000 bps represented the pBluescript fragment. Another fragment cut between *SalI* and *KpnI* smaller than 100 bps should have been produced but either ran off the gel, or was too faint to seen.

Next, the linear pBluescript and p8.6 were extracted from the agarose gel (2.3.2.2), and ligated to each other (2.3.2.3). The ligation mix was introduced into *E. coli* by electroporation and transformants were identified by blue/white selection (2.3.2.4). Seven colonies were picked for checking the existence of p8.6/pBS, but only p8.6/pBS_#4 and p8.6/pBS_#7 gave positive results. In Figure 4-4, plasmid DNA from p8.6/pBS_#4 and p8.6/pBS_#7 was examined by PCR reaction (4.2.1) and restriction digestion. A DNA product of about 4,000 bps was amplified in both #4 and #7 by using the T7 forward and M13 reverse primer pair. Two bands, 3,000 and 4,000 bps, respectively, were produced in both #4 and #7 cut by *SalI* and *KpnI*. However, there was also an unknown band of about 2,000 bps in the *SalI/KpnI* cutting product of #4. Therefore, p8.6/pBS_#7 was used in following procedures, as it was composed of purely p8.6 (~4,000 bps) and pBluescript (~3,000 bps).

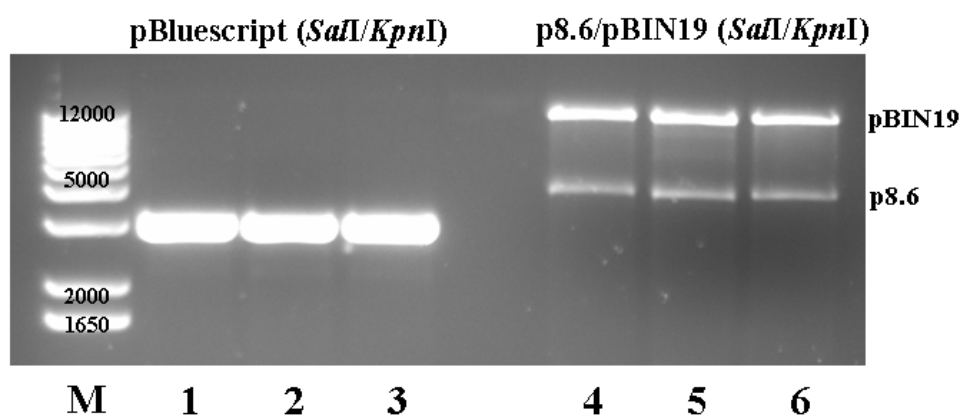


Figure 4-3 *SalI/KpnI* digestion of pBluescript and p8.6/pBIN19. An amount of 15 μ L of the double digestion product was loaded onto each lane. Marker (M) was a DNA ladder. pBluescript cut with *SalI* and *KpnI* was loaded onto lanes 1, 2, and 3. p8.6/pBIN19 cut with *SalI* and *KpnI* was loaded onto lanes 4, 5, and 6.

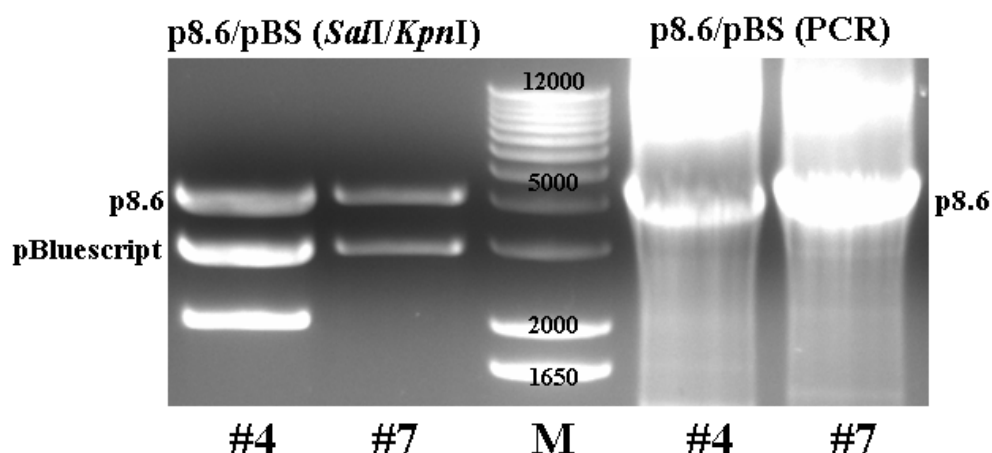


Figure 4-4 Identification of the p8.6/pBS candidates. Two candidates, #4 and #7, were examined. An amount of 10 μ L of the double digestion or PCR products were loaded onto each lane. Marker (M) was a DNA ladder. The linear p8.6 and pBluescript were marked next to the DNA bands.

4.3.2 p8.6-RFP Construction Using the Gateway[®] Cloning System

In the Gateway[®] cloning procedure, a PCR product suitable for use as substrates in a Gateway[®] BP recombination reaction with a donor vector has to be made. For this, an *attB* recombination site was incorporated into both ends of p8.6 by high fidelity PCR amplification (4.2.2). The purified *attB*-PCR product, and the *attP*-containing donor vector, pDONRTM221, was used in the Gateway[®] BP recombination to create an entry clone, p8.6/pDONRTM221, which was then introduced into DH10BTM *E. coli* by electroporation. Because the negative selection gene, *ccdB*, in pDONRTM221 was exchanged with p8.6 after recombination, the donor vector would not be able to grow on normal LB medium (page 16-25, Gateway[®] Technology with ClonaseTM II user manual).

To identify p8.6/pDONRTM221 constructs, PCR reaction (4.2.1) and restriction digestion were both used. In Figure 4-5, results for 8 candidates are shown, and colonies #1, #3, #4, #5, #7 and #8 gave two bands of approximately 4,000 bps and 12,000 bps, which correspond to p8.6 and pDONRTM221, respectively. These 6 candidates also gave

a single PCR product of about 4,000 bps (Figure 4-5), which corresponds to p8.6, suggesting that p8.6 had exchanged into the pDONRTM221 vector in #1, #3, #4, #5, #7 and #8.

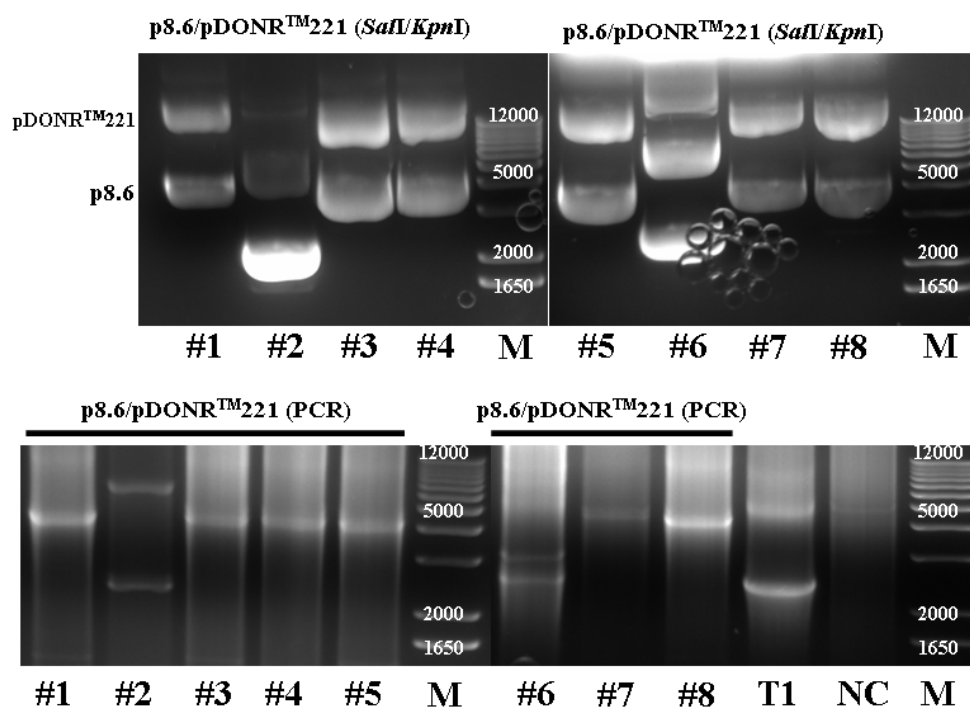


Figure 4-5 Identification of the p8.6/ pDONRTM221 candidates. Eight candidates were examined here. An amount of 10 μ L of the double digestion or PCR products were loaded onto each lane. Marker (M) was a DNA ladder. T1 was a p8.6/ pDONRTM221 candidate from previous selection. pDONRTM221 was used as negative control (NC).

To further confirm the presence of p8.6 and the specificity of the *pCOII* primers, pCOI1f01 and pCOI1f02 (Table 4-1), three sets of primer pairs, including ADs23 + ADa32, pCOI1f01 + ADa32, and pCOI1f02 + ADa32, were used to amplify DNA from p8.6/pDONRTM221 candidates. In Figure 4-6, a product of about 1,700 bps was amplified with primer pair ADs23 + ADa32 from #1, #3, #4, #5, #7 and #8. Likewise, a product of about 2,900 bps was amplified with primer pair pCOI1f01 + ADa32, and a product of about 2,400 bps was amplified with primer pair pCOI1f02 + ADa32, indicating #1, #3, #4, #5, #7 and #8 all contained p8.6 fragment, and that the *pCOII* primers are specific for the *COII* promoter.

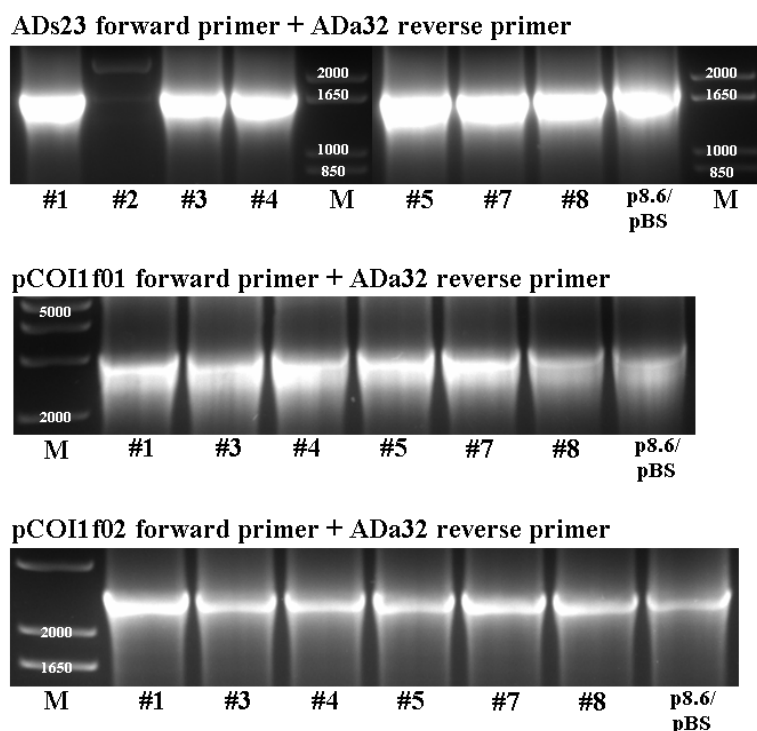


Figure 4-6 PCR reactions for p8.6/pDONRTM221 candidates using three sets of primer pairs. Primer pairs included ADs23 + ADa32, pCOI1f01 + ADa32, and pCOI1f02 + ADa32. An amount of 10 μ L of the PCR products were loaded onto each lane. Marker (M) was a DNA ladder. p8.6/pBS was used as positive control.

Before performing the LR recombination reaction for creating the expression clone, p8.6/pDONRTM221 #1, #3, #4, #5, #7 and #8 were all sequenced (2.3.3.3) with M13 forward primer to ensure there was no point mutation happened during the High Fidelity PCR. In addition, p8.6/pBS was sequenced with T7 forward primer to provide a template for DNA alignment along with the genome sequence from Tair (2.6.2). Results from the sequencing reactions gave approximately 1,200 bps DNA, but only the sequence after 50 until 900 base pairs (bps) were considered, because the quality of sequencing in the beginning was poor, and the sequence deteriorated in the end.

After aligning the sequencing results of p8.6/pDONRTM221 #1, #3, #4, #5, #7 and #8 with the Tair database and the sequencing result of p8.6/pBS, more than 2 point mutations were found in p8.6/pDONRTM221 #1, #3, #4, #5 and #7, but no mutation or

deletion was identified in p8.6/pDONRTM221 #8 (Table 4-2). Therefore, p8.6/pDONRTM221 #8 was further sequenced with pCOIIf01, pCOIIf02, ADs23, ADs25 and M13 reverse primer. p8.6/pBS was also sequenced with pCOIIf01, pCOIIf02, ADs23, ADs25 and M13 reverse primer for DNA alignment with p8.6/pDONRTM221 #8 and full-length analysis (4.3.3).

Table 4-2 List of base substitutions occurred in first 900 bps of the p8.6/pDONRTM221 candidates #1, #3, #4, #5, #7 and #8.

Candidate	Details and positions of base substitutions
p8.6/pDONR TM 221 #1	T-C (88), T-C (348)
p8.6/pDONR TM 221 #3	T-C (101), A-T (205), T-C (279), T-C (695)
p8.6/pDONR TM 221 #4	T-C (323), A-G (523)
p8.6/pDONR TM 221 #5	G-A (202), T-C (245), A-G (414), T-C (616)
p8.6/pDONR TM 221 #7	T-C (88), C-A (105), C-A (261), T-C (586)
p8.6/pDONR TM 221 #8	No error

Complete sequencing of p8.6/pDONRTM221 #8 revealed that there were 4 mutations (T to A transition (1004), T to C transition (1007), A to G transition (1360) and T to C transition (1431)) and 1 insertion (T/1024) in the *pCOII* region, and there were at least 5 mutations (T to A transition (577), T to C transition (590), G to A transition (724), T to C transition (817) and G to A transition (1346)), 1 deletion (A/1642) and 11 nucleotide insertions (AGCTTCCACCA) in the *COII* region (Figure 4-7 and 4-8). The mutations, deletion and insertions were all confirmed **twice** by overlapping (at least 150 bps) results from individual sequencing. In addition, all of the mutations in the *COII* region caused a change of amino acids after translation, for instance, the T to A transition (577) changed Ser to Thr, the T to C transition (590) changed Leu to Ser, the G to A transition (724) changed Ala to Thr, the T to C transition (817) changed Cys to Arg, and the G to A transition (1346) changed Ala to Thr.

Chapter 4: Construction of pCOII::COII::RFP

tair
p8.6
TGGAATCAGACAAATTATTGCTTTTGAAGAAGCAGAGTCAACACCAAGTACAATGACCGG
TGGAATCAGACAAATTATTGCTTTTGAAGAAGCAGAGTCAACACCAAGTACAATGACCGG

tair
p8.6
ACCTCCCCCATTTCTTTGAAGATGGGTCCACCAGTCTTTCTCCTTATTATTGCTGGTG
ACCTCCCCCATTTCTTTGAAGATGGGTCCACCAGTCTTTCTCCTTATTATTGCTGGTG

tair
p8.6
CCCTCCAACCACTTCATCGCTTCACGCACCATCTGCCTCTTATCAGTTCCCTCCACTATC
CCCTCCAACCACTTCATCGCTTCACGCACCATCTGCCTCTTATCAGTTCCCTCCACTATC

tair
p8.6
CATTGAGCTACCTTCCCTTCCGCCACTTTCTCCTTATTACCAGCATCGGGATCAGATGG
CATTGAGCTACCTTCCCTTCCGCCACTTTCTCCTTATTACCAGCATCGGGATCAGATGG

tair
p8.6
ATTCTTGATCCCGTCATCACCCTCGATCTCTCTGACATCCCTCCATTACCATTAGTCCA
ATTCTTGATCCCGTCATCACCCTCGATCTCTCTGACATCCCTCCATTACCATTAGTCCA

tair
p8.6
CCACATACCCATTCCAGGCTCATCATCATCATCATCCCAGCAACAGATGATGATTCTAT
CCACATACCCATTCCAGGCTCATCATCATCATCATCCCAGCAACAGATGATGATTCTAT

tair
p8.6
AATGTGCGACCTATTGTTTCATATTCCAGTTATCGATATCTTCTCTTCAGGTCAAAGCTA
AATGTGCGACCTATTGTTTCATATTCCAGTTATCGATATCTTCTCTTCAGGTCAAAGCTA

tair
p8.6
TCTGGTAAGCGCTGGACCCACCGGGATAATATCCACGGGCATCCCTCCGCTCCCAGTGGA
TCTGGTAAGCGCTGGACCCACCGGGATAATATCCACGGGCATCCCTCCGCTCCCAGTGGA

tair
p8.6
GAATGATTCGCTGGTCGAGAAAGGTGCAAGAGAAACACTACGATTGCTCATAAGCGGAGC
GAATGATTCGCTGGTCGAGAAAGGTGCAAGAGAAACACTACGATTGCTCATAAGCGGAGC

tair
p8.6
CAATGCAACAACATCTACACCTTTGAACCATCATGGAAGCAGAGGTCTATACAGTGTGAG
CAATGCAACAACATCTACACCTTTGAACCATCATGGAAGCAGAGGTCTATACAGTGTGAG

tair
p8.6
CCGGGATGTGAGTGGTGTGAGCTTGTGTTGCACCTATTGGGTTGCAACAACCGAGTTCAGT
CCGGGATGTGAGTGGTGTGAGCTTGTGTTGCACCTATTGGGTTGCAACAACCGAGTTCAGT

tair
p8.6
TGAGGGAGGAGATGGTGGTGGTGAGAGTGTGAGCTCAAGCGAAGCAGTGCCTGCGCCTCC
TGAGGGAGGAGATGGTGGTGGTGAGAGTGTGAGCTCAAGCGAAGCAGTGCCTGCGCCTCC

tair
p8.6
CAGAGAGACTTCTGGTTAATTTTTTTGGTTCTTTGTAAGTGTGGTCCGAGTTAAGTGTAT
CAGAGAGACTTCTGGTTAATTTTTTTGGTTCTTTGTAAGTGTGGTCCGAGTTAAGTGTAT

tair
p8.6
AGAAAACCTCATCTCTCGCCTAGTTTTTGGTTTTGTTTCAGCCCAAGTCTTTTGGTTTTCAGG
AGAAAACCTCATCTCTCGCCTAGTTTTTGGTTTTGTTTCAGCCCAAGTCTTTTGGTTTTCAGG

Chapter 4: Construction of pCOII::COII::RFP

tair p8.6	TGTAATTAGTCGGGTTTTTTGTAGCTTGCTTATATTACCTTTGTTATTTCCGAGTTTCAA TGTAATTAGTCGGGTTTTTTGTAGCTTGCTTATATTACCTTTGTTATTTCCGAGTTTCAA *****
tair p8.6	ATGAAGCTAAGAAATACGATCATAATAAAAAAGTTCTTTTGCGAGTATTCATTTTCTTTCA ATGAAGCTAAGAAATACGATCATAATAAAAAAGTTCTTTTGCGAGTATTCATTTTCTTTCA *****
tair p8.6	TGGTTCCTCCTTATTCATAGTCATTGTTGTTCTTTCTAATACTTTCTGAGCTTTTTT TGGTTCCTCCTTATTCATAGTCATTGTTGTTCTTTCTAATACATTCCTGAGCTTTTTT ***** ** *****
tair p8.6	TTT-CTATTGGAAAACTTTTGTCACTGAAAGAAATTTCAATGTGATTGGTCTTTTCGC TTTCTATTGGAAAACTTTTGTCACTGAAAGAAATTTCAATGTGATTGGTCTTTTCGC *** *****
tair p8.6	AACTGTAATAAGCACTAAAAGTTAATAATTGCTGCTTTTAAAGTCTTGTGCTGAATGA AACTGTAATAAGCACTAAAAGTTAATAATTGCTGCTTTTAAAGTCTTGTGCTGAATGA *****
tair p8.6	TTTAATCCCAAAGACGTTAAAAAAAAGACATGTAAATAGTCTTTGTTCCAAAAGTACCAT TTTAATCCCAAAGACGTTAAAAAAAAGACATGTAAATAGTCTTTGTTCCAAAAGTACCAT *****
tair p8.6	TTTGAGCGCTTTCTTTTCGACAATTGATGTTGAACTTGTACCAAATAAACCTTGAAAATCA TTTGAGCGCTTTCTTTTCGACAATTGATGTTGAACTTGTACCAAATAAACCTTGAAAATCA *****
tair p8.6	TACATCATTAATGTAGTTTTTTGTTATATACTTATATTCATATGGTCCATAATATATAG TACATCATTAATGTAGTTTTTTGTTATATACTTATATTCATATGGTCCATAATATATAG *****
tair p8.6	TTAACCATATTATGGACCATATAAATTCATGCAGTCAACAAGCTTTTTTTTCCTCATTA TTAACCATATTATGGACCATATAAATTCATGCAGTCAACAAGCTTTTTTTTCCTCATTA ***** *****
tair p8.6	AAGCTACTAATACTGTAGAAAATTTTTATCTTACAAAAGAAAGGAGAATTAATGTATTTT AAGCTACTAATACTGTAGAAAATTTTTATCTTACAAAAGAAAGGAGAATTAATGTATTTT ***** *****
tair p8.6	TATTTTAATCACATATAAAGCAACCAAGATAACATATACTAGTATTTAGTATTTTAAA TATTTTAATCACATATAAAGCAACCAAGATAACATATACTAGTATTTAGTATTTTAAA *****
tair p8.6	TTTTTTGCTTAGGATTCAGGTTATTAATACTCTATAAAGAAATAATTAAATCTATCCATC TTTTTTGCTTAGGATTCAGGTTATTAATACTCTATAAAGAAATAATTAAATCTATCCATC *****
tair p8.6	GAATAAATCACACAGCTTATTGGATCAGTTAAATATTCTAATAATATTGTCGTGTAGCTG GAATAAATCACACAGCTTATTGGATCAGTTAAATATTCTAATAATATTGTCGTGTAGCTG *****
tair p8.6	AGATCTGACCACTGCAAAAATGAAAAGAAAAACATAGAAGTAGAGAGAAGATCGCATCTC AGATCTGACCACTGCAAAAATGAAAAGAAAAACATAGAAGTAGAGAGAAGATCGCATCTC *****

Chapter 4: Construction of *pCOII::COII::RFP*

tair
p8.6
GACCGTCAACTTCAGTGTATGAAATAATGATCGTCCCACTTGATCCTCAAAAATATTATT
GACCGTCAACTTCAGTGTATGAAATAATGATCGTCCCACTTGATCCTCAAAAATATTATT

tair
p8.6
AACCAAACAAAATTTGATTCCATCGTCCCACTTTCTTCTTCTTCTCCTCCCAATCCGCCTCT
AACCAAACAAAATTTGATTCCATCGTCCCACTTTCTTCTTCTTCTCCTCCCAATCCGCCTCT

tair
p8.6
TCTTCTACGCGTGTCTTCTTCTCCTCACTCTCTCAATCTCTAGTCTTCTCCGATTAC
TCTTCTACGCGTGTCTTCTTCTCCTCACTCTCTCAATCTCTAGTCTTCTCCGATTAC

tair
p8.6
CGGATCTTTCCTTTCTTACTTCTTTCTTCTCACTCTGGTGGTTATGTGTGGATCTGCGAC
CGGATCTTTCCTTTCTTACTTCTTTCTTCTCACTCTGGTGGTTATGTGTGGATCTGCGAC

tair
p8.6
CTCGATTTCAATTGGAAGTCGTCGGTTTCTTCTCTAAATCGAATCTTTCAGGATTCGTT
CTCGATTTCAATTGGAAGTCGTCGGTTTCTTCTCTAAATCGAATCTTTCAGGATTCGTT

tair
p8.6
TGTTTTTTTCTTTTGTTTTTTTTTCGATCCGA-----TGGAGGATCCTGATATC
TGTTTTTTTCTTTTGTTTTTTTTTCGATCCGAAGCTTCCACCATGGAGGATCCTGATATC

tair
p8.6
AAGAGGTGTAAATTGAGCTGCGTCGCGACGGTTGATGATGTCATCGAGCAAGTCATGACC
AAGAGGTGTAAATTGAGCTGCGTCGCGACGGTTGATGATGTCATCGAGCAAGTCATGACC

tair
p8.6
TATATAACTGACCCGAAAGATCGCGATTTCGGCTTCTTTGGTGTGTCGGAGATGGTTCAAG
TATATAACTGACCCGAAAGATCGCGATTTCGGCTTCTTTGGTGTGTCGGAGATGGTTCAAG

tair
p8.6
ATTGATTCCGAGACGAGAGAGCATGTGACTATGGCGCTTTGCTACACTGCGACGCCTGAT
ATTGATTCCGAGACGAGAGAGCATGTGACTATGGCGCTTTGCTACACTGCGACGCCTGAT

tair
p8.6
CGTCTTAGCCGTCGATTCCCGAAGTTGAGTTCGCTCAAGCTTAAAGGCAAGCCTAGAGCA
CGTCTTAGCCGTCGATTCCCGAAGTTGAGTTCGCTCAAGCTTAAAGGCAAGCCTAGAGCA

tair
p8.6
GCTATGTTTAATCTGATCCCTGAGAAGTGGGAGGTTATGTTACTCCTTGGGTTACTGAG
GCTATGTTTAATCTGATCCCTGAGAAGTGGGAGGTTATGTTACTCCTTGGGTTACTGAG

tair
p8.6
ATTTCTAACAACCTTAGGCAGCTCAAATCGGTGCACTTCCGACGGATGATTGTCAGTGAC
ATTTCTAACAACCTTAGGCAGCTCAAATCGGTGCACTTCCGACGGATGATTGTCAGTGAC

tair
p8.6
TTAGATCTAGATCGTTTAGCTAAAGCTAGAGCAGATGATCTTGAGACTTTGAAGCTAGAC
TTAGATCTAGATCGTTTAGCTAAAGCTAGAGCAGATGATCTTGAGACTTTGAAGCTAGAC

tair
p8.6
AAGTGTTCTGGTTTTACTACTGATGGACTTTTGAGCATCGTTACACACTGCAGGAAAATA
AAGTGTTCTGGTTTTACTACTGATGGACTTTTGAGCATCGTTACACACTGCAGGAAAATA

Chapter 4: Construction of pCOII::COII::RFP

tair
p8.6
AAAACTTTGTAAATGGAAGAGAGTTCTTTTAGTGAAAAGGATGGTAAGTGGCTTCATGAG
AAAACTTTGTAAATGGAAGAGAGTTCTTTTAGTGAAAAGGATGGTAAGTGGCTTCATGAG

tair
p8.6
CTTGCTCAGCACAAACACA~~T~~CTCTTGAGGTTT~~T~~AAACTTCTACATGACGGAGTTTGCCAAA
CTTGCTCAGCACAAACACA~~A~~CTCTTGAGGTTT~~C~~AAACTTCTACATGACGGAGTTTGCCAAA

tair
p8.6
ATCAGTCCCAAAGACTTGGAACCATAGCTAGAAATTGCCGCTCTCTGGTATCTGTGAAG
ATCAGTCCCAAAGACTTGGAACCATAGCTAGAAATTGCCGCTCTCTGGTATCTGTGAAG

tair
p8.6
GTCGGTGACTTTGAGATTTTGGAACTAGTTGGGTTCTTTAAGGCT~~G~~CAGCTAATCTTGAA
GTCGGTGACTTTGAGATTTTGGAACTAGTTGGGTTCTTTAAGGCT~~A~~CAGCTAATCTTGAA

tair
p8.6
GAATTTTGTGGTGGCTCCTTGAATGAGGATATTGGAATGCCTGAGAAGTACATGAATCTG
GAATTTTGTGGTGGCTCCTTGAATGAGGATATTGGAATGCCTGAGAAGTACATGAATCTG

tair
p8.6
GTTTTTCCCCGAAAAC~~T~~A~~T~~CTCGGCTTGGTCTCTCTTACATGGGACCTAATGAAATGCCA
GTTTTTCCCCGAAAAC~~T~~A~~C~~CTCGGCTTGGTCTCTCTTACATGGGACCTAATGAAATGCCA

tair
p8.6
ATACTATTTCCATTTCGCGGCCCAAATCCGAAAGCTGGATTGCTTTATGCATTGCTAGAA
ATACTATTTCCATTTCGCGGCCCAAATCCGAAAGCTGGATTGCTTTATGCATTGCTAGAA

tair
p8.6
ACTGAAGACCATTGTACGCTTATCCAAAAGTGTCTAATTGGAAGTTCTCGAGACAAGG
ACTGAAGACCATTGTACGCTTATCCAAAAGTGTCTAATTGGAAGTTCTCGAGACAAGG

tair
p8.6
AATGTAATCGGAGATAGGGGTCTAGAGGTCCTTGCACAGTACTGTAAGCAGTTGAAGCGG
AATGTAATCGGAGATAGGGGTCTAGAGGTCCTTGCACAGTACTGTAAGCAGTTGAAGCGG

tair
p8.6
CTGAGGATTGAACGCGGTGCAGATGAACAAGGAATGGAGGACGAAGAAGGCTTAGTCTCA
CTGAGGATTGAACGCGGTGCAGATGAACAAGGAATGGAGGACGAAGAAGGCTTAGTCTCA

tair
p8.6
CAAAGAGGATTAATCGCTTTGGCTCAGGGCTGCCAGGAGCTAGAATACATGGCGGTGTAT
CAAAGAGGATTAATCGCTTTGGCTCAGGGCTGCCAGGAGCTAGAATACATGGCGGTGTAT

tair
p8.6
GTCTCAGATATAACTAACGAATCTCTTGAAAGCATAGGCACATATCTGAAAAACCTCTGT
GTCTCAGATATAACTAACGAATCTCTTGAAAGCATAGGCACATATCTGAAAAACCTCTGT

tair
p8.6
GACTTCCGCCTTGTCTTACTCGACCGGGAAGAAAGGATTACAGATCTGCCACTGGACAAC
GACTTCCGCCTTGTCTTACTCGACCGGGAAGAAAGGATTACAGATCTGCCACTGGACAAC

tair
p8.6
GGAGTCCGATCTCTTTTGATTGGATGCAAGAACTCAGACGATTTGCATTCTATCTGAGA
GGAGTCCGATCTCTTTTGATTGGATGCAAGAACTCAGACGATTTGCATTCTATCTGAGA

```

tair      CAAGGCGCTTAACCGACTTGGGCTTAAGCTACATCGGACAGTACAGTCCAAACGTGAGA
p8.6      CAAGGCGACTTAACCGACTTGGGCTTAAGCTACATCGGACAGTACAGTCCAAACGTGAGA
          *****

tair      TGGATGCTGCTGGGTTACGTAGGTGAATCAGATGAAGGTTTAATGGAATTCTCAAGAGGC
p8.6      TGGATGCTGCTGGGTTACGTAGGTGAATCAGATGAAGGTTTAATGGAATTCTCAAGAGGC
          *****

tair      TGTCCAAATCTACAGAAGCTAGAGATGAGAGGTTGTTGCTTCAGTGAGCGAGCAATCGCT
p8.6      TGTCCAAATCTACAGAAGCTAGAGATGAGAGGTTGTTGCTTCAGTGAGCGAGCAATCGCT
          *****

tair      GCAGCGGTTACAAAATTGCCTTCACTGAGATACTTGTGGGTACAAGGTTACAGAGCATCG
p8.6      GCAGCGGTTACAAAATTGCCTTCACTGAGATACTTGTGGGTACAAGGTTACAGAGCATCG
          *****

tair      ATGACGGGACAAGATCTAATGCAGATGGCTAGACCGTACTGGAACATCGAGCTGATTCCA
p8.6      ATGACGGGACAAGATCTAATGCAGATGGCTAGACCGTACTGGAACATCGAGCTGATTCCA
          *****

tair      TCAAGAAGAGTCCCGGAAGTGAATCAACAAGGAGAGATAAGAGAGATGGAGCATCCGGCT
p8.6      TCA-GAAGAGTCCCGGAAGTGAATCAACAAGGAGAGATAAGAGAGATGGAGCATCCGGCT
          *** *****

tair      CATATATTGGCTTACTACTCTCTGGCTGGCCAGAGAACAGATTGTCCAACAACGTGTTAGA
p8.6      CATATATTGGCTTACTACTCTCTGGCTGGCCAGAGAACAGATTGTCCAACAACGTGTTAGA
          *****

tair      GTCCTGAAGGAGCCAATAT
p8.6      GTCCTGAAGGAGCCAATAT
          *****

```

Figure 4-7 DNA alignment of the Tair genome sequence and the completely sequenced p8.6/pBS and p8.6/pDONRTM221 #8. Mutations, insertions and deletion happened in p8.6/pDONRTM221 #8 are marked in red. Mutation, insertion and deletion happened in both p8.6/pBS and p8.6/pDONRTM221 #8 are bold and marked in red.

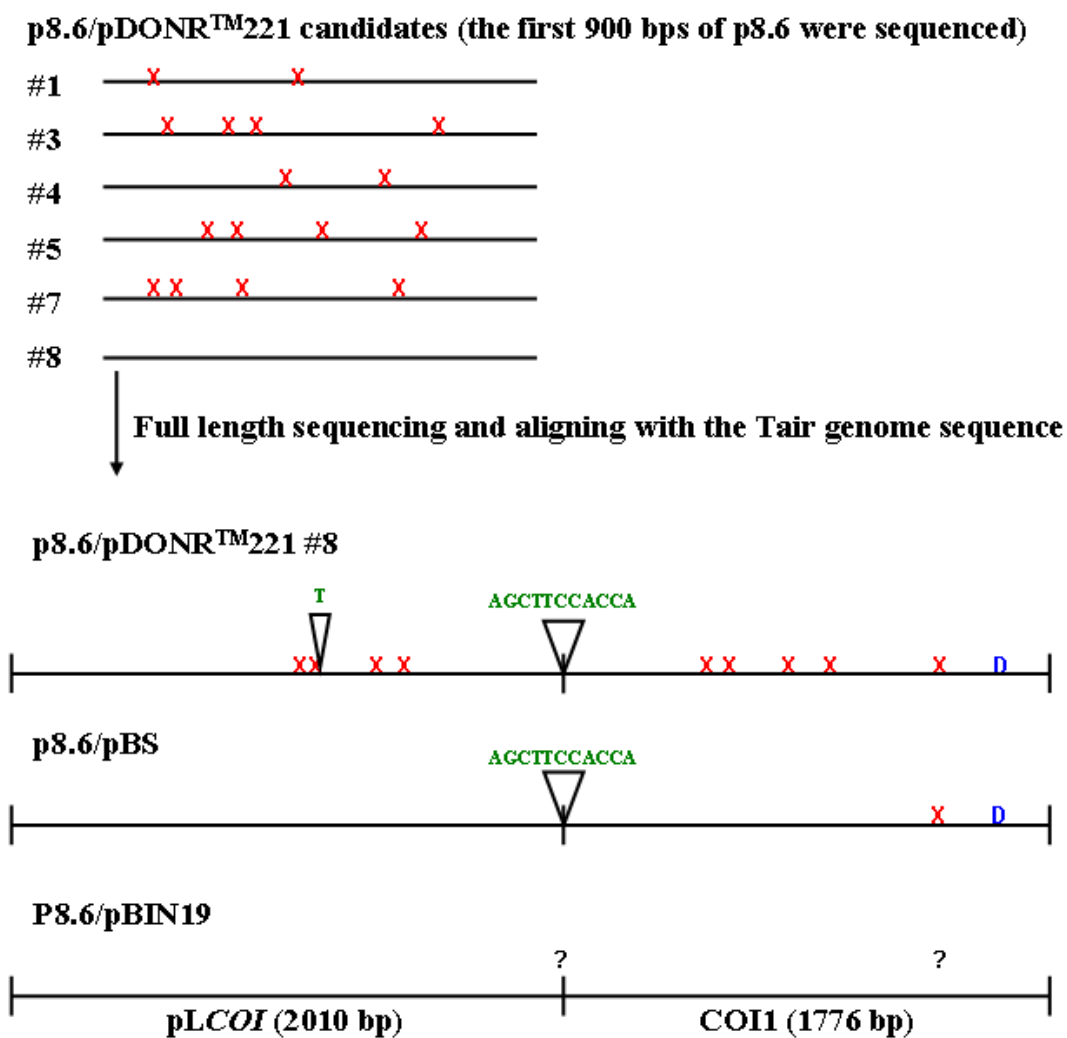


Figure 4-8 Diagram of sequencing and aligning processes of the p8.6/pDONRTM221 candidates, p8.6/pBS and p8.6/pBIN19. Nucleotide substitutions are marked as red X corresponding to Table 4-2. A single nucleotide deletion is marked as blue D. Insertions are marked as triangles and the inserted nucleotides are indicated in green.

Complete sequencing of p8.6/pBS also revealed one mutation, one deletion and one insertion already existed in the p8.6/pBS before the *attB*-PCR amplification. They were the G to A transition (1346), the A/1642 deletion, and the 11 nucleotides insertion (AGCTTCCACCA) in the middle of the start codon (Figure 4-6 and 4-7). These results indicated that at least 8 mutations probably occurred during the high fidelity PCR amplification. The differences between the Tair database and p8.6 is puzzling, and suggesting that errors were introduced during previous construction.

Due to the higher error rate of the high fidelity PCR, an alternative strategy to clone p8.6-RFP, using restriction enzyme fragment and pENTRTM vector for example, were hence considered. Before that, p8.6 in p8.6/pBIN19 was partially sequenced to confirm the mutations and to ensure that p8.6 would be cloned in frame (4.3.3).

4.3.3 Analysis of the p8.6 Construct

Full-length sequencing and aligning with the Tair genome sequence revealed that there was a mutation and a deletion in p8.6/pBS (4.3.2). To examine if these errors happened when inserting the p8.6 fragment into pBlueScript (4.3.1), the ADs29 forward primer was used to sequence p8.6/pBIN19. Although the sequencing results did not cover the G to A transition (1346) in p8.6/pBS (4.3.2), the A/1642 deletion, however, was not detected in p8.6/pBIN19 (Figure 4-8). This suggested that the processes of *SalI/KpnI* double digestion, DNA purification and ligation caused the nucleotide deletion, and that p8.6/pBS was not suitable for constructing p8.6-RFP. Furthermore, the ADs29 sequencing also discovered an unknown fragment of 225 bps between the *COII* gene and the HA tag (Figure 4-9). Online searching using the NCBI blast (<http://blast.ncbi.nlm.nih.gov/Blast.cgi>) revealed this fragment might be derived from plant expression vectors, such as pMENCHU or pPILY (Figure 4-10 and Table 4-3. The most identical alignments, AY720438.1 and AY720433.1, are included after Table 4-3).

```

GAGAGGTTGTTGCTTCAGTGAGCGAGCAATCGCTGCAGCGGTTACAAAAT-50
TGCCTTCAC TGAGATACTTGTGGGTACAAGGTTACAGAGCATCGATGACG-100
GGACAAGATCTAATGCAGATGGCTAGACCGTACTGGAACATCGAGCTGAT-150
TCCATCAAGAAGAGTCCCGGAAGTGAATCAACAAGGAGAGATAAGAGAGA-200
TGGAGCATCCGGCTCATATATTGGCTTACTACTCTCTGGCTGGCCAGAGA-250
ACAGATTGTCCAACAACTGTTAGAGTCTGAAGGAGCCAATACCCGGGTC-300
TAGAAGATCTTATCCATACGATGTAAGTTTCTGCTTCTACCTTTGATATA-350
TATATAATAATTATCATTAAATTAGTAGTAATATAATATTTCAAATATTTT-400
TTTCAAATAAAAAGAATGTAGTATATAGCAATTGCTTTTCTGTAGTTTAT-450
AAGTGTGTATATTTTAATTTATAACTTTTCTAATATATGACCAAAATTTG-500
TTGATGTGCAGGTTCCAGATTATGCTGAGTCGACGGATCCACTGCAGTGA-550
ATTCTCGTTCAAACATTTGGCAATAAAGTTTCTTAAGATTGAATCCTGTT-600
GCCGGTCTTGCGATGATTATCATATAATTTCTGTTGAATTACGTTAAGCA-650
TGTAATAATTAACATGTAATGCATGACGTTATTTATGAGATGGGTTTTTA-700
TGATTAGAGTCCCGCAATTATACATTTAATACGCGATAGAAAACAAAATA-750
TAGCGCGCAAAC TAGGATAAATTATCGCGCGCGGTGTCATCTGTCGAGGG-800
GGGGGCCCGGGGTACCGAGCTCGAATTCTTAATTAACAATTCAGTGGGCC-850
GTCGTTTTTACAACGTCGTGACTGGGAAAACCTGGCGTTACCCAAC TTAA-900
TCGCCCTTGACGACATCCCCCTTTGCCAGCTGGCGTAATAGCGAAGAGG-950
CCCGCACCGATCGCCCTTCCCAACAGTTGCGCAGCCTGAATGGCGCCCGC-1000

```

Figure 4-9 The result of p8.6/pBIN19 sequenced with the ADs29 forward primer. The *COII* region is marked in green bold. The 225 bps unknown fragment is bold. The 12 nucleotide HA tag is underlined. The *SaII* cutting site in 3' end of p8.6 is marked in red bold.

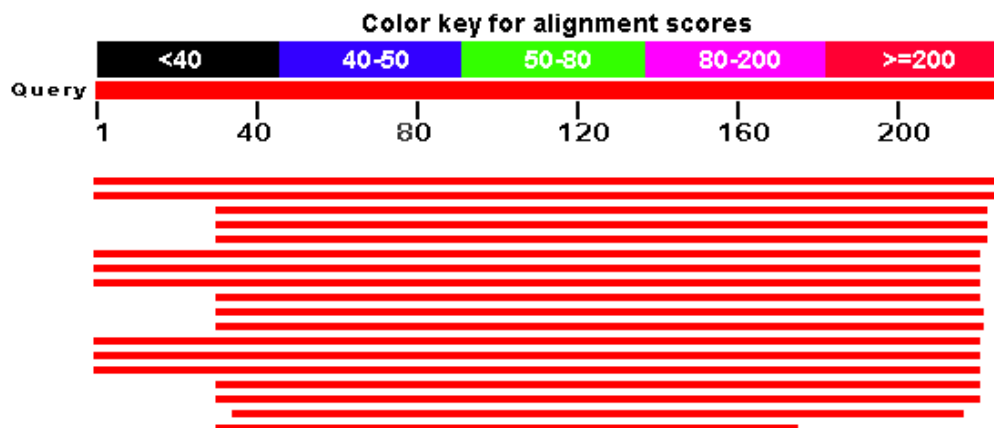


Figure 4-10 Online searching result of the 225 bps unknown fragment between *COII* and the HA tag in p8.6 from NCBI blast. Distribution of the 18 Blast hits on the query sequence are shown as red lines. Description of each hit is listed in Table 4-3.

Table 4-3 Description of 18 Blast hits from the NCBI blast searching result in Figure 4-10. The alignment detail of the bolded hits, AY720438.1 and AY720433.1, are included after this table at page 101.

Accession	Description	Total score	Max score Query coverage	Max ident
AY720438.1	Plant expression vector pMENCHU, complete sequence	405	100%	99%
AY720433.1	Plant expression vector pPILY, complete sequence	405	100%	99%
EU223249.1	Transposition Vector MightyMu_GUSB, complete sequence	353	84%	100%
U84006.1	Expression vector pBSII-LUCINT firefly luciferase (LUCINT), beta-galactosidase (lacZ) and beta-lactamase (ampR) genes, complete cds and lac operon promoter sequence	353	84%	100%
X84105.1	Artificial sequences T-DNA of binary vector pMOG553	353	84%	100%
AY720440.1	Plant expression vector pGIGI, complete sequence	351	97%	95%
AY720439.1	Plant expression vector pLOLA, complete sequence	351	97%	95%
AY720437.1	Plant expression vector pMESHI, complete sequence	351	97%	95%
EU161577.1	Cloning vector pSB156, complete sequence	350	84%	100%
EF569215.1	Expression vector PPV-NK-GFP, complete sequence	346	84%	99%
EF569214.1	Expression vector PPV-D, complete sequence	346	84%	99%
AY720436.1	Plant expression vector pPESiTa, complete sequence	344	97%	95%
AY720435.1	Plant expression vector pPESiTb, complete sequence	344	97%	95%
AY720434.1	Plant expression vector pPESiTc, complete sequence	344	97%	95%
HM066935.1	Nicotiana tabacum transgenic chloroplast kr2.2 DNA integrant, complete sequence	337	84%	98%
AJ616346.1	Nicotiana tabacum chloroplast kr1 DNA integrant	331	84%	98%
X04753.1	Potato light-inducible tissue-specific ST-LS1 gene	318	80%	98%
AJ517467.2	Nicotiana tabacum chloroplast inverse PCR product of 4.9-kb neo-hybridizing nuclear <i>Xba</i> I fragment	219	64%	93%

[AY720438.1](#) Plant expression vector pMENCHU, complete sequence

Length=4152

Score = 405 bits (219), Expect = 6e-110
 Identities = 223/225 (99%), Gaps = 0/225 (0%)
 Strand=Plus/Plus

```

Query 1   CCCGGGTCTAGAAGATCTTATCCATACGATGTAAGTTTCTGCTTCTACCTTTGatata 60
          |||
Sbjct 776 CCCGGGTCTAGAAGATCTTATCCATACGATGTAAGTTTCTGCTTCTACCTTTGATATATA 835

Query 61   tataataattatcattaattagtagtaataataatatttcaaataatttttttCAAAATAAA 120
          |||
Sbjct 836 TATAATAATTATCATTAATTAGTAGTAATATAATATTTTAAATATTTTTTCAAAATAAA 895

Query 121  AGAATGTAGTATATAGCAATTGCTTTTCTGTAGTTTATAAGTGTGTATATTTTAATTTAT 180
          |||
Sbjct 896 AGAATGTAGTATATAGCAATTGCTTTTCTGTAGTTTATAAGTGTGTATATTTCAATTTAT 955

Query 181  AACTTTTCTAATATATGACCAAAATTTGTTGATGTGCAGGTTCCA 225
          |||
Sbjct 956 AACTTTTCTAATATATGACCAAAATTTGTTGATGTGCAGGTTCCA 1000
    
```

[AY720433.1](#) Plant expression vector pPILY, complete sequence

Length=4153

Score = 405 bits (219), Expect = 6e-110
 Identities = 223/225 (99%), Gaps = 0/225 (0%)
 Strand=Plus/Plus

```

Query 1   CCCGGGTCTAGAAGATCTTATCCATACGATGTAAGTTTCTGCTTCTACCTTTGatata 60
          |||
Sbjct 776 CCCGGGTCTAGAAGATCTTATCCATACGATGTAAGTTTCTGCTTCTACCTTTGATATATA 835

Query 61   tataataattatcattaattagtagtaataataatatttcaaataatttttttCAAAATAAA 120
          |||
Sbjct 836 TATAATAATTATCATTAATTAGTAGTAATATAATATTTTAAATATTTTTTCAAAATAAA 895

Query 121  AGAATGTAGTATATAGCAATTGCTTTTCTGTAGTTTATAAGTGTGTATATTTTAATTTAT 180
          |||
Sbjct 896 AGAATGTAGTATATAGCAATTGCTTTTCTGTAGTTTATAAGTGTGTATATTTCAATTTAT 955

Query 181  AACTTTTCTAATATATGACCAAAATTTGTTGATGTGCAGGTTCCA 225
          |||
Sbjct 956 AACTTTTCTAATATATGACCAAAATTTGTTGATGTGCAGGTTCCA 1000
    
```

These findings led to a conclusion that perhaps it is more practical to insert RFP directly into the 3' end of the *COII* gene in p8.6/pBIN19. To achieve this, the RFP gene from the Gateway[®] destination vectors, pH7RWG2 and/or pH7WGR2 (Karimi *et al.*, 2002), would be PCR-amplified to add restriction sites for the insertion. For this, full length of p8.6 and the multiple restriction sites after the HA tag in pBIN19 were analysed using NEB cutter V2.0 (2.6.4) (Figure 4-11 and 4-12). The results indicated that some commonly-used restriction sites, such as *Bam*HI, *Eco*RI and *Sma*I, are present in p8.6. Moreover, considering the restriction sites after the HA tag and the restriction enzymes that needed to be avoided, *Sal*I and *Pst*I were selected to be added to the 5' and 3' end of the RFP fragment from pH7RWG2 or pH7WGR2.

Before inserting PCR-amplified RFP fragment into p8.6/pBIN19, this construct was cut by different sets of restriction enzymes to confirm the presence of particular restriction enzyme sites. In Figure 4-13, the *Sal*I single digestion (lane 1 and 2) produced two bands, about 12,000 bps and 4,000 bps, in similar size to the products from *Sal*I + *Kpn*I double digestion (lane 3). This indicates that there are two *Sal*I cutting sites in p8.6/pBIN19, and one of which is close to the 5' end of p8.6 adjacent to the *Kpn*I site. It may be concluded that the 12,000 bps band represented the pBIN19 vector, and the 4,000 bps band represented p8.6 fragment predicted in Figure 4-13. Products from *Sal*I + *Sma*I double digestion also produced two bands of approximately 12,000 bps and 4,000 bps (lane 6), agreeing with the finding that one *Sma*I site was found near the 3' end of p8.6 (Figure 4-11). The *Sal*I + *Bam*HI double digestion of p8.6/pBIN19 produced two bands of about 12,000 bps and 2,000 bps (lane 5), agreeing with the finding that there is one *Bam*HI site in the middle of p8.6 (Figure 4-11). Evidently, the 2,000 bps band represented two fragments from p8.6. However, two bands of about 12,000 bps and 3,000 bps from the *Sal*I + *Xba*I double digestion (lane 4) is difficult to interpret, because *Xba*I was found in neither p8.6 nor the multiple restriction site. Therefore, *Xba*I was not used further.

Display: - NEB single cutter restriction enzymes
- Main non-overlapping, min. 100 aa ORFs

GC=41%, AT=59%



Figure 4-11 Restriction sites in p8.6, including *pCOII*, *COII*, the 225 bps unknown fragment, and HA tag.

Display: - NEB single cutter restriction enzymes
- Main non-overlapping, min. 100 aa ORFs

GC=46%, AT=54%

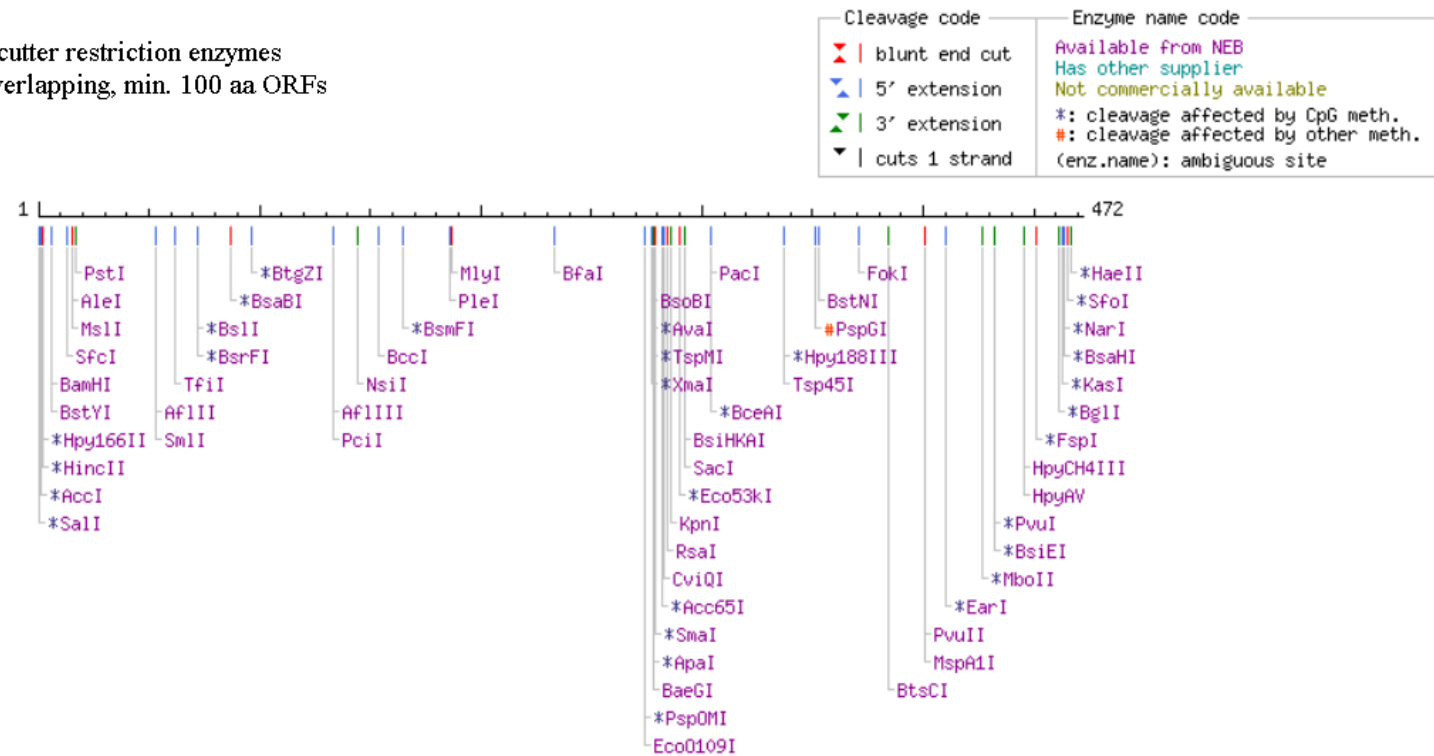


Figure 4-12 Restriction sites in the multiple restriction site region from the sequencing result of p8.6/pBIN19.

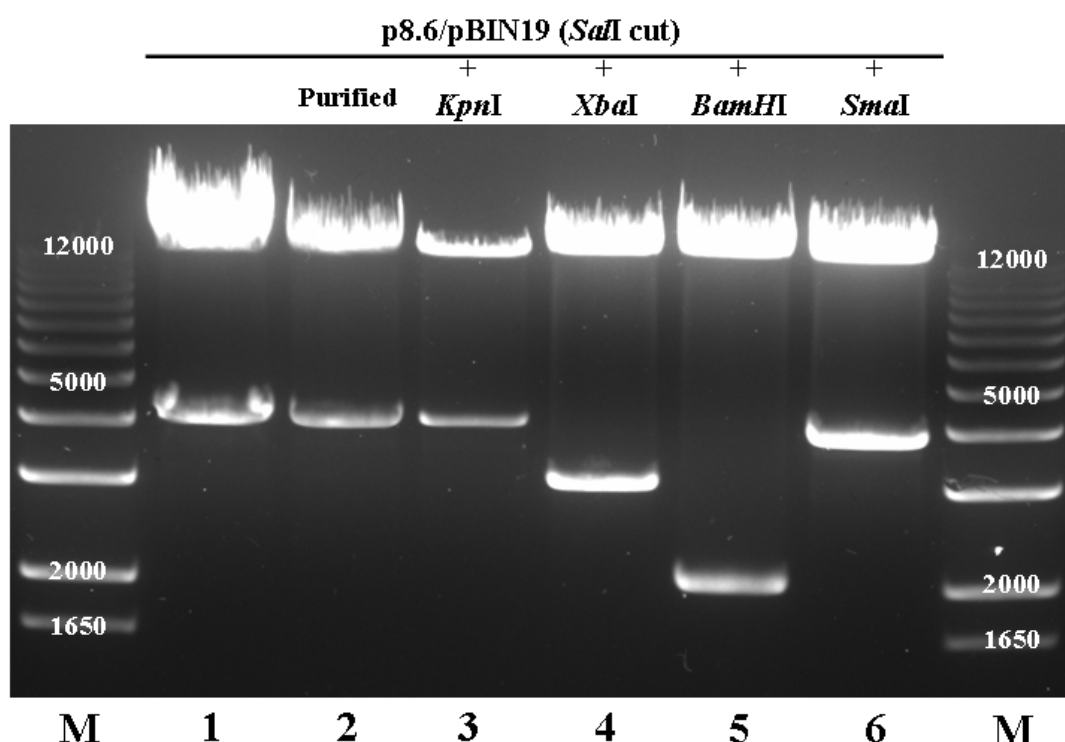


Figure 4-13 Restriction enzyme digestion for p8.6/pBIN19. The plasmid was firstly digested by *Sa*II (lane 1), purified (lane2), and then digested by *Kpn*I (lane3), *Xba*I (lane 4), *Bam*HI (lane 5) or *Sma*I (lane 6). An amount of 10 μ L of the reaction products were loaded onto each lane. Marker (M) was a DNA ladder.

4.4 Discussion

p8.6-RFP would be useful for colocalisation of the COI1 protein with other protein components from the JA signal pathway, and for avoiding the green autofluorescence that shared similar emission wavelength with GFP. However, the initial attempt to amplify p8.6 from p8.6/pBS (the *att*B-PCR reaction) using the Expand High Fidelity PCR System (4.2.2) apparently introduced sequence errors. It is unlikely that the errors occurred during DNA sequencing because the listed errors were all confirmed twice by overlapping the sequencing results. Although the enzyme mix was designed to generate PCR product of high yield, high fidelity and

high specificity from all kinds of DNA (Barnes, 1994), and the proofreading ability of Tgo DNA polymerase should have given a 3-fold increase in fidelity compared to Taq DNA polymerase, the error rate of Expand High Fidelity PCR System in 4.3.2 was found to be even higher than 1 in 9,000 nucleotides, the reported error rate of Taq DNA polymerase (Tindall and Kunkel, 1988). In the *attB*-PCR reaction product, there were 12 sequence differences from the Tair genome database. Nine base substitutions and one deletion were present in p8.6 (about 3,800 bps), suggesting the Expand High Fidelity PCR System did not function as well as it was claimed to be. It is uncertain if the fact that this enzyme mix was an old lab stock instead of recently ordered reduced its quality.

Among the 9 base substitutions and one deletion in p8.6/pDONRTM221 #8, the deletion (A/1642) and one substitution (G to A transition/1346) were also detected in p8.6/pBS, the parent clone of p8.6/pDONRTM221 #8, but the deletion (A/1642) was absent from the parent clone p8.6/pBIN19. Whether the substitution (G to A transition/1346) was present in p8.6/pBIN19 was not confirmed. The quality of the fluorescent peaks in all sequencing data was good and the possibility of misreading could be ruled out. These findings suggested that at least the deletion (A/1642) happened when transferring p8.6 from p8.6/pBIN19 to pBluescript. Molecular procedure, such as electrophoresis (2.3.5.1), is likely to cause DNA mutagenesis. As a mutagen, ethidium bromide in agarose gel intercalates double stranded DNA, which then fluoresces under UV light. Both intercalation with ethidium bromide and imaging under UV light can mutagenise DNA sample, and possibly cause the deletion (A/1642). Therefore, it is important to keep the construction steps as few as possible. Further sequencing of p8.6/pBIN19 with the other *COII* specific primer, ADs25 for instance, would help to clarify if the substitution (G to A transition/1346) also happened when transferring p8.6 from p8.6/pBIN19 to pBluescript.

In addition to the sequence changes in p8.6 mentioned above, two insertions, the 11 nucleotide (AGCTTCCACCA) right before the start codon of *COII* (**Figure 4-7** and **4-8**) and the 225 bps unknown fragment between the *COII* gene and the HA tag (**Figure 4-9**) were found by sequencing both p8.6/pBS and p8.6/pDONRTM221 #8. However, the 11 nucleotide (AGCTTCCACCA) insertion does not alter the start codon of *COII*. Because p8.6/pBIN19 was constructed by A. Devoto (Devoto and Turner, unpublished data, 2002) and no explanation was found from her lab note, it is difficult to speculate if these two insertions were included in p8.6 accidentally or

for a particular purpose. It is also possible that the 225 bps unknown fragment might be inserted into p8.6 unexpectedly from the pPILY vector, which was extensively used to construct the *COII* gene in Turner's lab. Nevertheless, the transgenic line, p8.6/*coil*-16, had doubtlessly proved that the expression of *COII* was not affected (3.3.3), and the function of *COII* was uncompromised by the two insertions in p8.6 (Devoto and Turner, unpublished data, 2002).

The making of p8.6-RFP was unfortunately not completed because of the high error rate of the Expand High Fidelity PCR System and the unexpected deletion (A/1642), which apparently happened when transferring p8.6 from p8.6/pBIN19 to pBluescript. However, p8.6/pBIN19 was sequenced thoroughly, and an alternative strategy for inserting RFP to p8.6/pBIN19 has been planned so that further work can construct p8.6-RFP/pBIN19.

Chapter 5

***Arabidopsis* Root Growth in Response to MeJA: the Cell Pattern in QC-LEH**

5.1 Introduction

An aim of this project was to study the growth inhibition caused by MeJA treatment. JA and its related compounds have long been regarded as growth inhibitors and promoters of senescence, and their role in plant development is as significant as in stress and disease defense. JA's growth inhibitory effect on seedlings was initially studied in wheat (Dathe *et al.*, 1981), rice (Yamane *et al.*, 1980) and sunflower (Corbineau *et al.*, 1988). Change of sensitivity to MeJA and coronatine, a phytotoxin structurally similar with JAs, was then used to screen *Arabidopsis* mutants in JA pathway (Staswick *et al.*, 1992, Feys *et al.*, 1994).

Our understanding of JA-mediated growth inhibition is preliminary when compared to the studies on JA-mediated disease resistance and JA signal transduction. It has been shown that exogenous JA can inhibit the synthesis of cell wall polysaccharides, which prevents IAA-induced oat coleoptile elongation (Ueda *et al.*, 1995). Moreover, MeJA sensitivity in *Arabidopsis* root does not involve ethylene accumulation (Berger *et al.*, 1996). In tobacco BY-2 cells, MeJA treatment disrupts microtubules in a cell cycle-dependent manner (Abe *et al.*, 1990). It is also clear that JA is able to block G1/S and G2/M transitions in BY-2 cells, indicating that interruption of meristem activity plays a role in restraining plant growth (Świątek *et al.*, 2002). Likewise, endogenous JA has effects on growth arrest as well. In *Arabidopsis*, wounding-caused JA synthesis can suppress growth by reducing mitotic cell number in a COI1, JAZ and MYC2-dependent manner (Zhang and Turner, 2008). Furthermore, based on the regulated expression of resistance traits

following herbivore attack in *N. attenuata*, it has been suggested that JA-mediated growth inhibition is the way plants reallocate resources in dealing with environmental stresses (Zavala and Baldwin, 2006).

In this chapter, I focused on the cellular reactions caused by MeJA treatment, which resulted in root growth inhibition in *Arabidopsis*. Growth medium was firstly decided for achieving optimised growth condition. Confocal and CCD upright microscopy was then used to measure the Length of the first Epidermal cell with a visible root Hair bulge (LEH), number of epidermal cells in a single file from the QC to first LEH (QC-LEH), and length of each root cell in QC-LEH. In QC-LEH, the first cell that started elongating rapidly was marked as the beginning of the transition zone (TZ), a transitional area between the meristem and the elongation zone. Observations at particular time point and time lapse photography were both used. Some of the JA and auxin mutants, including *coi1-16*, *aos*, *jin1-1* and *aux1-7*, were recruited to compare the cell pattern differences caused by MeJA treatment under dissimilar mutant background. Moreover, *CYCBI::GUS* was used to examine the impact of MeJA treatment on cell division.

5.2 Results

5.2.1 Johnson's Medium and Half MS Medium

For years, half MS medium had been used for growing *Arabidopsis* in this laboratory. However, it was announced at the *Arabidopsis* conference in Edinburgh that MS medium was growth inhibitory, and that Johnson's medium was superior (Doerner, 2009).

To clarify which medium is better for growing *Arabidopsis*, experiments were conducted to compare the growth of *Col-gl Arabidopsis* seedlings in Johnson's medium and half MS medium. In Figure 5-1, 4 day old *Col-gl* seedlings grown in Johnson's medium had thinner roots and light-green cotyledon, which made these seedlings look slightly unhealthy. Meanwhile, seedlings grown in half MS medium had longer roots and wide-open green cotyledon.

To investigate further, root length and the LEH were measured in *Col-gl* seedlings untreated or treated with 20 μ M MeJA for 24 hrs. Figure 5-2 shows that 5

day old seedlings grown in half MS medium had longer roots and larger LEH, and the differences between the treated and untreated groups were also significant. In contrast, seedlings grown in Johnson's medium had shorter roots and shorter LEH, and the differences between the treated and untreated groups were hardly distinguishable. Half MS was therefore chosen as the medium that would be used for all experiments in this project.

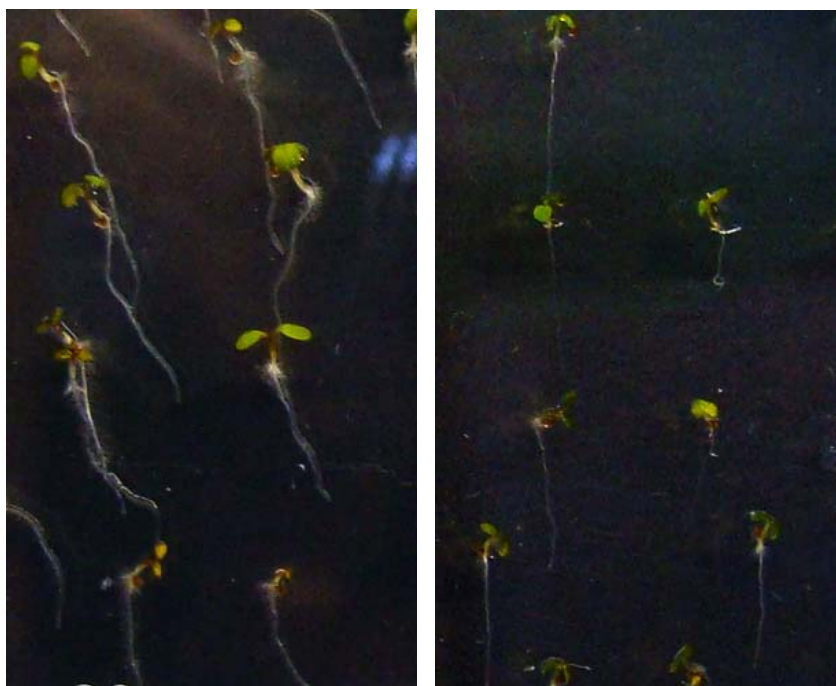


Figure 5-1 Four day old Col-*gl* *Arabidopsis* seedlings grown in half MS medium (left) and Johnson's medium (right).

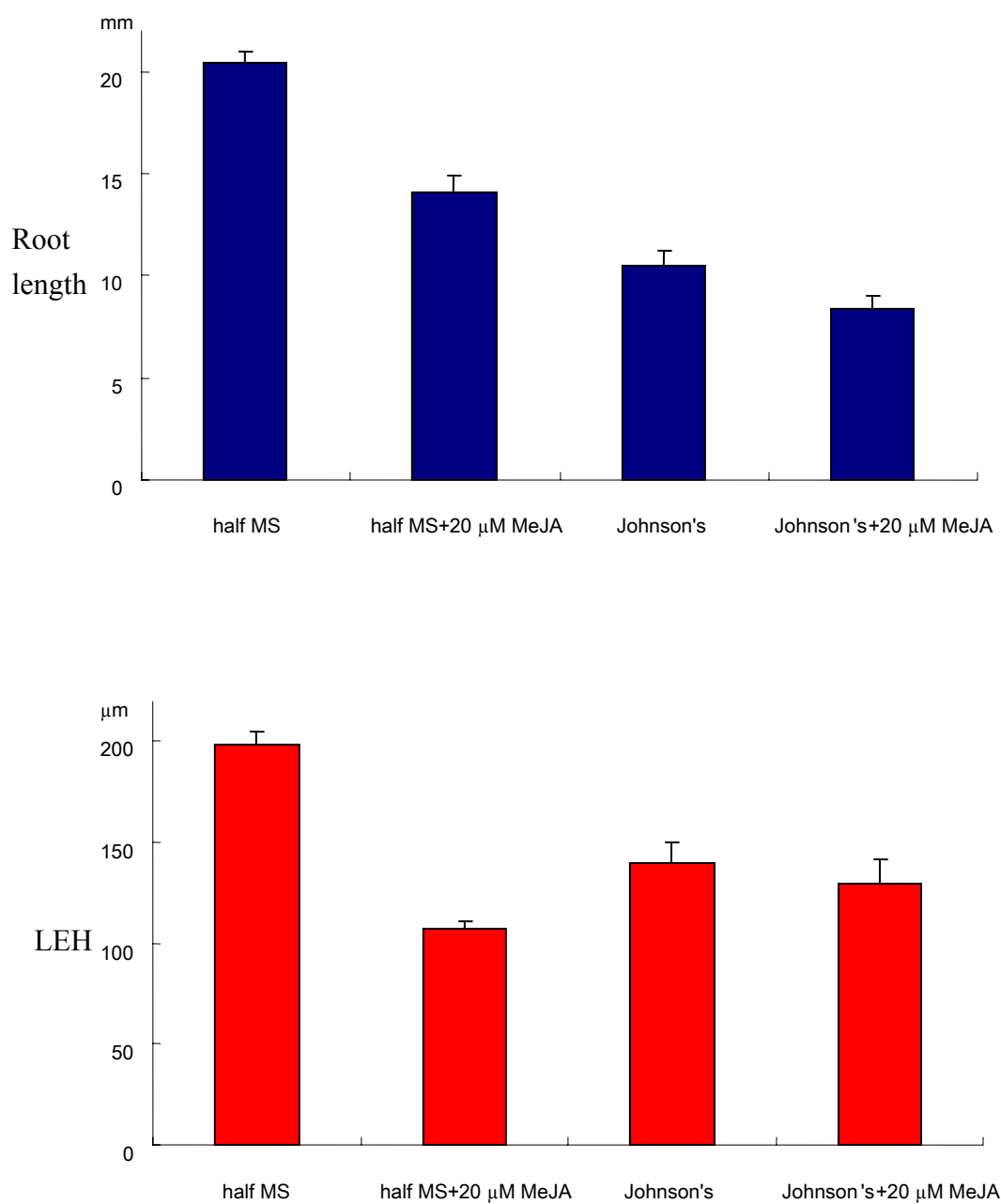


Figure 5-2 Five day old Col-*gl* *Arabidopsis* seedlings grown in half MS medium and Johnson's medium. +20 μ M MeJA: 24 hrs, 20 μ M MeJA treatment.

5.2.2 Root Growth Response to MeJA

MeJA inhibits root growth and has been used to isolate JA-insensitive mutants (Yamane *et al.*, 1980, Staswick *et al.*, 1992). In 3.3.2, I had shown that 20 μ M MeJA was the most suitable concentration to treat *Arabidopsis* seedlings. In next few sections, I studied the molecular and cellular responses to MeJA treatment in WT and several JA and auxin signal pathway mutants.

5.2.2.1 Effect of MeJA Treatment on Root Cells in Meristem and Elongation Zone

Based on the findings from the effect of MeJA treatment on primary root length and LEH, it was clear that the MeJA-mediated growth inhibition could be observed in 3 hrs after the treatment started, and shorter LEH had contribution to stunted root length (3.3.2). This raised the question whether MeJA also reduced the rate of cell expansion and the number of root cells. For this, a 150 minutes time-lapse imaging was planned.

The *GFP-TUA6* transgenic line was used considering the visible microtubules-GFP could reveal if the dynamic change of cytoskeletons was influenced by MeJA treatment (Hashimoto and Nakajima, 2001). To make image analysis easier, FM4-64, an amphiphilic styryl dye, was applied in the medium. FM4-64 can insert into the outer leaflet of the plasma membrane, and is commonly used as a fluorescent reporter of endocytosis (Fischer-Parton *et al.*, 2000). Moreover, FM4-64 allowed the seedlings to grow normally, while being stained. Three day old *GFP-TUA6* seedlings were transferred to half MS medium containing 0.35% low melting point agarose and 1 μ M FM4-64 with or without 20 μ M MeJA, covered with glass slide, and then observed under confocal microscope for 150 minutes (2.5.3). Images were taken every 15 minutes from the area of apical meristem to the elongation zone. To analyse the data, length of each root cell in one single file, from QC to LEH, was marked, measured and plotted, to compare the difference between MeJA treated and non-treated root growth pattern (Figure 5-3).

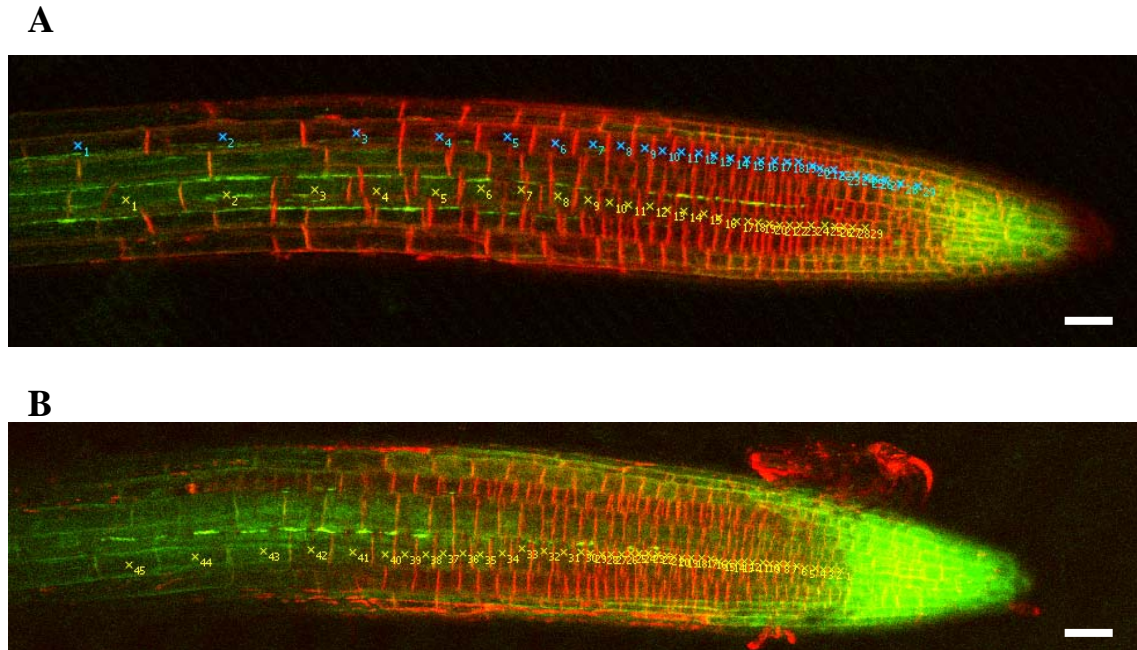


Figure 5-3 Three day old *GFP-TUA6* seedlings were observed under confocal microscope continuously for 150 min. Images were taken every 15 minutes and the root cell, from QC to LEH, was marked and numbered individually. All of the marked root cells were measured accordingly. Scale bar 50 μ m. (A) Untreated *GFP-TUA6* root. (B) 20 μ M MeJA-treated *GFP-TUA6* root.

As expected, the MeJA treated LEH was approximately 100 μ m (Figure 5-4 B), whereas the non-treated LEH lengthened longer than 140 μ m (Figure 5-4 A). The calculated growth rate of MeJA treated and untreated roots were 1.204 μ m/min and 1.294 μ m/min, respectively. There were 34 root cells from first cell in meristem to first LEH in non-treated root, but only 27 root cells were counted under the same criterion in MeJA treated root, suggesting that rate of cell production might be reduced in the latter. In addition, fewer root cells underwent rapid expansion (the notable cell elongation before the root cells gave birth of the root hair bulge, judging from the slope) in the presence of MeJA, although surprisingly, the rapid cell expansion rate in the MeJA treated root was not lower than the control root.

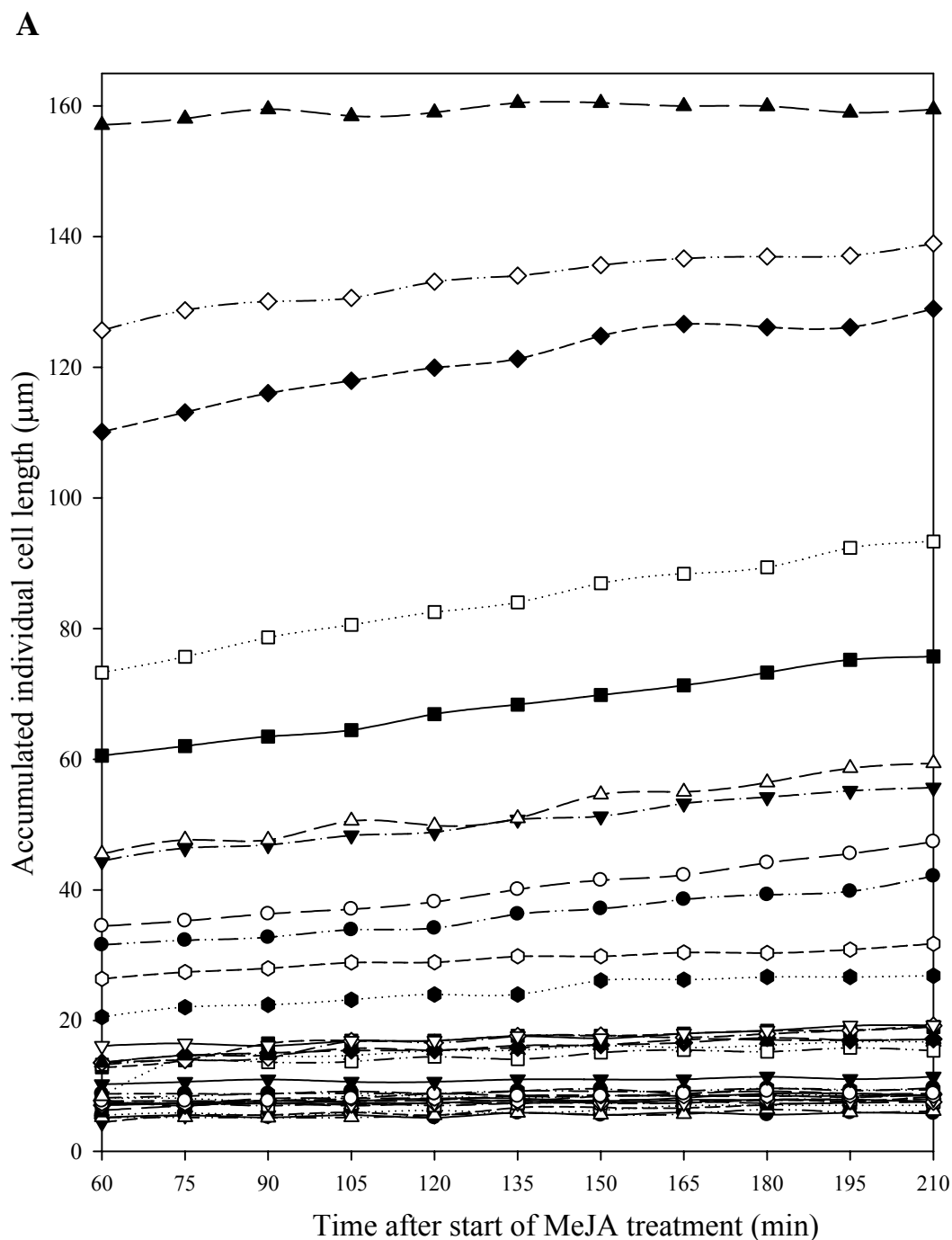
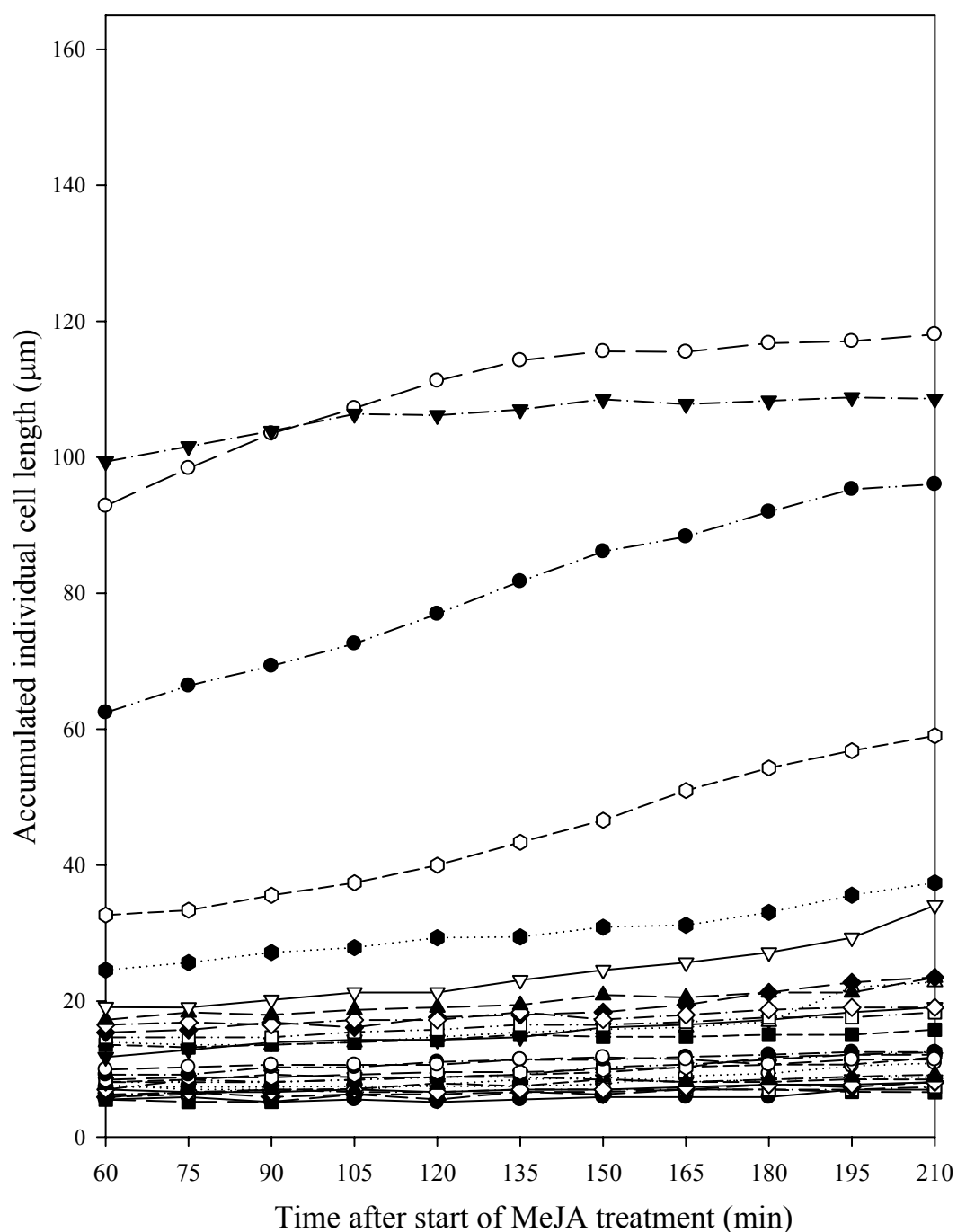


Figure 5-4 Three day old *GFP-TUA6* seedlings were observed under confocal microscope continuously for 150 min. Images were taken every 15 minutes and the length of each root cell, from QC to LEH, were measured and plotted. (A) Untreated *GFP-TUA6*: 34 root cells. (B) MeJA-treated *GFP-TUA6*: 27 root cells.

B



To investigate further how root growth pattern was influenced by MeJA treatment, 20 μM MeJA incubation was extended to 24 hrs, 48 hrs and 72 hrs. Six day old *GFP-TUA6* seedlings with differential treating were stained with 5 $\mu\text{g/ml}$

propidium iodide before being observed under the confocal microscope (2.5.3). Length of each root cell in QC-LEH was marked, measured and plotted to compare the difference of growth patterns between multiple days MeJA treated and untreated roots.

The root cell length accumulation curve from the multiple days MeJA treatment revealed that, in the untreated root, the rapid expansion started at the 28th root cell counting from the QC (Figure 5-5, red arrow), whereas in MeJA treated roots (24 hrs, 48 hrs and 72 hrs), the rapid expansion did not begin after the 42nd root cells (Figure 5-5, green arrow). This suggested that the growth pattern of the treated roots appeared similar after 24 hrs treating, because there was no significant difference among the curves of 24 hrs, 48 hrs and 72 hrs (Figure 5-5). The data also indicated that, after more than 24 hrs MeJA treatment, about 14 cells were held and waited between the meristem and the elongation zone before entering the rapid expansion stage. In addition, there were 14 rapidly expanding cells in control root, while there were only 8 rapidly expanding cells in MeJA-treated roots.

Both Figure 5-4 and Figure 5-5 also showed that the MeJA treated roots had shorter LEH. However, the result of cell number in meristem did not agree with each other in these two experiments. In Figure 5-4, the MeJA treated root had less root cells in meristem, whereas in Figure 5-5, there were more root cells piled up in this area in MeJA-treated roots (50 cells) than in control root (41 cells).

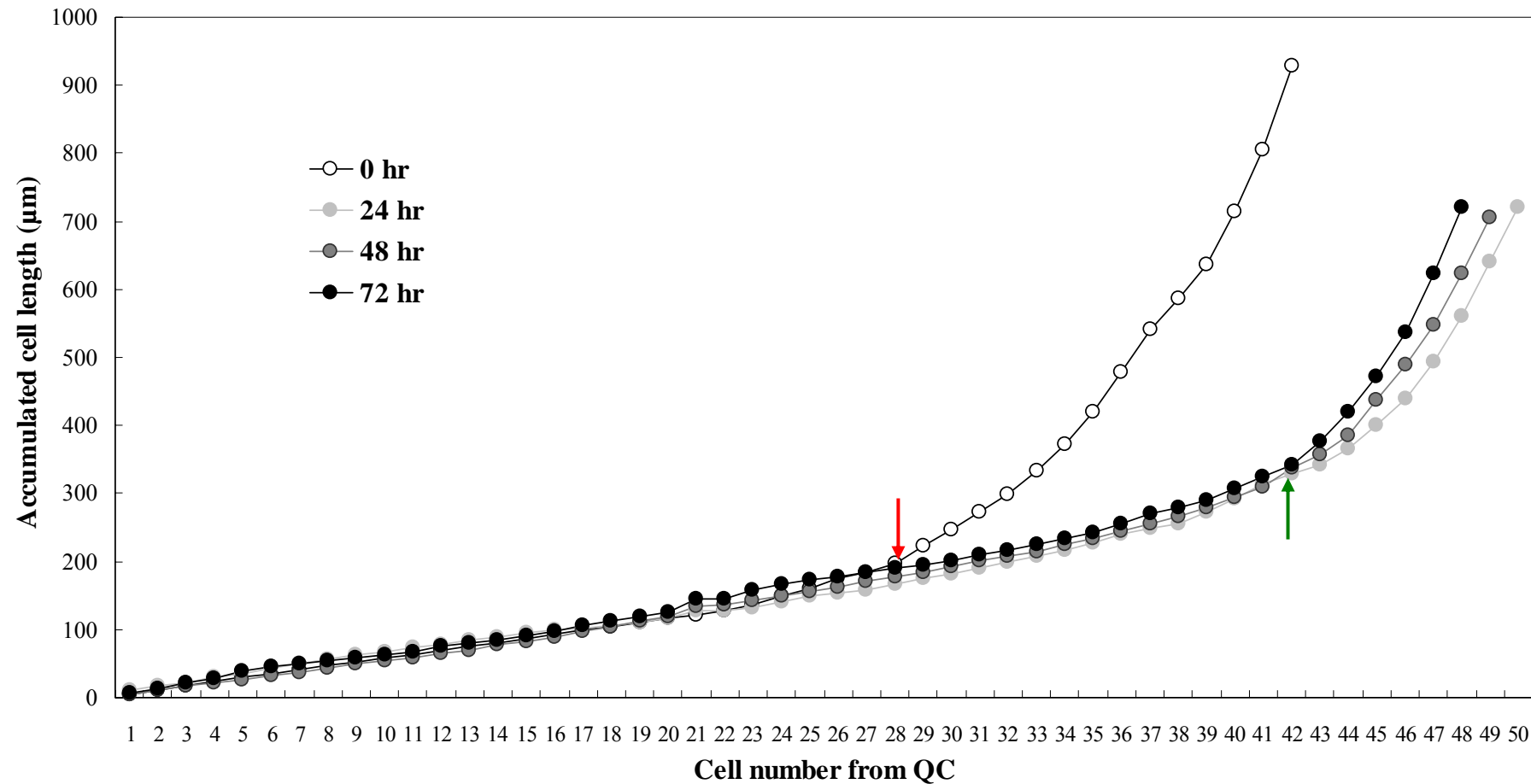


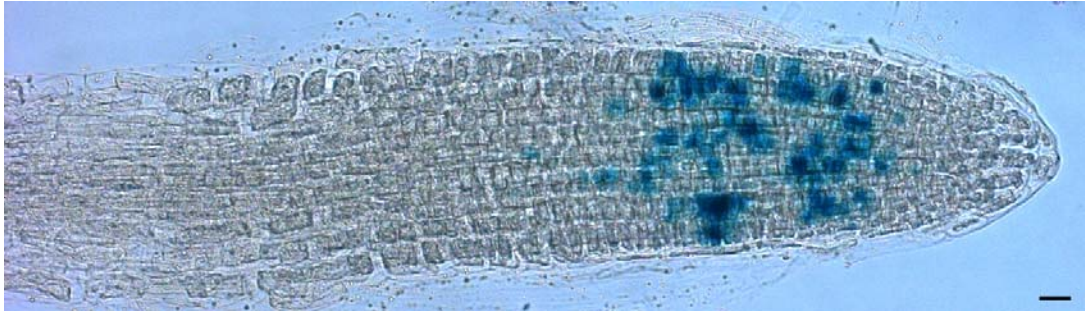
Figure 5-5 Six day old *GFP-TUA6* seedlings untreated or treated with 20 μ M MeJA (24 hr, 48 hr or 72 hr). In each group, length of a file of epidermal root cells, from the start of meristem to first LEH, was measured, and accumulation of root cell length was plotted. The first root cells that started rapidly expanding were marked in red arrow (0 hr) and green arrow (24 hr, 48 hr and 72 hr).

5.2.2.2 Effect of MeJA Treatment on Cell Division

It was shown in Figure 5-5 that in the MeJA treated roots, there were 42 cells before the rapid expansion zone compared to 28 cells in the untreated root. This raised the question whether these 14 cells that queued between the meristem and the elongation zone were either developmentally halted or remained in mitotic state. An experiment was subsequently planned by using *CYCB1::GUS* transgenic line. *CYCB1* expressed particularly at the G2/M transition, therefore offered a marker to specify the cells in mitosis status (Ferreira *et al.*, 1994). In *CYCB1::GUS* transgenic line, the cells underwent mitotic state appeared as blue dots after the histochemical detection of GUS activity.

Three day old *CYCB1::GUS* seedlings were untreated or treated with 20 μ M MeJA for 24 hrs before GUS activity was detected, and observed under a CCD upright microscope (2.5.1). The number of dots, which represent cells in mitosis, was reduced in the MeJA treated root (Figure 5-6). However, the area of cell division zone, where the dots appeared, was not longer in the MeJA treatment root (Figure 5-6, B). This indicated that albeit there were more root cells stayed short and were held before they entered the rapid expansion state (5.2.2.1), they did not have the ability for cell division. Although the reason why the developmental stage of these 14 cells were held is not known, it is possible that they would enter the rapid expansion state eventually, and form the root hair bulge at a shorter cell length compared to untreated root cells.

A



B

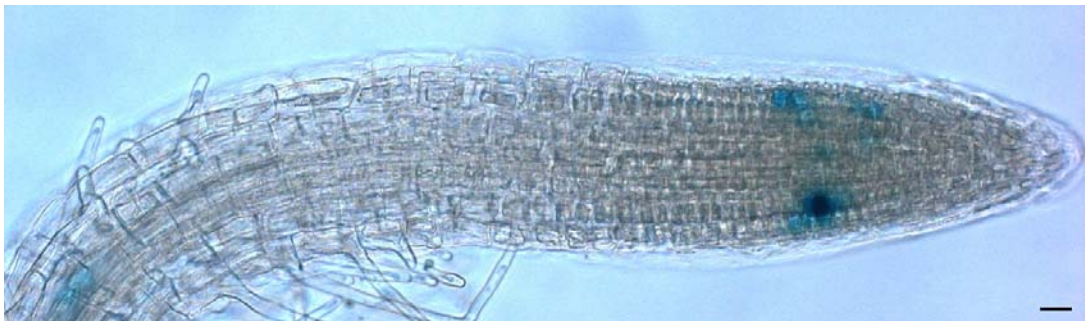


Figure 5-6 Three day old *CYCB1::GUS* seedlings were treated with 20 μ M MeJA for 24 hrs and observed under a confocal microscope. Scale bar 20 μ m. (A) Non-treated *CYCB1::GUS* root. (B) Treated *CYCB1::GUS* root.

5.2.2.3 Effect of MeJA Treatment on Root Cells in JA and Auxin Mutants

In 5.2.2.1 (Figure 5-5), I showed that MeJA treatment increased the cell number in QC-LEH, decreased the length of QC-LEH, and decreased the LEH. Here I have tested the role of JA and auxin signaling on these parameters, by using three JA signaling pathway mutants, *aos*, *jin1-1* and *coil-16*, and one auxin mutant, *aux1-7*. *aos*, *jin1-1* and *aux1-7* were already crossed into the *GFP-TUA6* background (2.2.4) in order to observe microtubules easily. Therefore, the control root for *aos*, *jin1-1* and *aux1-7* was *GFP-TUA6*. All of the 6 day old seedlings were untreated or treated with 20 μ M MeJA for 24 hrs, and stained with 5 μ g/ml propidium iodide, before being observed under the confocal microscope (2.5.3).

Data from each mutant are plotted separately in Figure 5-7 (*aos* and *GFP-TUA6*), Figure 5-8 (*coil-16* and *Col-gl*), Figure 5-9 (*jin1-1* and *GFP-TUA6*)

and Figure 5-10 (*aux1-7* and *GFP-TUA6*). The cell number in QC-LEH, the length of QC-LEH and the LEH in each group are summarised in Table 5-1 for comparison.

Table 5-1 Summary of parameters from Figure 5-7, 5-8, 5-9 and 5-10.

	Cell number in QC-LEH	Length of QC-LEH (µm)	LEH (µm)
<i>GFP-TUA6</i>	37	1162.04	225.234
<i>GFP-TUA6</i> + JA	45	793.467	78.574
<i>aos</i>	36	864.432	161.283
<i>aos</i> + JA	47	615.999	63.927
<i>jin1-1</i>	39	1191.71	190.971
<i>jin1-1</i> + JA	36	654.904	157.716
<i>aux1-7</i>	39	981.567	129.672
<i>aux1-7</i> + JA	43	1179.854	140.419
<i>Col-gl</i>	37	1159.987	226.214
<i>Col-gl</i> + JA	45	929.48	147.078
<i>coil-16</i>	44	1227.495	224.809
<i>coil-16</i> + JA	49	1142.045	192.766

Like *GFP-TUA6*, *aos* showed similar changes in parameters when treated with MeJA, including increased cell number in QC-LEH, decrease of the length of QC-LEH, and shorter LEH (Figure 5-7 and Table 5-1). As a JA biosynthesis mutant, *aos* is still capable of sensing and responding to MeJA treatment (Zhang and Turner, 2008). However, the length of QC-LEH was even shorter in treated *aos* than in *GFP-TUA6* (Figure 5-7). Evidently, MeJA appeared to have greater inhibitory effect on *aos* than on *GFP-TUA6*. The plot of accumulated cell length against cell number of the untreated *aos* was almost identical with *GFP-TUA6*. However, LEH appeared 1 cell earlier in *aos* than in *GFP-TUA6*, and LEH appeared in *aos* root approximately 300 µm shorter than in *GFP-TUA6*.

Surprisingly, the root cell pattern of *coil-16* also changed after MeJA treatment (Figure 5-8 and Table 5-1), which contradicted the understanding that *coil-16* is insensitive to MeJA treatment. Although the length of QC-LEH in untreated and treated *coil-16* was similar (1227.495 µm and 1142.045 µm), the latter contained 5 more cells in QC-LEH and had slightly shorter LEH. Comparing

with *Col-gl*, *coi1-16* root tips had longer meristem, which contains more cells (Figure 5-8, arrows). These data suggested that one of the roles of *COI1* is to reduce cell number in the meristem.

jin1-1 is defective in MYC2, a key TF in the JA signaling pathway, and is partially insensitive to MeJA treatment. In Figure 5-9, the length of QC-LEH in the treated *jin1-1* was shorter than untreated *jin1-1* and treated *GFP-TUA6*. Nevertheless, the LEH of the treated *jin1-1* was not reduced as much as the LEH of the treated *GFP-TUA6*, and the cell number of QC-LEH is even fewer in the treated *jin1-1*, suggesting that there were no cells accumulated between the meristem and TZ in the treated *jin1-1*. This indicated that *jin1-1* reacted to MeJA treatment by forming LEH 3 cells earlier, and in root tips 550 μm shorter, compared to the *jin1-1* control. However, the meristem cell numbers were not very different between the treated and untreated *jin1-1*, which also showed the partial insensitivity of *jin1-1* to MeJA.

aux1-7 was the only auxin mutant studied here. In Figure 5-10, the MeJA treated *aux1-7* had 4 more cells in the QC-LEH and a slightly longer LEH than untreated *aux1-7*. Moreover, the plots of accumulated cell length against cell number of MeJA treated and untreated *aux1-7* were relatively similar, which suggested that *aux1-7* was partially insensitive to MeJA, at least in the QC-LEH area. Evidently, this mutation in the auxin signaling pathway interferes with the MeJA-mediated growth inhibition.

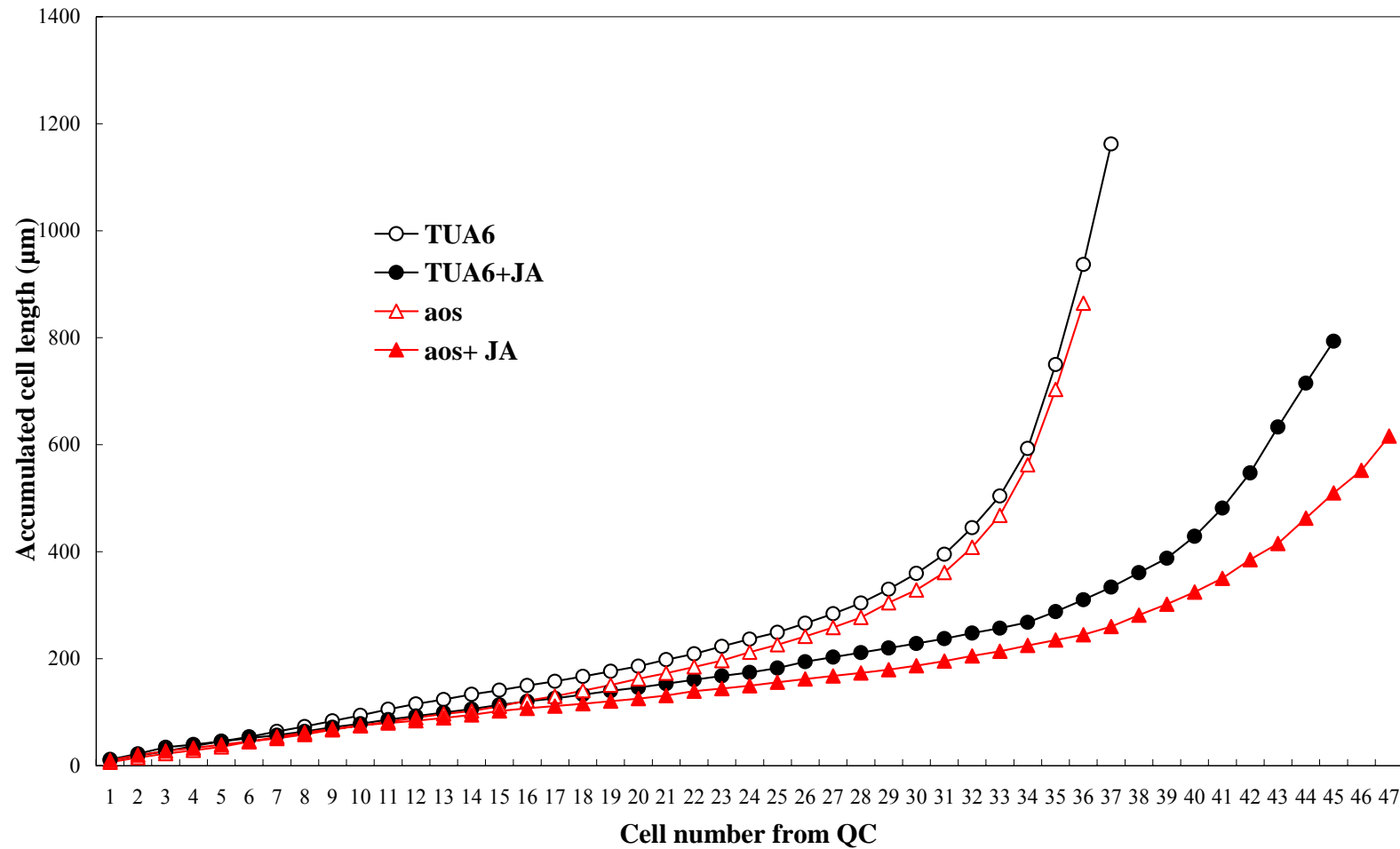


Figure 5-7 Six day old *GFP-TUA6* and *aos* seedlings untreated or treated with 24 hr, 20 μ M MeJA. In each group, length of a file of epidermal root cells, from the start of meristem to first LEH, was measured, and accumulation of root cell length was plotted.

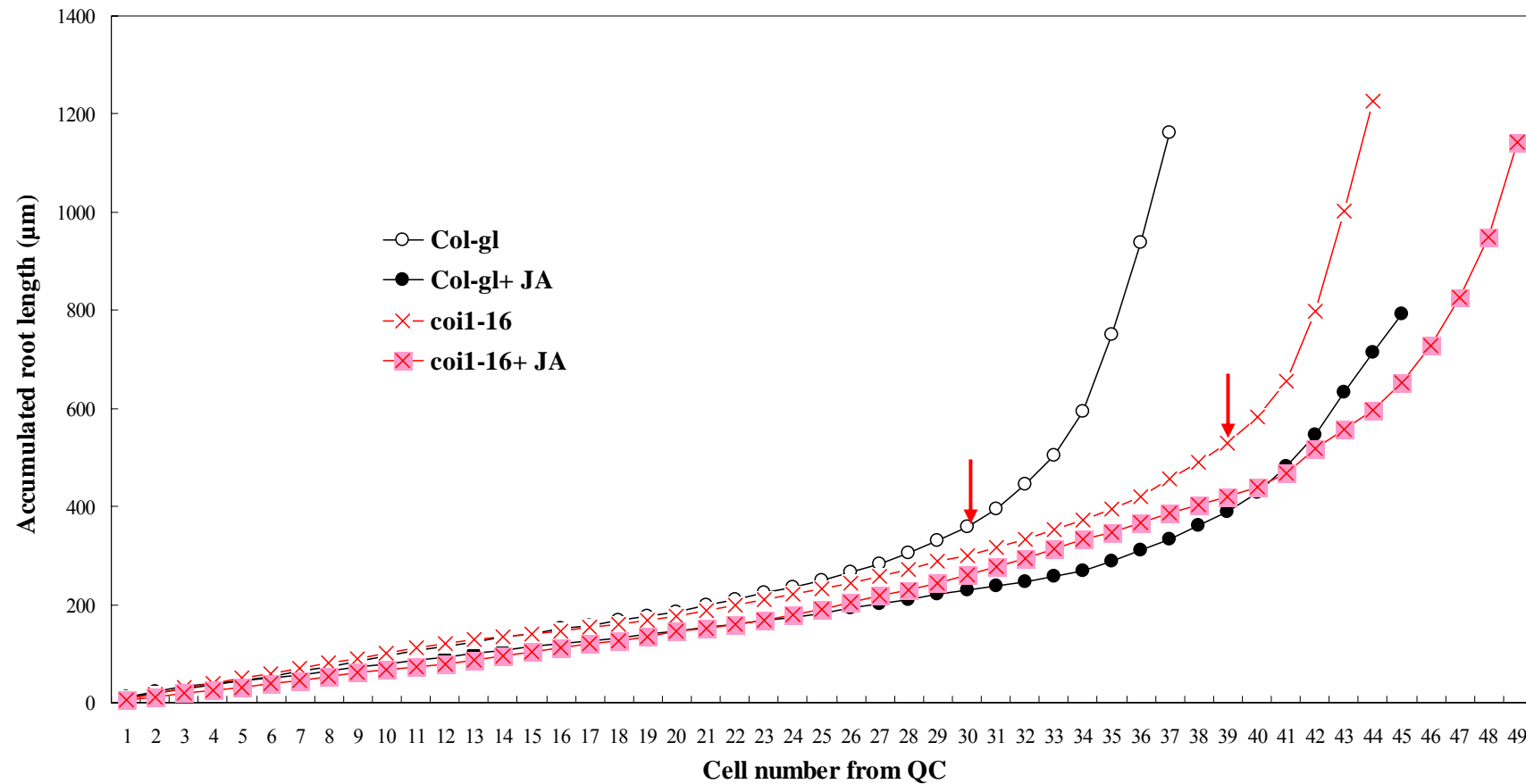


Figure 5-8 Six day old *Col-gl* and *coi1-16* seedlings untreated or treated with 24 hr, 20 µM MeJA. In each group, length of a file of epidermal root cells, from the start of meristem to first LEH, was measured, and accumulation of root cell length was plotted. The first root cells that started rapidly expanding were marked in red arrows.

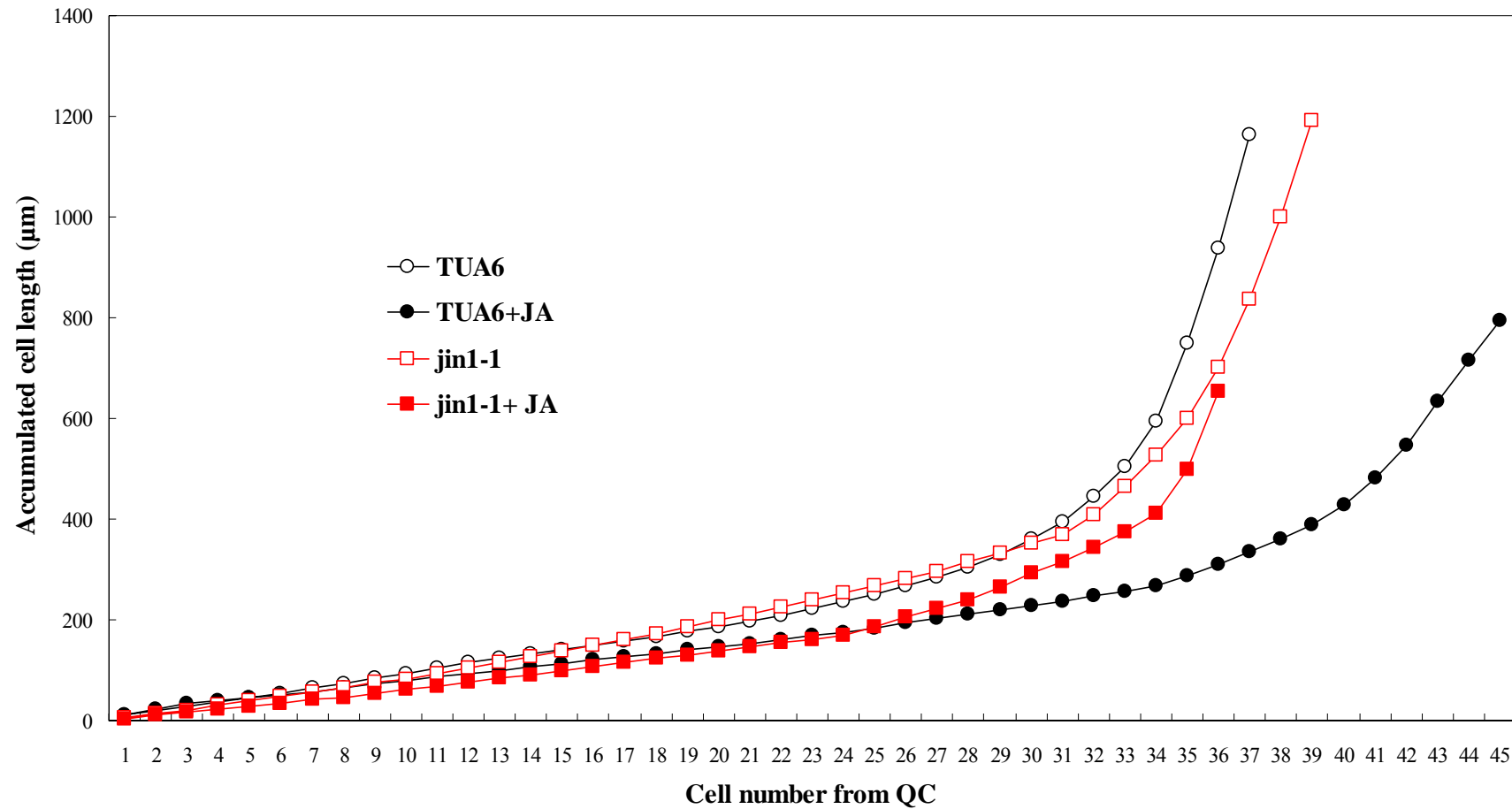


Figure 5-9 Six day old *GFP-TUA6* and *jin1-1* seedlings untreated or treated with 24 hr, 20 μM MeJA. In each group, length of a file of epidermal root cells, from the start of meristem to first LEH, was measured, and accumulation of root cell length was plotted.

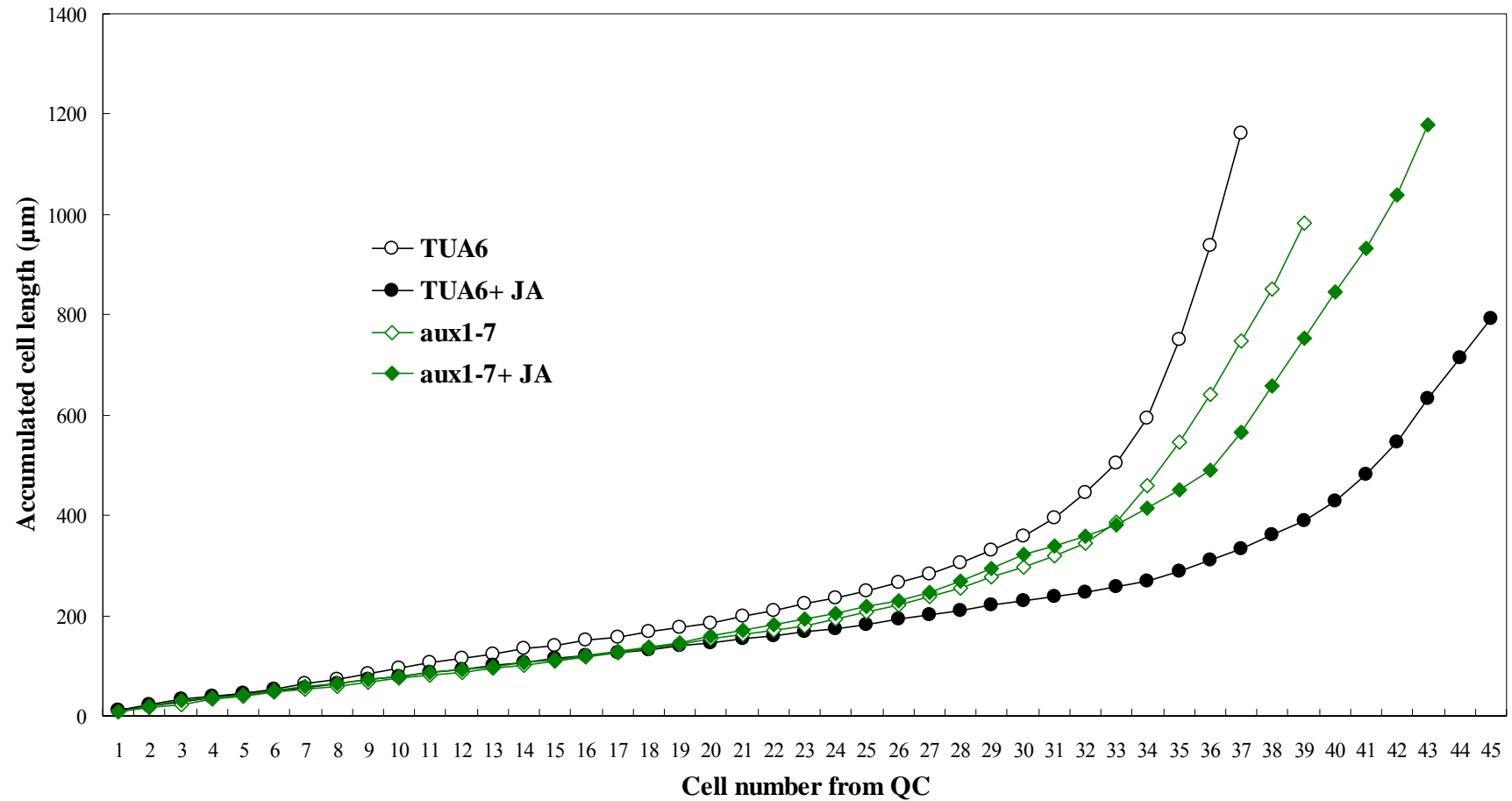


Figure 5-10 Six day old *GFP-TUA6* and *aux1-7* seedlings untreated or treated with 24 hr, 20 μM MeJA. In each group, length of a file of epidermal root cells, from the start of meristem to first LEH, was measured, and accumulation of root cell length was plotted.

5.3 Discussion

Growth inhibition caused by JA has been known for more than 20 years in plant physiological research field (Yamane *et al.*, 1980, Ueda and Kato, 1982). Subsequent studies have indicated that JA is also involved in reproductive and developmental regulation (Li *et al.*, 2004, Cipollini, 2005, Mandaokar *et al.*, 2006). In this chapter, I focused on MeJA-mediated growth inhibition in the primary root, by examining the effect of MeJA on cell pattern in the QC-LEH area and mitosis in WT and mutant background.

Before the experiment, it was hypothesized that four factors had contribution to root growth. These were: the rate of mitosis; the number of elongating cells; the rate of cell elongation; and the length of mature cells. It was already clear that the MeJA treated roots were shorter in length and LEH (3.3.2). The time-lapse photography described in this chapter further revealed unexpected events at the cell level. It was shown that stunting of roots by MeJA was due to a decrease in the number of expanding cells, and shorter LEH, i.e. root cells that began to form root hair bulge were shorter in the MeJA-treated roots than in the untreated roots (**Figure 5-4**). Surprisingly, the rate of cell expansion was not reduced by MeJA (**Figure 5-4**).

It was also found that another effect of MeJA was to delay the development of root cells before they entered the TZ. This led to an increase in the number of small undifferentiated cells between the meristem and the cell elongation zone (**Figure 5-5**). However, this phenomenon was not observed in the time-lapse photography, which actually showed there were fewer cells in the QC-LEH area of the MeJA-treated root. This might be because in the time-lapse photography experiment (**Figure 5-4**), the seedlings were exposed to MeJA for only 60 min before start of observation, whereas in **Figure 5-5**, the cell accumulation between the meristem and the elongation zone was observed after 24 hrs of MeJA treatment. This suggests that the developmental delay in cell elongation became obvious only after prolonged treatment with MeJA.

It should be noted that unlike the time-lapse imaging (**Figure 5-4**), the accumulation curve of root cell length in QC-LEH (**Figure 5-5** and **Figure 5-7** to **5-10**) only represented the root cell pattern at one time point. Therefore, it is impossible to examine if the growth rate and single cell expansion rate were affected by the MeJA treatment in **Figure 5-5** and onwards. The determination of

time-dependent changes in growing cells requires kinematics analysis adapted from the study of fluid dynamics, which enables evaluation of material derivatives and material integrals of variables associated with the moving elements in plant cells (Silk and Erickson, 1979).

The GUS activity assay of untreated and treated *CYCB1::GUS* seedlings indicated that there were fewer mitotic cells in the treated root (**Figure 5-6**), consistent with Zhang's finding in the shoot apical meristem (Zhang and Turner, 2008). It was also discovered previously that JA arrests cell cycle in both the G1/S and G2/M transitions in tobacco BY-2 cells (Świątek *et al.*, 2002, **Figure 5-11**). These authors claimed that JA is exclusively in charge of the G2/M disturbance (Świątek *et al.* 2004a, and **Figure 5-11**). However, these studies only observed an effect of MeJA on cell division at the non-physiological concentration of 100 μ M. The experiments in this chapter observed a block in cell division at 20 μ M, which is the upper range of the physiological concentration (Albrecht *et al.*, 1993).

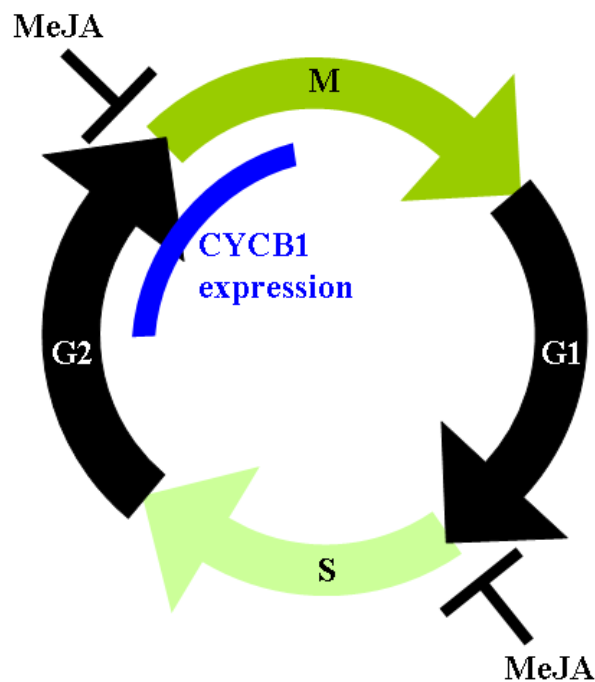


Figure 5-11 The cell cycle in root meristem. Disruptions by MeJA treatment and expression of *CYCB1* are indicated. M: Mitosis. G1: Gap1. G2: Gap2. S: Synthesis

In brief, the MeJA treatment delayed root cell elongation, reduced LEH length and number of mitotic cells, but did not decrease the rate of elongation of individual cells. These findings therefore enhance our knowledge about the mechanism of MeJA-mediated root growth inhibition.

Examination of the QC-LEH area in the MeJA-treated JA and auxin mutants revealed more information about the cause of growth inhibition. To begin with, MeJA-induced reduction of LEH was both *COI1*- and *Jin1*-dependent (**Figure 5-8** and **Figure 5-9**). Moreover, there were more cells in the meristem of *coi1-16* roots than in *Col-gl* (**Figure 5-8**), suggesting that *COI1* is involved in decreasing the cell production in root meristem. Therefore, it will be informative to examine the rate of cell production and mature cell length in *coi1-16*.

Interestingly, *jin1-1* and *coi1-16* did not exhibit apparent developmental delay before their root cells entered the TZ (**Figure 5-9**), which suggests that *COI1* and *JIN1* is responsible for the delayed rapid expansion caused by MeJA. Indeed, *ATMYC2/JIN1* plays a key role in JA-mediated growth inhibition in both *Arabidopsis* and tomato (Boter *et al.*, 2004). The growth arrest by MeJA is more severe in loss-of-function mutants of the MKK3–MPK6 cascade, which is activated by JA and negatively regulates *ATMYC2/JIN1* expression (Takahashi *et al.*, 2007).

AUX encodes an influx carrier that is involved in polar auxin transport. The *aux1* mutant exhibits insensitivity to auxin and defective root gravitropism (Bennett *et al.*, 1996). *aux1-7* had reduced sensitivity to MeJA-induced root growth inhibition (**Figure 5-10**), indicating that disruption of auxin transport suppresses the MeJA-mediated growth inhibition. In fact, auxin and JA have similar signal transduction pathways (Kazan and Manners, 2009). Mutations in genes encoding several different signaling components, for example, *AXR1*, *MYC2* and *JAR1*, affect both signal pathways (Tiryaki and Staswick, 2002. Staswick *et al.*, 2002. Dombrecht *et al.*, 2007). Clearly, auxin is therefore involved in the JA responses and this raises the possibility that other hormones are involved as well.

Chapter 6

***Arabidopsis* Root Growth in Response to MeJA: Setting Up the Parameters**

6.1 Introduction

In Chapter 5, I studied the cellular reactions to MeJA treatment in *Arabidopsis* root. The data indicated that MeJA treatment delayed root cell development before elongation, reduced the LEH length and number of dividing cells, but did not decrease the rate of individual cell elongation. However, some questions remained unanswered. For example, the MeJA treated root had fewer dividing cells in the meristem, but more cells accumulated in the meristem after 24 hrs treatment (Figure 5-5 and Figure 5-6). This indicated that the rate of cell production must have been reduced, and the number of cells in the meristem should have decreased. To confirm and extend these observations in this chapter, the rate of cell production was measured by both mitosis and an independent method, and the cell number in the meristem was also measured.

Root growth in young *Arabidopsis* seedlings is in fact a dynamic progress, i.e., the size of meristem and the cell number in meristem are not constant until the primary root become mature (Beemster and Baskin, 1998). Therefore, in this chapter, we applied a kinetic method to quantify the parameters of root growth under an identical conditions.

Several approaches had been developed to investigate the growth in roots. Using carbon particles to mark the *Zea mays* roots, which was photographed through a slit onto a moving strip of film, gave a series of curves for each carbon particle (Erickson and Sax, 1956). Recently, the automatic and comprehensive merits of

high-throughput quantification have made it become a popular method to trace growth of *Arabidopsis* seedlings grown on agarose (French *et al.*, 2009). At the cell level, a dye loading method was used to trace *Arabidopsis* root cells developing from the meristem to the elongation zone, and to examine the symplastic connection between these cells before they start to differentiate (Duckett *et al.*, 1994). It is now clear that a growth acceleration happens shortly after germination, and the growth rate doubles over a few days until root growth reaches a stable pace; however, the cell expansion rate rarely changes (Baskin *et al.*, 1995. Ubeda-Tomás *et al.*, 2009). In addition, the number of dividing cells and the mature cell length contribute to the increased root length (Beemster and Baskin, 1998).

In this Chapter, I worked with N. Kunpratem as indicated in the text. Following previous investigation (Ubeda-Tomás *et al.*, 2009), parameters were set up to study the dynamic growth of root cells from dividing to reaching their final length in the presence and absence of MeJA. These parameters were: increased root length per day; mature cell length; cell number in meristem; and size of meristem. The meristem was identified as the area from the first cell after QC to the TZ (Figure 6-1). The rate of cell production (cell/day) was calculated from the increased root length ($\mu\text{m}/\text{day}$) divided by the mature cell length ($\mu\text{m}/\text{cell}$). In addition, cell production was measured as the number of mitotic cells in the root meristem (2.3.6) for comparing two independent measures of cell production. The seedlings were observed from 2nd day after germination (DAG) to 7th DAG.

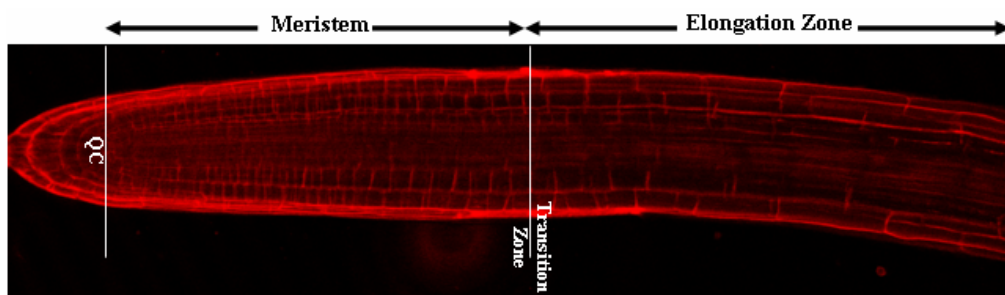


Figure 6-1 Confocal microscopy image of the *Arabidopsis* root apex. The distance between the QC and the transition zone gave the length of meristem.

6.2 Results

The *CYCBI::GUS* transgenic line was used here for its accessibility to monitor the number of dividing cells. Seeds were surface sterilized (2.2.2) and sown on half MS containing 0, 1 μ M, 5 μ M or 20 μ M MeJA (2.1.3 and 2.2.1). Six plates were prepared for each concentration. Plates were left in 4°C in the dark for 5 days to synchronise the germination, before they were moved to a short-day (SD) growth room at 22-23°C, where the plates were held in a vertical plane.

Because the primary roots were still short at 0 and 1st DAG, observations were conducted at 2nd, 3rd, 4th, 5th, 6th and 7th DAG. At each day, one plate of each MeJA concentration was taken out from the growth room, and seedlings were collected for the histochemical detection of GUS activity (by N. Kunpratam) and for observation under the confocal microscope (2.5.3) with staining of 5 μ g/ml propidium iodide to highlight cell walls (Figure 6-2). The number of dividing cells, the increased root length per day, the size of meristem, the meristem cell number, and the mature cell length were measured and plotted. The increased root length per day and the mature cell length were used to calculate the rate of cell production per day.

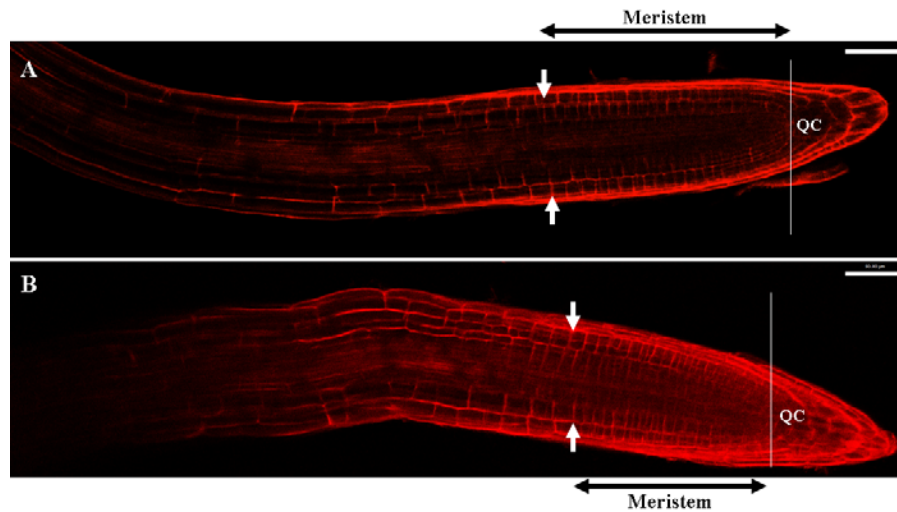


Figure 6-2 Confocal microscopy image of 4 day old *Arabidopsis* root apex. (A) The control root. (B) The 20 μ M MeJA-treated root. The distance between the QC and the TZ (white arrows) addressed the size of meristem. Scale bar 50 μ m.

The meristem size of the untreated *CYCBI::GUS* seedlings grew from 225 μ m

until they reached a stable size, about 280 μm , at day 7 (Figure 6-3). In MeJA treated groups, the meristem size decreased in a concentration-dependent manner. The 1 μM and 5 μM MeJA treatment had similar effects and decreased the meristem size after day 4. The 20 μM MeJA-treated roots exhibited significantly inhibited meristem size at day 2 and day 4-7, and the percentage of inhibition was approximately 20% from day 2 to day 6, and 10% at day 7 (Figure 6-3 and Table 6-1).

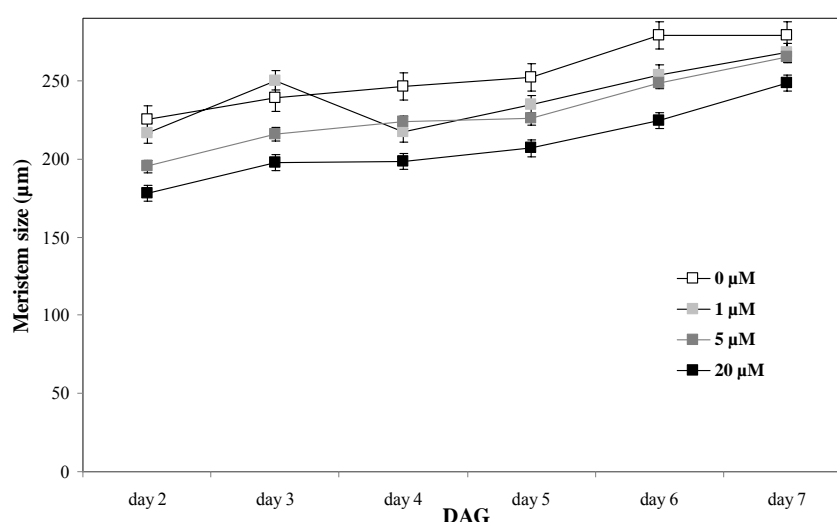


Figure 6-3 Meristem size of the *CYCB1::GUS* seedlings sown on half MS medium containing 0, 1 μM , 5 μM or 20 μM MeJA. Seedlings were observed under confocal microscope from 2nd to 7th DAG. The meristem was identified as the first cell after QC to the TZ.

Table 6-1 Mean meristem size from Figure 6-3 and the statistical significance. Numbers in brackets are the percentage of inhibition (%).

MeJA (μM)	Days after germination					
	2	3	4	5	6	7
0	225.5	238.9	246.5	252.5	279.3	279.0
1	216.6 (3.9)	250.2 (-4.7)	217.5* (11.8)	234.5 (7.1)	253.6 (9.2)	268.0 (4.0)
5	195.2 (13.4)	215.9 (9.6)	223.7* (9.2)	225.8 (10.6)	248.8 (10.9)	265.4 (4.9)
20	178.1* (21.0)	197.6 (17.3)	198.6* (19.4)	206.8* (18.1)	224.4* (19.6)	248.8* (10.8)

* Numbers with asterisk are significantly different ($p < 0.05$, p -value was computed by one-way ANOVA) from the untreated mean value.

Interestingly, the effect of MeJA on the cell number in the meristem was not as obvious as its effect on size. The number of cells in the meristem of the control roots increased from 29 to 34 from day 2 to day 7. Initially, the MeJA-treated roots contained significantly fewer cells than the control roots, about 23 to 26, in the meristem, at day 2 and day 3. However, the meristem cell number in these MeJA-treated roots also increased gradually. In the end, there was no significant difference between the control and treated roots at day 7 (Figure 6-4 and Table 6-2). This suggested that the length of each cell in the meristem was shorter in the MeJA-treated roots than in the control roots.

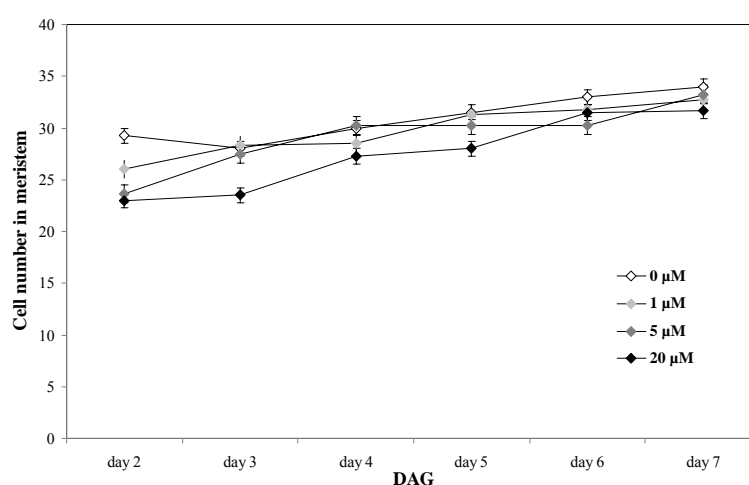


Figure 6-4 Cell number in meristem of the *CYCB1::GUS* seedlings sown on half MS medium containing 0, 1 μ M, 5 μ M or 20 μ M MeJA. Seedlings were observed under confocal microscope from 2nd to 7th DAG. The meristem cells were counted from the first cell after QC to the TZ.

Table 6-2 Mean cell number in meristem from Figure 6-4 and the statistical significance. Numbers in brackets are the percentage of inhibition (%).

MeJA (μ M)	Days after germination					
	2	3	4	5	6	7
0	29.3	28.0	30.0	31.5	33.0	34.0
1	26.0 (11.1)	28.3 (-1.2)	28.5 (5.0)	31.3 (7.9)	31.8 (3.6)	32.8 (3.7)
5	23.7* (19.1)	27.5 (1.8)	30.3 (-8.3)	30.3 (4.0)	30.3 (8.3)	33.3 (2.2)
20	23.0* (21.4)	23.5* (16.1)	27.3* (9.2)	28.0 (11.1)	31.5 (4.5)	31.7 (6.9)

* Numbers with asterisk are significantly different ($p < 0.05$, p -value was computed by one-way ANOVA) from the untreated mean value.

In Chapter 3, I showed that the LEH was reduced by MeJA treatment in *Col-gl* and *35S::COII::HA/coi1-16* seedlings (Figure 3-4). Here, it is shown that the mature cell length of *CYCBI::GUS* roots treated with 0 μM , 1 μM , 5 μM and 20 μM MeJA was reduced in a concentration-dependent manner (Figure 6-5 and Table 6-3). For instance, compared to the untreated seedlings, the 1 μM MeJA-treated roots showed inhibition of cell length less than 10%, the 5 μM MeJA-treated roots showed inhibition of approximately 15%, and the 20 μM MeJA-treated roots showed inhibition of higher than 20% after day 4.

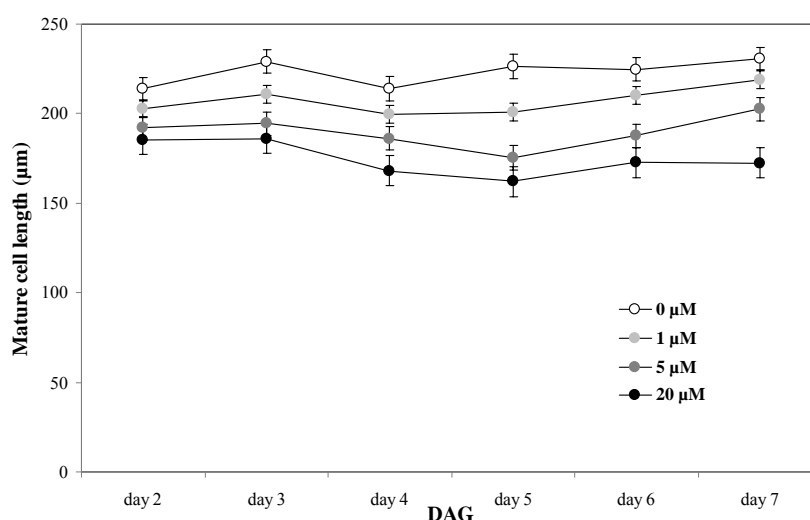


Figure 6-5 Mature cell length of the *CYCBI::GUS* seedlings sown on half MS medium containing 0, 1 μM , 5 μM or 20 μM MeJA. Seedlings were observed under confocal microscope from 2nd to 7th DAG. The mature cells were picked randomly from the differentiation zone.

Table 6-3 Mean mature cell length from Figure 6-5 and the statistical significance. Numbers in brackets are the percentage of inhibition (%).

MeJA (μM)	Days after germination					
	2	3	4	5	6	7
0	213.7	229.0	213.9	226.3	224.7	230.5
1	202.6 (5.2)	210.7 (8.0)	199.4 (6.8)	200.7 (11.3)	210.2 (6.5)	219.2 (4.9)
5	192.0 (10.1)	194.5 (15.0)	186.1 (13.0)	175.4* (22.5)	187.5* (16.6)	202.5 (12.2)
20	185.6 (13.1)	186.2 (18.7)	168.1* (21.4)	162.1* (28.4)	172.8* (23.1)	172.5* (25.2)

* Numbers with asterisk are significantly different ($p < 0.05$, p -value was computed by one-way ANOVA) from the untreated mean value.

Data from the rate of cell production (cell/day) also supported the hypothesis that the MeJA treatment decreased the cell production rate in the meristem. In Figure 6-6, the cell production rate doubled from 11 cells to 22 cells per day during the 7 days observation, and reached a stable production rate after day 6. In the MeJA-treated roots, it was apparent that the higher the MeJA concentration, the greater the inhibition. The 1 μM MeJA treatment caused an inhibition of cell production of 10%, averagely over day 2 to day 7. The 5 μM MeJA treatment initially gave higher reduction rate, 26% and 23% at day 2 and day 3, respectively, but the reduction rate became similar with the 1 μM MeJA treatment after day 4. The 20 μM MeJA treatment caused the highest reduction of the cell production rate. The rate was reduced by 50% before day 5, but increased to more than 60% at day 6 and day 7 (Figure 6-6 and Table 6-4).

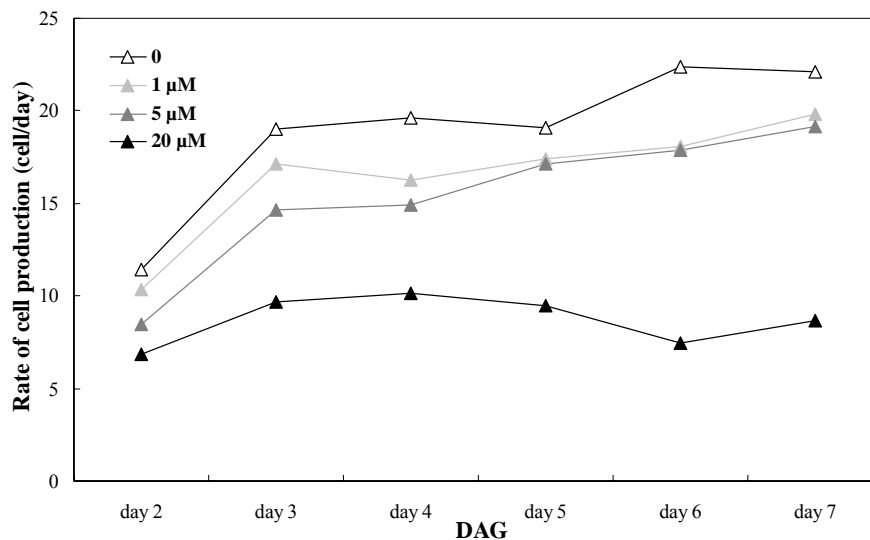


Figure 6-6 Rate of cell production of the *CYCB1::GUS* seedlings sown on half MS medium containing 0, 1 μM , 5 μM or 20 μM MeJA. Seedlings were observed from 2nd to 7th DAG. The rate of cell production (cell/day) was calculated from the increased root length ($\mu\text{m}/\text{day}$, Figure 6-8) divided by the mature cell length ($\mu\text{m}/\text{cell}$, Figure 6-5).

Table 6-4 Mean rate of cell production from Figure 6-6 and the statistical significance. Numbers in brackets are the percentage of inhibition (%).

MeJA (μ M)	Days after germination					
	2	3	4	5	6	7
0	11.4	19.1	19.6	19.1	22.4	22.1
1	10.4 (9.2)	17.1* (10.0)	16.2* (17.3)	17.4* (9.0)	18.1* (19.1)	19.8 (10.2)
5	8.4* (26.1)	14.7* (23.0)	14.9* (24.0)	17.1* (10.3)	17.9* (20.0)	19.1* (13.4)
20	6.8* (40.2)	9.7* (49.2)	10.2* (48.3)	9.5* (50.3)	7.5* (66.5)	8.7* (60.8)

* Numbers with asterisk are significantly different ($p < 0.05$, p -value was computed by one-way ANOVA) from the untreated mean value.

The number of mitotic cells, measured from the number of blue staining cells after histochemical GUS localisation in the meristem of *CYCBI::GUS* plants, agreed with the data from the rate of cell production, and from the previous chapter (5.2.2.2). In control roots, the number of mitotic cells increased from 21 to 33 from day 2 to day 7. The 1 μ M and 5 μ M MeJA treatments both caused a reduction of an average of 13% in cell division, whereas the 20 μ M MeJA treatment caused a significant reduction of an average of 58% over the same period, in cell division (Figure 6-7 and Table 6-5).

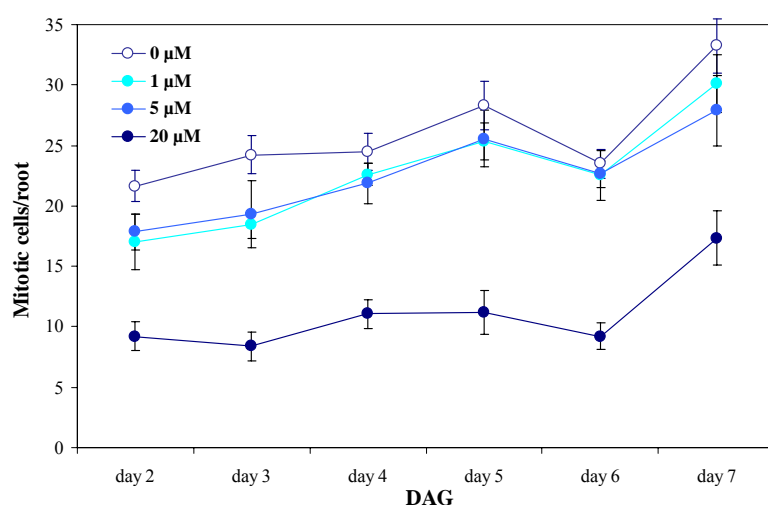


Figure 6-7 Number of mitotic cells at the meristem of the *CYCB1::GUS* seedlings sown on half MS medium containing 0, 1 μM , 5 μM or 20 μM MeJA. Seedlings were observed from 2nd to 7th DAG. The number of dividing cells was measured from the number of blue staining cells after histochemical GUS localisation in the meristem.

Table 6-5 Mean number of mitotic cells from Figure 6-7 and the statistical significance. Numbers in brackets are the percentage of inhibition (%).

MeJA (μM)	Days after germination					
	2	3	4	5	6	7
0	21.64	24.23	24.47	28.31	23.50	33.25
1	17.00 (21.4)	18.42 (24.0)	22.60 (7.6)	25.38 (10.4)	22.55 (4.1)	30.13 (9.4)
5	17.86 (17.5)	19.33 (20.2)	21.86 (10.7)	25.56 (9.7)	22.64 (3.7)	27.89 (16.1)
20	9.21* (57.4)	8.38* (65.4)	11.08* (54.7)	11.18* (60.5)	9.22* (60.8)	17.33* (47.9)

* Numbers with asterisk are significantly different ($p < 0.05$, p -value was computed by one-way ANOVA) from the untreated mean value.

Finally, all of the above growth parameters, including the meristem size, cell number in meristem, mature cell length, rate of cell production and mitotic cell number, had contribution to the increased root length per day (Figure 6-8). In control roots, the increased root length accelerated almost twice, from 0.244 cm/day to 0.436 cm/day, between day 2 and day 3. It was obvious that the increased root length per day was also reduced in a MeJA concentration-dependent manner. For

instance, compared to the untreated seedlings, the 1 μM MeJA-treated roots showed inhibition of increased root length between 14-24%, the 5 μM MeJA-treated roots showed inhibition of more than 30% from day 2 to day 6, and the 20 μM MeJA-treated roots showed inhibition of 50-70% during the observation period. In addition, the increased root length was significantly inhibited by MeJA in all concentrations from day 2 to day 7. The 1 μM MeJA treatment in day 2 was the only exception (Figure 6-8 and Table 6-6).

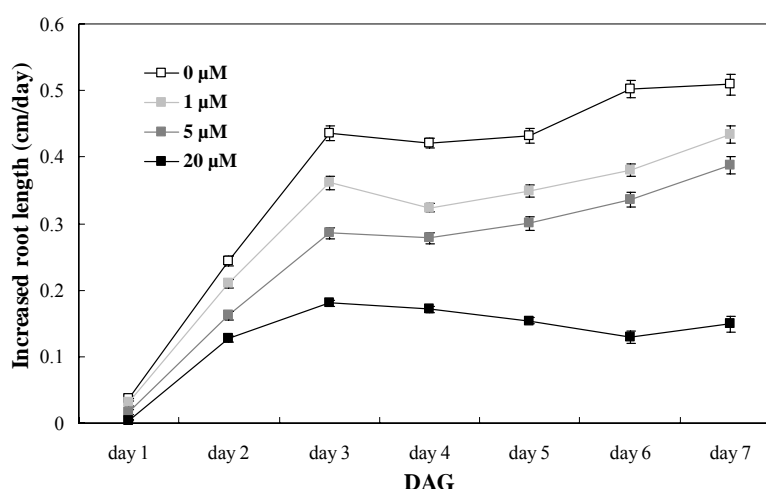


Figure 6-8 Increased root length per day of the *CYCBI::GUS* seedlings sown on half MS medium containing 0, 1 μM , 5 μM or 20 μM MeJA. Plates containing seedlings were scanned from 1st to 7th DAG. Root length of individual seedling was measured and plotted afterwards.

Table 6-6 Mean increased root length per day from Figure 6-8 and the statistical significance. Numbers in brackets are the percentage of inhibition (%).

MeJA (μM)	Days after germination					
	2	3	4	5	6	7
0	0.244	0.436	0.420	0.433	0.503	0.509
1	0.210 (13.9)	0.361* (17.2)	0.324* (22.9)	0.349* (19.3)	0.380* (24.4)	0.434* (14.7)
5	0.162* (33.6)	0.285* (34.6)	0.278* (33.9)	0.301* (30.5)	0.336* (33.2)	0.387* (23.9)
20	0.127* (48.0)	0.180* (58.7)	0.171* (59.3)	0.154* (64.4)	0.129* (74.2)	0.149* (70.7)

* Numbers with asterisk are significantly different ($p < 0.05$, p -value was computed by one-way ANOVA) from the untreated mean value.

6.3 Discussion

The growth of *Arabidopsis* roots is contributed by the number of dividing cells and their mature cell length (Beemster and Baskin, 1998). Evidently, cells in the primary meristem undergo cell cycles of similar duration and enter the TZ, where cells have the final division and start to elongate rapidly. In order to preserve resources such as water and nutrition from soil soon after germination, plants can raise the rate of cell production and/or the mature cell length. Conversely, in the MeJA-mediated root growth inhibition, plants may decrease these parameters to maintain their resources for defense activities (Zavala and Baldwin, 2006). In this chapter, we used methods adapted from previous investigations (Ubeda-Tomás *et al.*, 2009; Dello Ioio *et al.*, 2008). Here, these methods have been used not to simply study the growth patterns in young *Arabidopsis* roots, but to examine in a systematic and standardised way how MeJA affects growth.

Results from the effect of various concentration of MeJA on *CYCBI::GUS* roots showed that the size of meristem, the mature cell length, the rate of cell production, the number of mitotic cells, and the increased root length decreased in response to MeJA treatment (**Figure 6-3, 6-5, 6-6, 6-7 and 6-8**). However, the effect of 1 μ M and 5 μ M MeJA treatments was partly indistinguishable on the size of the meristem, the rate of cell production and the number of mitotic cells. The mature cell length was approximately constant over the observation period for each treatment, and was reduced in increasing concentrations of MeJA (**Figure 6-5**). Constant mature cell length over the observation period has been reported also in untreated and Gibberellin (GA) treated roots (Ubeda-Tomás *et al.*, 2009). The mitotic index in our result was nevertheless two times higher than Ubeda-Tomás' data, in which *CycB1;1::GFP* was used to monitor the effect of GA and PAC treatment on cell division at 6 DAG. Interestingly, MeJA did not reduce cell number in the meristem after day 4 (**Figure 6-4**). These data indicated that MeJA treatment caused a decrease of: the size of the meristem, the mature cell length, the rate of cell production and the number of dividing cells. These parameters would have contributed to the observed reduction in the increased root length (**Figure 6-8**).

It should be noted that the size of the meristem might not be an accurate

parameter when judging MeJA's effect on root growth because the size of meristem was either reduced, or increased, depending on the design of the experiments. In 5.2.2.1, extended (24 hrs, 48 hrs and 72 hrs) MeJA treatment on 6 day old *GFP-TUA6* revealed greater meristem length, due to the accumulation of pre-elongating cells. Nevertheless, in this chapter, MeJA caused a reduction in size of the meristem. It was possible that in this chapter where the seedlings were germinated on MeJA-containing medium, the treatment started to inhibit cell division in the meristem since day 0, which resulted in fewer mitotic cells, less cell production per day, and decreased meristem size, and the developmental delay before the cells entered the TZ was hence not reflected in the data. However, in 5.2.2.1, the seedlings were grown in control conditions before they were transferred to MeJA-containing medium. Possibly, the treatment started to inhibit root growth while the meristem size, the number of mitotic cells and the cell production rate were normal, and it took time for the treatment to have a comprehensive effect on all of the parameters. It was therefore likely that those pre-elongating cells were held in this stage soon after the treatment began and accumulated with newly formed cells before the TZ. This may therefore have created the situation where meristems contained more cells and were longer than controls, while in fact very few cells in this longer meristem maintained the mitosis function, and the accumulated pre-elongating cells did not divide further.

The growth acceleration theory (Baskin et al., 1995) is supported by our data. In untreated *CYCB1::GUS* seedlings, the rate of cell production doubled in 4 days (**Figure 6-6**), similar to a previous report for WT *Arabidopsis* roots shortly after germination (Ubeda-Tomás *et al.*, 2009). The meristem size and number of dividing cells increased during the 7 days observation as well, about 20% and 35%, respectively. Although the size of the meristem was smaller and its increase during the period of observation was not as dramatic as Ubeda-Tomás *et al.* reported, it remained apparent that the rate of cell production, the meristem size, and the number of dividing cells had a greater contribution to the accelerated growth after germination than the number of cells in the meristem. Under this assumption, it was more intriguing to find that the MeJA treatment suppressed the rate of cell production more than the other parameters mentioned above. Although the size of the meristem and the number of dividing cells were both inhibited by the MeJA treatment, these 2 parameters still increased with time. The rate of cell production was the only parameter that doubled in the untreated roots, but there was almost no

change in the 20 μ M MeJA-treated roots during the observation period.

In tobacco BY2 cells, JAs arrests the cell cycle in both G1/S and G2/M transitions (Świątek *et al.*, 2002). It is possible that the cell cycle in mitotic cells in the meristem was slowed down by the MeJA treatment in G1 and in G2, so that it took longer to produce a new cell. Cell cycle arrest is likely to be due to the decline of cyclin-dependent kinases (CDKs), which are a family of protein kinases regulating the cell cycle (Liu and Kipreos, 2000). For instance, the 200 μ M JA treatment sufficiently reduced the expression of cyclin B1;1 and CDK-B during G2 phase in BY2 cells, which revealed a possible link between JA signaling and arrest of cell cycle (Świątek *et al.*, 2004b). However, it remains unknown whether the mitotic cells merely spend more time at G1 and G2 and eventually enter the next phase without further activation, or the arrested cells are needed to be activated to enter the next phase.

In conclusion, it is shown here that the MeJA treatment reduced the rate of cell production and the number of mitotic cells in the meristem, resulting in a decreased meristem size, and inhibition of root growth. In the TZ, MeJA had a different effect, and caused decreased mature cell length. However, the rate of cell production was inhibited more than the other above parameters.

The experiments in this chapter had set up a system that helped us to thoroughly investigate how primary root growth is altered by various treatments in *Arabidopsis* transgenic lines. Clearly, this system could be used to examine MeJA's effect on mutants in different backgrounds to further study the involvement detail of genes in JA signaling.

Chapter 7

***Arabidopsis* Root Growth in Response to MeJA, GA and ABA: Crosstalk Between Plant Hormone Signal Pathways**

7.1 Introduction

The plant hormone signal pathways form a network that integrates developmental processes and response to the environment. The regulation of the crosstalk between hormones may be highly specific and occur only in certain tissues, plant species, or may have resulted from interactions with certain types of pests and pathogens. Usually, connections between two hormone signal pathways were discovered by identifying mutants defective in one signal pathway also have an altered physiological condition or gene expression in the other pathway. In addition, many components in JA signaling have been shown to take part in other hormones' signal transduction as well (Kazan and Manners, 2008).

Among the hormone signaling pathways which are often connected with the JA signal pathway, SA is considered to have an antagonistic relationship with JA in disease resistance (Spoel *et al.*, 2003). Mutations that compromise JA signaling lead to induction of the SA marker genes, and vice versa. Reviewers also suggested that SA and JA signaling work together in controlling the balance of different anti-disease strategies (Smith *et al.*, 2009).

JA and ethylene are both antagonistically and synergistically correlated depending on the condition of the stresses applied. A mutation in the cellulose synthase gene *CeSA3/CEVI* causes constitutive expression of JA- and

ethylene-induced genes, and enhances the resistance to pathogens and pests, indicating that disruption of the cell wall biosynthesis can activate JA and ethylene signaling (Ellis and Turner, 2001; Ellis *et al.*, 2002).

ABA is another plant hormone that can act either antagonistically or synergistically with JA. As a positive regulator of ABA signaling, *AtMYC2/JIN1* can negatively regulate the defense gene expression in JA signaling (Anderson *et al.*, 2004). Moreover, the JA level is induced in ABA treated *Arabidopsis*, suggesting that ABA might activate JA biosynthesis (Adie *et al.*, 2007).

JA's positive relation with the growth hormone auxin has provided a link between development and defense. JA and auxin signaling share many similarities; for instance, the perception of both hormones requires F-box proteins (COI1 for JA and TIR1 for auxin) that mediate the degradation of protein repressors (JAZ proteins for JA and AUX/IAA for auxin) via ubiquitination (Mockaitis and Estelle, 2008). Furthermore, mutations in genes encoding protein components in the signaling pathways, such as *MYC2*, *JASMONATE RESISTANT1 (JAR1)*, *AUXIN RESISTANT1 (AXR1)* and *SGT1b*, suppress both pathways (Dombrecht *et al.*, 2007; Staswick *et al.*, 2002; Tiriyaki and Staswick, 2002; Gray *et al.*, 2003). Auxin is believed to be involved in the MeJA-mediated root growth inhibition, because MeJA suppresses the expression of the auxin reporter *DR5:GUS* in the elongation zone, resulting in blocked polar auxin transportation (T. Nguyen, 2007, unpublished data).

The crosstalk between GA and JA largely depends on DELLA proteins. DELLAs are protein repressors of GA signaling (Fu and Harberd, 2003). By destabilizing DELLAs, such as RGA, RGL2 and GAI, GA signaling promotes cell expansion in stamen filament elongation and root elongation in the endodermis (Cheng *et al.*, 2004; Ubeda-Tomás *et al.*, 2008). The promotion of JA synthesis by GA was found to be DELLA-dependent, and results in induction of the *MYB21*, *MYB24*, and *MYB57* expression (Cheng *et al.*, 2009). Recently, DELLAs were reported to up-regulate the expression of JA-responsive genes through competing with MYC2 for JAZ1 binding in *Arabidopsis*, revealing further details of the molecular mechanism (Hou *et al.*, 2010).

In Chapter 5 and Chapter 6, it is reported that when seedlings are germinated on medium containing MeJA, the root growth was inhibited, the meristem was shorter and contained fewer cells, and the LEH was also shorter. This indicated that

different aspects of cellular development contribute to root growth inhibition by MeJA. In this chapter, I have extended these findings by studying the interaction between the hormones MeJA, auxin, GA, and ABA in the regulation of root growth. For this, root growth was monitored, at intervals, by seven parameters (primary root length, root growth rate, mature cell length, rate of cell production, mitotic index, cell number in meristem, and meristem size) in WT seedlings and the mutants, including *coil-16* (JA signaling), *abi* (ABA signaling), *aux1-7* (auxin signaling), and *della 4* (GA signaling). The *CYCBI::GUS/Col-0* transgenic line was used to monitor mitosis.

To further study the crosstalk between JA and GA, the effect of paclobutrazol (PAC), a GA biosynthesis inhibitor (Olszewski *et al.*, 2002), was tested on root growth rate of *coil-16*, *della 4*, and *gal-3*. The effect of MeJA on root growth was also tested on several GA mutants, including *gai*, *della 4*, and *gal-3* (2.2.5). For the crosstalk between JA and ABA, I used various concentrations of ABA to treat JA mutants from different part of the signaling pathway, including *aos*, *coil-16*, *jai3*, *jin1-1* and *jut* (2.2.5).

7.2 Results

7.2.1 The Effect of MeJA, GA and ABA Treatments on Root Growth of *coil-16*, *abi*, *aux1-7*, and *della4* Mutants Insensitive to JA, ABA, auxin and GA, Respectively

The experiments for root growth responses to JA, GA and ABA were conducted in three WT backgrounds. The first genotype included Col-*gl* and *coil-16*. The second genotype included *CYCBI::GUS/Col-0*, Col-0, *abi* and *aux1-7*. The third genotype included Ler and *della 4*. The transgenic line, *CYCBI::GUS/Col-0* was assumed as WT in its response to the treatments, and a WT control would not therefore be required.

Originally, 10 μ M ABA was used as the treatment concentration. However, this concentration seriously inhibited the germination of the first batch seeds (data not shown). Therefore, the concentration of the ABA treatment was adjusted to 0.5 μ M (Belin *et al.*, 2009) when we handled the second batch. The ABA treatment for

the first batch was conducted separately later with the adjusted concentration to complement the data; hence the data are presented in separate figures (**Figures 7-3, 7-4, 7-11 and 7-12**).

For all the experiments conducted for 7.2.1, seeds were surface sterilised (2.2.2) and approximately 50 were sown on half MS as control, and half MS containing 20 μ M MeJA, 0.5 μ M ABA, or 2 μ M GA (2.1.3 and 2.2.1). For experiments where seedlings were sacrificed to make measurements (meristem size, cell number in meristem, mature cell length and histochemical detection of GUS activity specially prepared for *CYCBI::GUS/Col-0*), six plates were prepared for each of the four treatments, and one plate for each of the 6 days of observation. Plates were left in 4°C in the dark for 5 days to synchronise germination, before they were moved to a SD growth room at 22-23°C, where the plates were held in a vertical plane. Because the primary roots were still short at 0 and 1st DAG, observations were conducted at 2nd, 3rd, 4th, 5th, 6th and 7th DAG. At each day, one plate of each treatment was taken out from the growth room, and seedlings were collected for either the histochemical detection of GUS activity or observation under the confocal microscope (2.5.3) with staining of 5 μ g/ml propidium iodide to highlight cell walls (Figure 6-2). The number of dividing cells per day, the meristem cell number, the mature cell length (μ m) and the meristem size (μ m) were measured and plotted.

Root length was measured continuously and did not involve sacrifice of seedlings. For this, seedlings were grown on plates held in a vertical plane, and the plates were scanned in a Canon CanoScan 5600F document scanner, and root lengths were subsequently measured using Image J software. For each genotype (*Col-0*, *abi*, *aux1-7*, *CYCBI::GUS/Col-0*, *Col-gl*, *coi1-16*, *Ler* and *della*) and treatment (control, 20 μ M MeJA, 0.5 μ M ABA, and 2 μ M GA), 1 plate containing approximately 40 seedlings was prepared, and scanned on seven successive days (0, 1st, 2nd, 3rd, 4th, 5th, 6th and 7th DAG). From these measurements, the increased root length per day was calculated. The increased root length per day and the mature cell length measured from the confocal images were used to calculate the cell production rate per day (Ubeda-Tomás *et al.*, 2008).

7.2.1.1 The Role of *COI1* on JA, GA and ABA Signaling

MeJA, GA and ABA moderate root growth in different ways. The *coil-16* mutant shows insensitivity to MeJA-induced root growth inhibition. Here, I have compared the effects of MeJA, GA and ABA on root growth of *coil-16* and its WT parent, Col-*gl*. The significance of the comparison is based on *p* value < 0.05 according to one-way ANOVA.

Data for cell number in meristem, meristem size, mature cell length, primary root length, root growth rate and cell production rate of Col-*gl* and *coil-16* from 1st to 7th DAG are shown in Figure 7-1, 7-2, 7-3, and 7-4. Data from 7th DAG are summarised in Table 7-1 for ease of comparison.

In the untreated Col-*gl* and *coil-16*, primary root length, root growth rate, cell production rate, cell number in meristem and meristem size were all significantly longer or larger in *coil-16* than in Col-*gl*. The mature cell length was the only parameter which was not different in *coil-16*. These data showed that endogenous JA signaling might inhibit root growth in parameters such as primary root length, root growth rate, cell production rate, cell number in meristem and meristem size, and that *COI1* is required for this inhibition effect.

In the MeJA treatment, primary root length, root growth rate, cell production rate, mature cell length and meristem size were all reduced in Col-*gl*. Cell number in meristem was the only parameter unaffected in the MeJA-treated Col-*gl*. In the MeJA-treated *coil-16*, all of the parameters were significantly higher than those in the MeJA-treated Col-*gl*. However, some of the parameters, such as primary root length, root growth rate and cell production rate were also reduced in the MeJA-treated *coil-16* comparing to untreated *coil-16*, although the reduction in these parameters were not as high as those reduced in the MeJA-treated Col-*gl*. This insensitivity of *coil-16* to the MeJA treatment is predictable, considering *COI1* is a main factor in JA perception, and MeJA-mediated root growth inhibition is reduced in the absence of functional *COI1* (5.2.2.3).

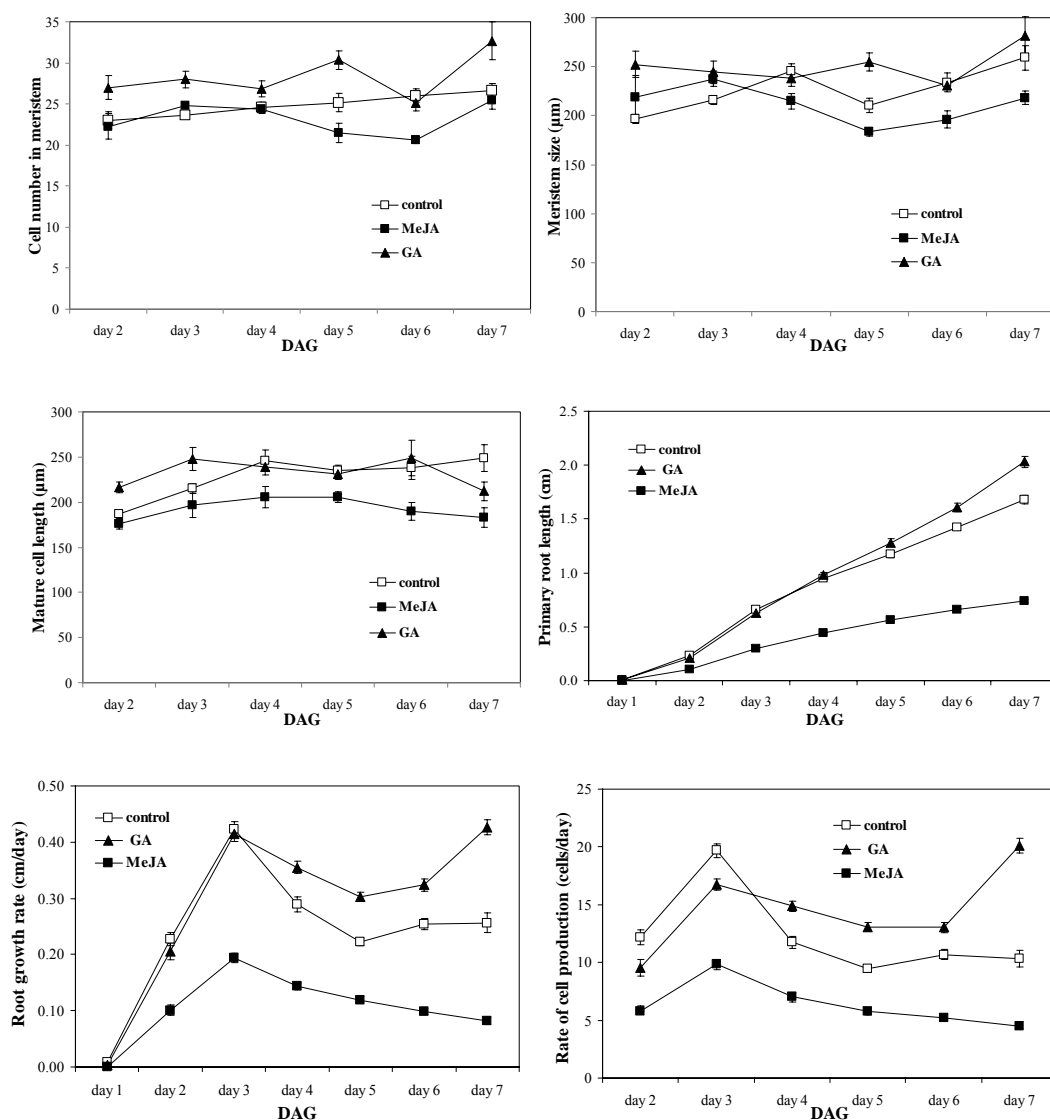


Figure 7-1 Cell number in the meristem, the meristem size, mature cell length, primary root length, root growth rate and rate of cell production of the **Col-*gl*** seedlings sown on half MS medium containing 20 μ M MeJA or 2 μ M GA. Seedlings were observed under microscope from 2nd to 7th DAG. The meristem was identified as the first cell after QC to the TZ.

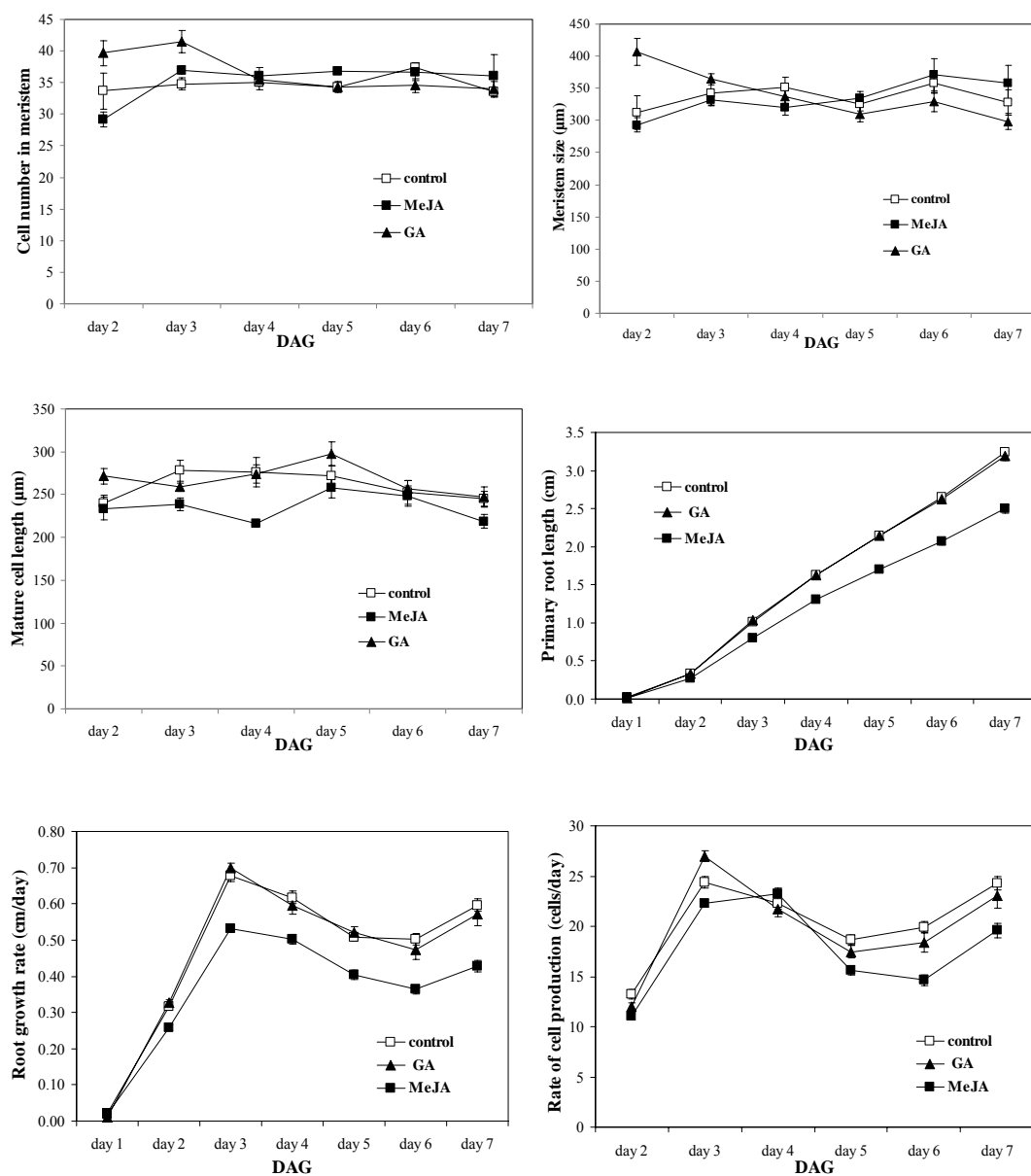


Figure 7-2 Cell number in the meristem, the meristem size, mature cell length, primary root length, root growth rate and rate of cell production of the *coil-16* seedlings sown on half MS medium containing 20 μM MeJA or 2 μM GA. Seedlings were observed under microscope from 2nd to 7th DAG. The meristem was identified as the first cell after QC to the TZ.

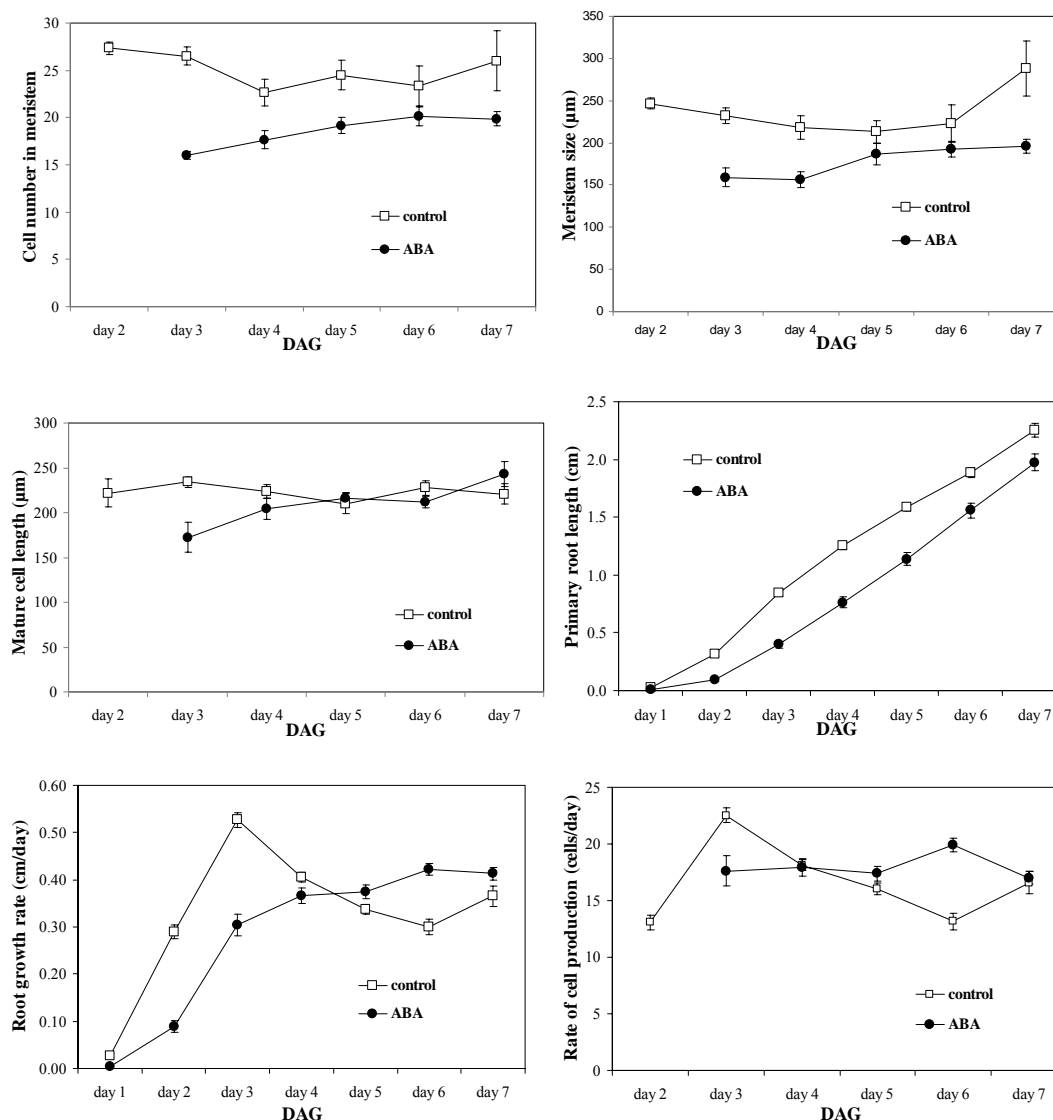


Figure 7-3 Cell number in the meristem, the meristem size, mature cell length, primary root length, root growth rate and rate of cell production of the **Col-*gl*** seedlings sown on half MS medium containing 0.5 μM ABA. Seedlings were observed under microscope from 2nd to 7th DAG. The meristem was identified as the first cell after QC to the TZ.

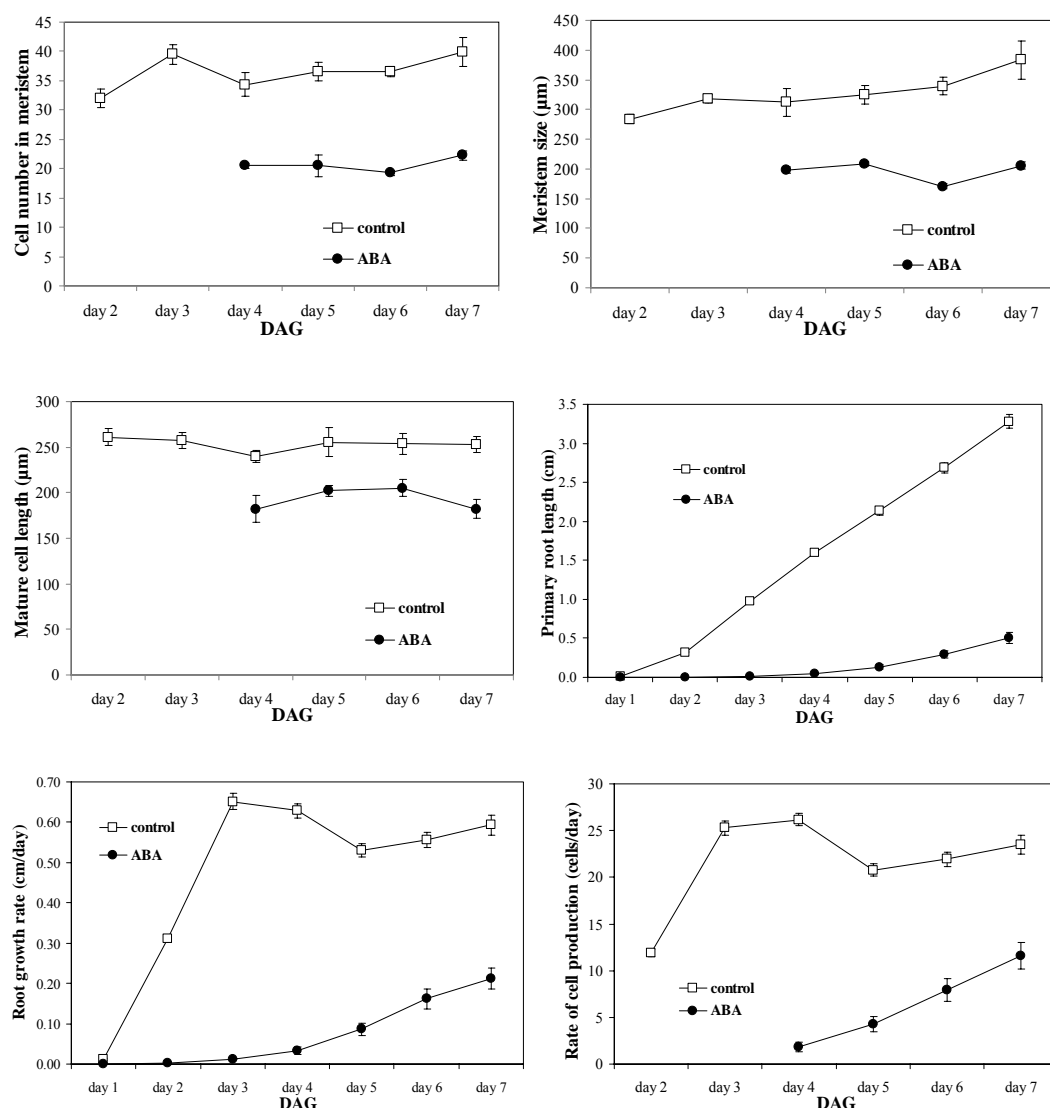


Figure 7-4 Cell number in the meristem, the meristem size, mature cell length, primary root length, root growth rate and rate of cell production of the *coi1-16* seedlings sown on half MS medium containing 0.5 μM ABA. Seedlings were observed under microscope from 2nd to 7th DAG. The meristem was identified as the first cell after QC to the TZ.

Table 7-1 The significance of the parameters differences between Col-*gl* and *coil*-16 at 7th DAG. Y: Significantly different ($p < 0.05$, p -value was computed by one-way ANOVA) from the WT value. N: not significantly different.

		WT (Col- <i>gl</i>)	<i>coil</i> -16	Significant difference
Control	Primary root length (cm)	1.68± 0.04	3.24± 0.05	Y
	Root growth rate (cm/d)	0.11± 0.008	0.25± 0.007	Y
	Mature cell length (µm)	248.70± 14.52	252.50± 13.85	N
	Rate of cell production	10.31±0.73	24.29± 0.70	Y
	Cell number in meristem	26.6±0.93	33.5± 0.62	Y
	Meristem size (µm)	259.04±12.38	328.17± 19.48	Y
MeJA	Primary root length	0.74±0.02	2.50± 0.05	Y
	Root growth rate	0.03± 0.003	0.18± 0.007	Y
	Mature cell length	183.09± 10.74	248.17± 11.49	Y
	Rate of cell production	4.51± 0.36	19.6± 0.73	Y
	Cell number in meristem	25.4± 1.03	36± 3.36	Y
	Meristem size	217.95± 6.87	358.59± 26.63	Y
GA	Primary root length	2.03± 0.05	3.19± 0.06	Y
	Root growth rate	0.18± 0.006	0.24± 0.01	Y
	Mature cell length	212.03± 10.75	256.62± 9.44	Y
	Rate of cell production	20.11± 0.66	23.09± 1.26	Y
	Cell number in meristem	32.67± 2.30	34± 1.21	N
	Meristem size	281.26± 20.02	329.15± 15.16	N
ABA	Primary root length	1.97± 0.07	0.51± 0.07	Y
	Root growth rate	0.17± 0.006	0.09± 0.01	Y
	Mature cell length	242.73± 14.02	181.92± 10.56	Y
	Rate of cell production	17.01± 0.58	11.63± 1.42	Y
	Cell number in meristem	19.88± 0.72	22.25± 0.80	N
	Meristem size	196.32± 8.16	205.64± 6.45	N

In the GA treatment, primary root length, root growth rate, cell production rate and cell number in meristem increased in Col-*gl*. Mature cell length was reduced in the GA-treated Col-*gl*, but only at 7th DAG. In GA-treated *coil*-16, none of the parameters were promoted or inhibited. However, primary root length, root growth rate and cell production rate were significantly higher in the GA-treated *coil*-16 than in Col-*gl*. This suggested that the *coil*-16 roots are insensitive to the GA treatment and *COII* might be required for GA-mediated root growth promotion. Alternatively, considering all parameters were already bigger in untreated *coil*-16 than in Col-*gl*, it is possible that those in *coil*-16 had reached their maximum range and could not be promoted further.

In the ABA treatment, primary root length, cell number in meristem and meristem size were reduced in the ABA-treated Col-*gl*. However, in the ABA treated *coil*-16, all parameters were reduced severely compared to the untreated *coil*-16. The primary root length, root growth rate, cell production rate and mature cell length were significantly smaller/lower in the treated *coil*-16 than in the treated Col-*gl*. This indicated that *COIL* might be required for resistance of ABA-mediated growth reduction. Considering the delayed seed germination of ABA-treated *coil*-16, it is also possible that the parameters were lower/smaller because the ABA effect on the *coil*-16 seeds persists for several days after germination. Further experiments need to be conducted to test if this hyper-sensitivity of *coil*-16 to the ABA treatment was due to an effect on the seed, or to an effect on the root.

7.2.1.2 The Role of *AUX1* on JA, GA and ABA Signaling

Auxin is another important hormone in moderating plant root growth. The *aux1*-7 mutant exhibits insensitivity to MeJA-induced root growth inhibition (5.2.2.3). Here, I have compared the effects of MeJA, GA and ABA on root growth of *aux1*-7 and its WT parent, Col-0. The significance of the comparison is based on *p* value < 0.05 according to one-way ANOVA.

Data for cell number in meristem, meristem size, mature cell length, primary root length, root growth rate and cell production rate of Col-0 and *aux1*-7 from 1st to 7th DAG are shown in Figure 7-5 and Figure 7-6. Data from 7th DAG were summarised in Table 7-2 for the ease of comparison.

In the control group, the primary root length, root growth rate, cell production rate, cell number in meristem and meristem size were reduced in *aux1*-7 compared to Col-0, suggesting that disruption of auxin transportation can inhibit root growth by affecting several parameters apart from the mature cell length.

In the MeJA treatment, all the parameters in both treated Col-0 and *aux1*-7 were reduced. However, the mature cell length of the MeJA-treated Col-0 was significantly smaller than those in the MeJA-treated *aux1*-7, and the cell production rate of the MeJA-treated Col-0 was significantly higher than those in the MeJA-treated *aux1*-7. This indicated that *aux1*-7 is less sensitive to the MeJA treatment in primary root length, root growth rate, cell number in meristem,

meristem size and particularly mature cell length. This suggests that auxin transportation or auxin response is important for MeJA-mediated root growth inhibition.

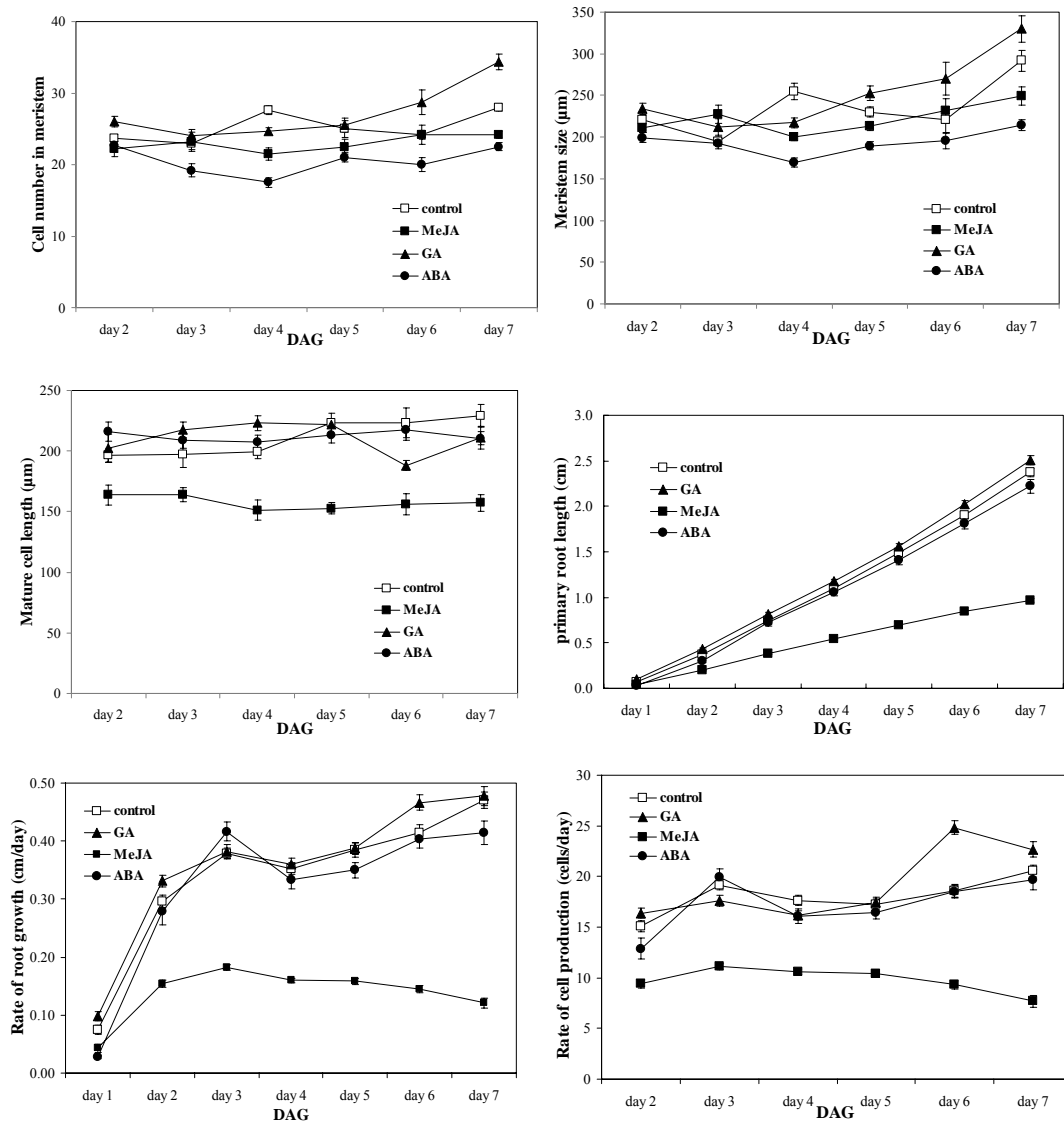


Figure 7-5 Cell number in the meristem, the meristem size, mature cell length, primary root length, root growth rate and rate of cell production of the **Col-0** seedlings sown on half MS medium containing 20 μM MeJA, 0.5 μM ABA, or 2 μM GA. Seedlings were observed under microscope from 2nd to 7th DAG. The meristem was identified as the first cell after QC to the TZ.

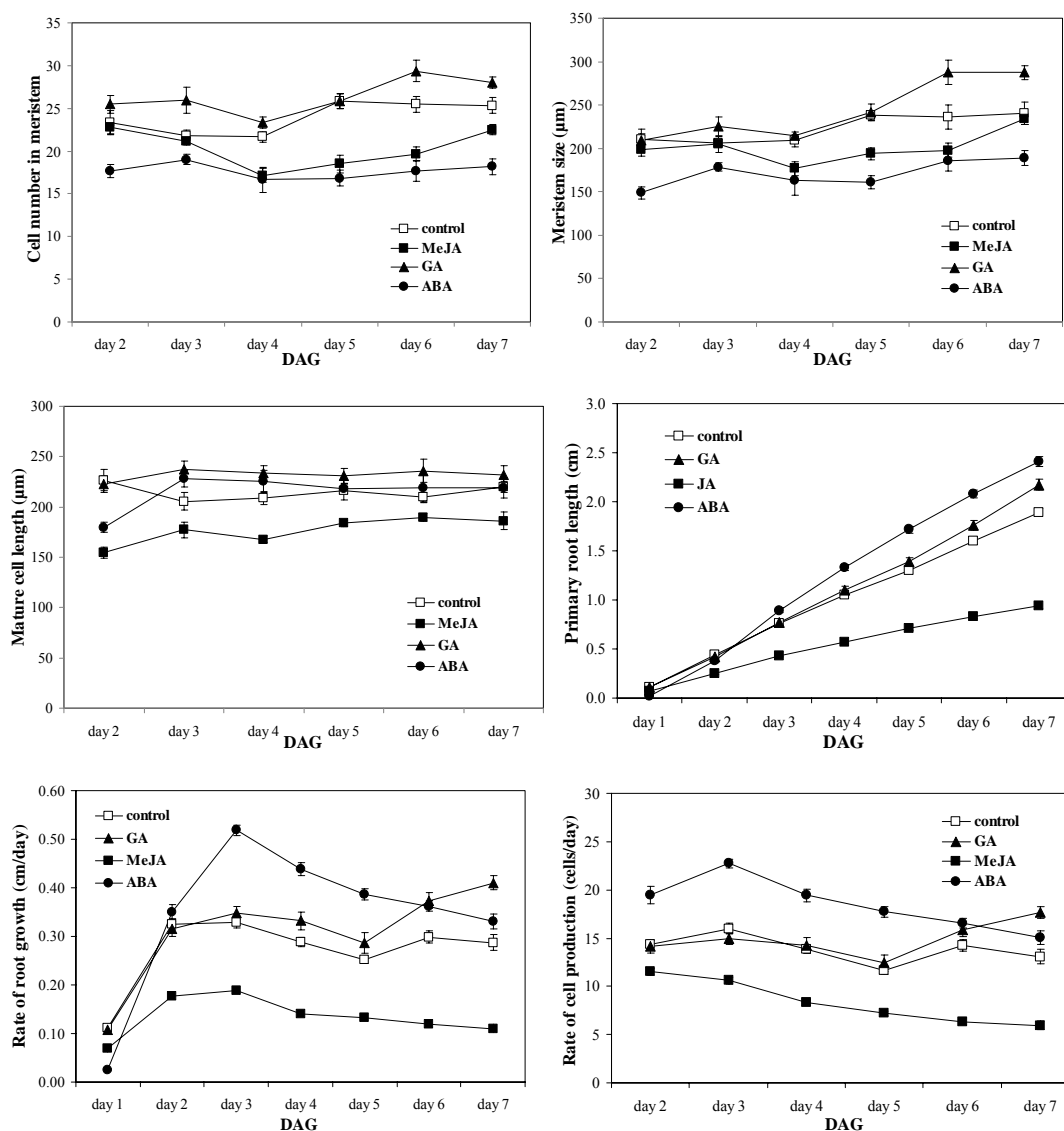


Figure 7-6 Cell number in the meristem, the meristem size, mature cell length, primary root length, root growth rate and rate of cell production of the *aux1-7* seedlings sown on half MS medium containing 20 μM MeJA, 0.5 μM ABA, or 2 μM GA. Seedlings were observed under microscope from 2nd to 7th DAG. The meristem was identified as the first cell after QC to the TZ.

Table 7-2 The significance of the parameters differences between Col-0 and *aux1-7* at 7th DAG. Y: Significantly different ($p < 0.05$, p -value was computed by one-way ANOVA) from the WT value. N: not significantly different.

		WT (Col-0)	<i>aux1-7</i>	Significant difference
Control	Primary root length (cm)	2.37± 0.05	1.89± 0.04	Y
	Root growth rate (mm/h)	0.20± 0.006	0.12± 0.007	Y
	Mature cell length (µm)	229.02± 9.13	219.81± 5.81	N
	Rate of cell production	20.55± 0.59	13.08± 0.74	Y
	Cell number in meristem	28± 0.52	25.33± 0.95	Y
	Meristem size (µm)	291.53± 12.52	240.67± 12.85	Y
MeJA	Primary root length	0.96± 0.02	0.94± 0.03	N
	Root growth rate	0.05± 0.004	0.05± 0.004	N
	Mature cell length	157.17± 6.60	185.94± 8.72	Y
	Rate of cell production	7.70± 0.56	5.93± 0.45	Y
	Cell number in meristem	24.17± 0.54	22.5± 0.56	N
	Meristem size	249.22± 10.87	233.69± 6.58	N
GA	Primary root length	2.50± 0.05	2.17± 0.06	Y
	Root growth rate	0.20± 0.007	0.17± 0.006	Y
	Mature cell length	210.97± 9.17	232.29± 8.67	N
	Rate of cell production	22.65± 0.77	17.65± 0.62	Y
	Cell number in meristem	34.33± 1.12	28± 0.68	Y
	Meristem size	329.8± 15.86	287.42± 8.02	Y
ABA	Primary root length	2.22± 0.07	2.41± 0.05	N
	Root growth rate	0.17± 0.008	0.14± 0.007	Y
	Mature cell length	210.60± 5.74	219.10± 10.35	N
	Rate of cell production	19.67± 0.95	15.08± 0.72	Y
	Cell number in meristem	22.5± 0.56	18.17± 0.95	Y
	Meristem size	214.29± 6.63	188.73± 8.77	Y

In the GA treatment, only the cell number in the meristem and meristem size increased in the GA-treated Col-0. However, the primary root length, root growth rate, cell production rate and meristem size also increased in the GA-treated *aux1-7*. Although there were more parameters promoted in the GA-treated *aux1-7* than in the GA-treated Col-0, the primary root length, root growth rate, cell production rate, cell number in meristem and meristem size were significantly smaller in the GA-treated *aux1-7* than those in the GA-treated Col-0. This suggested that disruption of auxin transportation does not interrupt the GA-mediated growth promotion. It is also possible that GA treatment restores root growth defects in the *aux1-7* mutant.

In the ABA treatment, both cell number in meristem and meristem size were reduced in the ABA-treated Col-0 and *aux1-7*, but primary root length increased in the ABA-treated *aux1-7*. In addition, the root growth rate, cell production rate, cell number in meristem and meristem size remained significantly smaller in the ABA-treated *aux1-7* than those in the ABA-treated Col-0. This indicated that the 0.5 μ M ABA treatment has inhibitory effect mainly on the meristem. This effect not only caused no reduction on the growth rate, but even increased the primary root length of the ABA-treated *aux1-7*. It is possible that other growth parameters, such as rate of cell elongation and number of dividing cells, were promoted by the ABA treatment in contributing to the increased root length in *aux1-7*. This experiment also showed that disruption of auxin transportation does not interfere with ABA-mediated growth arrest or promotion.

7.2.1.3 The Role of *ABI* on JA, GA and ABA Signaling

The ABA-insensitive mutant, *abi*, was included to study if the defective ABA signaling could affect JA, GA and ABA signaling in the growing roots. The significance of the comparison is based on p value < 0.05 according to one-way ANOVA.

Data for cell number in meristem, meristem size, mature cell length, primary root length, root growth rate and cell production rate of Col-0 and *abi* from 1st to 7th DAG are shown in Figure 7-5 (7.2.1.2) and Figure 7-7. Data from 7th DAG are summarised in Table 7-3 for the ease of comparison.

In the control group, *abi* has a larger meristem size and more cells in the meristem than Col-0, indicating that endogenous ABA signaling might contribute to controlling the primary root growth by decreasing the meristem parameters. However, this change on meristem size and cell numbers in meristem does not affect the primary root length, suggesting that there must be other root growth parameters influenced by the ABA signaling. In this case, a reduction of meristem cell number and meristem size did not result in a change in root length.

In the MeJA treatment, all root parameters were reduced in both Col-0 and *abi*, showing that ABA signaling is not required for MeJA-mediated root growth inhibition.

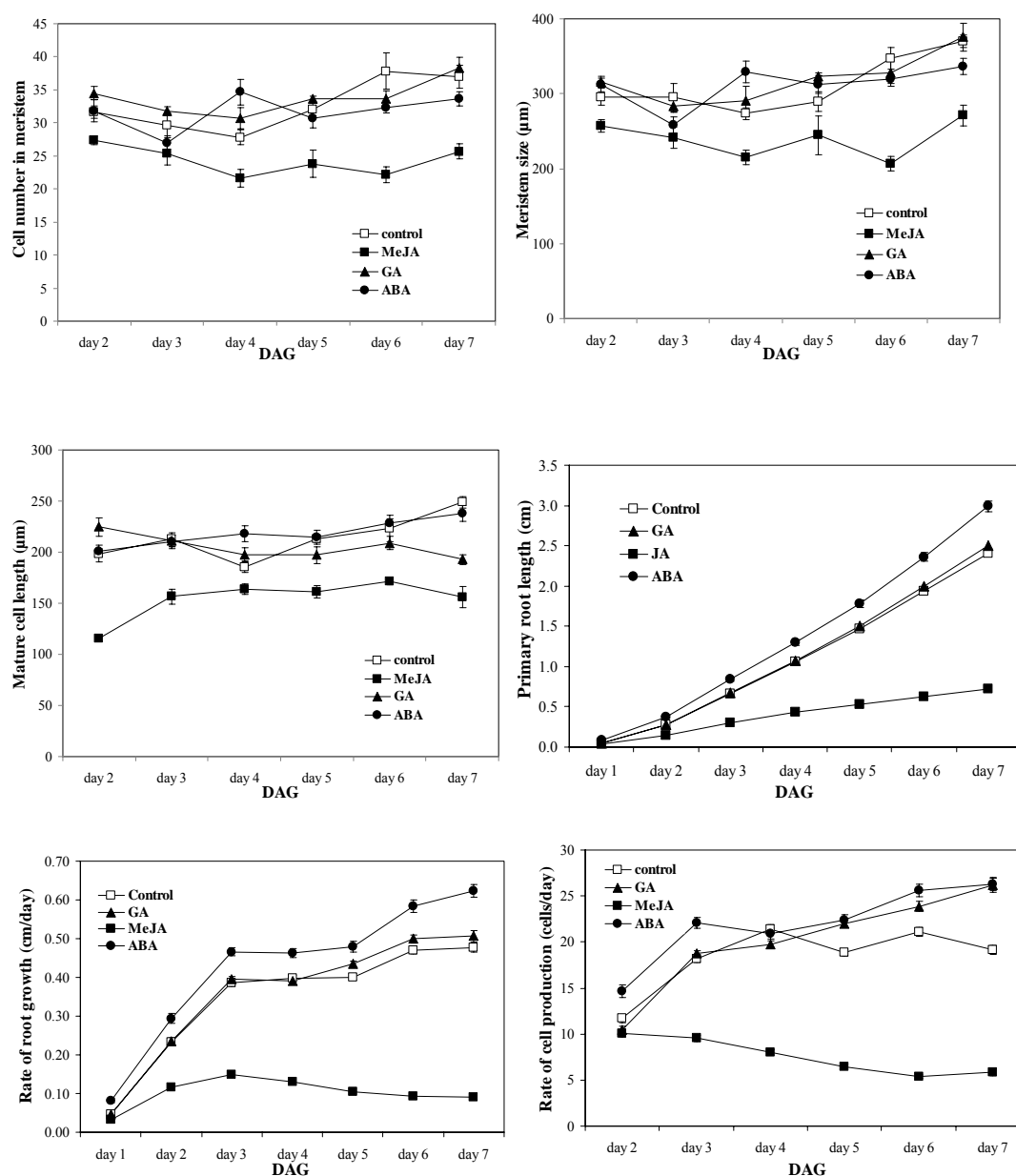


Figure 7-7 Cell number in the meristem, the meristem size, mature cell length, primary root length, root growth rate and rate of cell production of the *abi* seedlings sown on half MS medium containing 20 μM MeJA, 0.5 μM ABA, or 2 μM GA. Seedlings were observed under microscope from 2nd to 7th DAG. The meristem was identified as the first cell after QC to the TZ.

Table 7-3 The significance of the parameters differences between Col-0 and *abi* at 7th DAG. Y: Significantly different ($p < 0.05$, p -value was computed by one-way ANOVA) from the WT value. N: not significantly different.

		WT (Col-0)	<i>abi</i>	Significant difference
Control	Primary root length (cm)	2.37± 0.05	2.41± 0.04	N
	Root growth rate (mm/h)	0.20± 0.006	0.20± 0.005	N
	Mature cell length (µm)	229.02± 9.13	248.94± 5.51	N
	Rate of cell production	20.55± 0.59	19.14± 0.50	N
	Cell number in meristem	28± 0.52	37± 1.77	Y
	Meristem size (µm)	291.53± 12.52	370.02± 7.96	Y
MeJA	Primary root length	0.96± 0.02	0.72± 0.02	Y
	Root growth rate	0.05± 0.004	0.04± 0.002	Y
	Mature cell length	157.17± 6.60	155.83± 10.46	N
	Rate of cell production	7.70± 0.56	5.83± 0.37	Y
	Cell number in meristem	24.17± 0.54	25.67± 1.12	N
	Meristem size	249.22± 10.87	270.98± 13.46	N
GA	Primary root length	2.50± 0.05	2.51± 0.03	N
	Root growth rate	0.20± 0.007	0.21± 0.006	N
	Mature cell length	210.97± 9.17	209.01± 6.34	N
	Rate of cell production	22.65± 0.77	26.22± 0.79	Y
	Cell number in meristem	34.33± 1.12	38.33± 1.56	Y
	Meristem size	329.8± 15.86	375.71± 18.39	N
ABA	Primary root length	2.22± 0.07	2.99± 0.07	Y
	Root growth rate	0.17± 0.008	0.26± 0.007	Y
	Mature cell length	210.60± 5.74	237.64± 7.69	Y
	Rate of cell production	19.67± 0.95	26.26± 0.68	Y
	Cell number in meristem	22.5± 0.56	33.67± 1.09	Y
	Meristem size	214.29± 6.63	336.43± 10.38	Y

In the GA treatment of Col-0, the cell number in meristem and meristem size increased. However, the GA treatment of *abi* had no effect on cell number in meristem and meristem size, but reduced the mature cell length and increased the cell production rate. Considering that the cell number in meristem and meristem size were promoted in the untreated *abi*, it is possible that these parameters could not be promoted further by the GA treatment. Because GA treatment reduces the mature cell length in *abi*, but does not alter the root growth rate, it follows that there must be a compensating increase in the rate of cell production in GA-treated *abi*. Apparently, *ABI* suppresses these effects of GA in WT plants.

In the ABA treatment, the cell number in meristem and meristem size were reduced in the treated Col-0, whereas primary root length, root growth rate and cell production rate increased in the treated *abi*. The fact that the ABA treatment could decrease the meristem parameters in Col-0 but not in *abi* echoes the finding that in the untreated Col-0, the meristem parameters were smaller than in *abi*. Presumably, this is due to the action of endogenous ABA. In addition, because *abi* remained sensitive to the ABA treatment in root growth rate and cell production rate, which were not induced by exogenous ABA in Col-0, this suggests not only that *abi* is not insensitive to ABA, but also that *ABI* suppresses the ABA-induced promotion in root growth rate and cell production rate.

7.2.1.4 The Role of *DELLAs* on JA, GA and ABA Signaling

GA increases plant root growth by promoting cell number in meristem, mature cell length, primary root length, root growth rate and cell production rate in Col-*gl*, and cell number in meristem and meristem size in Col-0. The *della 4* mutant, which lacks in 4 DELLA proteins (GAI, RGA, RGL1 and RGL2) and is insensitive to GA, was therefore used. Here, I have compared the effects of MeJA, GA and ABA on root growth of *della 4* and its WT parent, Ler. The significance of the comparison is based on p value < 0.05 according to one-way ANOVA.

Data for cell number in meristem, meristem size, mature cell length, primary root length, root growth rate and cell production rate of Ler and *della 4* from 1st to 7th DAG are shown in Figure 7-8 and Figure 7-9. Data from 7th DAG were summarised in Table 7-4 for the ease of comparison.

In the untreated control group, no difference in parameters could be found between Ler and *della 4*. This indicated that the mutated 4 DELLA proteins are not responsible for these root growth-related parameter at least within 7 days after germination.

In the MeJA treatment, all parameters in both Ler and *della 4* were reduced, and the reduction degree showed no difference between treated Ler and treated *della 4* either. It is apparent that GAI, RGA, RGL1 and RGL2 are not required for the MeJA-mediated root growth inhibition.

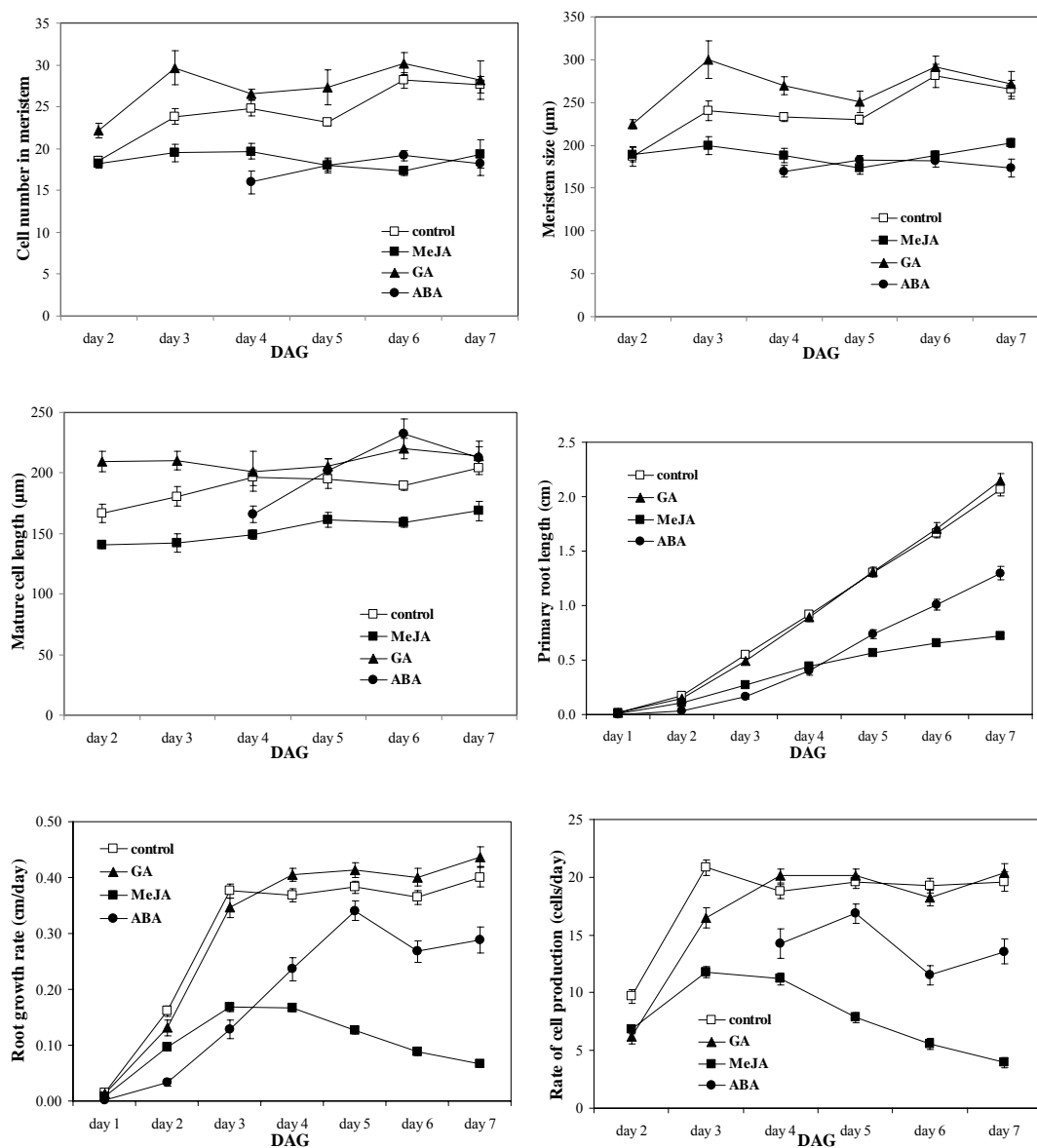


Figure 7-8 Cell number in the meristem, the meristem size, mature cell length, primary root length, root growth rate and rate of cell production of the **Ler** seedlings sown on half MS medium containing 20 μ M MeJA, 0.5 μ M ABA, or 2 μ M GA. Seedlings were observed under microscope from 2nd to 7th DAG. The meristem was identified as the first cell after QC to the TZ.

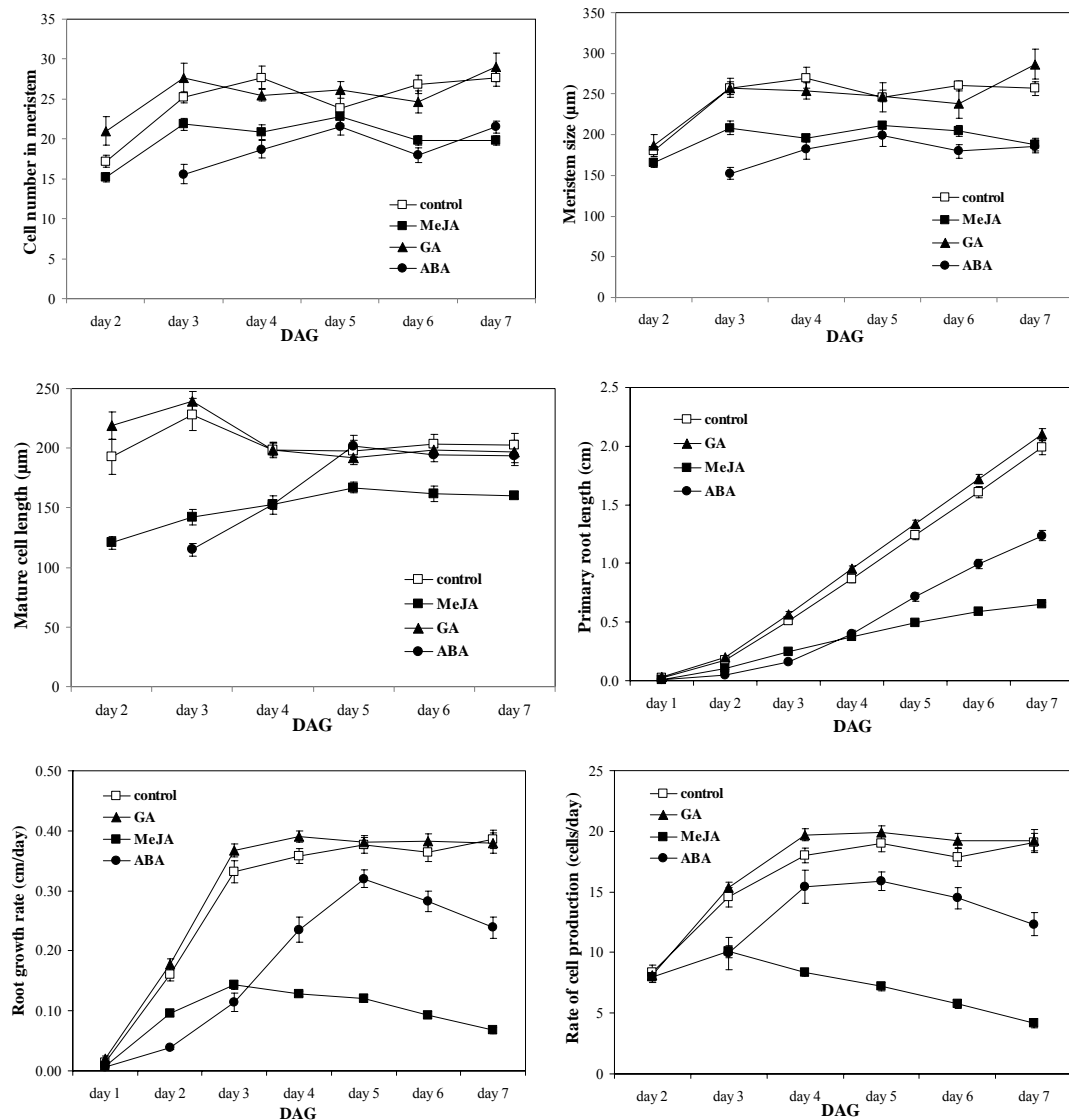


Figure 7-9 Cell number in the meristem, the meristem size, mature cell length, primary root length, root growth rate and rate of cell production of the *della 4* seedlings sown on half MS medium containing 20 μM MeJA, 0.5 μM ABA, or 2 μM GA. Seedlings were observed under microscope from 2nd to 7th DAG. The meristem was identified as the first cell after QC to the TZ.

Table 7-4 The significance of the parameters differences between Ler and *della 4* at 7th DAG. Y: Significantly different ($p < 0.05$, p -value was computed by one-way ANOVA) from the WT value. N: not significantly different.

		WT (Ler)	<i>della 4</i>	Significant difference
Control	Primary root length (cm)	2.07± 0.06	1.99± 0.06	N
	Root growth rate (mm/h)	0.17± 0.007	0.16± 0.007	N
	Mature cell length (µm)	204.37± 5.63	202.32± 10.17	N
	Rate of cell production	19.61± 0.82	19.07± 0.8	N
	Cell number in meristem	27.67± 1.02	27.67± 1.02	N
	Meristem size (µm)	264.87± 11.43	256.72± 8.82	N
MeJA	Primary root length	0.72± 0.02	0.66± 0.02	N
	Root growth rate	0.03± 0.003	0.03± 0.003	N
	Mature cell length	168.76± 8.07	160.45± 2.82	N
	Rate of cell production	3.96± 0.42	4.19± 0.37	N
	Cell number in meristem	19.33± 1.71	19.83± 0.60	N
	Meristem size	202.96± 5.44	187.64± 8.14	N
GA	Primary root length	2.15± 0.07	2.10± 0.05	N
	Root growth rate	0.18± 0.007	0.16± 0.007	N
	Mature cell length	214.30± 11.71	197.24± 9.14	N
	Rate of cell production	20.42± 0.80	19.25± 0.86	N
	Cell number in meristem	28.17± 2.30	29± 1.79	N
	Meristem size	271.79± 14.93	286.66± 18.76	N
ABA	Primary root length	1.30± 0.06	1.24± 0.04	N
	Root growth rate	0.12± 0.01	0.10± 0.008	N
	Mature cell length	212.56± 9.45	193.40± 7.80	N
	Rate of cell production	13.56± 1.09	12.35± 0.93	N
	Cell number in meristem	18.17± 1.40	21.5± 0.76	N
	Meristem size	173.73± 10.38	185.44± 7.66	N

In the GA treatment, both Ler and *della 4* were insensitive to the treatment, and there were no difference between parameters in treated Ler and treated *della 4*. It was expected that *della 4* would be insensitive to the GA treatment. However, because Ler was also insensitive to the treatment, this raised the question that the Ler ecotype is generally insensitive to GA.

In the ABA treatment, the cell number in meristem, meristem size, primary root length, root growth rate and cell production rate were all reduced in the treated Ler and *della 4*. In addition, there were no significant difference between these parameters in treated Ler and treated *della 4*. This suggested that ABA-mediated growth reduction does not require functional GAI, RGA, RGL1 and RGL2.

7.2.1.5 The Effect of MeJA, GA and ABA Treatment on Cyclin B1 Expression

CYCBI::GUS/Col-0 was treated with MeJA, GA and ABA to examine their effects on Cyclin B1 index, which represents mitotic cell number and could be compared with the cell production rate calculated from mature cell length and root growth rate per day.

MeJA significantly reduced the mature cell length, the primary root length, the root growth rate and the rate of cell production of *CYCBI::GUS/Col-0*, but the cell number in meristem and the meristem size were not reduced as much as other parameters (Figure 7-10). GA's effect on *CYCBI::GUS/Col-0* was most obvious in the promoted rate of cell production, while other parameters were not altered significantly (Figure 7-10). In Figure 7-12, the Cyclin B1 expression was promoted only by the GA treatment at 6th DAG, whereas the Cyclin B1 expression was decreased by MeJA and ABA treatment to a similar degree from 5th to 7th DAG (about 5 mitotic cells/ day, Figure 7-12). Surprisingly, the cell production rate was the only parameter that increased in the ABA-treated *CYCBI::GUS/Col-0* (Figure 7-11), while Cyclin B1 expression, cell number in meristem, meristem size and primary root length were all reduced by ABA. These data indicated that the Cyclin B1 expression might correspond to the cell production rate in the case of MeJA and GA treatment, whereas the Cyclin B1 expression was inhibited, but rate of cell production was increased by the ABA treatment. Apparently, Cyclin B1 expression and cell production rate do not always relate to each other. It is possible that ABA reduces the time taken for the mitotic cycle, giving an apparent reduction in the mitotic index.

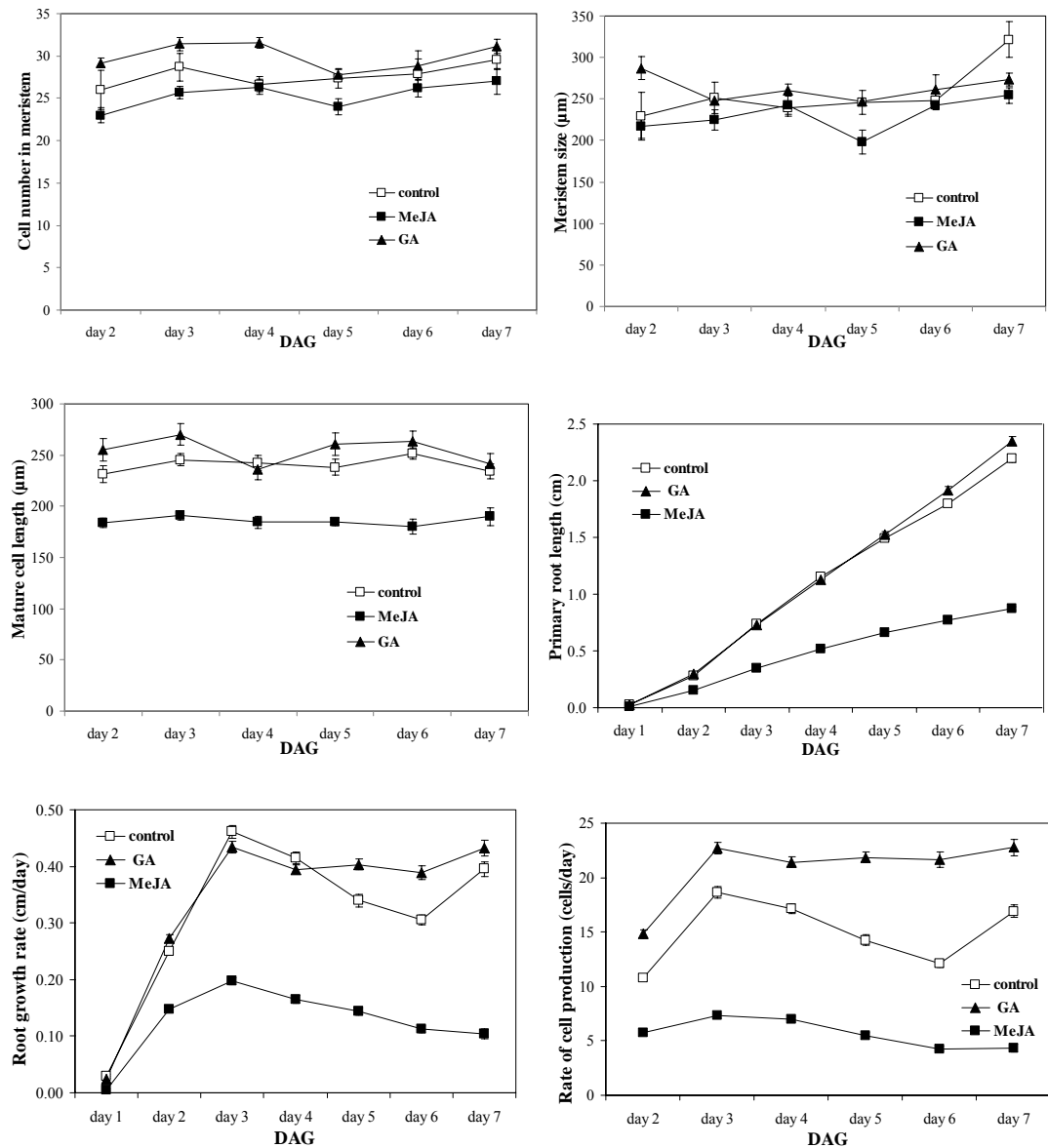


Figure 7-10 Cell number in the meristem, the meristem size, mature cell length, primary root length, root growth rate and rate of cell production of the *CYCB1::GUS/Col-0* seedlings sown on half MS medium containing 20 μM MeJA or 2 μM GA. Seedlings were observed under microscope from 2nd to 7th DAG. The meristem was identified as the first cell after QC to the TZ.

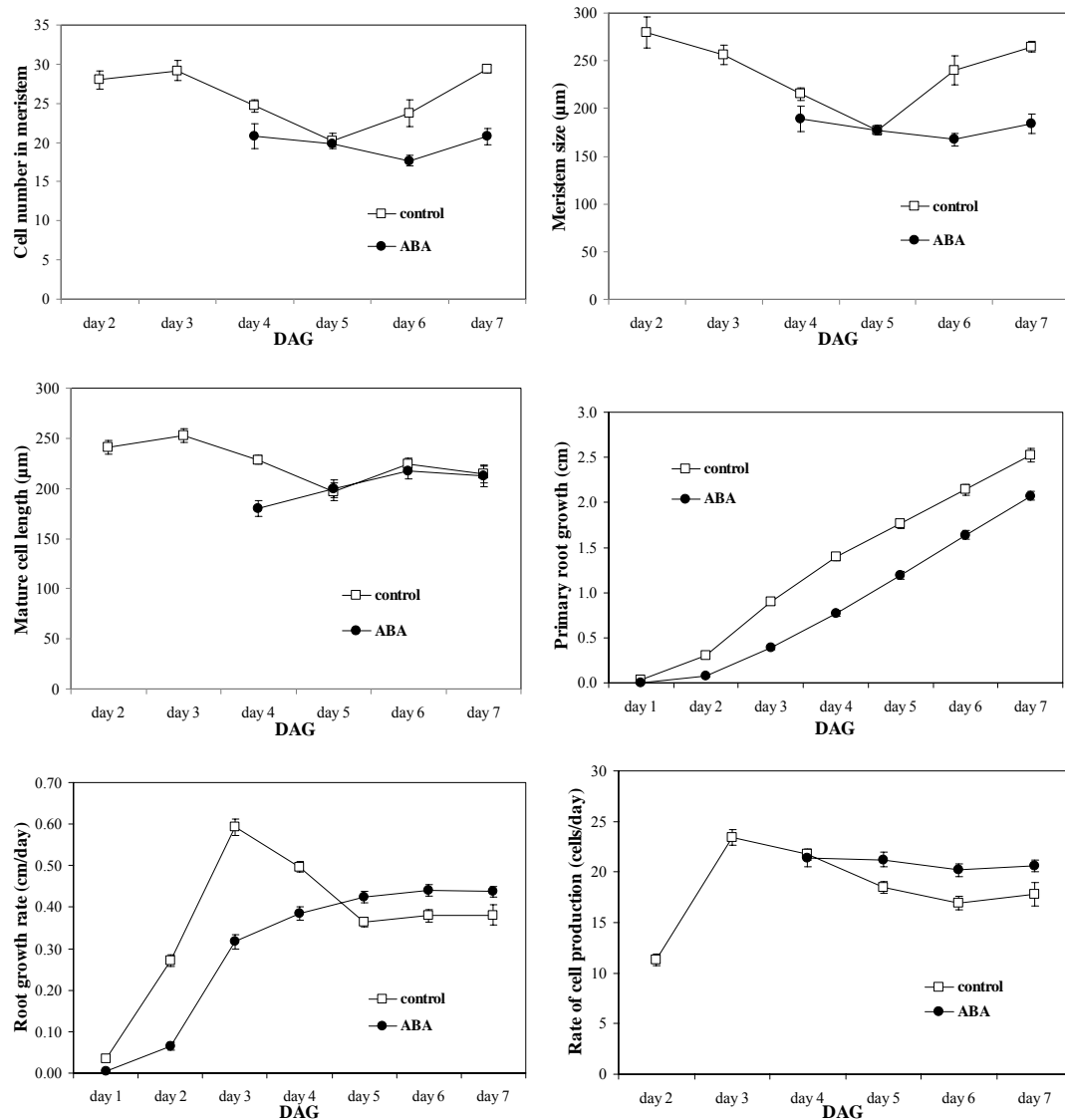


Figure 7-11 Cell number in the meristem, the meristem size, mature cell length, primary root length, root growth rate and rate of cell production of the *CYCB1::GUS/Col-0* seedlings sown on half MS medium containing 0.5 μM ABA. Seedlings were observed under microscope from 2nd to 7th DAG. The meristem was identified as the first cell after QC to the TZ.

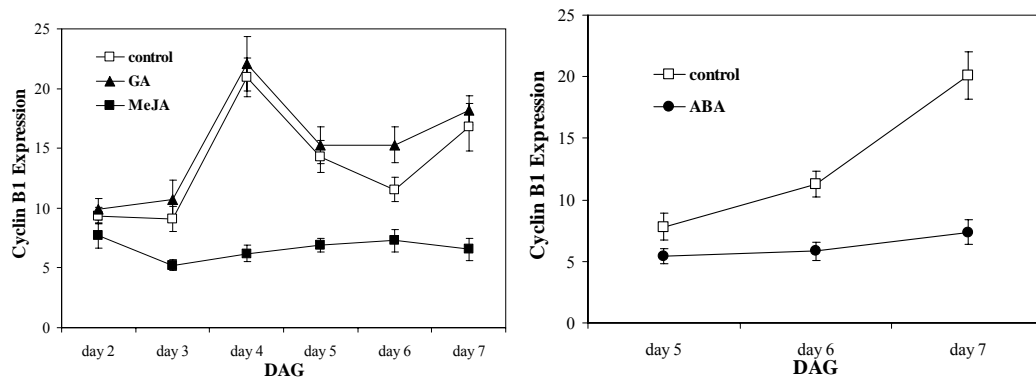


Figure 7-12 Cyclin B1 expression of the *CYCB1::GUS/Col-0* seedlings sown on half MS medium containing 20 μ M MeJA, 2 μ M GA, or 0.5 μ M ABA. Seedlings were observed under microscope from 2nd to 7th DAG. The cyclin B1 expression was identified as the number of blue dots in the root tip.

7.2.2 The Effect of the MeJA and paclobutrazol Treatments on *della 4*, *gal-3*, *gai* and *coil-16*

To understand further the crosstalk between JA and GA signaling, three GA mutants, *della 4*, *gal-3* and *gai*, and one JA mutant, *coil-16*, were treated with MeJA and/or PAC to study whether COI1 and DELLA proteins are required in the crosstalk between the GA and JA pathways.

Seeds of Ler, *della 4*, *gal-3*, *Col-gl* and *coil-16* were prepared and germinated as stated in 7.2.1. Three days after germination, seedlings were transferred to half MS medium containing 0.1 μ M PAC (2.1.3 and 2.2.1) and held vertically in long-day growth chamber. The plates were scanned and root lengths were measured on the 3rd, 4th, 5th, 6th and 7th DAG for each genotype and treatment as stated in 7.2.1.

Seeds of Ler, *della 4*, *gal-3* and *gai* were also prepared and germinated as stated in 7.2.1. Three days after germination, seedlings were transferred to half MS medium containing 20 μ M MeJA (2.1.3 and 2.2.1) and held vertically in LD growth chamber. The plates were scanned and root lengths were measured on the 3rd, 4th, 5th, 6th and 7th DAG for each genotype and treatment as stated in 7.2.1.

MeJA inhibited root growth of each of the four lines similarly (Figure 7-13 and 7-14). This indicated that functional DELLA proteins, GA biosynthesis, and sensitivity to GA were not required for the MeJA-mediated growth inhibition, and that DELLA proteins inhibit root growth via different mechanism from the MeJA-mediated growth inhibition. However, *della 4* was actually less sensitive to the MeJA treatment at 7th DAG compared to MeJA-treated Ler (Figure 7-13), suggesting that DELLA proteins might be partially required for sensitivity to MeJA in older roots.

The PAC treatment inhibited root growth of Ler, *della 4*, *gal-3* (Figure 7-13), *Col-gl* and *coil-16* (Figure 7-15). Because both *gal-3* and *gai* were inhibited by PAC, the most likely explanation is that PAC was toxic to root growth independently of its effect on GA biosynthesis.

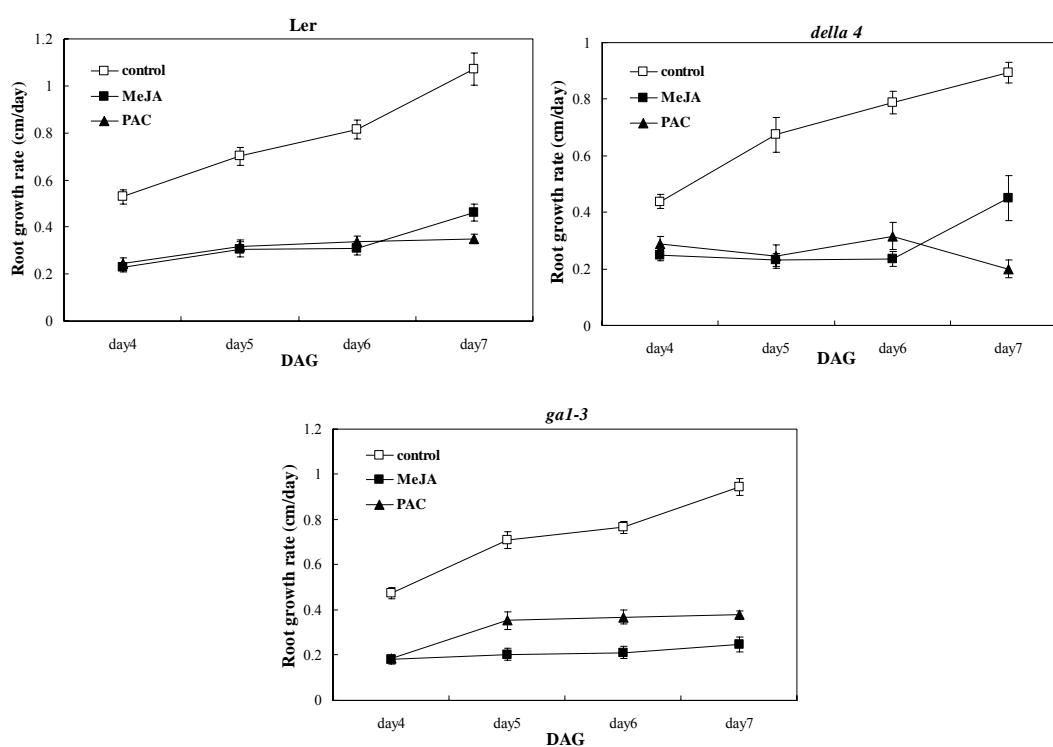


Figure 7-13 Rate of root growth of the **Ler**, **della 4** and **gal-3** seedlings transferred to half MS medium containing 20 μ M MeJA or 0.1 μ M PAC. Plates containing the seedlings were scanned from 3rd to 7th DAG, and the length of each seedling at each day was measured and analysed.

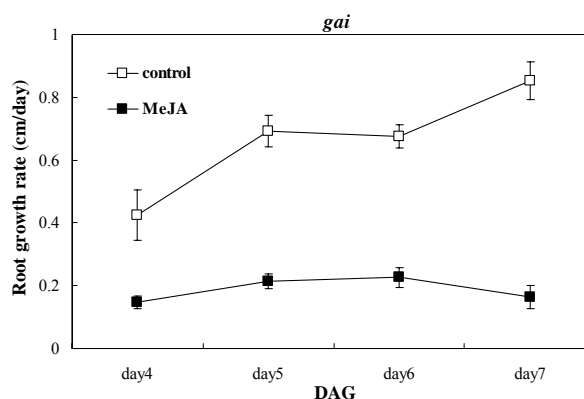


Figure 7-14 Rate of root growth of the *gai* seedlings transferred to half MS medium containing 20 μ M MeJA. Plates containing the seedlings were scanned from 3rd to 7th DAG, and the length of each seedling at each day was measured and analysed.

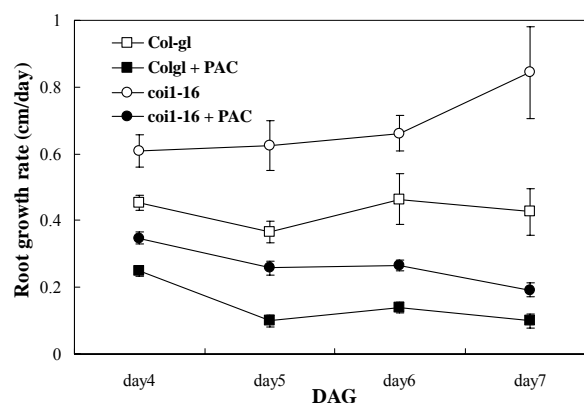


Figure 7-15 Rate of root growth of the 3 day old *Col-gl* and *coi1-16* seedlings transferred to half MS medium containing 0.1 μ M PAC. Plates containing the seedlings were scanned from 3rd to 7th DAG, and the length of each seedling at each day was measured and analysed.

7.2.3 The Effect of the ABA Treatment on *aos*, *coil-16*, *jai3*, *jin1-1* and *jut*

ABA severely inhibited root growth of *coil-16* (7.2.1.1). To determine whether this was a specific consequence of the mutation, or due to a deficiency in JA signaling, the response of *coil-16* to two concentrations of ABA, was compared with that of other mutants in the JA pathway: *aos*, *jai3*, *jin1-1* and *jut*, and their corresponding WT parents. The treatments started three days after germination, in order to exclude possible inhibitory effect of the ABA treatment on seed germination.

Seeds of *Col-gl*, *coil-16*, *aos*, *Col-0*, *jai3*, *jin1-1* and *jut* were prepared and germinated as stated in 7.2.1. Three days after germination, seedlings were transferred to half MS medium containing 0.5 μ M or 10 μ M ABA (2.1.3 and 2.2.1), transferred to a LD growth chamber and grown in vertically held plates. The plates were scanned, and root lengths were measured at 3rd, 4th, 5th, 6th and 7th DAG for each genotype and treatment as stated in 7.2.1.

For *Col-gl*, *coil-16* and *aos*, the root growth rates were slightly promoted by 0.5 μ M ABA at 4th and 5th DAG (Figure 7-16). However, root growth was largely inhibited by the 10 μ M ABA treatments. Evidently, ABA-mediated root growth inhibition and promotion are not affected by lack of JA biosynthesis or JA perception. Similar results were found for *Col-0*, and mutants in the *Col-0* background, *jai3* and *jin1-1*: growth was slightly promoted by 0.5 μ M ABA at 4th and 5th DAG, but largely inhibited by 10 μ M ABA (Figure 7-17). Growth of *jut* was not promoted by 0.5 μ M ABA, but its roots were inhibited by 10 μ M ABA, similar to *Col-0*, *jai3* and *jin1-1* (Figure 7-17). This suggested that *JAZ3*, *MYC2* and *JUT* are not required for the ABA-mediated growth inhibition, and that *JUT* might participate in a minor role in ABA-mediated growth promotion by low ABA concentrations.

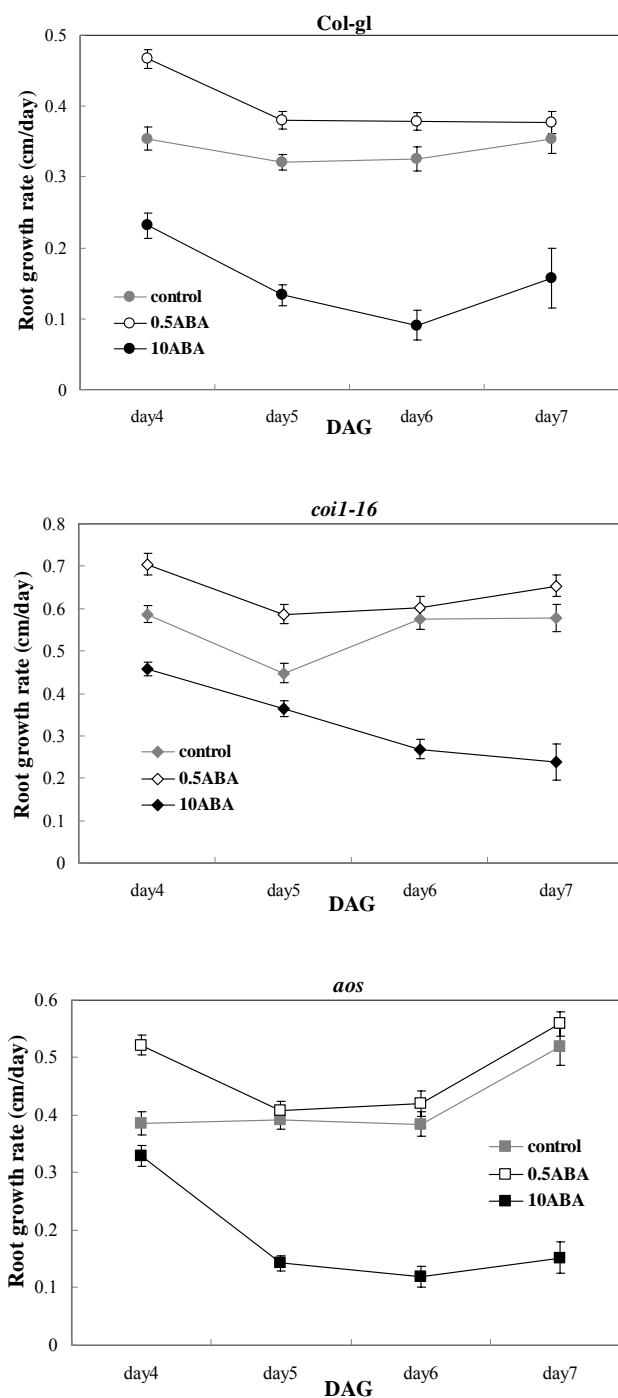


Figure 7-16 Rate of root growth of the 3 day old *Col-gl*, *coil-16* and *aos* seedlings transferred to half MS medium containing 0.5 μ M or 10 μ M ABA. Plates containing the seedlings were scanned from 3rd to 7th DAG, and the length of each seedling at each day was measured and analysed.

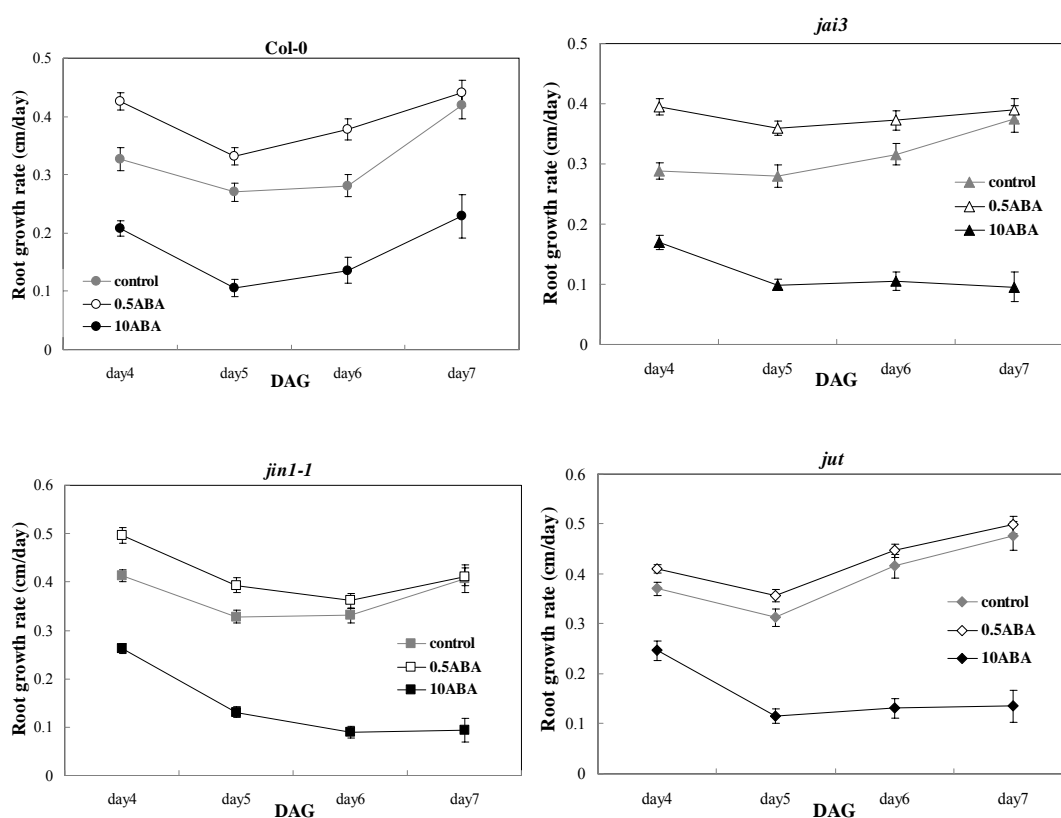


Figure 7-17 Rate of root growth of the 3 day old *Col-0*, *jai3*, *jin1-1* and *jut* seedlings transferred to half MS medium containing 0.5 μM or 10 μM ABA. Plates containing the seedlings were scanned from 3rd to 7th DAG, and the length of each seedling at each day was measured and analysed.

7.3 Discussion

Experiments in chapter 5 and 6 demonstrated that MeJA suppresses root growth by reducing the rate of cell production in the meristem, and by decreasing the length of mature cells, apparently without reducing the rate of cell elongation. Obviously, other hormones also affect plant root growth. This chapter therefore investigated the interaction between MeJA, auxin, GA, and ABA in the regulation of root growth of *Arabidopsis*. Theoretically, if a mutant of a certain hormone signaling pathway exhibits altered responses to a different hormone signaling pathway compared to WT, this would indicate that there should be interaction between the two hormone pathways in the observed response. Following the methods used in chapter 6, the

same parameters (primary root length, root growth rate, cell production rate, mature cell length, cell number in meristem and meristem size) were also measured in this chapter.

JA signaling contributes to vegetative and reproductive development besides its role in resistance to pathogens and stress (Koo and Howe, 2009). **COI1** is a main component of JA perception (Xie *et al.*, 1998), and the significant differences of parameters between *coil-16* and *Col-gl* indicated that endogenous JA suppresses primary root length, root growth rate, cell production rate, cell number in meristem and meristem size, but not mature cell length. However, root growth of *coil-16* and *Col-gl* were similarly affected by GA and ABA, indicating that this *COI1*-dependent growth arrest was independent from GA and ABA signaling.

ABA-treated *coil-16* responded similarly to ABA-treated *Col-gl* in root growth, indicating no interaction between JA and ABA signaling. The MeJA-treated *abi* had similar responses to MeJA-treated *Col-0*, suggested that *ABI* also does not interact with MeJA-mediated growth inhibition (**Figure 7-5** and **7-7**). Similarly, several ABA-treated JA mutants (*aos*, *jai3* and *jin1-1*) exhibited no significant differences in root growth compared to the ABA-treated WT (*Col-gl* and *Col-0*) (**Figure 7-16** and **7-17**). These results further confirm that JA and ABA control root growth via distinctive mechanisms. However, originally isolated as an ABA-insensitive mutant, JUT did not show promoted growth by 0.5 μ M ABA, implying a possible link between JA and ABA signaling in this aspect of vegetative growth. In fact, both MeJA and ABA induce reactive oxygen species (ROS) production and nitric oxide (NO) production, and activate I_{Ca} channels and S-type anion channels in guard cells via the same pathway, but the *coil* mutation disrupts only the MeJA-mediated stomatal closing (Munemasa *et al.*, 2007), suggesting that JA and ABA signaling share part of the signaling mechanism in some plant responses.

When *coil-16* was germinated in ABA-containing medium, its germination was inhibited and all of the root growth parameters were severely inhibited (**Figure 7-4**). However, if *coil-16* seedlings germinated in MS medium were transferred to ABA-contained medium, their growth response was the same as WT seedlings (**Figure 7-16**). Apparently, ABA not only inhibited germination of *coil-16*, but also caused growth reduction of those seedlings that eventually germinated. Other JA insensitive mutants, such as *jin4* and *jar1*, are also more sensitive to ABA-induced

inhibition of germination (Berger *et al.*, 1996 and Staswick *et al.*, 1992). This indicated that JA signaling might repress ABA-mediated cell cycle arrest in the seed embryo. Indeed, ABA was reported to hold back seed germination by inducing the expression of a cyclin-dependent kinase inhibitor (ICK1), which arrests cell cycle at the G1/S transition (Wang *et al.*, 1998). It is hence possible that JA signaling interferes with the ABA-mediated cell cycle arrest.

It was shown in **Figure 5-10** that *aux1-7* had reduced sensitivity to MeJA. In this Chapter, it was confirmed that **AUX1** is involved in MeJA-mediated root growth inhibition, and is required for the reduction of several root growth parameters. Primary root growth is not the only developmental process affected by both JA and auxin. *ANTHRANILATE SYNTHASE α 1* (*ASAI*), an auxin biosynthetic gene, was defective in a mutant compromised in MeJA-mediated lateral root formation (Sun *et al.*, 2009). This mutant was defective in up-regulating the expression of auxin transport components, such as PIN1, PIN2 and AUX1, indicating the close relationship between regulation of auxin transport and MeJA-mediated growth responses. Interestingly, disruption of AUX1-mediated auxin influx has also been shown to negatively affect JA signaling, and caused increased susceptibility to necrotrophic pathogens (Llorente *et al.*, 2008). These results demonstrated the crosstalk between auxin and JA signaling in regulating both vegetative growth and resistance to pathogens.

GA-treated *aux1-7* exhibited WT responses, indicating no evident role of *AUX1* in GA-mediated root growth responses. However, ABA-treated *aux1-7* had increase root length, while ABA-treated Col-0 had decreased root length (**Figure 7-5** and **7-6**). Indeed, the crosstalk between auxin and ABA has been demonstrated in root tissue by showing the hypomorphic effect on the expression pattern of an ABA-inducible chimaeric reporter: *Daucus carota* (L.) Dc3 promoter: *uidA* (ProDc3:GUS) in *aux1* and *auxin-resistant-4* (*axr4*) mutants, suggesting that ABA and IAA signaling pathways interact in roots (Rock and Sun, 2005). In addition, *AUX1* is also responsible for ABA-mediated repression of embryonic axis elongation during early seedling development (Belin *et al.*, 2009). Therefore, *AUX1* not only has a role in ABA signaling in expression of ProDc3:GUS and seed embryo, but also participates in the ABA-mediated root growth responses.

The experiment with *abi* provided more information about the inhibitory effects of ABA on growth, and the antagonisms between GA and ABA signaling.

abi had a significantly larger meristem and higher cell number in meristem than those in Col-0 root, but the root length of *abi* was not longer than Col-0, suggesting that although endogenous ABA regulates meristem parameters, this does not affect root growth. Additionally, exogenous ABA reduces mitotic cell number. This is consistent with the report that ABA arrests the cell cycle at the G1 phase (Liu *et al.*, 1994). In GA-treated *abi*, the mature cell length decreased, but the rate of cell production increased compared to WT, and as a consequence there was no change in primary root length (**Figure 7-5** and **7-7**). The crosstalk between GA and ABA signaling hence would not be detected if only root length was measured. However, induction of epidermal cell death by accumulation of ethylene and GA and reduction of ABA level in adventitious roots of deepwater rice (Steffens and Sauter, 2005) also suggested that there might be more hormones involved in the interaction between ABA and GA in controlling vegetative growth.

Ler roots were insensitive to exogenous GA. This was unexpected because GA treatment caused Col-*gl* to have longer roots, higher root growth rate, longer mature cells, higher cell production rate, and more cells in the meristem. However, GA treatment only caused Col-0 to have an increase in cell number in the meristem. Evidently, WT *Arabidopsis* lines vary in their response to GA, and Ler was the most insensitive of those tested. Roots of *Arabidopsis gal-3* are stunted, and application of GA promotes growth of its roots to WT length (Fu and Harberd, 2003). GA causes disappearance of DELLA proteins, and this might be expected to promote root growth (Silverstone *et al.*, 2001). However, *della 4* roots were not significantly longer than roots of Ler (**Figure 7-8** and **7-9**, Figure 1A of Achard *et al.*, 2006). In addition, there was no significant difference between Ler and *della 4* in meristem size and cell number in meristem during the observation period (**Figure 7-8** and **7-9**, Figure 2B of Achard *et al.*, 2009). Presumably, endogenous GA in Ler roots is saturating any response to exogenous GA.

della 4 exhibited WT (Ler) root responses to MeJA and ABA. This indicated that *DELLAs* are not involved in MeJA- and ABA-mediated growth responses. However, *della 4* is reported to be more resistant to ABA-mediated growth inhibition than WT (Achard *et al.*, 2006), but this was not tested for statistical significance. Ler, *della 4*, *gal-3*, and *gai* were inhibited to similar level by MeJA, suggesting that *DELLA* proteins and GA biosynthesis are not required for MeJA-mediated growth inhibition. However, the growth recovery of the 7 day old

della 4 seedlings treated with MeJA compared with the MeJA treated Ler, *gal-3* and *gai* had implied an involvement of DELLAs in JA signaling in older roots. Indeed, it was shown that 8 day old *della* mutants, including *rga-t2*, *gai-t6* and a penta mutant (*gal-3 rga-t2 gai-t6 rgl1-1 rgl2-1*) in the *gal-3* background, exhibited less sensitivity to 10 μ M JA treatment compared to *gal-3*. In addition, DELLA proteins compete with MYC2 by interacting with JAZs (Hou *et al.*, 2010). However, this conclusion was based on a comparison of root lengths of JA treated *della* mutants and *gal-3* (Figure 1C of Hou *et al.*, 2010). Without showing root length of untreated and JA treated WT, it is difficult to tell if *rga-t2* and *gai-t6* in the *gal-3* background truly had reduced sensitivity to JA. During stamen development, DELLA proteins suppress JA biosynthesis, suppressing the expression of *MYB21*, *MYB24*, and *MYB57*, (Cheng *et al.*, 2009). However, JA biosynthesis in *Arabidopsis* flowers uses the DAD1 phospholipase for the release of linolenic acid from membrane lipids, whereas this is not required for JA biosynthesis in leaves (Ishiguro *et al.*, 2001). Although there are evidences supporting the hypothesis that the crosstalk between JA and GA signaling largely depends on DELLA proteins, this crosstalk might happen in tissue- and circumstance-dependant manner, and growth of young seedlings may not be included.

Root growth of Ler, *della 4*, *gal-3*, *Col-gl* and *coil-16* were inhibited to similar level by 0.1 μ M PAC. This might suggest that JA signaling is not required for growth repression caused by DELLA proteins. Nevertheless, *della 4*, which is a *gal-3* mutant lacks functional GAI, RGA, RGL1 and RGL2 (Cheng *et al.*, 2004), is expected to be PAC-insensitive. Although there is no reference about PAC-treated *della 4*, *rgl1 Δ 17*, a transgenic line with a 17–amino acid deletion identical to the dominant mutation that causes GA insensitivity in the *gai-1* mutant, is shown to be insensitive to PAC treatment up to 60 μ M (Wen and Chang, 2002). This indicated that the PAC used here might have toxicity to root growth other than blocking GA biosynthesis. Therefore, it is difficult to tell if the growth of *coil-16* was inhibited due to lack of GA biosynthesis, or due to PAC's unexpected toxicity.

All in all, the data presented here indicate that root growth is regulated by an interaction between JA, ABA, auxin and GA signaling, and MeJA-mediated growth inhibition largely relies on auxin transportation, but not ABA and GA signaling.

Chapter 8

***Arabidopsis* Root Growth in Response to MeJA: Role of Microtubules, Acid Efflux and Water Potential**

8.1 Introduction

In Chapter 5 and Chapter 6, I show that MeJA treatment reduced the rate of cell production and the number of mitotic cells in the root apical meristem, resulting in a decreased meristem size, and inhibition of root growth. In the TZ, MeJA had a different effect, and decreased mature cell length. However, MeJA did not decrease the rate of elongation of individual cells. These data gave information about the morphological change of MeJA-treated roots, nevertheless, the cellular process of growth arrest remain unclear.

The size of root cells formed in the meristem does not change dramatically until the cells enter the elongation zone, where the length of cells increases rapidly until they reach the mature cell length. The control of root cell elongation depends on many factors. Generally, turgor pressure inside the cell and cell wall extensibility are considered to determine the degree of cell elongation (Cleland, 1971). During cell elongation, the expanding cells have a lower water potential (Ψ_w) than mature cells, and this is because the turgor pressure (Ψ_p) is prevented from reaching its maximum by the extension of cell walls (Nonami and Boyer, 1987, Boyer, 2001). Cell wall extensibility is largely decided by the orientation of the cellulose microfibrils, whose direction is correlated with microtubules which direct the cellulose synthases to the plasma membrane (Delmer, 1987). The microtubule

orientation, which determines the orientation of the cellulose microfibrils, changes following the developmental stages. In young growing cells, cellulose microfibrils are initially arranged isotropically and then laterally (Figure 8-1). The lateral orientation allows cells to expand in a direction that is perpendicular to cellulose microfibrils. In mature cells, the cellulose microfibrils become overlapping and form a cross-hatched pattern, which gives a similar pattern to the microtubules, and prohibits cells from elongating further (Brett, 2000). This raises the possibility that MeJA suppresses cell elongation by re-orientating microtubules and cellulose microfibrils.

In potato, JA causes expansion of tubers and tuber cells. Microtubules have been reported to be indispensable for this JA and MeJA-induced cell expansion (Koda, 1997). JA-induced cell expansion is due to accumulation of sucrose, which increases the osmotic pressure, and due to changes in cell wall structure, which affects the cell wall extensibility. By contrast, in tobacco BY-2 cells, MeJA suppresses growth by inhibiting mitosis at both the G1/S and G2/M transitions (Swiatek *et al.*, 2002). Significantly, MeJA at 10 μ M or higher can disrupt microtubules in the S phase (Ade *et al.*, 1990). Apparently, MeJA can affect the orientation of microtubules during both cell division and cell expansion. This raises the possibility that MeJA-induced root growth inhibition is associated with reorientation of microtubules in the meristem and in the elongation zone. Although it is not known yet whether the cell cycle arrest can be directly linked to microtubule disruption, observing microtubule orientation in untreated and MeJA-treated roots would provide more evidence.

In an elongating cell, H-bonds between cell wall components are broken temporarily to loosen the wall, and this is due to cell wall acidification, which activates the wall-loosening enzymes, such as expansins (Cosgrove *et al.*, 2002). Indeed, it was shown that IAA promotes cell wall loosening and cell wall synthesis, which resulted in higher elongation rate in maize coleoptiles (Kutschera and Schopfer, 1986). In addition, exogenous IAA treatment decreases cytosolic pH in maize cells, coleoptiles and parsley hypocotyls (Brummer *et al.*, 1985, Gehring *et al.*, 1990). The acidification of the cytosol and the stimulation of a proton pump can possibly be connected with the acid efflux during cell wall acidification, which occurs at the same region of root elongation in maize (Mulkey and Evans, 1981). Evidently, MeJA inhibits the IAA-induced elongation of maize coleoptile, and

causes alkalization of cytosol to approximately 0.2 pH unit (Irving *et al.*, 1999). It is hence important to investigate if MeJA-mediated growth inhibition in *Arabidopsis* roots is related to disruption of microtubule orientation and change of turgor pressure as mentioned above, and suppression of the acid efflux and cell wall acidification.

In this Chapter, microtubule orientation in root cells, change of pH around the root tissue, and root growth against low water potential were examined in untreated- and MeJA-treated maize and *Arabidopsis* roots.

8.2 Results

8.2.1 Effect of MeJA Treatment on Microtubule Orientation

MeJA was shown to disrupt microtubules in BY-2 cells in the S phase (Ade *et al.*, 1990). To test if microtubules have a role in MeJA-mediated root growth inhibition, two experiments were designed. The first experiment was to observe the microtubule orientation in untreated and MeJA-treated *GFP-TUB6*, *aos/GFP-TUB6*, *jin1-1/GFP-TUB6* and *aux1-7/GFP-TUB6* roots (2.2.1-2.2.5 and 2.5.3). *GFP-TUB6* is a transgenic line, which expresses GFP-labeled β -tubulin and whose microtubules can be observed easily (Hashimoto and Nakajima, 2001). Crossing *aos*, *jin1-1* and *aux1-7* respectively with *GFP-TUB6* produced the corresponding mutants with visible microtubules. It was expected that in MeJA-treated roots, the pattern of microtubule orientation might change in meristem or mature cells. If JA alters microtubule orientation, the JA biosynthesis and insensitive mutants and auxin insensitive mutant might be expected to have distinguishable differences of microtubule orientation compared to *GFP-TUB6*.

Confocal microscope images of untreated *GFP-TUB6* revealed the microtubules distributed both isotropically and laterally in the meristem (Figure 8-1 B, arrows), and they became more oblique and scattered in mature cells (Figure 8-1 A, arrow). Although the cross-hatched pattern in mature cells reported by others

(Brett, 2000) is not obvious, the differences between young cells and mature cells are apparent. In the 50 μ M MeJA treated *GFP-TUB6*, the microtubule orientation in the meristem and mature cells were similar to those in untreated roots (Figure 8-1 D and C)

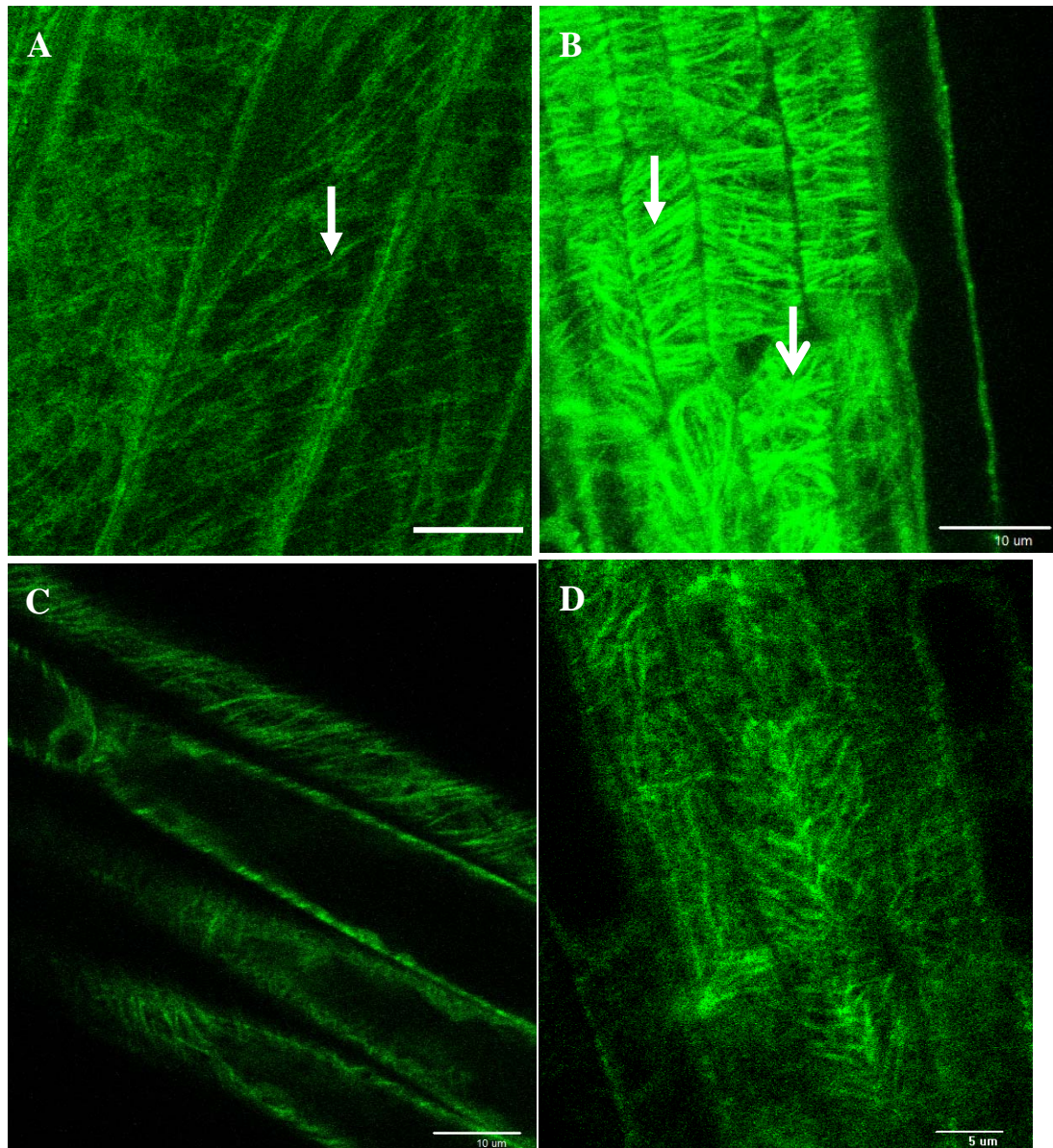


Figure 8-1 Confocal microscope image of 5 day old *GFP-TUB6* roots. (A) Untreated mature root cells. Oblique and scattered microtubules (arrow) (B) Untreated meristem. Isotropic (open arrow) and lateral (solid arrow) microtubules. (C) Mature root cells treated with 50 μ M MeJA, 24 hrs. (D) Meristem treated with 50 μ M MeJA, 24 hrs.

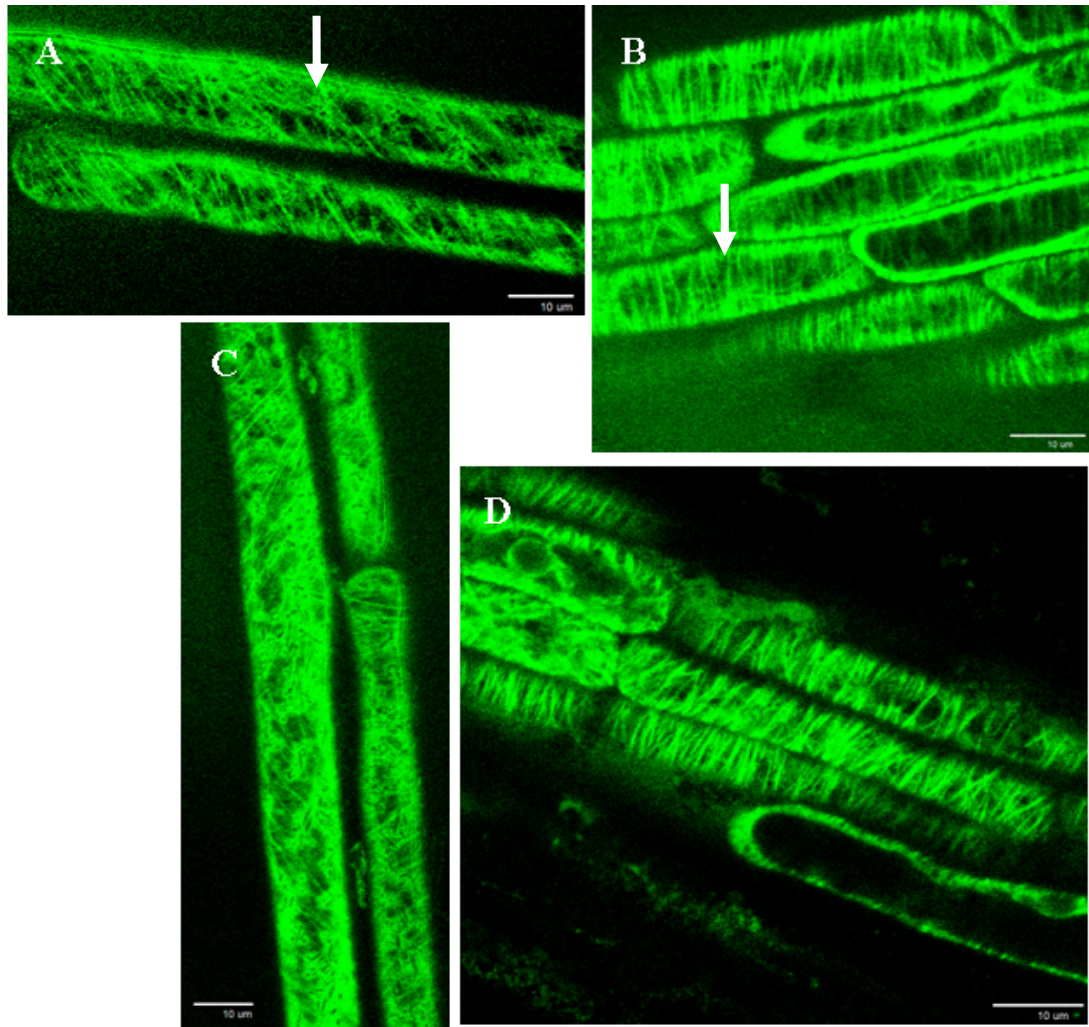


Figure 8-2 Confocal microscope image of 5 day old *aos/GFP-TUB6* roots. (A) Untreated mature root cells. Cross-hatched microtubules (arrow) (B) Untreated meristem. Lateral microtubules (arrow) (C) Mature root cells treated with 50 μ M MeJA, 24 hrs. (D) Meristem treated with 50 μ M MeJA, 24 hrs.

In *aos/GFP-TUB6*, microtubules in the meristem were distributed mostly laterally (Figure 8-2 B, arrow), and the cross-hatched pattern was obvious in mature cells (Figure 8-2 A, arrow). However, in the MeJA-treated *aos/GFP-TUB6*, the meristem and mature cells did not show any difference from the untreated *aos/GFP-TUB6* (Figure 8-2 D and C). In *jin1-1/GFP-TUB6*, the JA (partially) insensitive mutant, microtubules in the meristem were also distributed laterally, and

the cross-hatched pattern in mature cells was obvious (Figure 8-3 B and A, arrows). However, in the MeJA-treated *jin1-1/GFP-TUB6*, the meristem and mature cells did not show any difference from the untreated *jin1-1/GFP-TUB* (Figure 8-3 D and C). Again, in *aux1-7/GFP-TUB6*, the untreated and MeJA-treated meristem both had laterally distributed microtubules (Figure 8-4 A and B), and the untreated and MeJA-treated mature cells also showed similar cross-hatched pattern (data not shown). In short, although the change of microtubule orientation from meristem to mature tissue were observed in *GFP-TUB6*, *aos/GFP-TUB6*, *jin1-1/GFP-TUB6* and *aux1-7/GFP-TUB6* roots, the MeJA treatment did not alter the microtubule orientation in any of the tested lines.

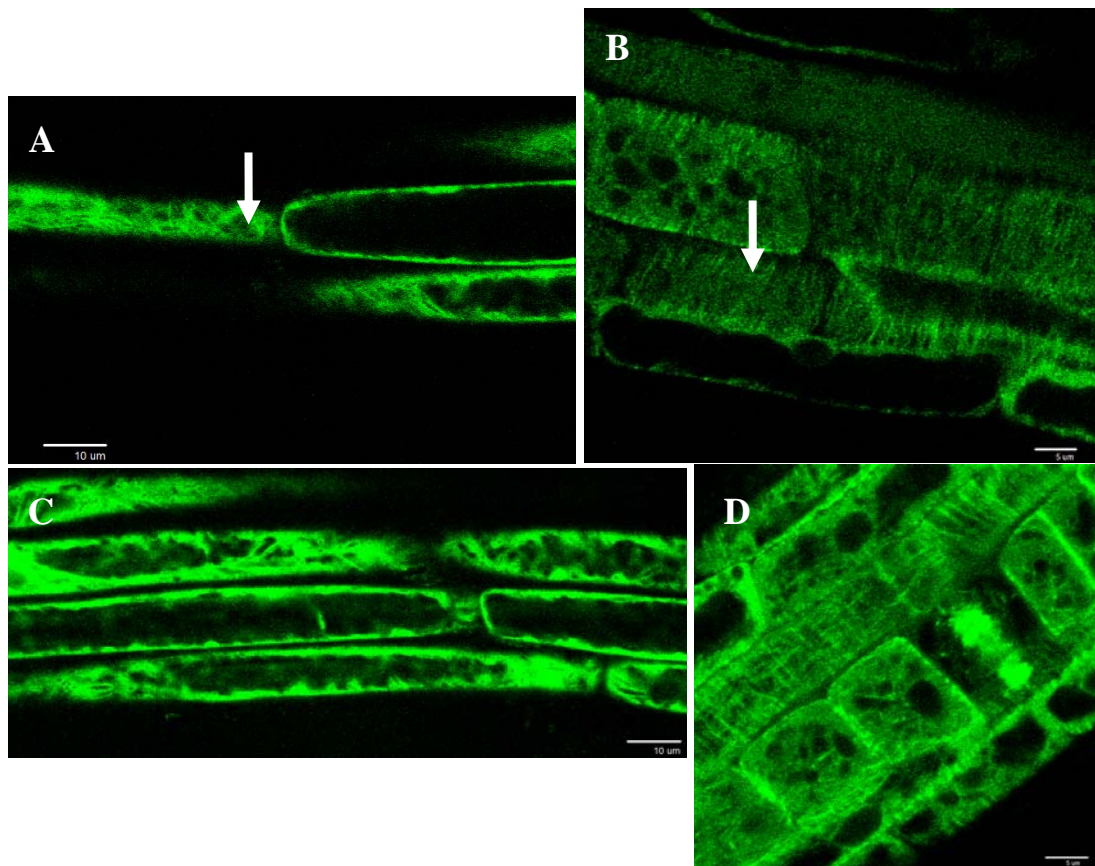


Figure 8-3 Confocal microscope image of 5 day old *jin1-1/GFP-TUB6* roots. (A) Untreated mature root cells. Cross-hatched microtubules (arrow) (B) Untreated meristem. Lateral microtubules (arrow) (C) Mature root cells treated with 50 μ M MeJA, 24 hrs. (D) Meristem treated with 50 μ M MeJA, 24 hrs.

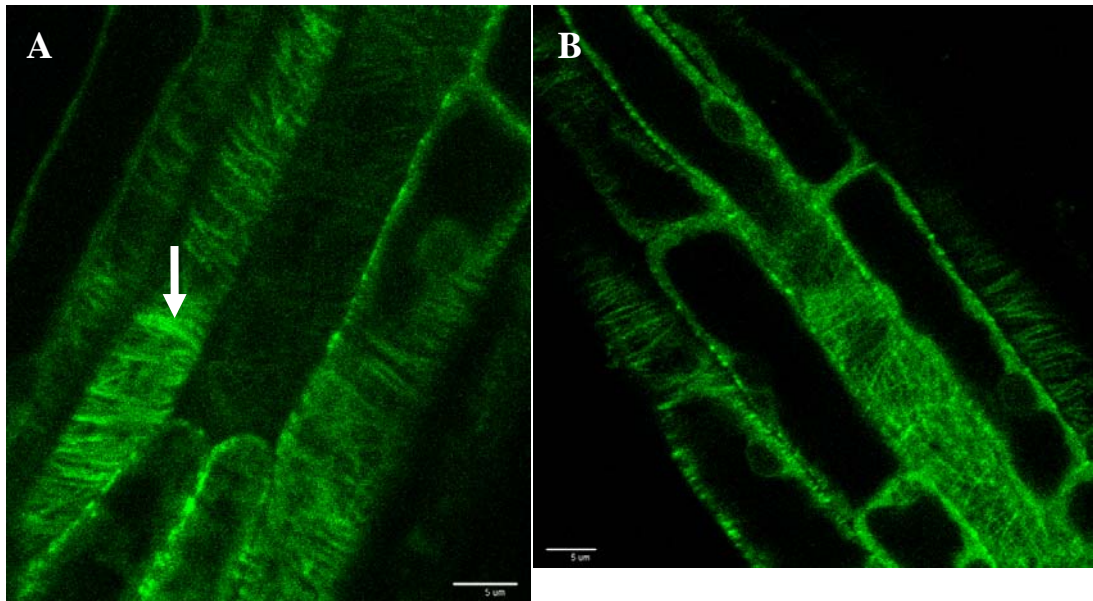


Figure 8-4 Confocal microscope image of 5 day old *aux1-7/GFP-TUB6* roots. (A) Untreated meristem. Lateral microtubules (arrow) (C) Meristem treated with 50 μ M MeJA, 24 hrs.

The preceding experiment indicated that the orientation of microtubules is unlikely to contribute to MeJA-mediated root growth inhibition. To further confirm if microtubules are required for MeJA-mediated root growth inhibition, oryzalin, a herbicide that disrupt microtubules, was used to depolymerise microtubules in untreated and MeJA treated *GFP-TUB6*. Five day old *GFP-TUB6* seedlings were transferred to MS medium containing 200 nM or 500 nM oryzalin (2.2.1-2.2.4). After 24 hrs incubation, morphological change could be observed in the root apical area. Compared to untreated *GFP-TUB6* (Figure 8-5 A), the 200 nM oryzalin-treated *GFP-TUB6* showed an irregular-shaped root apex, with swollen meristem cells and crooked root hairs (Figure 8-5 B). In the 500 nM oryzalin-treated *GFP-TUB6*, most of the meristem cells were approximately spherical (Figure 8-5 C). Under the confocal microscope (2.5.3), it was also clear that there were laterally orientated microtubules in untreated meristem cells (Figure 8-6 A). In roots exposed to 200 nM oryzalin, cells became swollen, and had fragmented microtubules (Figure 8-6 B, arrow). In 500 nM oryzalin-treated roots, the microtubules were not in fibrils (Figure 8-6 C), indicating that most of the microtubules had been depolymerised by the treatment. Besides oryzalin's remarkable effect on root apex, it was however

obvious that oryzalin had small or no effect on mature tissue, where root cells remained intact.

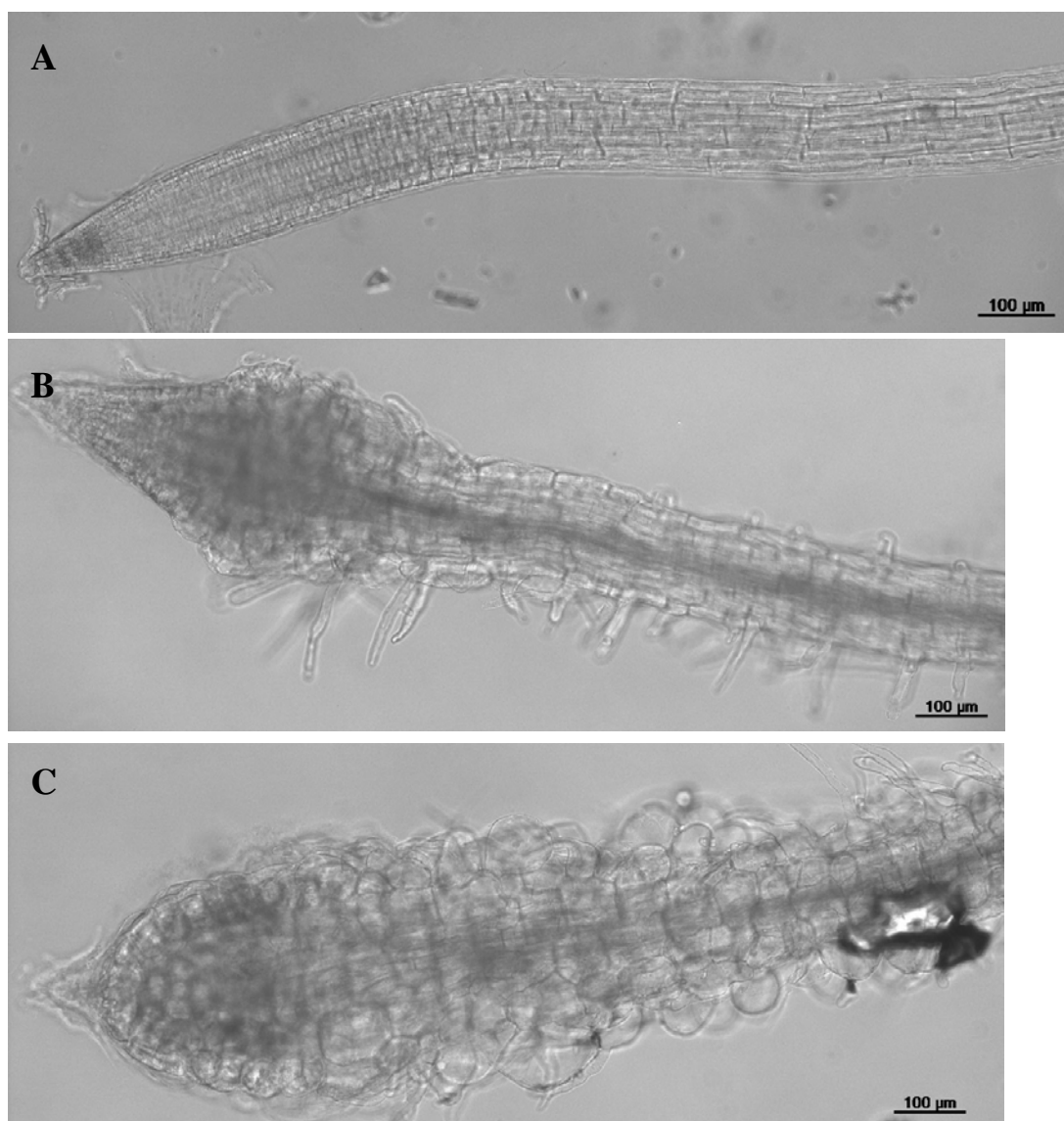


Figure 8-5 Bright field microscope image of 6 day old *GFP-TUB6* roots. (A) Untreated root. (B) Root treated with 200 nM oryzalin, 24 hrs. (C) Root treated with 500 nM oryzalin, 24 hrs.

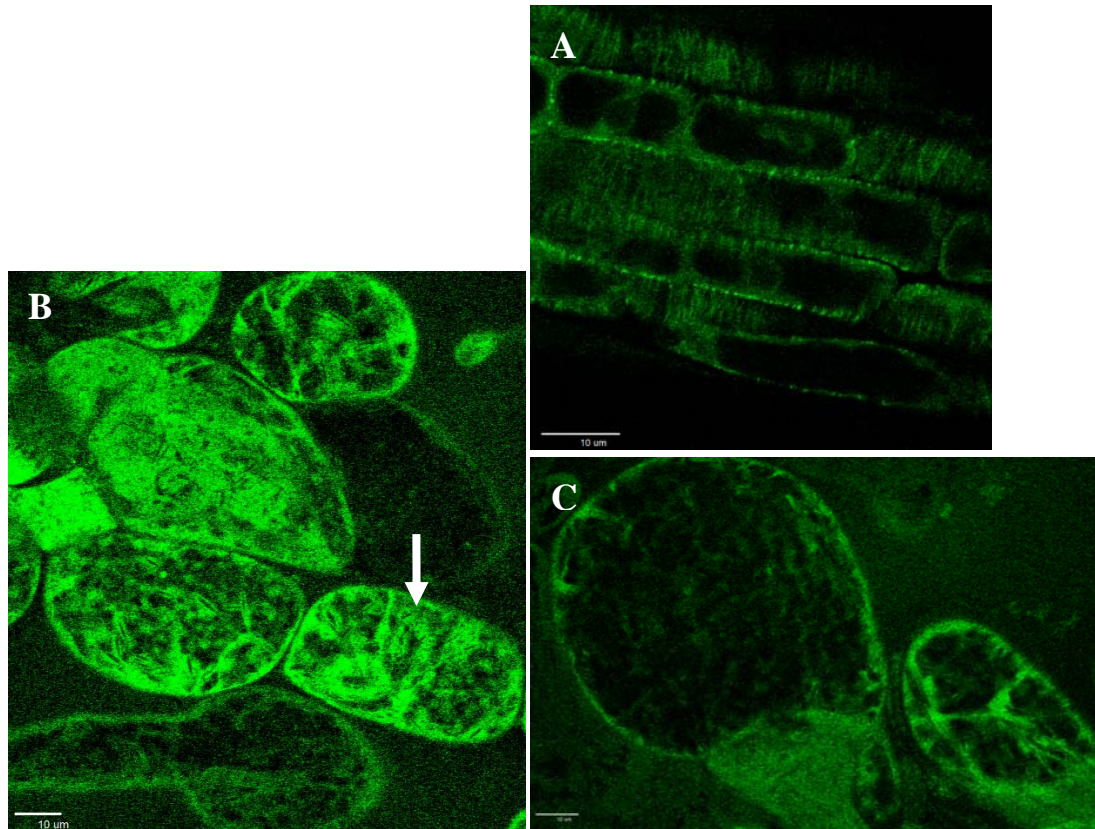


Figure 8-6 Confocal microscope image of 6 day old *GFP-TUB6* roots. (A) Untreated meristem. (B) Meristem treated with 200 nM oryzalin, 24 hrs. Swollen cells (arrow) (C) Meristem treated with 500 nM oryzalin, 24 hrs.

After confirming the effect of oryzalin treatment, 5 day old *GFP-TUB6* seedlings were transferred to MS medium containing both oryzalin and MeJA, incubated for 24 hrs, and then observed under bright field microscope (2.2.1-2.2.4 and 2.5.4). it was hypothesised that if intact microtubules were required for response to MeJA, then the oryzalin-treated cells would not respond to MeJA. In *GFP-TUB6* seedlings treated with 200 nM oryzalin and 50 μ M MeJA, the shape of meristem was similar to untreated meristem (Figure 8-7 A), although most of the elongating cells were slightly swollen (Figure 8-7 B). In *GFP-TUB6* seedlings treated with 500 nM oryzalin and 50 μ M MeJA, the apical root looked very similar to the 200 nM oryzalin-treated one (Figure 8-7 D and A). According to the hypothesis, if microtubules are required for MeJA-mediated root growth inhibition, the disruption of microtubules would prevent the swollen cells from being smaller due to MeJA's effect; whereas if microtubules are not required for MeJA-mediated root growth inhibition, the swollen cells would be smaller than those treated with oryzalin alone (Figure 8-9). The diameter of swollen cells in *GFP-TUB6* treated with 500 nM oryzalin, and those in *GFP-TUB6* treated with 500 nM oryzalin and 50 μ M MeJA were measured. The 500 nM oryzalin-treated cells were averagely 80 μ m in diameter, while the 500 nM oryzalin and 50 μ M MeJA-treated cells were about 50-60 μ m in diameter (Figure 8-8). These results strongly indicate that microtubules are not required for MeJA-mediated root growth inhibition.

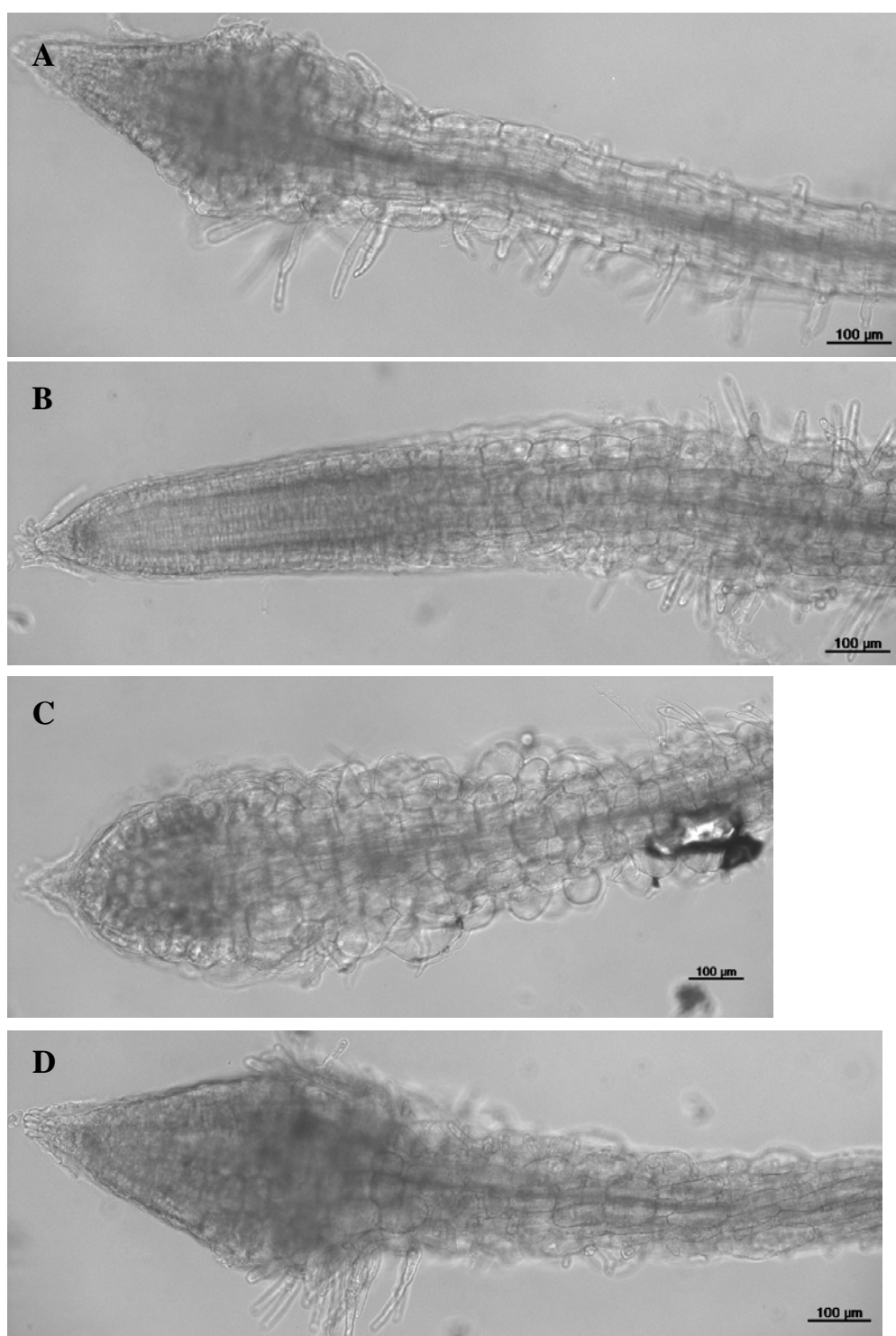


Figure 8-7 Bright field microscope image of 6 day old *GFP-TUB6* roots. (A) Root treated with 200 nM oryzalin, 24 hrs. (B) Root treated with 200 nM oryzalin and 50 μM MeJA, 24 hrs. (C) Root treated with 500 nM oryzalin, 24 hrs. (D) Root treated with 500 nM oryzalin and 50 μM MeJA.

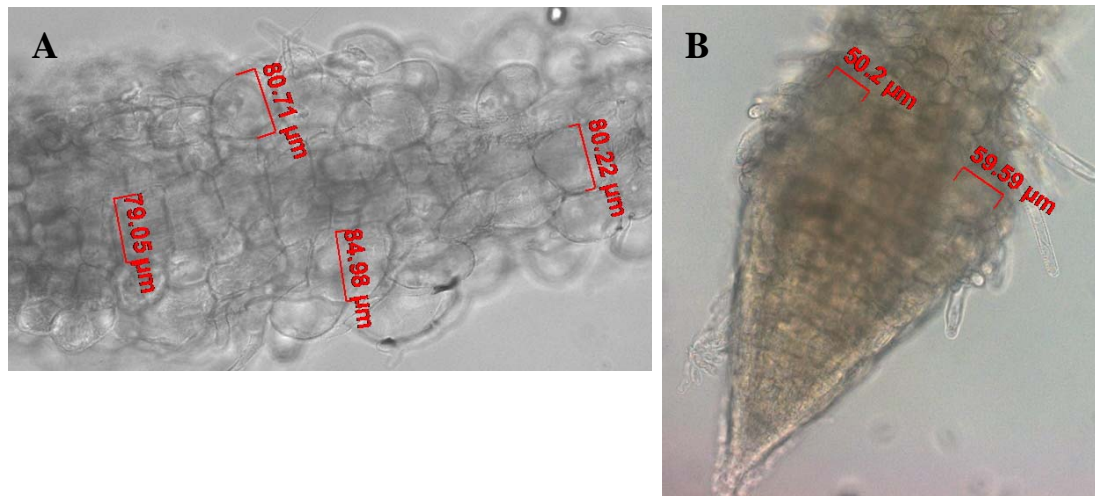


Figure 8-8 Bright field microscope image of 6 day old *GFP-TUB6* roots with individual cell diameter measurement. (A) Root treated with 500 nM oryzalin, 24 hrs. (B) Root treated with 500 nM oryzalin and 50 μ M MeJA, 24 hrs.

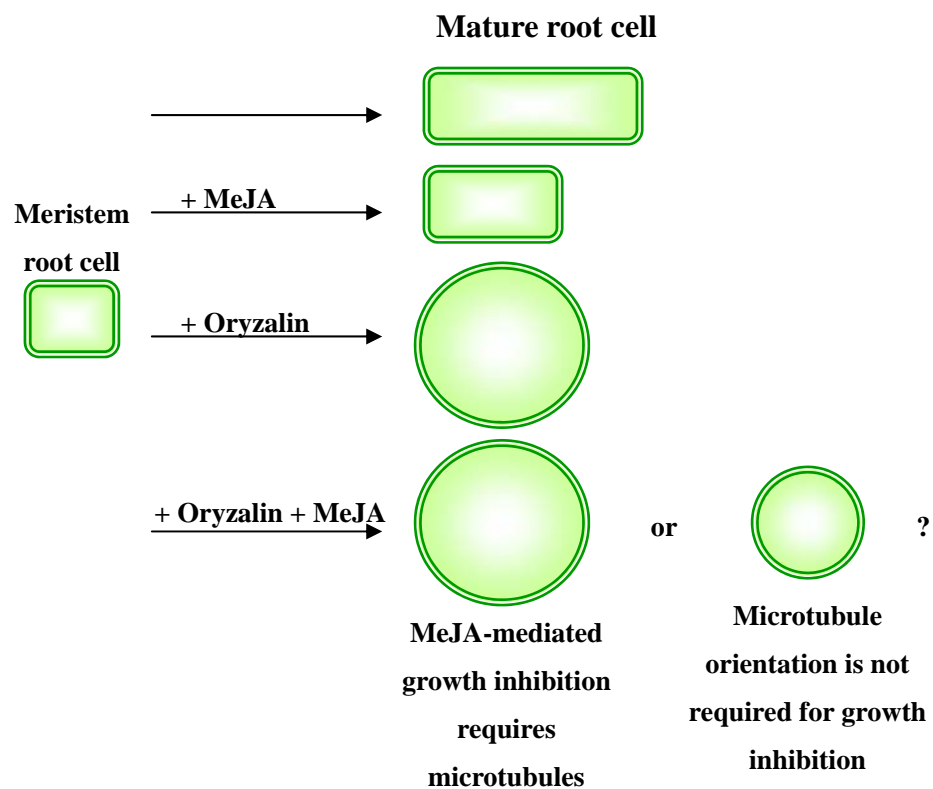


Figure 8-9 Hypothesis of testing if microtubules are required for MeJA-mediated root growth inhibition by using oryzalin treatment on *GFP-TUB6*.

8.2.2 Effect of MeJA Treatment on Acid Efflux

It has been reported that elongating cells release protons to the cell wall matrix. To test this, *Zea mays* and *Arabidopsis* were used to test the pH pattern of the root surface in response to MeJA. *Zea mays* has been used previously for these experiments (Mulkey and Evans, 1981). In larger root, the surface pH can be easily detected with a pH indicator dye: bromocresol purple, which turns yellow (pH <5), orange (pH= 5), red or purple (pH>5) (2.1.5). Maize seeds were surface sterilized, germinated, and untreated or treated with 50 μ M MeJA, before transferred to medium containing bromocresol purple and without or with 50 μ M MeJA (2.2.6 and 2.2.7). Although it was potential that the pH pattern of the root surface should be reflected in a change of medium colour within 3 to 8 minutes (Mulkey and Evans, 1981), there was no colour change within 18 hrs after transfer.

In medium at pH 5.5, the untreated maize seedlings grew many lateral roots 4 days after transfer. The colour of the medium was bright yellow near the elongation zone, orange near the root apex, and red/purple around the seed coat (Figure 8-10 A). The MeJA-treated seedlings had shorter apical and shorter lateral roots. The stunted roots were also thicker than the untreated ones. Moreover, the colour of medium remained orange 4 days after transfer (Figure 8-10 B). In medium at pH 6.5, the untreated seedlings had bright yellow near the elongation zone and red/purple near the root apical 18 hrs after transfer (Figure 8-10 C). In MeJA-treated seedlings, the colour of medium yellowed very slightly near the elongation zone 18 hrs after transfer (Figure 8-10 D). With maize roots and bromocresol purple, it is clear that MeJA treatment reduces acid efflux from the elongating cells, which is possibly a result of growth arrest in this area. However, there was no JA insensitive maize mutant available for further examination, and *Arabidopsis* was hence used with an adapted method to measure the acid efflux.



Figure 8-10 *Zea mays* seedlings in medium containing pH indicator dye bromocresol purple. (A) and (B) Five day old seedlings in pH 5.5 medium. (A) Untreated. (B) Treated with 50 μ M MeJA, 4 days. (C) and (D) Three day old seedlings in pH 6.5 medium. (C) Untreated. (D) Treated with 50 μ M MeJA, 18 hrs.

Because *Arabidopsis* roots are thinner than maize roots, when they were transferred to medium containing bromocresol purple, there was no detectable change of medium colour (data not shown). Therefore, it would be difficult to examine pH pattern of *Arabidopsis* root surface with pH indicator dye or to detect pH directly at root surface. Here, 7 day old *Arabidopsis* roots were cut from the

seedlings and suspended in MS medium minus MES, and the pH was recorded (2.3.9). Because the initial pH value of the medium was at 6.5, it was expected that the acid efflux from elongating cells would decrease this pH value. Over the first minute, the pH dropped from 6.5 to 6.3, possibly due to transfer of protons in the roots. Therefore, the subsequent change in pH was recorded, i.e., from 5 to 35 minutes after transfer. The pH of the medium containing the untreated *Col-gl* roots dropped from 6.25 to 6.18 over the period 5 to 30 minutes. The pH of the medium containing the MeJA-treated *Col-gl* roots rose from 6.28 to 6.32 over the period 5 to 35 minutes. These results indicated acid efflux in untreated *Col-gl* roots and lack of acid efflux, or even alkaline efflux/ acid influx in MeJA-treated *Col-gl* roots (Figure 8-11). The pH of the medium containing the untreated *coil-16* roots dropped from 6.27 to 6.20 over the period 5 to 35 minutes. The pH of the medium containing the MeJA-treated *coil-16* roots also dropped from 6.26 to 6.23 over the period 5 to 35 minutes. These results suggested similar acid efflux from both untreated and MeJA-treated *coil-16* (Figure 8-11).

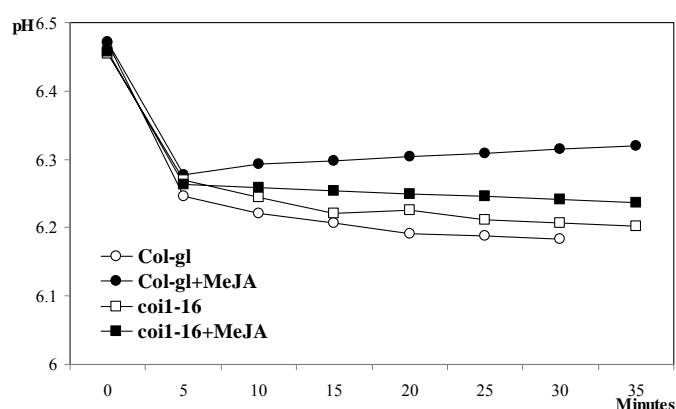


Figure 8-11 pH measuring of medium with 7 day old *Col-gl* and *coil-16* roots, untreated or treated with 20 μ M MeJA.

8.2.3 Effect of MeJA Treatment on Cellular Water Potential

The water potential is lower in the elongating cells than in the mature cells, so that elongating cells are better able to enlarge by taking more water/fluid (Boyer, 2001). It was hypothesised that the MeJA-treated roots are less able to take up water from

the medium, and the JA insensitive mutant would have lower water potential even when treated with MeJA. To examine this hypothesis, a low-water-potential medium with PEG 8000 was specially made (2.1.6). Three day old *Col-gl* and *coil-16* seedlings were transferred to the control medium or to 18% PEG8000 and 30% PEG8000 medium without or with 20 μ M MeJA, and then transferred to a SD growth chamber and held vertically. The plates containing seedlings were scanned for 3 consecutive days, and the root length was measured. Increased root length and rate of root growth inhibition were calculated for each day. Because the results from 1st, 2nd and 3rd day were similar, only results from 2nd day were chosen to show in Figure 8-12.

The root growth of *Col-gl* in the low-water-potential medium decreased dramatically compared with the untreated *Col-gl*. The growth inhibition rate of *Col-gl* was 48.7% with 18% PEG8000 and 77.5% with 30% PEG8000. The growth inhibition rate of the MeJA-treated *Col-gl* was 65.9%. The growth inhibition rate of *Col-gl* treated with 20 μ M MeJA was 80.9% on 18% PEG8000, and 85.6% on 30% PEG8000 (Figure 8-12). These results indicated that the low-water-potential medium created a higher osmotic pressure outside the root cells, and lack of water uptake led to reduction of root growth in a PEG8000 concentration dependent manner. In addition, the MeJA-mediated growth inhibition caused further reduction of root growth under high osmotic pressure. However, these results did not reveal if the MeJA-treated cells have higher water potential than the untreated ones.

The root growth of *coil-16* in the low-water-potential medium also decreased compared with the untreated *coil-16*. The growth inhibition rate of *coil-16* was 15.5% with 18% PEG8000 and 62.1% with 30% PEG8000. The growth inhibition rate of the MeJA-treated *coil-16* is 15.0%. The growth inhibition rate of *coil-16* treated with 20 μ M MeJA was 38.3% on 18% PEG8000, and 85.9% on 30% PEG8000 (Figure 8-12). These results indicated that the higher osmotic pressure also inhibited root growth of *coil-16* in a PEG8000 concentration dependent manner. *coil-16* was apparently less sensitive to 18% PEG8000 than *Col-gl*, which suggested that the water potential in the *coil-16* elongating cells might be lower than those in *Col-gl*. When treated with both MeJA and 18% PEG8000, *coil-16* also exhibited lower growth inhibition rate than *Col-gl* under the same treatment; whereas when treated with both MeJA and 30% PEG8000, the growth inhibition rate of *coil-16* was almost the same with *Col-gl* under the same treatment. This suggested that the

insensitivity of *coil-16* to PEG8000 is more evident at the lower PEG8000 concentration.

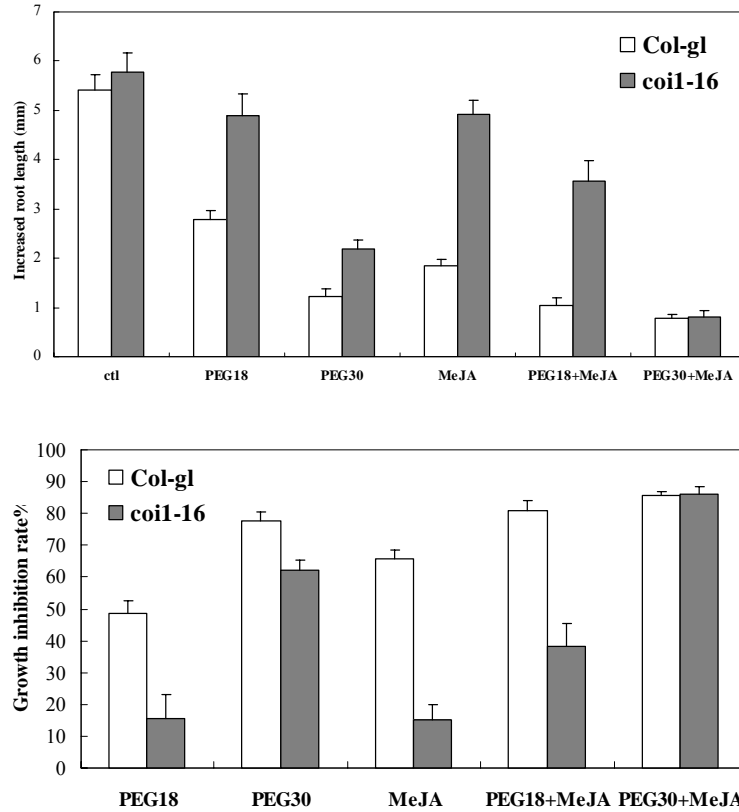


Figure 8-12 Increased root length (mm) and growth inhibition rate (%) of untreated and PEG8000 and 20 μ M MeJA-treated Col-*gl* and *coil-16*. **ctl**: untreated control. **PEG18**: 18% PEG 8000. **PEG30**: 30% PEG 8000.

8.3 Discussion

To understand the mechanical aspect of the MeJA-mediated root growth inhibition, the microtubule orientation in root cells, the change of root surface pH and acid efflux, and the root growth against low water potential were examined in this chapter.

Surprisingly, although microtubules were shown to be indispensable for JA and MeJA-induced cell cycle arrest in BY-2 suspension cells and tuber cell

expansion in potato (Ade *et al.*, 1990, Koda, 1997), the result here demonstrated that the MeJA-induced root growth inhibition in *Arabidopsis* does not require microtubules (**Figure 8-7**). In addition, the microtubule orientation is not affected by MeJA in both the meristem and the mature cells, and no obvious differences of microtubule orientation can be found in the JA and auxin mutants compared with *GFP-TUB6* (**Figure 8-1** to **8-4**). Therefore, *Arabidopsis* microtubules were not affected by MeJA as they are in the tobacco and potato cells reported previously (Ade *et al.*, 1990, Koda, 1997).

Microtubules are considered to guide the cellulose synthesising complexes, and control the orientation of the cellulose microfibrils and the direction of cell expansion (Giddings and Staehelin, 1991). The results here demonstrated differences of microtubule orientation between the meristem and the mature cells as laterally orientated and cross-hatched pattern (**Figure 8-1**). Verbelen *et al.* used an indirect immunofluorescent staining of microtubules with monoclonal anti-tubulin antibodies, and reported a change in orientation between elongating cells and differentiating cells. In *Arabidopsis* roots, the epidermis cells in elongation zone have cortical microtubules as parallel loops, while the epidermis cells in the differentiation zone also have parallel microtubules, which are oblique in different angles to the long axis of the cells (Verbelen *et al.*, 2001, Figure 2). Taken together, the results of Verbelen and those presented here indicate that the pattern of microtubules from meristem to mature tissues changes from isotropical, to lateral/parallel, to parallel but more oblique, and then cross-hatched in the mature cells. The capacity of these different cell types to expand can be related to the orientation of the microtubules. However, the orientation does not seem to be affected by exposure to MeJA.

During cell expansion, the release of protons from the cytoplasm activates the wall-loosening proteins, which break the weak hydrogen bonds between the cellulose microfibrils, allowing cell wall expansion (Cosgrove *et al.*, 2002). Maize roots have been used to illustrate surface pH pattern with pH indicator dye, and direct measurement of root surface acidification with a pH electrode (Mulkey and Evans, 1981, Zidan *et al.*, 1990). The results presented here indicate that maize seedlings treated with MeJA have reduced root growth rate and decreased acid efflux from the elongation zone (**Figure 8-10**). Similarly, maize roots treated with 2 μ M IAA had reduced growth, and decreased acid efflux from the elongation zone

(Mulkey and Evans, 1981). However, the acid efflux was observed in 3-8 minutes after seedlings were transferred to the medium as stated by Mulkey and Evans, but it took at least 18 hrs to observe the same change of medium colour in the results presented here. Possibly, this difference in acid efflux rate reflects the different growth condition and maize lines used.

The measurement of acid efflux from the *Arabidopsis* root was achieved by recording the pH of the medium incubating the roots (**Figure 8-11**). To my knowledge, this is the first time acid efflux was shown with living *Arabidopsis* roots. The MeJA-treated *Arabidopsis* roots caused an increase of the medium pH, suggesting acid influx, or alkaline efflux. Interestingly, JA caused intracellular alkalization of *Paphiopedilum* guard cells and maize coleoptiles (Gehring *et al.*, 1997, Irving *et al.*, 1999), indicating that a change of cytosolic pH is probably one of the features in MeJA-treated tissues. It is very likely though, the cytosolic alkalization can be directly linked with the acid influx/alkaline efflux observed here. The acid efflux from *coi1-16* roots was not affected by MeJA, further confirming the correlation of acid efflux and root cell elongation. This suggested that the MeJA-mediated root growth inhibition is caused by reduced acid efflux, and presumably decreased cell wall acidification and wall loosening.

Low water potential at elongating cells is created by cell wall expansion (Boyer, 2001). The PEG8000 treatment strongly inhibited *Arabidopsis* root growth by preventing water uptake to the elongating cells. The results suggested that the elongating cells of *coi1-16* had more plastic walls, or lower water potential than those in *Col-gl*. In addition, the MeJA-treated roots showed higher sensitivity to low water potential stress (**Figure 8-12**). Although there is so far no evidence of a connection between JA signaling and change of water potential/ turgor pressure, other plant hormone was already shown to affect these factors. In roots of sunflower and soybean suffering chilling-induced water stress, endogenous ABA increases water transport in the roots by enhancing hydraulic conductivity (Ludewig *et al.*, 1988, Albert and Markhart, 1984). It is possible that one of the ways used by endogenous JA to inhibit vegetative growth is by preventing water uptake of elongating cells. Possibly, the exogenous MeJA causes growth arrest also by the same mechanism.

Chapter 9

General Discussion

In this thesis, I described my investigation into the effect of MeJA on the expression and subcellular localisation of the COI1 protein, and the physiological and morphological basis of MeJA-mediated root growth inhibition. This has revealed two main discoveries: that the COI1 protein is localised in the nucleus together with the JAZ3 protein (**Chapter 3**), and that MeJA inhibits root growth by suppressing mitosis and cell elongation, which is independent from ABA and GA signaling (**Chapter 5, 6, 7 and 8**).

It was hypothesised that the perception of JA and the induction of JA-responsive genes take place in the nucleus. This project initially aimed at localising protein components that participate in the perception and the activation of the JA signal pathway. As a result, localisation of COI1 and co-localisation of COI1 and JAZ3 to the nucleus in *Arabidopsis* roots were successfully revealed for the first time (**Chapter 3**). Significantly, some other components of the JA signal pathway, including MYC2, JAZ1, JAZ6, JAI3/JAZ3 and JAS1/JAZ10, have been localised to the nucleus. However, with the exception of JAI3/JAZ3, these proteins were expressed either in transiently transformed BY-2 cells, or by biolistic delivery to onion cells (Lorenzo *et al.*, 2004, Thines *et al.*, 2007, Chini *et al.*, 2007, Yan *et al.*, 2007). Co-localisation of COI1 and JAZ3 expressed in the *Arabidopsis* transgenic line confirmed for the first time that the perception of JA-Ile by the COI1-JAZ co-receptor must take place in the nucleus. Therefore, it is almost certain that the other untested protein components in the JA signal pathway, such as JAZ2, JAZ4, JAZ5, JAZ7 and JAZ 8, and other TFs such as MYC3 and MYC4 (Ferna'ndez-Calvo *et al.*, 2011), accumulate in the nucleus as well.

It was also revealed for the first time that the sub-nuclear localisation is altered,

and the expression of COI1 is induced, by MeJA in the root tissue under the regulation of the native promoter (**Chapter 3**). The expression of the *COI1* transcript is constitutive, and is not induced by wounding or JA (Xie *et al.*, 1998). It was hence surprising to see a change in protein level in response to the MeJA treatment. This suggests that there might be post-transcriptional or translational regulation of COI1 when the JA signal pathway is activated. Another interesting finding was the speckle-like distribution of COI1::HA in the nucleus under the regulation of the 35S promoter (**Chapter 3**). Sub-nuclear domains, such as nucleolus, cajal bodies, speckles, and different types of nuclear bodies, bear distinctive functions, and some of the nuclear bodies are involved in RNA metabolism and hormonal responses (Shaw and Brown, 2004). The phytochrome-containing speckle domains, for example, are light-inducible and consist of phytochromes imported from cytosol and form protein complexes for light-triggered responses. Phytochrome A is required for JA-mediated root growth inhibition, and degradation of JAZ1 is the link between phytochrome A and JA signaling (Robson *et al.*, 2010). In addition, root-localised phytochrome chromophore deficiencies impair JA-mediated root growth inhibition (Costigan *et al.*, 2011). These studies suggest that the JA-signaling components are also likely to form nuclear bodies, and the sub-nuclear localisation of JAZ1/TIFY10A in BY-2 cells as unidentified nuclear bodies definitely supports this hypothesis (Grunewald *et al.*, 2009). Further examinations on COI1 and JAZ3 under regulation of the 35S promoter and/or the native promoter by high-resolution confocal microscopy will certainly reveal more detail.

Another focus of this project was to investigate the JA-mediated growth inhibition, which is one of the first physiological effects discovered for JAs (Dathe *et al.*, 1981; Staswick *et al.*, 1992). However, the studies on JA-mediated growth inhibition so far revealed only fragmented results. This project examined the effect of MeJA on every part of the root, and the results give a more comprehensive picture.

The increased length of a root is contributed mainly by two factors, the number of the dividing cells and the length of the mature cells (Beemster and Baskin, 1998). By examining the growth-contributing morphological parameters, including meristem size, meristem cell number, mitotic cell number, length of LEH, number of rapidly-elongating cells, rate of elongation, and mature cell length, it was revealed

that MeJA affects the meristem, the TZ and the elongation zone (**Figure 9-1; Chapter 5 and 6**). Unexpectedly, the rate of individual cell elongation was not inhibited, which corresponds to Beemster and Baskin's finding that the cellular expansion rate rarely changes even when roots undergo accelerated growth shortly after germination (Beemster and Baskin, 1998). In addition, MeJA's inhibitory effects on the meristem and the cell expansion zone were possibly two distinctive processes which do not relate to each other.

In previous studies, the reduction of cell division in the SAM and the reduction of cell elongation in oat coleoptile segments by JA had been shown (Zhang and Turner, 2008; Ueda *et al.*, 1995). In this thesis, the reduction of mitosis in the root apical meristem was observed (**Chapter 5 and 6**). However, it was shown for the first time that the reduction of cell elongation is due to a combination of the reduced number of rapidly elongating cells, and the decreased mature cell length (**Chapter 5 and 6**). Interestingly, a developmental pause of cells in the meristem before they entered the TZ was observed in the seedlings transferred from half MS to MeJA-containing medium (**Chapter 5**), but not in those germinated directly in MeJA-containing medium (**Chapter 6**). This indicates that MeJA causes the developmental delay of cells prior to their entry to the TZ only on rapidly growing roots, and that certain changes of the morphological factors in MeJA-treated roots can be treatment-dependent. Furthermore, there are distinctive differences between a piece of coleoptile segment and an intact root. The coleoptile segment consists of morphologically similar cells which are all specialised to elongating growth, while an intact root consists of cells undergoing mitosis, elongation and differentiation. The *Arabidopsis* root, therefore, is able to display JA's diverse effects on cells at different developmental stages, and is a more comprehensive model to study MeJA-mediated growth inhibition.

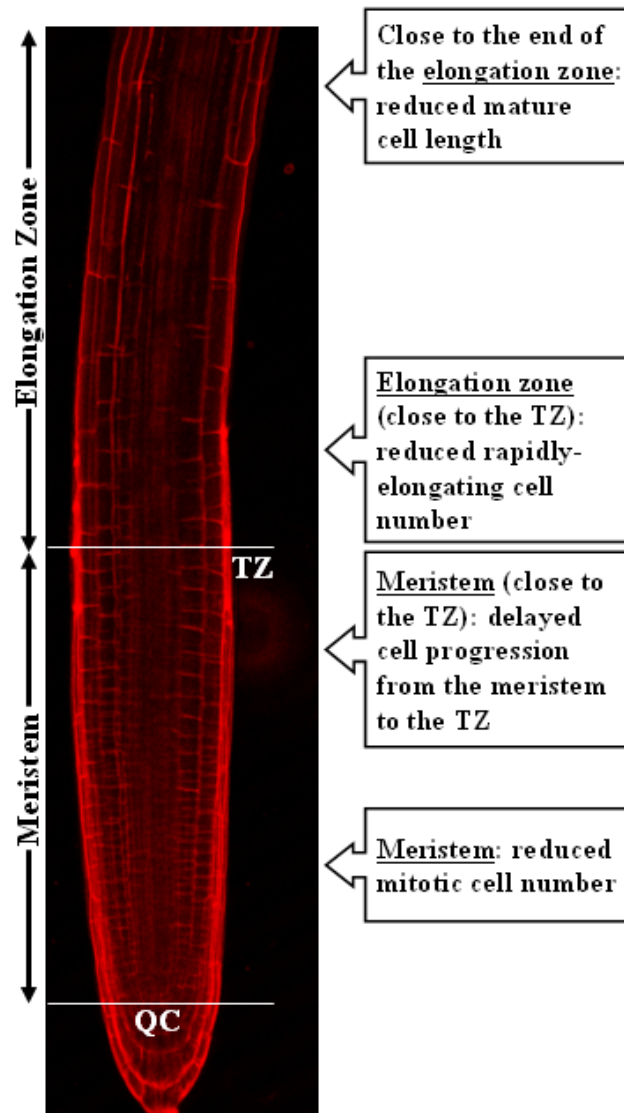


Figure 9-1 An *Arabidopsis* root and the listed effects of MeJA that cause root growth inhibition. TZ: transition zone, and QC: quiescent centre.

Examination of physiological factors of the elongating cells revealed that the MeJA-treated roots exhibited less acid efflux than the untreated ones in the elongation zone, while microtubule orientation, surprisingly, was not involved in the MeJA-mediated growth inhibition (**Chapter 8**). Additionally, the MeJA-treated roots showed higher sensitivity to low water potential stress, and *coil-16* was more resistant to the same stress, suggesting that MeJA reduces cell elongation by lowering the osmotic pressure (**Chapter 8**). Although, to my knowledge, the change

of water uptake in the MeJA-treated root has not previously been investigated, the microtubule orientation had been studied in MeJA-treated BY-2 cells, and the cytosolic pH had been studied in the JA-treated maize coleoptile segments (Abe *et al.*, 1990; Irving *et al.*, 1999). BY-2 cell line has high homogeneity and high growth rate, and has been used as a model system to study general biochemical phenomena of plant cells. This cell suspension culture may be sufficient enough for studying the cell cycle, but may not be a system to compare with a developing root, in which cells divide, elongate, and differentiate. It was observed that in BY-2 cells, microtubules are depolymerised by MeJA only in the S-phase, but after the cell cycle proceeds, the microtubule polymerisation takes place again and is insensitive to MeJA. However, in the present study, the microtubule orientation was not altered by MeJA in both the meristem and the mature cells, indicating that MeJA does not inhibit root growth by disrupting microtubules (**Chapter 8**). This finding was also supported by experiments in which microtubules were depolymerised with oryzalin, but cell enlargement was still inhibited by MeJA, confirming that microtubules are not required for MeJA-mediated growth inhibition (**Chapter 8**). Possibly, MeJA arrests cell cycle via different mechanisms in the BY-2 cells and in the root meristem, and mediates growth inhibition in a cell type-specific and tissue-specific manner.

Acid growth refers to the rapid stimulation of cell enlargement in response to acid wall pH. This response is characteristic of the growing cells of many plant tissues and is the result of wall-loosening proteins bound to the cell wall. Much, if not all, of the acid growth response of cell walls has been attributed to the action of expansins

JA inhibits the elongation of maize coleoptile segments by increasing the cytosolic pH (Irving *et al.*, 1999), which is in agreement with less acid efflux from the elongating cells (**Chapter 8**). The acid efflux from cytosol and decrease of cell wall pH are both the features of the growing plant cells. These features had been linked to the action of the wall-loosening proteins, such as expansins, which weaken the hydrogen bonds of wall components to one another or to the cellulose surface (Cosgrove *et al.*, 2002). Evidently, JA increases the cytosolic pH in the elongating cells before they reach their normal mature length. This action prevents acid efflux from the cytosol, which in turn limits the cell wall extensibility and ceases the elongation.

Taken together, the respective effects of MeJA on cells in the meristem and elongation zone are concluded below. In the meristem, MeJA decreases the number of the dividing cells by disrupting the cell cycle, which delays cells entering the TZ, where cells are having their final division, and begin to elongate rapidly. This results in either less cells in the meristem, if the seedlings are germinated in MeJA-containing medium, or cells accumulate between the meristem and the elongation zone, if the seedlings are treated with MeJA after germination. Once the cells have entered the TZ, MeJA does not inhibit the rate of expansion of individual cells, but causes fewer cells to elongate, which also cease elongating before they reach the normal mature length. Considering the rate of cell elongation is unchanged, it is likely that the few rapidly-elongating cells in the MeJA-treated root still keep normal acid efflux and water uptake. Presumably, these cells cease elongation due to increased cytosolic pH, which decreases acid efflux from cytosol to cell wall, and reduced turgor pressure, which prevents further water uptake. This hypothesis should be investigated further.

How JA-responsive genes modulate these physiological effects, however, remains unknown. Nevertheless, auxin, the most predominant hormone in regulating plant growth, is perhaps able to provide an explanation. The IAA-induced elongation of oat and maize coleoptile segments was inhibited by JA, indicating that the two hormone pathways interact (Ueda *et al.*, 1995; Irving *et al.*, 1999). Sun *et al.* further demonstrated that exogenous MeJA regulates the expression of *PIN1*, *PIN2* and *AUX1* in controlling the lateral root formation in *Arabidopsis*, indicating that JA inhibits growth by modulating auxin transportation (Sun *et al.*, 2009). *AUX1*, the auxin influx carrier, has been reported to be involved in both phloem-based and polar transport of auxin (Swarup *et al.*, 2001). The insensitivity of *aux1-7* to MeJA, especially in reaching to mature cell length (**Chapter 7**), suggests that the MeJA-mediated root growth inhibition depends on controlling auxin transportation. Although the link between JA signaling and altered expression of the auxin carrier genes is not yet clear, it is hypothesised that flavonoid biosynthesis might have a role. Flavonoid biosynthesis is up-regulated by JA, and the flavonoid-deficient mutants display altered protein level and localisation of the *PIN* genes in a tissue-specific manner, indicating that JA might mediate auxin transportation via the flavonoid signaling pathway (Peer *et al.*, 2004; Sun *et al.*, 2009).

JA is not the only plant hormone that influences vegetative and developmental

growth in the root. GA controls root proliferation in a DELLA-dependent manner. To increase the meristem size, activated GA signaling targets degradation of the DELLA proteins in a subset of endodermal cells in the meristem (Ubeda-Tomás *et al.*, 2009). Achard *et al.* also showed that the DELLA-mediated root growth inhibition largely depends on DELLAs reducing the cell division rate in the meristem (Achard *et al.*, 2009). On the other hand, ABA inhibits plant growth by limiting cell wall extensibility in maize coleoptiles, and disrupting cell division by arresting the G1 phase of the cell cycle in tomato seeds (Kutschera and Schopfer, 1986; Liu *et al.*, 1994). Considering the complex crosstalk between these hormones reported so far, it is hard not to assume that there might also be interactions between the JA, ABA and GA signaling components in root growth.

The results presented in this thesis, however, demonstrate that MeJA-mediated root growth inhibition is both DELLA- and ABA-independent (**Chapter 7**). Despite extensive evidence showing that DELLA proteins regulate JA biosynthesis and interact with the JAZ proteins (Cheng *et al.*, 2009; Hou *et al.*, 2010), and ABA works synergistically with JA in defending against hemi-biotroph and necrotrophic pathogens (de Torres-Zabala *et al.*, 2007; Adie *et al.*, 2007), it seems the crosstalk between JA and ABA, and JA and GA signaling does not extend to MeJA-mediated growth inhibition. This finding is also supported by the fact that JA-induced growth inhibition in maize coleoptile segments is ABA-independent (Irving *et al.*, 1999). Therefore, although JA, GA, and ABA may interact in other hormone-induced responses, their effect on regulating root growth is evidently independent. This suggests that MeJA-mediated root growth inhibition is unique among the JA-induced responses, in that it does not involve an interaction with GA or ABA, and the fine-tuning of root growth and development between different plant hormones is more diversified and delicate than our comprehension so far.

Future work:

There remain many unanswered questions regarding the MeJA-mediated growth inhibition. Below is a list of the top questions and the suggested approaches.

- Function of the individual JAZ genes in the regulation of root growth is still unknown. JAS1/JAZ10, a nuclear mediator that represses the MeJA-induced root growth inhibition in a COI1-dependent manner (Yan *et al.*, 2007), should

be a nice candidate to start with. If *JAZ* mutants are made to test their insensitivity to MeJA, mutation of multiple *JAZ* genes will be necessary, because some of the JAZ proteins work redundantly with each other (Thines *et al.*, 2007).

- Function of the TFs repressed by JAZ proteins in root growth is not completely identified yet. *myc2* is only partially sensitive to MeJA-mediated growth inhibition (**Chapter 5** and Lorenzo *et al.*, 2004), and the recently discovered MYC3 and MYC4 TFs only have minor contribution to the JA response in root (Fernández-Calvo *et al.*, 2011), indicating that there must be other TFs involved. Despite MYC3 and MYC4, Fernández-Calvo *et al.* also identified several other MYC TFs containing similar JAZ-interaction domain, which can be used for further screening.
- How JA regulates the cell cycle? Previous research showed that in BY-2 cells, JA suppresses the CDK activity and inhibits the accumulation of cyclin B1, which result in arrest of the cell cycle in the G2-M transition (Świątek *et al.*, 2004a). It will be interesting to examine the expression pattern of the cell cycle-related genes in the root meristem of JA mutants.
- How JA regulates cell elongation? Future studies based on measuring the turgor pressure (e.g., Tomos and Leigh, 1999) in untreated and MeJA-treated WT plant and JA mutants should be able to test whether the MeJA-induced elongation inhibition is due to reduced osmotic potential in the elongating cells.

Bibliography

- Abe M., Shibaoka H., Yamane H., and Takahashi N.** (1990). Cell cycle-dependent disruption of microtubules by methyl jasmonate in tobacco BY-2 cells. *Protoplasma* **156**, 1-8.
- Achard P., Cheng H., De Grauwe L., Decat J., Schoutteten H., Moritz T., Van Der Straeten D., Peng J., and Harberd N.P.** (2006). Integration of Plant Responses to Environmentally Activated Phytohormonal Signals. *Science* **311**, 91-94.
- Achard P., Gusti A., Cheminant S., Alioua M., Dhondt S., Coppens F., Beemster G.T., and Genschik P.** (2009). Gibberellin signaling controls cell proliferation rate in Arabidopsis. *Curr Biol.* **19**, 1188-1193.
- Adie B.A., Pérez-Pérez J., Pérez-Pérez M.M., Godoy M., Sánchez-Serrano J.J., Schmelz E.A., and Solano R.** (2007). ABA is an essential signal for plant resistance to pathogens affecting JA biosynthesis and the activation of defenses in Arabidopsis. *Plant Cell* **19**, 1665-1681.
- Albert H. and Markhart III.** (1984). Amelioration of Chilling-Induced Water Stress by Absciscic Acid-Induced Changes in Root Hydraulic Conductance. *Plant Physiol.* **74**, 81-83.
- Albrecht T., Kehlen A., Stahl K., Knöfel H.D., Sembdner G., and Weiler E.W.** (1993). Quantification of rapid, transient increases in jasmonic acid in wounded plants using a monoclonal antibody. *Planta* **191**, 86-94.
- Anderson J.P., Badruzsaufari E., Schenk P.M., Manners J.M., Desmond O.J., Ehlert C., Maclean D.J., Ebert P.R., and Kazan K.** (2004). Antagonistic interaction between abscisic acid and jasmonate-ethylene signaling pathways modulates defense gene expression and disease resistance in Arabidopsis. *Plant Cell* **16**, 3460-3479.
- Ausubel F.M., Brent R., Kingston R.E., Moore D.D., Seidman J.G., Smith J.A., and Struhl K.** (1999). In *Current Protocols in Molecular Biology* John Wiley & Sons, Hoboken, N.J. .
- Barnes W.M.** (1994). PCR amplification of up to 35-kb DNA with high fidelity and high yield from lambda bacteriophage templates. *Proc Natl Acad Sci U S A.* **91**, 2216-2220.
- Baskin T.I., Cork, A., Williamson R.E., Gorst J.R.** (1995). STUNTED PLANT 1, A Gene Required for Expansion in Rapidly Elongating but Not in Dividing Cells and Mediating Root Growth Responses to Applied Cytokinin. *Plant Physiol.* **107**, 233-243.
- Beemster G.T. and Baskin T.I.** (1998). Analysis of cell division and elongation underlying the developmental acceleration of root growth in Arabidopsis thaliana. *Plant Physiol.* **116**, 1515-1526.

BIBLIOGRAPHY

- Belin C., Megies C., Hauserová E., and Lopez-Molina L.** (2009). Absciscic acid represses growth of the Arabidopsis embryonic axis after germination by enhancing auxin signaling. *Plant Cell* **21**, 2253-2268.
- Benedetti C.E., Xie D., and Turner J.G.** (1995). Coi1-dependent expression of an Arabidopsis vegetative storage protein in flowers and siliques and in response to coronatine or methyl jasmonate. *Plant Physiol.* **109**, 567-572.
- Bennett M.J., Marchant A., Green H.G., May S.T., Ward S.P., Millner P.A., Walker A.R., Schulz B., and Feldmann K.A.** (1996). Arabidopsis AUX1 Gene: A Permease-Like Regulator of Root Gravitropism. *Science* **273**, 948-950.
- Berger S., Bell E., Mullet J.E.** (1996). Two Methyl Jasmonate-Insensitive Mutants Show Altered Expression of AtVsp in Response to Methyl Jasmonate and Wounding. *Plant Physiol.* **111**, 525-531.
- Birnboim H.C., and Doly J.** (1979). A rapid alkaline extraction procedure for screening recombinant plasmid DNA. *Nucleic Acids Res.* **7**, 1513-1523.
- Boter M., Ruíz-Rivero O., Abdeen A., and Prat S.** (2004). Conserved MYC transcription factors play a key role in jasmonate signaling both in tomato and Arabidopsis. *Genes & Dev.* **18**, 1577-1591.
- Boyer J.S.** (2001). Growth-induced water potentials originate from wall yielding during growth. *J Exp Bot.* **52**, 1483-1488.
- Brett C.T.** (2000). Cellulose microfibrils in plants: biosynthesis, deposition, and integration into the cell wall. *Int Rev Cytol.* **199**, 161-199.
- Brummer B., Bertl A., Potrykusc I., Fellec H. and Parish R.W.** (1985). Evidence that fusaric acid and indole-3-acetic acid induce cytosolic acidification of Zea mays cells. *FEBS Lett.* **189**, 109-113.
- Buchanan-Wollaston V., Page T., Harrison E., Breeze E., Lim P.O., Nam H.G., Lin J.F., Wu S.H., Swidzinski J., Ishizaki K., and Leaver C.J.** (2005). Comparative transcriptome analysis reveals significant differences in gene expression and signalling pathways between developmental and dark/starvation-induced senescence in Arabidopsis. *Plant J.* **42**, 567-585.
- Cheng H., Qin L., Lee S., Fu X., Richards D.E., Cao D., Luo D., Harberd N.P., and Peng J.** (2004). Gibberellin regulates Arabidopsis floral development via suppression of DELLA protein function. *Dev.* **131**, 1055-1064.
- Cheng H., Song S., Xiao L., Soo H.M., Cheng Z., Xie D., and Peng J.** (2009). Gibberellin acts through jasmonate to control the expression of MYB21, MYB24, and MYB57 to promote stamen filament growth in Arabidopsis. *PLoS Genet.* **5**, e1000440.
- Chico J.M., Chini A., Fonseca S., and Solano R.** (2008). JAZ repressors set the rhythm in jasmonate signaling. *Curr Opin Plant Biol.* **11**, 486-494.
- Chini A., Fonseca S., Fernández G., Adie B., Chico J.M., Lorenzo O., García-Casado G., López-Vidriero I., Lozano F.M., Ponce M.R., Micol J.L., and Solano R.** (2007). The JAZ family of repressors is the missing link in jasmonate signalling. *Nature* **448**,

BIBLIOGRAPHY

666-671.

- Chini A., Fonseca S., Chico J.M., Fernández-Calvo P., and Solano R.** (2009). The ZIM domain mediates homo- and heteromeric interactions between Arabidopsis JAZ proteins. *Plant J.* **59**, 77-87.
- Chung H.S., and Howe G.A.** (2009). A critical role for the TIFY motif in repression of jasmonate signaling by a stabilized splice variant of the JASMONATE ZIM-domain protein JAZ10 in Arabidopsis. *Plant Cell* **21**, 131-145.
- Cipollini D.** (2005). Interactive Effects of Lateral Shading and Jasmonic Acid on Morphology, Phenology, Seed Production, and Defense Traits in Arabidopsis thaliana. *Int J Plant Sci.* **166**, 955-959.
- Cleland R.** (1971). Cell wall expansion. *Annu. Rev. Plant Physiol.* **22**, 197-222.
- Conconi A., Smerdon M., Howe G.A., and Ryan C.A.** (1996). The octadecanoid signalling pathway in plants mediates a response to ultraviolet radiation. *Nature* **383**, 826-829.
- Corbineau F., Rudnicki R.M., and Côme D.** (1988). The effects of methyl jasmonate on sunflower (*Helianthus annuus* L.) seed germination and seedling development. *Plant Growth Regulation* **7**, 157-169.
- Cosgrove D.J., Li L.C., Cho H.T., Hoffmann-Benning S., Moore R.C., and Blecker D.** The growing world of expansins. *Plant Cell Physiol.* **43**, 1436-1444.
- Costigan S.E., Warnasooriya S., Humphries B.A., and Montgomery B.L.** (2011). Root-localized phytochrome chromophore synthesis is required for photoregulation of root elongation and impacts root sensitivity to jasmonic acid in Arabidopsis thaliana. *Plant Physiol.* DOI:10.1104/pp.1111.184689.
- Creelman R.A., and Mullet J.E.** (1997). Biosynthesis and action of jasmonates in plants. *Annu Rev Plant Physiol Plant Mol Biol* **48**, 355-381.
- Dathe W., Rönch H., Preiss A., Schade W., Sembdner G. and Schreiber K.** (1981). Endogenous plant hormones of the broad bean, *Vicia faba* L. (-)-jasmonic acid, a plant growth inhibitor in pericarp. *Planta* **153**, 530-535.
- de Torres-Zabala M., Truman W., Bennett M.H., Lafforgue G., Mansfield J.W., Rodriguez Egea P., Bögre L., and Grant M.** (2007). *Pseudomonas syringae* pv. tomato hijacks the Arabidopsis abscisic acid signalling pathway to cause disease. *EMBO J.* **26**, 1434-1443.
- Dellaporta S.L., Wood J., and Hicks J.B.** (1983). A plant DNA miniprep: version II. *Plant Mol Bio Rep.* **1**, 19-21.
- Dello Ioio R., Nakamura K., Moubayidin L., Perilli S., Taniguchi M., Morita M.T., Aoyama T., Costantino P., and Sabatini S.** (2008). A genetic framework for the control of cell division and differentiation in the root meristem. *Science* **322**, 1380-1384.
- Delmer D.** (1987). Cellulose biosynthesis. *Annu Rev Plant Physiol* **38**, 259.
- Delmer D.P., and Amor Y.** (1995). Cellulose Biosynthesis. *Plant Cell* **7**, 987-1000.

BIBLIOGRAPHY

- Devoto A., Nieto-Rostro M., Xie D., Ellis C., Harmston R., Patrick E., Davis J., Sherratt L., Coleman M., and Turner J.G.** (2002). COI1 links jasmonate signalling and fertility to the SCF ubiquitin–ligase complex in Arabidopsis. *Plant J.* **32**, 457-466.
- Devoto A., Ellis C., Magusin A., Chang H.S., Chilcott C., Zhu T., and Turner J.G.** (2005). Expression profiling reveals COI1 to be a key regulator of genes involved in wound- and methyl jasmonate-induced secondary metabolism, defence, and hormone interactions. *Plant Mol Biol.* **58**, 497-513.
- Doerner P.** (2009). Root systems architecture workshop in ICAR2009.
- Dolan L., Janmaat K., Willemsen V., Linstead P., Poethig S., Roberts K., and Scheres B.** (1993). Cellular organisation of the Arabidopsis thaliana root. *Dev.* **119**, 71-84.
- Dolan L., and Davies J.** (2004). Cell expansion in roots. *Curr Opin Plant Biol.* **7**, 33-39.
- Dombrecht B., Xue G.P., Sprague S.J., Kirkegaard J.A., Ross J.J., Reid J.B., Fitt G.P., Sewelam N., Schenk P.M., Manners J.M., and Kazan K.** (2007). MYC2 differentially modulates diverse jasmonate-dependent functions in Arabidopsis. *Plant Cell* **19**, 2225-2245.
- Duckett C.M., Oparka K.J., DAM. Prior, Dolan L., and Roberts K.** (1994). Dye-coupling in the root epidermis of Arabidopsis is progressively reduced during development. *Dev.* **120**, 3247-3255.
- Ellis C., and Turner J.G.** (2001). The Arabidopsis mutant *cev1* has constitutively active jasmonate and ethylene signal pathways and enhanced resistance to pathogens. *Plant Cell* **13**, 1025-1033.
- Ellis C., and Turner J.G.** (2002). A conditionally fertile *coil* allele indicates cross-talk between plant hormone signalling pathways in Arabidopsis thaliana seeds and young seedlings. *Planta* **215**, 549-556.
- Ellis C., Karafyllidis I., Wasternack C., and Turner J.G.** (2002). The Arabidopsis mutant *cev1* links cell wall signaling to jasmonate and ethylene responses. *Plant Cell* **14**, 1557-1566.
- Erickson R.O., and Sax K.B.** (1956). Elementary growth rate of the primary root of *Zea mays*. *Proc. Am. Philos. Soc.* **100**, 487-498.
- Evans M.L.** (1974). Rapid responses to plant hormones. *Annu Rev Plant Physiol* **25**, 195-233.
- Evans M.L., and Vesper M.J.** (1980). An Improved Method for Detecting Auxin-induced Hydrogen Ion Efflux from Corn Coleoptile Segments. *Plant Physiol.* **66**, 561-565.
- Farmer E.E., and Ryan C.A.** (1990). Interplant communication: airborne methyl jasmonate induces synthesis of proteinase inhibitors in plant leaves. *Proc Natl Acad Sci U S A.* **87**, 7713-7716.
- Fernández-Calvo P., Chini A., Fernández-Barbero G., Chico J.M., Gimenez-Ibanez S., Geerinck J., Eeckhout D., Schweizer F., Godoy M., Franco-Zorrilla J.M., Pauwels L., Witters E., Puga M.I., Paz-Ares J., Goossens A., Reymond P., De Jaeger G., Solano R.** (2011). The Arabidopsis bHLH transcription factors MYC3 and MYC4 are targets of JAZ repressors and act additively with MYC2 in the activation of jasmonate

BIBLIOGRAPHY

- responses. *Plant Cell* **23**, 701-715.
- Ferreira P.C., Hemerly A.S., Engler J.D., van Montagu M., Engler G., and Inzé D.** (1994). Developmental Expression of the Arabidopsis Cyclin Gene *cyclAt*. *Plant Cell* **6**, 1763-1774.
- Feys B., Benedetti C.E., Penfold C.N., and Turner J.G.** (1994). Arabidopsis Mutants Selected for Resistance to the Phytotoxin Coronatine Are Male Sterile, Insensitive to Methyl Jasmonate, and Resistant to a Bacterial Pathogen. *Plant Cell* **6**, 751-759.
- Fischer-Parton S., Parton R.M., Hickey P.C., Dijksterhuis J., Atkinson H.A., and Read N.D.** (2000). Confocal microscopy of FM4-64 as a tool for analysing endocytosis and vesicle trafficking in living fungal hyphae. *J Microsc.* **198**, 246-259.
- Fonseca S., Chico J.M., and Solano R.** (2009). The jasmonate pathway: the ligand, the receptor and the core signalling module. *Curr Opin Plant Biol.* **12**, 539-547.
- French A., Ubeda-Tomás S., Holman T.J., Bennett M.J., and Pridmore T.** (2009). High-throughput quantification of root growth using a novel image-analysis tool. *Plant Physiol.* **150**, 1784-1795.
- Friml J., Benková E., Mayer U., Palme K., and Muster G.** (2003). Automated whole mount localisation techniques for plant seedlings. *Plant J.* **34**, 115-124.
- Fu X., and Harberd N.P.** (2003). Auxin promotes Arabidopsis root growth by modulating gibberellin response. *Nature* **421**, 740-743.
- Gehring C.A., Irving H.R., McConchie R., and Parish R.W.** (1997). Jasmonates Induce Intracellular Alkalinization and Closure of *Paphiopedilum* Guard Cells. *Ann Bot* **80**, 485-489.
- Gehring C.A., Irving H.R., and Parish R.W.** (1990). Effects of auxin and abscisic acid on cytosolic calcium and pH in plant cells. *Proc Natl Acad Sci U S A.* **87**, 9645-9649.
- Giddings T.H., and Staehelin L.A.** (1991). Staehelin, Microtubule—mediated control of microfibril deposition: a re-examination of the hypothesis In: C.W. Lloyd, Editors, *The cytoskeletal basis of plant growth and form*. Academic Press, London, 85–99.
- Gray W.M., Muskett P.R., Chuang H.W., and Parker J.E.** (2003). Arabidopsis SGT1b is required for SCF(TIR1)-mediated auxin response. *Plant Cell* **15**, 1310-1319.
- Grunewald W., Vanholme B., Pauwels L., Plovie E., Inzé D., Gheysen G., and Goossens A.** (2009). Expression of the Arabidopsis jasmonate signalling repressor JAZ1/TIFY10A is stimulated by auxin. *EMBO Rep.* **10**, 923-928.
- Hager, A., Debus, G., Edel, H.G., Stransky, H., and Serrano, R.** (1991). Auxin induces exocytosis and the rapid synthesis of a high-turnover pool of plasma-membrane H⁺-ATPase. *Planta* **185**, 527-537.
- Hashimoto T., and Nakajima K.** (2001). FY2001 Ground-based Research Announcement for Space Utilization Research Report.
- Hedden P.** (2008). Gibberellins close the lid. *Nature* **456**, 455-456.
- Hou X., Lee L.Y., Xia K., Yan Y., and Yu H.** (2010). DELLAs modulate jasmonate signaling

BIBLIOGRAPHY

- via competitive binding to JAZs. *Dev Cell.* **19**, 884-894.
- Irving H.R., Dyson G., McConchie R., Parish R.W., and Gehring C.A.** (1999). Effects of Exogenously Applied Jasmonates on Growth and Intracellular pH in Maize Coleoptile Segments. *J Plant Growth Regul.* **18**, 93-100.
- Ishiguro S., Kawai-Oda A., Ueda J., Nishida I., and Okada K.** (2001). The DEFECTIVE IN ANTHHER DEHISCENCE gene encodes a novel phospholipase A1 catalyzing the initial step of jasmonic acid biosynthesis, which synchronizes pollen maturation, anther dehiscence, and flower opening in Arabidopsis. *Plant Cell* **13**, 2191-2209.
- Jefferson R.A., Kavanagh T.A., and Bevan M.W.** (1987). GUS fusions: beta-glucuronidase as a sensitive and versatile gene fusion marker in higher plants. *EMBO J.* **6**, 3901-3907.
- Johnson C.M., Stout P.R., Broyer T.C., and Carlton A.B.** (1956). Comparative chlorine requirements of different plant species. *Plant and Soil* **8**, 337-353.
- Karban R., and Baldwin I.T.** (1997). *Induced Response to Herbivory*. Chicago: University of Chicago Press.
- Karimi M., Inzé D., and Depicker A.** (2002). GATEWAY vectors for Agrobacterium-mediated plant transformation. *Trends Plant Sci.* **7**, 193-195.
- Kazan K., and Manners J.M.** (2008). Jasmonate Signaling: Toward an Integrated View. *Plant Physiol.* **146**, 1459-1468.
- Kazan K., and Manners J.M.** (2009). Linking development to defense: auxin in plant-pathogen interactions. *Trends Plant Sci.* **14**, 373-382.
- Kessler A., Halitschke R., and Baldwin I.T.** (2004). Silencing the jasmonate cascade: induced plant defenses and insect populations. *Science* **305**, 665-668.
- Khan S., Stone J.M.** (2007). Arabidopsis thaliana GH3.9 influences primary root growth. *Planta* **226**, 21-34.
- Koda Y.** (1997). Possible involvement of jasmonates in various morphogenic events. *Physiologia Plantarum* **100**, 639-646.
- Koo A.J., and Howe G.A.** (2009). The wound hormone jasmonate. *Phytochemistry* **70**, 1571-1580.
- Kutschera U., and Schopfer P.** (1986). Effect of auxin and abscisic acid on cell wall extensibility in maize coleoptiles. *Planta* **167**, 527-535.
- Li L., Zhao Y., McCaig B.C., Wingerd B.A., Wang J., Whalon M.E., Pichersky E., and Howe G.A.** (2004). The tomato homolog of CORONATINE-INSENSITIVE1 is required for the maternal control of seed maturation, jasmonate-signaled defense responses, and glandular trichome development. *Plant Cell* **16**, 126-143.
- Liu Y., Bergervoet J.H.W., Ric Vos C. H., Hilhorst H.W.M., Kraak H.L., Karssen C.M., and Bino R.J.** (1994). Nuclear replication activities during imbibition of abscisic acid- and gibberellin-deficient tomato (*Lycopersicon esculentum* Mill.) seeds. *Planta* **194**, 368-373.
- Llorente F., Muskett P., Sánchez-Vallet A., López G., Ramos B., Sánchez-Rodríguez C.,**

BIBLIOGRAPHY

- Jordá L., Parker J., and Molina A.** (2008). Repression of the auxin response pathway increases Arabidopsis susceptibility to necrotrophic fungi. *Mol Plant* **1**, 496-509.
- Lorenzo O., Chico J.M., Sánchez-Serrano J.J., and Solano R.** (2004). JASMONATE-INSENSITIVE1 Encodes a MYC Transcription Factor Essential to Discriminate between Different Jasmonate-Regulated Defense Responses in Arabidopsis. *Plant Cell* **16**, 1938-1950.
- Ludewig M., Dörffling K., and Seifert H.** (1988). Abscissic acid and water transport in sunflowers. *Planta* **175**, 325-333.
- Mandaokar A., Thines B., Shin B., Lange B.M., Choi G., Koo Y.J., Yoo Y.J., Choi Y.D., Choi G., and Browse J.** (2006). Transcriptional regulators of stamen development in Arabidopsis identified by transcriptional profiling. *Plant J.* **46**, 984-1008.
- Mauch-Mani B., and Mauch F.** (2005). The role of abscisic acid in plant-pathogen interactions. *Curr Opin Plant Biol.* **8**, 409-414.
- McConn M., and Browse J.** (1996). The Critical Requirement for Linolenic Acid Is Pollen Development, Not Photosynthesis, in an Arabidopsis Mutant. *Plant Cell* **8**, 403-416.
- McConn M., Creelman R.A., Bell E., Mullet J.E., and Browse J.** (1997). Jasmonate is essential for insect defense in Arabidopsis. *Proc Natl Acad Sci U S A.* **94**, 5473-5477.
- Melotto M., Mecey C., Niu Y., Chung H.S., Katsir L., Yao J., Zeng W., Thines B., Staswick P., Browse J., Howe G.A., and He S.Y.** (2008). A critical role of two positively charged amino acids in the Jas motif of Arabidopsis JAZ proteins in mediating coronatine- and jasmonoyl isoleucine-dependent interactions with the COI1 F-box protein. *Plant J.* **55**, 979-988.
- Mockaitis K., and Estelle M.** (2008). Auxin receptors and plant development: a new signaling paradigm. *Annu Rev Cell Dev Biol.* **24**, 55-80.
- Moons A., Prinsen E., Bauw G., and Van Montagu M.** (1997). Antagonistic effects of abscisic acid and jasmonates on salt stress-inducible transcripts in rice roots. *Plant Cell* **9**, 2243-2259.
- Mulkey T.J., Evans M.L.** (1981). Geotropism in Corn Roots: Evidence for Its Mediation by Differential Acid Efflux. *Science* **212**, 70-71.
- Munemasa S., Oda K., Watanabe-Sugimoto M., Nakamura Y., Shimoishi Y., and Murata Y.** (2007). The coronatine-insensitive 1 Mutation Reveals the Hormonal Signaling Interaction between Abscissic Acid and Methyl Jasmonate in Arabidopsis Guard Cells. Specific Impairment of Ion Channel Activation and Second Messenger Production. *Plant Physiol.* **143**, 1398-1407.
- Nagpal P., Ellis C.M., Weber H., Ploense S.E., Barkawi L.S., Guilfoyle T.J., Hagen G., Alonso J.M., Cohen J.D., Farmer E.E., Ecker J.R., and Reed J.W.** (2005). Auxin response factors ARF6 and ARF8 promote jasmonic acid production and flower maturation. *Dev.* **132**, 4107-4118.
- Navarro L., Bari R., Achard P., Lisón P., Nemri A., Harberd N.P., and Jones J.D.** (2008). DELLAs control plant immune responses by modulating the balance of jasmonic acid

BIBLIOGRAPHY

- and salicylic acid signaling. *Curr Biol.* **18**, 650-655.
- Nonami H., and Boyer J.S.** (1987). Origin of growth-induced water potential : solute concentration is low in apoplast of enlarging tissues. *Plant Physiol.* **83**, 596-601.
- Olszewski N., Sun T.P., and Gubler F.** (2002). Gibberellin signaling: biosynthesis, catabolism, and response pathways. *Plant Cell* **14**, S61-80.
- Paredez A.R., Somerville C.R., and Ehrhardt D.W.** (2006). Visualization of Cellulose Synthase Demonstrates Functional Association with Microtubules. *Science* **312**, 1491-1495.
- Pauwels L., Morreel K., De Witte E., Lammertyn F., Van Montagu M., Boerjan W., Inzé D., and Goossens A.** (2008). Mapping methyl jasmonate-mediated transcriptional reprogramming of metabolism and cell cycle progression in cultured Arabidopsis cells. *Proc Natl Acad Sci U S A.* **105**, 1380-1385.
- Pauwels L., Barbero G.F., Geerinck J., Tilleman S., Grunewald W., Pérez A.C., Chico J.M., Bossche R.V., Sewell J., Gil E., García-Casado G., Witters E., Inzé D., Long J.A., De Jaeger G., Solano R., and Goossens A.** (2010). NINJA connects the co-repressor TOPLESS to jasmonate signalling. *Nature* **464**, 788-791.
- Peer W.A., Bandyopadhyay A., Blakeslee J.J., Makam S.N., Chen R.J., Masson P.H., and Murphy A.S.** (2004). Variation in Expression and Protein Localization of the PIN Family of Auxin Efflux Facilitator Proteins in Flavonoid Mutants with Altered Auxin Transport in Arabidopsis thaliana. *Plant Cell* **16**, 1898-1911.
- Pickett F.B., Wilson A.K., and Estelle M.** (1990). The auxi Mutation of Arabidopsis Confers Both Auxin and Ethylene Resistance. *Plant Physiol.* **94**, 1462-1466.
- Quint M., Ito H., Zhang W., and Gray W.M.** (2005). Characterization of a novel temperature-sensitive allele of the CUL1/AXR6 subunit of SCF ubiquitin-ligases. *Plant J.* **43**, 371-383.
- Rayle D.L., and Cleland R.** (1977). Control of plant cell enlargement by hydrogen ions. *Curr Topics Dev Biol* **11**, 187-214.
- Richards D.E., King K.E., Ait-Ali T., and Harberd N.P.** (2001). How gibberellin regulates plant growth and development: A molecular genetic analysis of gibberellin signaling. *Annu Rev Plant Physiol Plant Mol Biol.* **52**, 67-88.
- Rober-Kleber N., Albrechtová J.T., Fleig S., Huck N., Michalke W., Wagner E., Speth V., Neuhaus G., and Fischer-Iglesias C.** (2003) Plasma membrane H⁺-ATPase is involved in auxin-mediated cell elongation during wheat embryo development. *Plant Physiol.* **131**, 1302-1312
- Robson F., Okamoto H., Patrick E., Harris S.R., Wasternack C., Brearley C., and Turner J.G.** (2010). Jasmonate and phytochrome A signaling in Arabidopsis wound and shade responses are integrated through JAZ1 stability. *Plant Cell* **22**, 1143-1160.
- Rock C.D., and Sun X.** (2005). Crosstalk between ABA and auxin signaling pathways in roots of Arabidopsis thaliana (L.) Heynh. *Planta* **222**, 98-106.
- Sambrook J., Fritsch E.F., and Maniatis T.** (1989). *Molecular Cloning: A Laboratory Manual.*

BIBLIOGRAPHY

- (Cold Spring Harbor Laboratory Press).
- Santner A., and Estelle M.** (2009). Recent advances and emerging trends in plant hormone signalling. *Nature* **459**, 1071-1078.
- Sedbrook J.C., and Kaloriti D.** (2008). Microtubules, MAPs and plant directional cell expansion. *Trends Plant Sci.* **13**, 303-310.
- Sembdner G., and Parthier B.** (1993). The biochemistry and the physiological and molecular actions of jasmonates. *Annu Rev Plant Physiol Plant Mol Biol.* **44**, 569-589.
- Seo H.S., Song J.T., Cheong J.J., Lee Y.H., Lee Y.W., Hwang I., Lee J.S., and Choi Y.D.** (2001). Jasmonic acid carboxyl methyltransferase: a key enzyme for jasmonate-regulated plant responses. *Proc Natl Acad Sci U S A.* **98**, 4788-4793.
- Shaw P.J., and Brown J.W.** (2004). Plant nuclear bodies. *Curr Opin Plant Biol.* **7**, 614-620.
- Sheard L.B., Tan X., Mao H., Withers J., Ben-Nissan G., Hinds T.R., Kobayashi Y., Hsu F.F., Sharon M., Browse J., He S.Y., Rizo J., Howe G.A., and Zheng N.** (2010). Jasmonate perception by inositol-phosphate-potentiated COI1-JAZ co-receptor. *Nature* **468**, 400-405.
- Silk W.K., and Erickson R.O.** (1979) Kinematics of plant growth. *J Theor Biol.* **76**, 481-501.
- Silverstone A.L., Jung H.S., Dill A., Kawaide H., Kamiya Y., and Sun T.P.** (2001). Repressing a repressor: gibberellin-induced rapid reduction of the RGA protein in *Arabidopsis*. *Plant Cell* **13**, 1555-1566.
- Smith J.L., De Moraes C.M., and Mescher M.C.** (2009). Jasmonate- and salicylate-mediated plant defense responses to insect herbivores, pathogens and parasitic plants. *Pest Manag Sci.* **65**, 497-503.
- Somerville C.** (2006). Cellulose synthesis in higher plants. *Annu Rev Cell Dev Biol.* **22**, 53-78.
- Spoel S.H., Koornneef A., Claessens S.M., Korzeliuss J.P., Van Pelt J.A., Mueller M.J., Buchala A.J., Métraux J.P., Brown R., Kazan K., Van Loon L.C., Dong X., and Pieterse C.M.** (2003). NPR1 modulates cross-talk between salicylate- and jasmonate-dependent defense pathways through a novel function in the cytosol. *Plant Cell* **15**, 760-770.
- Staswick P.E., Su W., and Howell S.H.** (1992). Methyl jasmonate inhibition of root growth and induction of a leaf protein are decreased in an *Arabidopsis thaliana* mutant. *Proc Natl Acad Sci U S A.* **89**, 6837-6840.
- Staswick P.E., Tiriyaki I., and Rowe M.L.** (2002). Jasmonate response locus JAR1 and several related *Arabidopsis* genes encode enzymes of the firefly luciferase superfamily that show activity on jasmonic, salicylic, and indole-3-acetic acids in an assay for adenylation. *Plant Cell* **14**.
- Staswick P.E., and Tiriyaki I.** (2004). The oxylipin signal jasmonic acid is activated by an enzyme that conjugates it to isoleucine in *Arabidopsis*. *Plant Cell* **16**, 2117-2127.
- Steffens B., and Sauter M.** (2005). Epidermal cell death in rice is regulated by ethylene, gibberellin, and abscisic acid. *Plant Physiol.* **139**, 713-721.

BIBLIOGRAPHY

- Stelmach B.A., Müller A., Hennig P., Laudert D., Andert L., and Weiler E.W.** (1998). Quantitation of the octadecanoid 12-oxo-phytodienoic acid, a signalling compound in plant mechanotransduction. *Phytochemistry* **47**, 539-546.
- Stepansky A., and Galili G.** (2003). Synthesis of the Arabidopsis bifunctional lysine-ketoglutarate reductase/saccharopine dehydrogenase enzyme of lysine catabolism is concertedly regulated by metabolic and stress-associated signals. *Plant Physiol.* **133**, 1407-1415.
- Sugimoto K., Williamson R.E., and Wasteneys G.O.** (2000). New Techniques Enable Comparative Analysis of Microtubule Orientation, Wall Texture, and Growth Rate in Intact Roots of Arabidopsis. *Plant Physiol.* **124**, 1493-1506.
- Sun J., Xu Y., Ye S., Jiang H., Chen Q., Liu F., Zhou W., Chen R., Li X., Tietz O., Wu X., Cohen J.D., Palme K., and Li C.** (2009). Arabidopsis ASA1 is important for jasmonate-mediated regulation of auxin biosynthesis and transport during lateral root formation. *Plant Cell* **21**, 1495-1511.
- Sun T.P., and Kamiya Y.** (1994). The Arabidopsis GA1 locus encodes the cyclase ent-kaurene synthetase A of gibberellin biosynthesis. *Plant Cell* **6**, 1509-1518.
- Swarup R., Friml J., Marchant A., Ljung K., Sandberg G., Palme K., and Bennett M.** (2001). Localization of the auxin permease AUX1 suggests two functionally distinct hormone transport pathways operate in the Arabidopsis root apex. *Genes & Dev.* **15**, 2648-2653.
- Swiatek A., Lenjou M., Van Bockstaele D., Inzé D., and Van Onckelen H.** (2002). Differential Effect of Jasmonic Acid and Abscissic Acid on Cell Cycle Progression in Tobacco BY-2 Cells. *Plant Physiol.* **128**, 201-211.
- Swiatek A., Van Dongen W., Esmans E.L., and Van Onckelen H.** (2004a). Metabolic Fate of Jasmonates in Tobacco Bright Yellow-2 Cells. *Plant Physiol.* **135**, 161-172.
- Swiatek A., Azmi A., Stals H., Inzé D., and Van Onckelen H.** (2004b). Jasmonic acid prevents the accumulation of cyclin B1;1 and CDK-B in synchronized tobacco BY-2 cells. *FEBS Lett.* **572**, 118-122.
- Takahashi F., Yoshida R., Ichimura K., Mizoguchi T., Seo S., Yonezawa M., Maruyama K., Yamaguchi-Shinozaki K., and Shinozaki K.** (2007). The mitogen-activated protein kinase cascade MKK3-MPK6 is an important part of the jasmonate signal transduction pathway in Arabidopsis. *Plant Cell* **19**, 805-818.
- Thines B., Katsir L., Melotto M., Niu Y., Mandaokar A., Liu G., Nomura K., He S.Y., Howe G.A., and Browse J.** (2007). JAZ repressor proteins are targets of the SCF(COI1) complex during jasmonate signalling. *Nature* **448**, 661-665.
- Tindall K.R., and Kunkel T.A.** (1988). Fidelity of DNA synthesis by the *Thermus aquaticus* DNA polymerase. *Biochemistry* **27**, 6008-6013.
- Tiryaki I., and Staswick P.E.** (2002). An Arabidopsis mutant defective in jasmonate response is allelic to the auxin-signaling mutant *axr1*. *Plant Physiol.* **130**, 887-894.
- Tomos A.D., and Leigh R.A.** (1999). The pressure probe: A versatile tool in plant cell

BIBLIOGRAPHY

- physiology. *Annu Rev Plant Physiol Plant Mol Biol.* **50**, 447-472.
- Turner J.G.** (2007). Stress Responses: JAZ Players Deliver Fusion and Rhythm. *Curr Biol.* **17**, 847-849.
- Tyler L., Tomas S.G., Hu J., Dill A., Alonso J.M., Ecker J.R., and Sun T.P.** (2004). DELLA proteins and gibberellin-regulated seed germination and floral development in *Arabidopsis*. *Plant Physiol.* **135**, 1008-1019.
- Ubeda-Tomás S., Swarup R., Coates J., Swarup K., Laplaze L., Beemster G.T., Hedden P., Bhalerao R., and Bennett M.J.** (2008). Root growth in *Arabidopsis* requires gibberellin/DELLA signalling in the endodermis. *Nat Cell Biol* **10**, 625-628.
- Ubeda-Tomás S., Federici F., Casimiro I., Beemster G.T., Bhalerao R., Swarup R., Doerner P., Haseloff J., and Bennett M.J.** (2009). Gibberellin signaling in the endodermis controls *Arabidopsis* root meristem size. *Curr Biol.* **19**, 1194-1199.
- Ueda J., and Kato, J.** (1982). Inhibition of cytokinin-induced plant growth by jasmonic acid and its methyl ester. *Physiologia Plantarum* **54**, 249-252.
- Ueda J., Miyamoto K., and Kamisaka S.** (1995). Inhibition of the synthesis of cell wall polysaccharides in oat coleoptile segments by jasmonic acid: relevance to its growth inhibition. *J Plant Growth Regul.* **14**, 69-76.
- Ueda M., Koshino-Kimura Y., and Okada K.** (2005). Stepwise understanding of root development. *Curr Opin Plant Biol.* **8**, 71-76.
- Ueguchi-Tanaka M., Ashikari M., Nakajima M., Itoh H., Katoh E., Kobayashi M., Chow T.Y., Hsing Y.I., Kitano H., Yamaguchi I., and Matsuoka M.** (2005). GIBBERELLIN INSENSITIVE DWARF1 encodes a soluble receptor for gibberellin. *Nature* **437**, 693-698.
- Vanholme B., Grunewald W., Bateman A., Kohchi T., and Gheysen G.** (2007). The tify family previously known as ZIM. *Trends Plant Sci.* **12**, 239-244.
- Verbelen J.P., Vissenberg K., Kerstens S., and Le J.** (2001). Cell expansion in the epidermis: microtubules, cellulose orientation and wall loosening enzymes. *J Plant Physiol.* **158**, 537-543.
- Vick B.A., and Zimmerman D.C.** (1984). Biosynthesis of jasmonic Acid by several plant species. *Plant Physiol.* **75**, 458-461.
- Vijayan P., Shockey J., Lévesque C.A., Cook R.J., and Browse J.** (1998). A role for jasmonate in pathogen defense of *Arabidopsis*. *Proc Natl Acad Sci U S A.* **95**, 7209-7214.
- Wang H., Qi Q., Schorr P., Cutler A.J., Crosby W.L., and Fowke L.C.** (1998). ICK1, a cyclin-dependent protein kinase inhibitor from *Arabidopsis thaliana* interacts with both Cdc2a and CycD3, and its expression is induced by abscisic acid. *Plant Journal* **15**, 501-510.
- Wasilewska A., Vlad F., Sirichandra C., Redko Y., Jammes F., Valon C., Frei dit Frey N., and Leung J.** (2008). An update on abscisic acid signaling in plants and more... . *Mol Plant* **1**, 198-217.

BIBLIOGRAPHY

- Wasternack C.** (2007). Jasmonates: An Update on Biosynthesis, Signal Transduction and Action in Plant Stress Response, Growth and Development. *Ann Bot* **100**, 681-697.
- Wen C.K., and Chang C.** (2002). Arabidopsis RGL1 encodes a negative regulator of gibberellin responses. *Plant Cell* **14**, 87-100.
- Xiao S., Dai L., Liu F., Wang Z., Peng W., and Xie D.** (2004). COS1: an Arabidopsis coronatine insensitive1 suppressor essential for regulation of jasmonate-mediated plant defense and senescence. *Plant Cell* **16**, 1132-1142.
- Xie D.X., Feys B.F., James S., Nieto-Rostro M., and Turner J.G.** (1998). COI1: An Arabidopsis Gene Required for Jasmonate-Regulated Defense and Fertility. *Science* **280**, 1091-1094.
- Xu L., Liu F., Lechner E., Genschik P., Crosby W.L., Ma H., Peng W., Huang D., and Xie D.** (2002). The SCF(COI1) Ubiquitin-Ligase Complexes Are Required for Jasmonate Response in Arabidopsis. *Plant Cell* **14**, 1919-1935.
- Yamane H., Sugawara J., Suzukiy, Shimamura E., and Takahashi N.** (1980). Syntheses of Jasmonic Acid Related Compounds and Their Structure-Activity Relationships on the Growth of Rice Seedlings. *Agric Biol Chem.* **44**, 2857-2864.
- Yan Y., Stolz S., Chételat A., Reymond P., Pagni M., Dubugnon L., and Farmer E.E.** (2007). A Downstream Mediator in the Growth Repression Limb of the Jasmonate Pathway. *Plant Cell* **19**, 2470-2483.
- Yoshida Y., Sano R., Wada T., Takabayashi J., and Okada K.** (2009). Jasmonic acid control of GLABRA3 links inducible defense and trichome patterning in Arabidopsis. *Dev.* **136**, 1039-1048.
- Zavala J.A., and Baldwin I.T.** (2006). Jasmonic acid signalling and herbivore resistance traits constrain regrowth after herbivore attack in *Nicotiana attenuata*. *Plant Cell Environ.* **29**, 1751-1760.
- Zhang Y., and Turner J.G.** (2008). Wound-induced endogenous jasmonates stunt plant growth by inhibiting mitosis. *PLoS ONE* **3**, e3699.
- Zheng N., Schulman B.A., Song L., Miller J.J., Jeffrey P.D., Wang P., Chu C., Koepp D.M., Elledge S.J., Pagano M., Conaway R.C., Conaway J.W., Harper J.W., and Pavletich N.P.** (2002). Structure of the Cul1-Rbx1-Skp1-F boxSkp2 SCF ubiquitin ligase complex. *Nature* **416**, 703-709.
- Zidan I., Azaizeh H., and Neumann P.M.** (1990). Does Salinity Reduce Growth in Maize Root Epidermal Cells by Inhibiting Their Capacity for Cell Wall Acidification? *Plant Physiol.* **93**, 7-11.